ACTA UNIVERSITATIS SZEGEDIENSIS

ACTA MINERALOGICA-PETROGRAPHICA

TOMUS XXVII

SZEGED, HUNGARIA
1985

NOTE TO CONTRIBUTORS

General

The Acta Mineralogica—Petrographica publishes original studies on the field of geochemistry, mineralogy and petrology, first of all studies of Hungarian researchers, papers resulted in by co-operation of Hungarian researchers and those of other countries and, in a limited volume, papers from abroad on topics of global interest.

Manuscripts should be written in English and submitted to the Editor-in-chief, Institute of Mineralogy, Geochemistry and Petrography, Attila József University, H-6701 Szeged, Pf. 651, Hungary.

The authors are responsible for the accuracy of their data, references and quotations from other sources.

Manuscript

Manuscripts should be typewritten with double spacing, 25 lines on a page and space for 50 letters in a line. Each new paragraph should begin with an indented line. Underline only words that should be typed in italics.

Manuscripts should generally be organized in the following order:

Title
Name(s) of author(s) and their affiliations, in foot-note the address of the author to whom the correspondence should be sent.
Abstract
Introduction
Methods, techniques, material studied, description of the area investigated, etc.
Results
Discussion or conclusions
Acknowledgement
Explanation of plates (if any)
Tables
Captions of figures (drawings, photomicrographs, etc.)

Abstract

The abstract cannot be longer than 500 words.

Tables

The tables should be typewritten on separate sheets and numbered according to their sequence in the text, which refers to all tables.

The title of the table as well as the column headings must be brief, but sufficiently explanatory.

The tables generally should not exceed the type-area of the journal, i. e. 12,5×18,5 cm. Fold-outs can only exceptionally be accepted.

ACTA UNIVERSITATIS SZEGEDIENSIS

ACTA MINERALOGICA-PETROGRAPHICA

TOMUS XXVII

SZEGED, HUNGARIA
1985

HU ISSN 0365—8066
HU ISSN 0324—6523

Adjuvantibus

BÉLA MOLNÁR et TIBOR SZEDERKÉNYI

Redigit

GYULA GRASSELLY

Edit

Institutum Mineralogicum, Geochimicum et Petrographicum
Universitatis Szegediensis de Attila József nominatae

Nota

Acta Miner. Petr., Szeged

Szerkeszti

GRASSELLY GYULA

a szerkesztőbizottság tagjai:
MOLNÁR BÉLA és SZEDERKÉNYI TIBOR

Kiadja

a József Attila Tudományegyetem Ásványtani, Geokémia és
Kőzettani Tanszéke
H—6722 Szeged, Egyetem u. 2—6.

Kiadványunk címének rövidítése
Acta Miner. Petr., Szeged

CONTENTS

Acta Mineralogica-Petrographica, Szeged, XXVII, 5—16, 1985

MAJOR AND TRACE ELEMENTS IN SOME GRANITIC ROCKS SOUTHEASTERN AT-TAIF AREA, SAUDI ARABIA — THEIR IMPLICATIONS TO MAGMA GENESIS AND TECTONIC SETTING

M. A. HEIKAL*

ABSTRACT

The Pan-African granites southeast At-Taif area represent the last episode in the Hijaz tectonic cycle. Granites are the youngest and most abundant rock unit in the studied area. Diorite and metamorphic rocks are mainly enclosed within these granites.

Major element studies have revealed the calc-alkaline nature of the examined granites and diorite. The trend of differentiation of these rocks is similar to that recognized in many worldwide studies of calc-alkaline rocks.

Chemical data suggest that the granitic rocks were evolved in a compressional environment by partial melting of the lower crust. The intermediate rocks might have been derived by interaction of melts derived from the oceanic crust and mantle with the rising magmas.

INTRODUCTION

The crystalline rocks of the Arabian Shield occupy a trapezoidal area that extend northwestward and southwestward into two elongated segments along the eastern margin of the Red Sea *(Fig. 1)*. Granitoids (quartzdiorite, tonalite to granite) form about 40% of the basement exposures (STOESER and ELLIOTT, 1979). The granitic plutons are emplaced into eruptive volcanics and volcano-clastics of similar composition. Numerous mafic-ultramafic bodies occupy narrow, discontinuous N. W.—S. E. zones. All rocks reliably dated ($\sim$1,100 to $\sim$500 m.y.) appear to be late Proterozoic in age (FLECK *et al.*, 1976, 1979; BAUBRON *et al.*, 1976). GREENWOOD *et al.*, (1976) coined the term "Hijaz Tectonic Cycle" to cover the 600 m.y. during which the late Proterozoic events have led to the formation of the southern part of the Arabian Shield. GASS (1979) considered the estimated age of the non-cratonic basement of the Arabian Shield to fall within the extended (1100—450 m.y.) Pan-African time scale.

The present paper deals with some granitic rocks, located 27 km southeast At-Taif in the southern Hijaz quadrangle of the Arabian Shield. The studied granitic rocks belong to the Younger Granites of BROWN *et al.*, (1962), and to the last episode (third) of the Hijaz tectonic cycle of GREENWOOD *et al.*, (1976) according to NASSEEF and GASS (1976). It is the purpose of this paper to describe in brief the general geologic setting and petrography of the granitic rocks southeast At-Taif area with emphasis on magma genesis and tectonic setting.

Worthy of remark, the granitic rocks northeast At-Taif city (north the studied area) were studied in detail by NASSEEF (1971) and NASSEEF and GASS (1977). Field, geochemical and petrographic studies carried out by these authors suggest that the granitic rocks of At-Taif area were emplaced in an island arc environment.

* Geology Department — Al-Azhar University, Cairo, Egypt

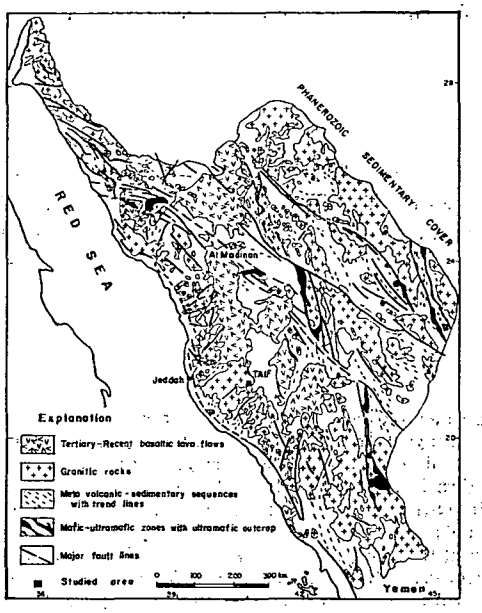

Fig. 1. Major rock types and structure of Arabian Shield and location of the studied area. Based on tectonic map of Arabian peninsula, compiled by BROWN (1970) and simplified by NASSEF and GASS (1977)

GEOLOGIC SETTING

Buff and grey granites are the youngest and most dominant plutonic rocks in the studied area. Local variation in colour of these two types and the difference between them appear to be due to varying in abundance of biotite and K-feldspar. Dykes of leucocratic granite are distinguished as the youngest rock unit in the studied area cutting all the older rock units.

Diorite is older than granites, being mainly enclosed within the granitic rocks. Metamorphic rocks represent the oldest rock unit in At-Taif area, and similar to diorite, they are mainly enclosed within the exposed granites. The metamorphic rocks consist mainly of hornblende-biotite schist, quartz-feldspathic schist and marble. Locally, the hornblende-biotite schist show evidence of assimilation by the granitic magma, while contacts of the quartz-feldspathic schists with the granites are sharp.

The investigated area is dissected by few minor faults, without any clear indication of apparent movement. These faults trend mainly in N—S and E. NE—W. SW directions, where they mainly control the courses of wadis (e.g. Wadi El-Shagrah, W. Hamem).

PETROGRAPHY

Granites are medium to coarse-grained, and grey to buff in colour with hypidiomorphic granular texture. Uncommonly, granites show porphyritic and gneissose textures. K-feldspars, plagioclase, quartz, and biotite are the essential minerals.

Sphene, zircon, and apatite are accessories. K-feldspars are usually present as orthoclase and microcline with abundant perthite intergrowths. Quartz and plagioclase are observed as inclusions in the K-feldspars. Plagioclase (An_{13}—An_{22}) forms subhedral to anhedral crystals, which are uncommonly zoned. Core and rim structure is observed in altered plagioclase. Quartz occurs as interstitial anhedral grains. Graphic quartz-potash feldspar intergrowths are common in these rocks. Biotite is the only mafic mineral and is observed in the examined granites with X=straw yellow, Y=Z= dark brown.

Leucocratic granite is medium-grained and pink in colour, with hypidiomorphic granular texture. Quartz, K-feldspars and plagioclase (An_{12}—An_{18}) are the essential minerals, while mafic minerals are minor constituents. Muscovite, apatite and zircon are accessories.

Diorite is fine- to medium-grained, dark to light grey in colour, and displays a hypidiomorphic texture. Plagioclase (An_{26}—An_{32}) si the most dominant feldspar and forms euhedral to subhedral tabular crystals with pronounced zoning. Plagioclase is accompanied by irregular interstitial quartz and small amounts of orthoclase. Biotite occurs as brown to greenish brown flakes and is mainly associated with hornblende. Sphene, opaque oxides and zircon are accessories.

CHEMISTRY AND MAGMA GENESIS

Eleven samples representing grey, buff, and leucocratic granites and diorite were selected for chemical and spectrographic analyses. The results of analyses for both major and trace elements and the CIPW norms of the examined rocks are given in Tables 1 and 2.

The chemical analyses of the examined rocks are plotted on O'CONNOR's (1965) variation diagram to classify the examined rocks according to their normative contents. All the plots of granites fall within the field of granite or lie along the border line separating the granite and trondhjemite fields. Diorite falls within the granodiorite field. For simplicity, the term "granitic rocks" is here used to cover all these rock types *(Fig. 2)*.

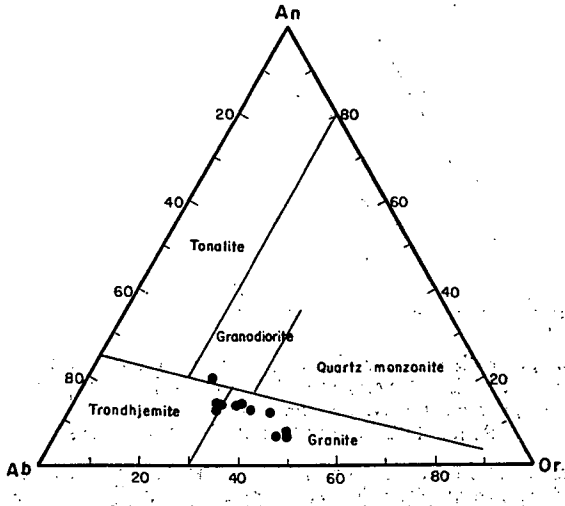

Fig. 2. Chemical classification of At-Taif granitic rocks using their normative feldspar ratios. Field boundaries are those of O'CONNOR (1965)

Fig. 3-A is a standard AFM triangular diagram which illustrates that the investigated rocks show a typical calc-alkaline trend (CARMICHAEL *et al.*, 1974). The plots of At-Taif granitic rocks also follow the average trend of the plutonic and volcanic rocks of the Arabian Shield (STOESER and ELLIOTT, 1979). *Fig. 3-B* and *Fig. 4* reveal again the calc-alkaline nature of the granitic rocks, where they plot in the fields defined by STOESER and ELLIOTT (1979) for the calc-alkaline granites of the Arabian Shield. The diorite plot falls outside the Arabian field since this field represents the calc-alkaline granites.

The chemical analyses of At-Taif plutonic rocks are plotted on a variation diagram against the differentiation index of THORNTON and TUTTLE (1960) in *Fig. 5*. It may be noted that the trend of differentiation is similar to that recognized in

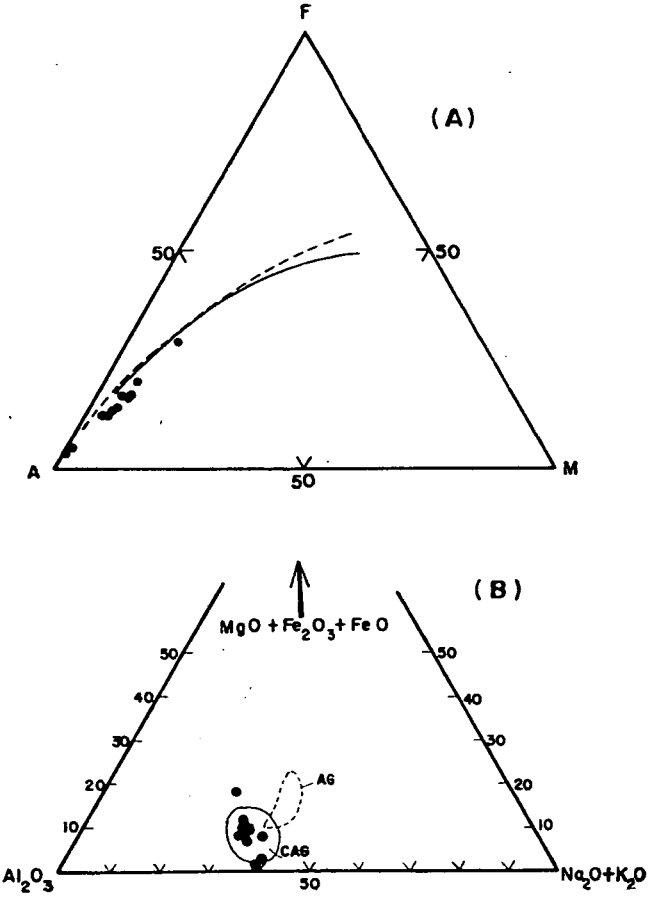

Fig. 3. A. AFM triangular diagram for At-Taif granitic rocks. A: Na_2O+K_2O, M: MgO and F: $FeO+Fe_2O_3$. The solid curve is the average trend line for the Sierra Nevada batholith (CARMICHAEL *et al.*, 1974). The dashed curve is the average trend line for the plutonic and volcanic rocks of the Arabian Shield (STOESER and ELLIOTT, 1979).

B. Total alkali-alumina-total iron oxide+magnesia ternary diagram (wt. %) for At-Taif granitic rocks. The two fields shown are for calc-alkaline granites (CAG) and alkali granites (AG) of the Arabian Shield (after STOESER and ELLIOTT, 1979)

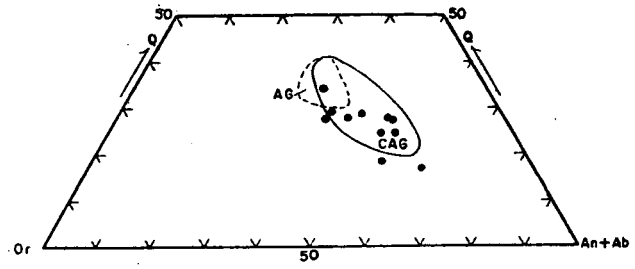

Fig. 4. Normative quartz-orthoclase-plagioclase (An+Ab) triangular diagram for the investigated granitic rocks. Diagram includes the fields designated by STOESER and ELLIOTT (1979) for calc-alkali (CAG) and alkali (AG) granites from Saudi Arabia

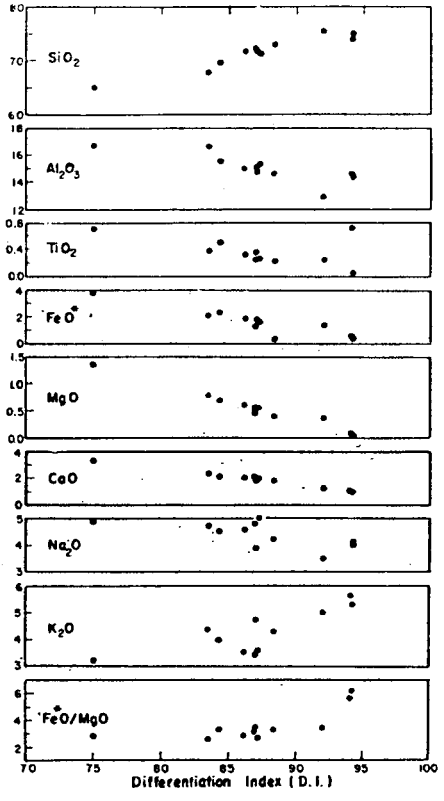

Fig. 5. Variation diagram of the major element (wt. %).

many worldwide studies of calc-alkaline rocks (NOCKOLDS and ALLEN, 1953; ALBUQUERQUE, 1971). SiO_2, K_2O and FeO* (total iron)/MgO show a steady increase toward the more differentiated types, while Al_2O_3, TiO_2, FeO*, MgO and CaO decrease in the same direction, which is the normal trend. Na_2O shows some scatter. The Na_2O content ranges from 3.51 to 4.99. Within this narrow range, it appears

TABLE 1

Chemical analyses and CIPW norms of At-Taif granitic rocks

%	1*	2	3	4	5	6	7	8	9	10	11
SiO_2	64.77	68.04	71.40	72.24	72.78	71.61	71.47	69.62	73.99	75.18	74.64
TiO_2	0.70	0.37	0.26	0.23	0.21	0.32	0.34	0.50	0.07	0.24	0.03
Al_2O_3	16.74	16.60	15.27	15.04	14.58	14.86	14.79	15.53	14.45	12.94	14.44
Fe_2O_3	1.50	0.81	0.68	0.56	0.63	0.94	0.91	1.05	0.38	0.63	0.21
FeO	2.49	1.32	0.87	0.84	0.68	0.90	0.98	1.34	0.16	0.74	0.12
MnO	0.06	0.03	0.02	0.01	0.02	0.03	0.05	0.03	0.0	0.02	0.0
MgO	1.37	0.78	0.55	0.44	0.38	0.60	0.53	0.70	0.09	0.38	0.05
CaO	3.32	2.29	1.88	2.03	1.81	1.96	1.76	2.09	0.99	1.06	0.96
Na_2O	4.87	4.74	4.99	4.75	4.17	4.59	3.87	4.51	3.98	3.51	4.05
K_2O	3.19	4.38	3.59	3.42	4.26	3.50	4.69	3.95	5.64	4.99	5.26
P_2O_5	0.32	0.13	0.10	0.09	0.07	0.12	0.11	0.16	0.02	0.08	0.02
H_2O	0.67	0.52	0.39	0.35	0.42	0.57	0.51	0.52	0.21	0.22	0.20
Total	100.00	100.01	100.00	100.00	100.01	100.00	100.01	100.00	99.98	99.99	99.98
FeO*/MgO	2.80	2.63	2.69	3.05	3.28	2.91	3.39	3.26	5.58	3.44	6.18
CIPW Norms											
Q	14.96	17.48	23.80	26.47	27.81	26.60	26.52	22.85	27.08	32.86	28.90
Or	18.85	25.88	21.21	20.21	25.17	20.68	27.71	23.34	33.32	29.48	31.08
Ab	41.19	40.09	42.20	40.17	35.27	38.82	32.73	38.14	33.66	29.69	34.25
An	14.38	10.51	8.67	9.48	8.49	8.94	8.01	9.32	4.78	4.74	4.63
C	0.01	0.21	0.00	0.05	0.0	0.25	0.41	0.42	0.05	0.03	0.39
En	3.41	1.94	1.37	1.10	0.94	1.49	1.32	1.74	0.22	0.95	0.12
Fs	2.29	1.20	0.64	0.72	0.42	0.40	0.58	0.82	0.0	0.48	0.0
Mt	2.17	1.17	0.99	0.81	0.91	1.36	1.32	1.52	0.31	0.91	0.30
Hm	0.0	0.0	0.0	0.0	0.0	0.0	0.0	0.0	0.16	0.0	0.0
Il	1.33	0.70	0.49	0.44	0.40	0.61	0.65	0.95	0.13	0.46	0.06
Ap	0.76	0.31	0.24	0.21	0.17	0.28	0.26	0.38	0.05	0.19	0.05
D.I.	75.00	83.45	87.21	86.85	88.25	86.10	86.96	84.33	94.06	92.02	94.23

* Sample 1: Diorite, Samples 2—7: Grey granite, 8—10: Buff granite, 11: Leucocratic granite.

TABLE 2

Trace element contents (ppm) and element ratios of At-Taif granitic rocks

	1*	2	3	4	5	6	7	8	9	10	11
Rb	88.4	114.1	86.0	78.0	105.1	87.7	147.0	92.7	102.6	80.8	119.2
Sr	882.8	726.2	770.2	585.4	394.6	511.6	389.2	563.8	329.8	438.6	232.3
Zr	201.2	213.2	119.3	152.9	120.6	156.8	149.5	210.5	77.7	168.0	79.5
Nb	9.9	7.0	3.2	4.9	5.8	6.8	17.7	10.9	2.8	11.9	2.0
Y	14.3	6.8	3.0	2.7	2.8	7.2	23.7	7.9	2.3	16.6	3.5
Zn	67.3	55.7	39.6	34.4	35.0	47.2	47.2	59.8	11.3	33.2	7.4
$\frac{Sr \times 10^3}{Ca}$	3.7	4.4	5.8	4.0	3.1	3.7	3.1	3.8	4.7	5.8	3.4
K/Rb	300	319	347	364	337	332	265	354	456	512	367

* Numbers refer to Table 1.

that the content of Na_2O does not vary systematically with differentiation (BATEMAN and DODGE, 1970, p. 414).

The trace elements and trace element ratios are also plotted against the differentiation index *(Fig. 6)*. Zr and Sr show a progressive decrease toward the highly differentiated granites, while K/Rb ratio increases in the same direction. The Rb, Y contents and Sr/Ca ratio are approximately constant throughout the examined rocks. However, Y shows a slight increase toward the diorite.

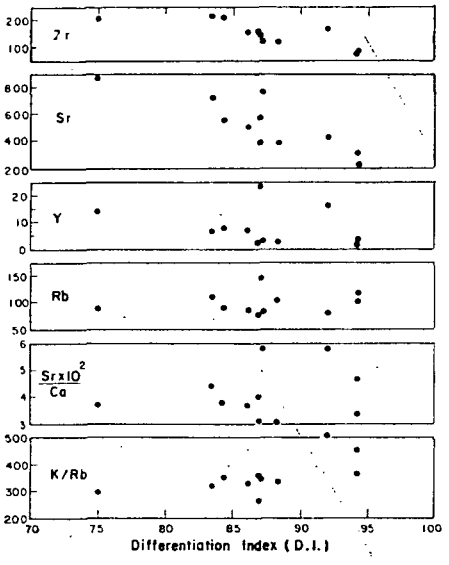

Fig. 6. Variation diagram of some trace elements and element ratios (ppm).

The normative albite, orthoclase and quartz proportions of At-Taif granitic rocks are plotted on the ternary diagram Ab-Or-Q, the residua diagram of TUTTLE and BOWEN (1958). The plots *(Fig. 7-A)* show a tight pattern that elongates toward the Ab corner. It is clear that all the analyses fall within or near the centre of the diagram. According to TUTTLE and BOWEN (*op. cit.*, p. 79) "the concentration of the analyses near the centre of the diagram is readily explained if a magmatic history is involved in the origin of most granites". Consequently, At-Taif granitic rocks are considered to possess a magmatic history. In addition, the concentration of most plots near the minimum of 1 kb pressure, suggested that the examined rock were formed at or near this particular pressure. The same points shown in *Fig. 7-A* are plotted on a figure showing the isobaric fractionation curves at 1000 bars water-vapour pressure *(Fig. 7-B)*, in order to reveal their fractionation behaviour. It is clear that most plots lie along the fractionation curves, suggesting their formation by fractional crystalization from a single magma (TUTTLE and BOWEN, 1958). This conclusion has been previously achieved from *Fig. 5* and *Fig. 6*.

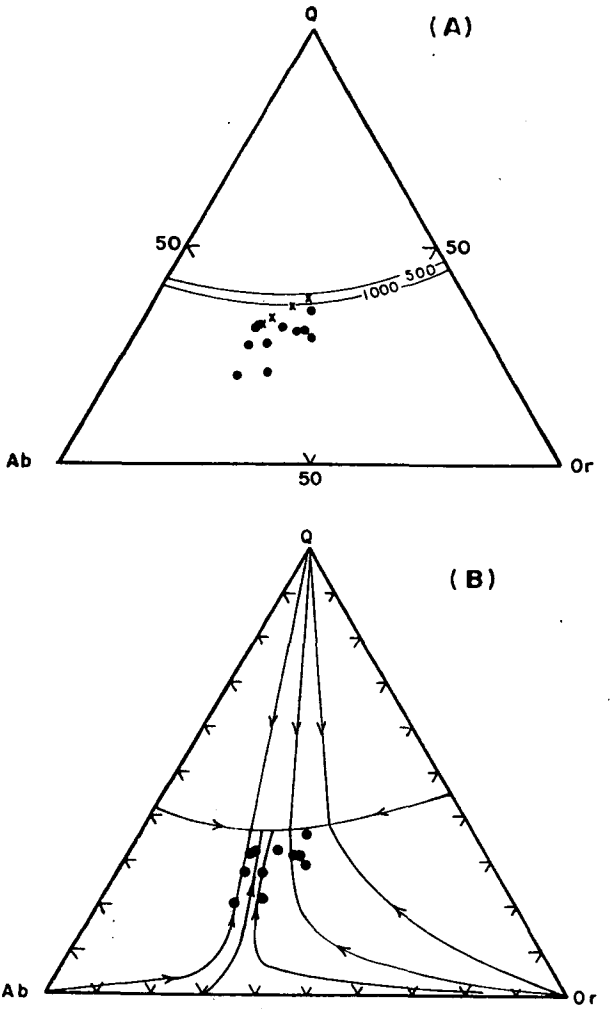

Fig. 7. A. Orthoclase-quartz-albite "residua diagram" (TUTTLE and BOWEN, 1958) for At-Taif granitic rocks. The projections of the boundary between quartz and feldspar fields at 500 and 1000 kg/cm² of water-vapour pressure, and the isobaric temperature minima for these pressures and for 2 and 3 kilobar pressures are also shown as crosses

B. The same plots shown in *Fig. 7-A* are plotted in relation to isobaric fractionation curves for 1000 bars water-vapour pressure (TUTTLE and BOWEN, 1958).

TECTONIC ENVIRONMENT

In the light of plate tectonic theory, it is generally accepted that the bulk of calc-alkaline granitic rocks lie above subduction zones. In the present study, two lines of evidence are used to predict the tectonic environment of the studied granitic rocks, *i*) the major elements content, and *ii*) the Nb, Zr and Ti concentrations of these rocks.

According to PETRO *et al.* (1979), it is assumed that on the AFM diagram, the variation trends of granites evolved in compressional environment (subduction zones) tend to be nearly perpendicular to the FM side for the entire trend. *Fig. 3-A* shows that the examined rocks follow the average trend of the plutonic and volcanic rocks of the Arabian Shield, which tends to be nearly perpendicular to the FM side. In addition, Table 1 shows that nearly all the analysed samples contain normative corundum (i.e. peraluminous rocks). The higher frequencies of peraluminous rocks are characteristic of compressional environment, while peralkaline rocks are characteristic of extensional environment (PETRO *et al.*, 1979).

Considering minor and trace elements, PEARCE and GALE (1977) have demonstrated that there are substantial geochemical variations between volcanic arc magmas and within-plate magmas. Igneous rocks of all SiO_2 values that evolved above subduction zones have Nb contents below 15 ppm, whereas for granitic rocks (60—75% SiO_2) Nb ranges from 50 to 500 ppm. According to GASS (1979, p. 12), the Nb content in 100 Sudan-Arabian granitic rocks are below 40 ppm and in over 80% the Nb content is below 15 ppm. All the investigated samples have Nb content below 15 ppm, except for sample 7 where the Nb content is 17.5 ppm. *Fig. 8* shows PEARCE and GALE's (1977) plot of Nb-SiO_2 for magmatic rocks of known tectonic setting. All the analysed samples plot in the field of volcanic arc magmas. The majority of plots fall in the field defined by PEARCE and GALE *(op. cit.)* for rocks derived from crustal melts by metamorphism of sediments.

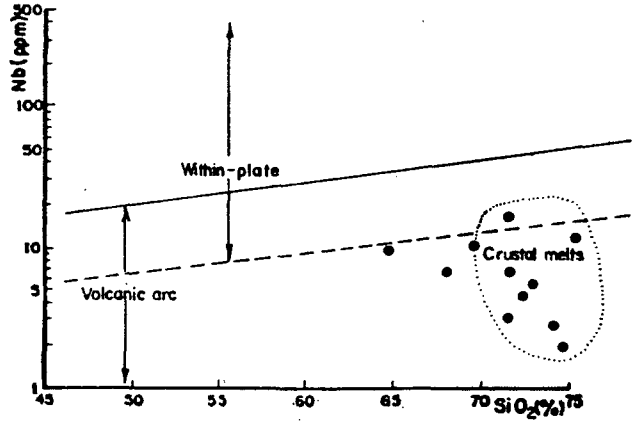

Fig. 8. Nb-SiO_2 diagram of the analysed granitic rocks. The dashed diagonal line gives lower limit for within-plate magma type, the solid diagonal line gives upper limit for volcanic arc magma type. Estimate of Nb-SiO_2 range of crustal melts derived from sediments metamorphosed up to and including amphibolite facies superimposed on diagram (PEARCE and GALE, 1977).

PEARCE (1980) regarded the immobile elements Ti and Zr as the most realistic geochemical discriminator between arc and within-plate magmatic products. All the studied rocks plot in the arc field *(Fig. 9)*.

To sum up, it is argued that the Pan-African granitic rocks of At-Taif area were evolved in a compressional environment by partial melting of the lower crust. The rising magmas may mix with melts derived from the subducted oceanic crust and mantle wedge to account for the origin of intermediate rocks (PETRO *et al.*, 1979).

Worthy of remark, the Rb/Sr ratio of At-Taif granitic rocks indicates a crustal thickness more that 30 km *(Fig. 10)*. The estimated thickness is in accordance with that reported by KNOPOFF and FOUNDA (1975) for the Pan-African crust.

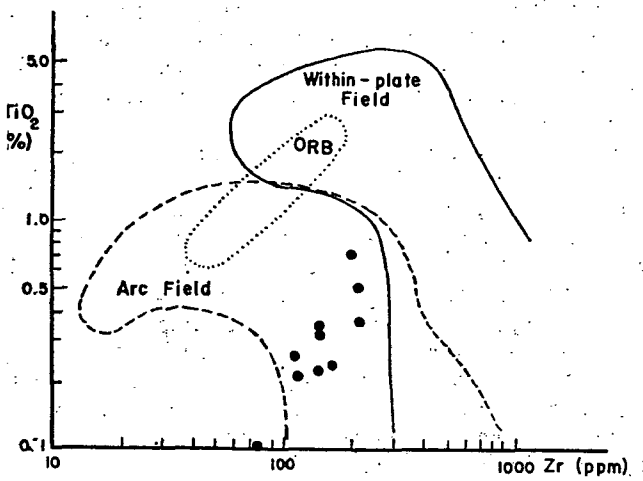

Fig. 9. TiO_2-Zr plots for At-Taif granitic rocks. Compositional fields for present-day volcanic rocks from island arc, ocean ridge basalts (ORB) and within-plate settings are after PEARCE (1980).

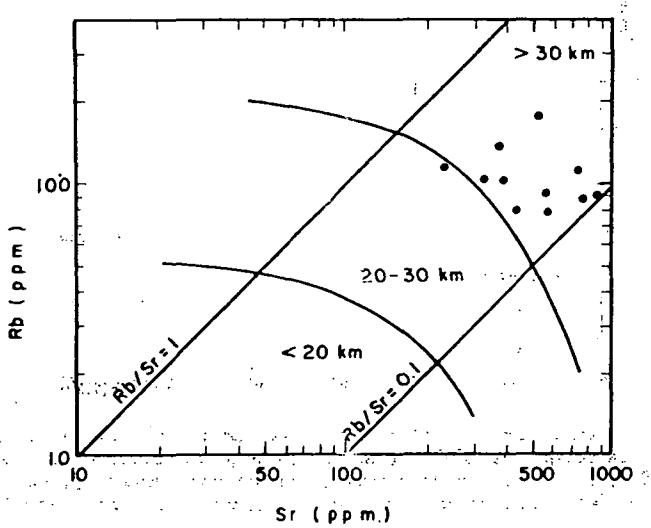

Fig. 10. Rb-Sr diagram showing distribution of At-Taif granitic rocks. Numbers in kilometers refer to crustal thickness as inferred from the Rb-Sr crustal thickness index (CONDIE, 1973).

The suggested tectonic environment for At-Taif granitic rocks is in harmony with previous studies on the Arabian-Nubian Shield (e.g. AL SHANTI and MITCHELL, 1976; BAKOR *et al.*, 1976; GARSON and SHALABY, 1976; NASSEEF and GASS, 1977; GASS, 1979) that led to the conclusion that the crystalline basement of Arabia and

northeast Africa is the product of cratonization of island arc over a period of 600 m.y. According to NASSEEF and GASS, (1977), At-Taif granitic rocks represent the final phases in the episodic cratonization process.

ACKNOWLEDGEMENT

The author wishes to express his deep thanks for Faculty of Earth Sciences, King Abdulaziz University — Saudi Arabia for facilities offered during field studies. Chemical and spectrographic analyses were carried out in the laboratories of Institute of Mineralogy and Petrography, Dell University, Italy, for such assistance the author feels indebted.

REFERENCES

ALBUQUERQUE, C. A. R. (1971): Petrochemistry of a series of granitic rocks from northern Portugal. Geol. Soc. Am. Bull., **82,** 2783—2798.

AL SHANTI, A. M. and A. H. G. MITCHELL (1976): Late Precambrian subduction and collision in the Al Amar-Idsas region, Arabian Shield, Kingdom of Saudi Arabia. Tectonophysics, **30,** T41—T47.

BAKOR, A. R., I. G. GASS and C. R. NEARY (1976): Jabal Al Wask, northwest Saudi Arabia: An Eocambrian back arc ophiolite. Earth Planet. Sci. Lett., **30,** 1—9.

BATEMAN, P. C. and F. C. W. DODGE (1970): Variations of major chemical constituents across the Central Sierra Nevada Batholith. Geol. Soc. Am. Bull., **81,** 409—420.

BAUBRON, J. C., J. DELFOUR and Y. VIALETTE (1976): Geochronological measurements (Rb/Sr; K/Ar) on rocks of Saudi Arabia. French Bureau de Recherches Géologiques et Miniéres open-file report 76—JED—22, 152 pp.

BROWN, G. F.: (1970): Eastern margin of the Red Sea and the coastal structures in Saudi Arabia. Royal Soc. London Philos. Trans., Ser. A, **267,** 75—87.

BROWN, G. F., R. O. JACKSON, R. G. ROGUE and W. H. MACLEAN (1962): Geology of southern Hijaz quadrangle, Kingdom of Saudi Arabia, Misc. Geol. Invest. U. S. Geol. Surv., Map—210 A.

CARMICHAEL, I. S. E., F. J. TURNER and J. VERHOOGEN (1974): Igneous petrology. McGraw-Hill Book Co., 739 pp.

CONDIE, K. C. (1973): Archean magmatism and crustal thickening. Geol. Soc. Am. Bull., **84,** 2981—2992.

FLECK, R. J. (1979): Rubidium-strontium geochronology and plate tectonic evolution of the southern part of the Arabian Shield. U. S. Geol. Surv. Saudi Arabian project report **245,** 105 pp.

FLECK, R. J., R. G. COLEMAN, H. R. CORNWALL, W. R. GREENWOOD, D. G. HADLEY, W. C. PRINZ, J. C. RATTE and D. L. SCHMIDT (1976): Potassium argon geochronology of the Arabian Shield, Kingdom of Saudi Arabia. Geol. Soc. Am. Bull., **87,** 9—21.

GARSON, M. S. and I. M. SHALABY (1976): Precambrian-Lower Paleozoic plate tectonics and metallogenesis in the Red Sea region. In: D. F. STRONG (ed.): Metallogeny and plate tectonics. Geol. Assoc. Can. Spec. Pap., **14,** 573—596.

GASS, I. G. (1979): Evolutionary model for the Pan-African crystalline basement. In: S. A. TAHOUN (ed.), Evolution and Mineralization of the Arabian-Nubian Shield, Bull., **3,** 1. Pergamon Press, Oxford, 11—20.

GREENWOOD, W. R., D. G. HADLEY, R. E. ANDERSON, R. J. FLECK and D. L. SCHMIDT (1976): Late Proterozoic cratonization in southwestern Saudi Arabia. Royal Soc. London Philos. Trans., Ser. A., **280,** 517—527.

KNOPOFF, L. and A. A. FOUNDA (1975) : Upper mantle structure under the Arabian Peninsula. Tectonophysics, **26,** 121—134.

NASSEEF, A. O. (1971): The geology of the northeastern At-Taif area, Saudi Arabia. Ph. D. Thesis, Leeds, Great Britain Univ. Leeds, 229 pp.

NASSEEF, A. O. and I. G. GASS (1977): Granitic and metamorphic rocks of the Taif area, western Saudi Arabia. Geol. Soc. Am. Bull., **88,** 1721—1730.

NOCKOLDS, S. R. and R. ALLEN (1953): The geochemistry of some igneous rock series. Geochim. et Cosmochim. Acta, **4,** 105—142.

O'CONNOR, J. T. (1965): A classification for quartz-rich igneous rocks based on feldspar ratios. U. S. Geol. Survey Prof. Paper **525—B,** 79—84.

PEARCE, J. A. (1980): Geochemical evidence for the genesis and eruptive setting of lavas from Tethyan ophiolites. Proc. Int. Ophiolite Symp. Nicosia, Cyprus, Geol. Surv. Cyprus Bull.
PEARCE, J. A. and G. H. GALE (1977): Identification of ore-deposition environment from trace-element geochemistry. In: Volcanic processes in ore genesis. Inst. Min. Metall. and Geol. Soc. London, 14—24.
PETRO, W. L., T. A. VOGEL and J. T. WILBAND (1979): Major element chemistry of plutonic rock suites from compressional and extensional plate boundaries. Chem. Geol., **26,** 217—235.
STOESER, D. B. and J. E. ELLIOTT (1979): Post-orogenic peralkaline and calc-alkaline granites and associated mineralization of the Arabian Shield, Kingdom of Saudi Arabia. U. S. Geol. Surv. Saudi Arabian project report **265,** 42 pp.
THORNTON, C. P. and TUTTLE, O. F. (1960): Chemistry of igneous rocks I. Differentiation Index. Amer. J. Sci., **258,** 644—684.
TUTTLE, O. F. and N. L. BOWEN (1958): Origin of granite in the light of experimental studies in the system: $NaAlSi_3O_8$—$KAlSi_3O_8$—SiO_2—H_2O. Mem. Geol. Soc. Am., 74 pp.

Manuscript received, June 21, 1984

Acta Mineralogica-Petrographica, Szeged, XXVII, 17—31, 1985

PETROCHEMISTRY, PETROGENESIS AND CLASSIFICATION OF UM HUQAB, GARF AND EL-MUEILHA GRANITIC MASSES, SOUTHEASTERN DESERT, EGYPT

A. K. A. SALEM[1], M. L. KABESH[1] and M. KH. GHAZALY[2]

ABSTRACT

The granitic masses of Um Huqab, Garf and El-Mueilha Southeastern Desert, Egypt, and belonging to synorogenic, late- and post-orogenic cycles are examined. Petrochemical characters based on major elements data of 13 newly analysed samples are clarified. Behaviour of major elements is discussed and chemical and modal classifications are presented based on normative feldspars and modal composition. Petrographical and petrochemical data suggest a magmatic origin for the examined granitic rocks. El-Mueilha granitic mass suffered along the peripheral parts, as well as along faults leading to albitization.

INTRODUCTION

The present paper deals with the petrochemistry, petrogenesis and classification of the granitic masses of Um Huqab, Garf and El-Mueilha *(Fig. 1)*. The examined masses occur among the basement rocks in the Southeastern Desert, Red Sea Hills, Egypt. The examined granitic rocks are considered by EL RAMLY and AKAAD (1960), SABET, (1972) and EL RAMLY (1972) as belonging to the younger group of granitoids. These authors gathered the granites outcropping in the Central Eastern Desert, Egypt, into two major groups, vis., *a)* older grey granites and *b)* younger granites of pink and red colours. These two granite groups are equivalent to EL SHAZLY's (1964); *a)* synorogenic plutonites and *b)* late orogenic plutonites, respectively. Broadly speaking the granitic rocks of Egypt are distinguished into three groups (EL GABY, 1975 and HUSSEIN *et al.*, 1982), namely: *1)* synorogenic granitoids, comprising the Shaitian and grey granites, *2)* late-orogenic granitoids (younger granitoids) and, *3)* post-orogenic granitoids, comprising the alkaline granites. The late-orogenic granitoids are further subdivided into three phases, based on field relations and mineralogical composition, (SABET *et al.*, 1976 and AKAAD and NOWEIR, 1980).

However, a comprehensive classification of the granites of Egypt has been advanced by GREENBERG, (1981). According to this author, the younger granites are divided into three groups, based on field relations, mineralogy, textural and chemical characteristics. Um Huqab and Garf granitic rocks are classified as older granites (grey granites) while El-Mueilha granitic complex is presented in Group I (*op. cit.*, 1981).

[1] Earth Sciences Laboratory, National Research Centre, Dokki, Cairo, Egypt
[2] Geology Department, Faculty of Science, Aswan, Assuit University, Egypt

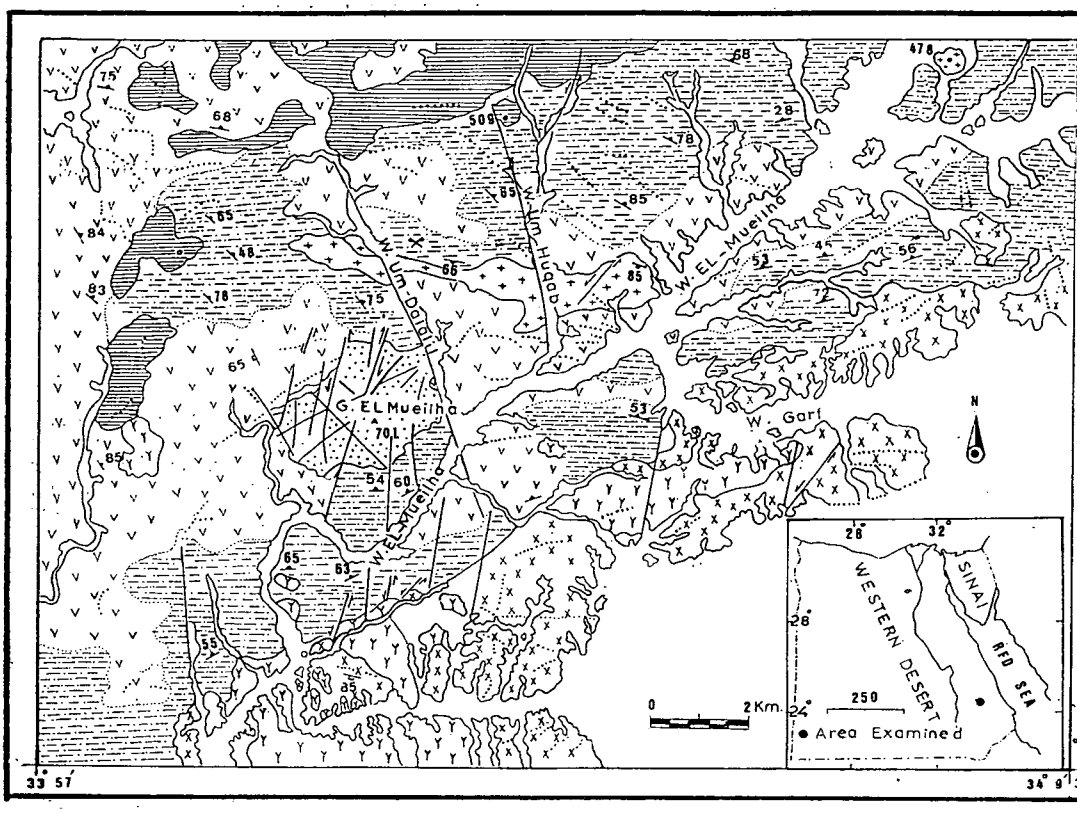

Explanation

1) Post-granit dykes; 2) El-Mueilha granite pluton (late- to post-orogenic granitoids); 3) Um Huqab granite body (synorogenic granitoids); 4) Garf granitic mass (synorogenic granitoids); 5) Metagabbro — diorite complex; 6) Serpentinites and related rocks; 7) Metavolcanics; 8) Geosynclinal metasediments; 9) Sharp contact; 10) Gradational contact; 11) Strike and dip of foliation and schistosity; 12) Inclined joints; 13) Fault (showing strike slip); 14) Fluorite quarry; 15) Elevation point; 16) Triangulation point

Fig. 1. Geological map of Um Huqab, Garf, and El-Mueilha granitic masses

GEOLOGICAL SETTING

The three examined granitic masses occur among the basement complex of Precambrian age. The basement rocks comprise a thick succession of geosynclinal metasediments alternating and partially overlain by metavolcanics. This succession is intruded by serpentinites, metagabbro-diorite complex and granitic massess of

various types. The previous basement rocks are cut by post-granitic dykes. The lithostratigraphy of the various rock units is given below (GHAZALY, 1984).

Youngest: 7) Post granite dykes
6) Late to post-orogenic granitoids:
— El-Mueilha granite pluton
5) Synorogenic granitoids:
— Um Huqab granitic rocks.
— Garf granitic mass
4) Metagabbro-diorite complex
3) Serpentinites and related rocks
2) Metavolcanics
Oldest: 1) Geosynclinal metasediments

The granitic rocks form moderately elevated features (Garf and El-Mueilha) to highly elevated (Um Huqab) and comprise four major distinct field types; tonalite, microdiorite (Um Huqab and Garf), muscovite and albitized granite (El-Mueilha). Field observations suggest a younger age for these granitic rocks. This is confirmed by cross-cutting relations and the presence of included xenoliths of the country rocks within the host granites. It is argued that the emplacement of the granitic rocks was of intrusive nature according to the following field observations:

— The contacts dip gently or moderately away from the granitic masses.
— Angular to subrounded xenoliths of dark basic volcanics are recorded along the peripheral parts of El Mueilha granite pluton. These xenoliths show no sign of interaction with the granite, pointing to the rather 'cold' nature of the granite magma (SOLIMAN. 1971 and 1975) or else the emplacement of the granite at shallow depth.
— A thin hornfelsic metamorphic aureole has developed around El-Mueilha mass. The contacts are characterized by abundant shear zones affecting the surrounding rocks and occasionally at right angles to the contacts. Also schistose structures has been recorded among the rocks near the shear planes (GHAZALY, 1984).

PETROGRAPHY OF THE GRANITIC ROCKS

The petrographic description of the examined granitic rocks is given under the following categories:

1) Synorogenic granitoids; these rocks are represented by Um Huqab and Garf granitic masses.
2) Late- to post-orogenic granitoids; this group comprises El-Mueilha granitic pluton.

Synorogenic granitoids:

Under the microscope, two types have been recognized among these granitic rocks namely tonalites and microdiorites. Generally, these rocks exhibit holocrystalline, hypidiomorphic granular texture. They are fine to coarse grained usually non-porphyritic and even-grained and occasionally porphyritic. The essential minerals are quartz, plagioclase, biotite, hornblende, muscovite and chlorite. Few micrograph-

ic intergrowths are observed. In Um Huqab granites many carlsbad twinning divide both normally and oscillatory zoned plagioclase megacrysts into two roughly equal parts, with the largest dimensions of these crystales parallel to the composition face. Accordingly the plagioclase twinning of Um Huqab granitic rocks is primary (SEIFERT, 1964). Plagioclase occurs as lath-shaped crystals 1.2×1.8 mm. The composition of plagioclase ranges from An_{32} to An_{36}. It is saussuritized to various degrees with epidote concentrated in the cores of normally zoned crystals. Oscillatory zoning is not uncommon. Hornblende occurs as long prismatic crystals ranging from 0.5 mm to 0.9 mm in length and from 0.2 mm to 0.4 mm in breadth. It has a deep green colour, pleochroic with X=green yellow Y=pale green and Z=deep green. Hornblende may show simple twinning and encloses iron granules, short prisms of zircon and sometimes quartz blebs. Hornblende is poikilitically sieved by small anhedral saussuritized plagioclase crystals. Sometimes, hornblende is chloritized and strongly pleochroic specially along peripheries and is usually cracked along cleavage perpendicular to the long dimensions of the crystals. Biotite occurs as stout, long flakes, 0.2 mm of deep brown, reddish brown and olive green colour. It is pleochroic from deep brown to straw yellow. The biotite flakes are usually clustered in patches, and slightly chloritized or charged with iron oxide rods and granules along cleavage planes. Muscovite forms fine interstitial aggregates, sometimes occurs as stout thick flakes 0.7 mm long, usually associated with biotite. Quartz occurs as anhedral crystals 1.2×0.8 mm, with sutured outlines. It is clear but may be undulosed and shows fine granulation along its peripheries. Quartz forms myrmekitic intergrowths with plagioclase, the latter is occasionally rimmed with quartz. Iron oxide, sphene, zircon and apatite are accessories.

Younger granitoids

Two phases could be distinguished among El-Mueilha granitic pluton: 1) muscovite granite and 2) albitized granite. Generally, these granites exhibit holocrystalline, hypidiomorphic granular texture. They are medium to coarse grained. The essential minerals are quartz, plagioclase, microcline, muscovite and lepidolite. Plagioclase occurs as subhedral crystals ranging from 1.7 mm to 2.0 mm in length and from 0.2 mm to 0.8 mm in breadth. Sometimes plagioclase forms aggregates of small subhedral albite crystals in the groundmass. It is slightly to moderately saussuritized and sericitized and corroded by quartz. Plagioclase is perthitically intergrown with microcline and twinned according to the albite law. Sometimes it shows intense undulose extinction. The alteration often begins in the interior which may be clouded or completely obscured while the margin remains clear. Microcline occurs either as subhedral to anhedral microcline-microperthite crystals, 5×3.5 mm, or as disseminated anhedral equal crystals, 1.5 mm across which are sieved and corroded by other constituents and display different degrees of alteration. In the microcline microperthite, the exsolved sodic plagioclase component occurs within the host microcline as microscopic lamellae which are frequently less altered than the host microcline. Drops of quartz inclusion are common within the microcline. Microcline is corroded by quartz, but itself replaces plagioclase and is sometimes intergrown with it forming perthite texture. It encloses minute prisms of zircon. Muscovite forms fine interstitial aggregates; sometimes occurs as short thick flakes 0.2×0.15 mm, usually associated with biotite and plagioclase of the groundmass or replacing them. Lepidolite occurs in fair amount, and possesses the same optical properties as muscovite, but the former has a large extinction angle (5°—7°). Lepidolite shows higher interference colour. It is recorded in El-Mueilha granites. Zircon, sphene, apatite and iron oxides are acces-

sories. Rarely, cataclasis affects the different minerals of the examined granites. Due to deformation quartz shows wavy extinction, marginal granulation, fracturing and granulation along fractures. The deformation of plagioclase is manifested by undulose extinction and curved and displaced twinning lamellae.

MODAL COMPOSITION

The quantitative mineral composition for 18 representative samples from Um Huqab, Garf and El-Mueilha granitic rocks are given in Table 1. *Fig. 2* shows the classification suggested by IUGS Subcommission on the Systematics of Igneous Rocks, (1973)* which was further reviewed by STRECKEISEN (1976), based on modal quartz-alkali feldspars and plagioclase relative proportions. According to this classification Um Huqab and Garf granites plot in the fields of tonalite and quartz diorite while the granites of El-Mueilha fall within the fields of granite and granodiorite.

PETROCHEMICAL CHARACTERS

The results of major oxide analyses for 13 samples, compared with reference high-calcium granites of TUREKIAN and WEDEPOHL (1961), and, in addition the average analysis of El-Mueilha (ZAGHLOUL *et al*, 1976) one analysis of leuco-granodiorite

TABLE 1

Modal analysis of the investigated granitic rocks

Granites and Sample No.	Mineral	Plagio-clase	Quartz	Alk. feldspar	Horn-blende	Biotite	Mus-covite	Acces-sories	Total
Garf granitic mass	1·	60.43	22.73	0.00	13.23	0.00	0.00	3.61	100
	2	52.87	19.36	0.56	14.42	6.91	0.00	5.88	100
	3	66.49	12.39	0.62	12.09	6.98	0.00	0.89	100
	4	56.63	16.00	0.00	17.17	8.67	0.00	1.53	100
	5·	46.87	26.65	0.94	20.13	2.81	0.00	2.60	100
	6·	52.80	32.23	1.20	0.00	12.67	0.00	0.80	100
	7·	52.68	24.05	0.90	13.67	7.67	0.00	1.03	100
	8·	62.68	15.25	0.84	4.43	15.57	0.00	1.23	100
	9·	50.82	19.80	0.42	22.22	6.00	0.00	0.74	100
Um Huqab granite	10·	61.70	26.43	1.20	4.03	1.00	4.31	1.33	100
	11	64.56	14.03	0.74	12.03	8.10	0.00	0.54	100
	12·	56.93	36.83	0.00	0.00	4.83	0.00	1.41	100
	13·	65.07	20.46	1.92	0.00	11.39	0.00	1.16	100
El-Mueilha granite	14·	55.03	31.63	10.72	0.00	0.00	2.53	0.09	100
	15·	44.09	38.30	14.66	0.00	0.00	2.52	0.43	100
	16·	47.23	37.23	13.17	0.00	0.00	2.37	0.00	100
	17·	41.30	29.97	24.80	0.00	0.00	3.93	0.00	100
	18·	40.23	44.60	10.67	0.00	0.00	4.50	0.00	100

· These samples have been analysed.

* IUGS Subcomission on the Systematics of Igneous Rocks. Classification and nomenclature of plutonic rocks. Recommendations. Geotimes **18** (1973) 10,26—30.

of Wadi Beizah (DIAB, 1979), and the average analyses of granodiorite (LE MAITRE, 1976) are given in Table 2. From the chemical point of view, the granitic rocks of Garf, Um Huqab and El-Mueilha are considered as high-calcium granites.

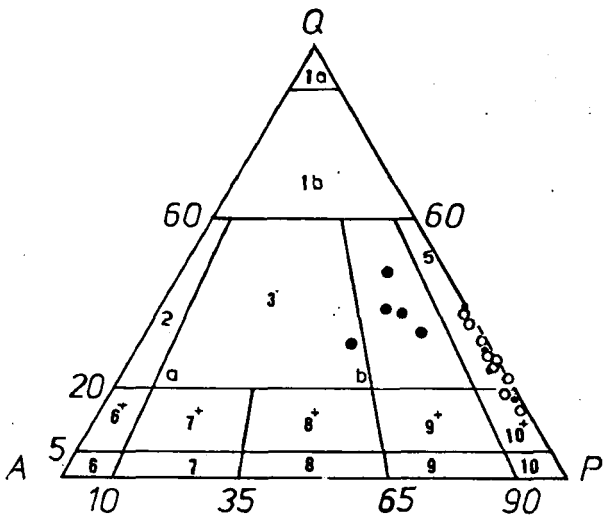

Fig. 2. Classification of the investigated granitic rocks on the basis of their quartz (Q), alkali feldspars (A), and plagioclase (P), (Diagram after the IUGS, 1973). *1a*: quartzolite (silexite), *1b:* quartz-rich granitoids, *2:* alkali-feldspar granite, *3:* granite, *4:* granodiorite, *5:* tonalite, *6:* alkali-feldspar quartz syenite (*6*:* alkali-feldspar quartz syenite), *7:* syenite (*7*:* quartz syenite), *8:* monzonite (*8*:* quartz monzonite, *9:* monzodiorite, monzogabbro, (*9*:* quartz monzodiorite, quartz monzogabbro), *10:* diorite, quartz gabbro), *10*:* quartz diorite, quartz gabbro, quartz anorthosite. Symbols: O Um Huqab granitic mass; · Garf granitic rocks; ● El-Mueilha pluton

The chemical analyses of the examined rocks are plotted on the AFM variation diagram. *Fig. 3* reveals a small differentiation trend which is similar to the late differentiation trends of common calc-alkaline igneous rocks series given by NOCKOLDS and ALLEN (1953). These trends are characterized by decrease of Mg and ($Fe^{3+} + Fe^{2+}$) with increase of alkalies. Trends of variation of these elements follow those defined by EL-GABY (1975) and HUSSEIN *et al.*, (1982) for Egyptian granitoids. On the AFM diagram, the trends are nearly prependicular to the FM side. Duch a trend is characteristic for granites formed under compressional environment, (PETRO *et al.*, 1979).

Fig. 4 shows the alkalinity ratio variation diagram proposed by WRIGHT (1969). It is clear from the diagram that Um Huqab and Garf granitic rocks fall within the cal-alkaline field. This field is defined by HUSSEIN *et al.*, (1982) for synorogenic granitoids (Group I), while El-Mueilha granite show an alkaline tendency and plot within the field of late-orogenic granitoids. The enrichment in soda seems to be a general feature of the late-orogenic granitoids with alkaline affinity (SILLITOE, 1979). In addition, petrographic data reveals that El-Mueilha granites suffered greatly from alkali metasomatism.

The agpaitic coefficient from Zavaritski-parameters (*c.f.* BAILY and MACDONALD, 1970) is plotted *vs.* SiO_2 showing the peralkaline nature of Um Huqab, Garf and El-Mueilha granitic rocks *Fig. 5*. There are two main groups, the agpaitic and the

TABLE 2

Chemical analyses of the investigated granitic rocks and some chemical analyses for comparison

	El-Mueilha granite pluton						Garf granitic mass				Um Huqab granitic mass						
Sample No	1	2	3	4	5	6	7	8	9	10	11	12	13	A	B	C	D
SiO_2	72.71	70.60	75.34	72.73	72.18	74.97	66.11	68.07	59.69	62.37	66.95	66.88	70.22	67.23	76.96	66.09	66.40
Al_2O_3	13.32	15.79	13.26	14.54	14.79	12.29	17.34	15.60	16.97	14.90	16.31	17.22	14.94	15.50	13.22	15.73	15.07
Fe_2O_3	1.15	0.20	0.11	0.27	0.96	0.45	1.24	0.97	2.36	3.09	2.46	0.75	0.26	4.23	1.05	1.38	1.74
FeO	0.49	0.22	0.44	0.30	0.18	0.37	2.74	1.92	3.26	3.83	1.92	1.11	1.06	—	0.33	2.73	2.99
TiO_2	0.02	0.02	0.03	0.04	0.02	0.03	0.83	0.36	0.84	0.69	0.28	0.37	0.17	0.57	0.06	0.57	0.50
CaO	1.40	1.72	1.05	1.40	0.98	2.25	1.61	2.18	3.81	5.27	2.40	4.38	3.71	3.54	1.12	3.83	3.57
MgO	0.50	0.05	0.28	0.04	0.05	0.10	0.86	1.46	2.11	2.52	0.63	1.02	0.42	1.56	0.31	1.74	1.65
Na_2O	5.17	5.99	4.78	4.57	5.33	4.33	4.24	4.12	4.33	4.54	4.99	4.99	4.50	3.83	3.13	3.75	3.86
K_2O	3.88	3.65	3.81	4.33	3.82	3.55	1.86	1.90	1.78	1.43	2.04	2.05	2.47	3.04	3.29	2.73	3.07
MnO	—	0.02	0.06	0.05	0.09	—	0.09	0.06	0.05	—	0.09	0.04	0.08	0.07	0.03	0.07	0.07
P_2O_5	0.10	0.07	0.27	0.07	0.07	0.07	0.27	0.37	0.34	0.17	0.13	0.18	0.08	0.21	0.05	0.10	0.20
H_2O^-	—	0.10	—	0.02	—	—	0.07	0.07	0.02	0.52	0.20	0.11	0.23	—	0.04	0.19	—
H_2O^+	0.98	0.67	0.40	0.76	0.75	0.63	1.79	1.44	3.18	0.60	1.60	0.97	0.92	—	0.37	0.25	0.79
Total	99.72	99.10	99.83	99.12	99.22	99.04	99.05	98.72	98.74	99.93	100	100.07	99.06	99.36	99.96	99.90	99.89
Agpaitic coef.	0.95	0.87	0.90	0.84	0.87	0.89	0.52	0.58	0.53	0.60	0.64	0.61	0.67	0.62	0.65	0.58	0.64
Alkalinity ratio	4.19	3.45	4.00	3.53	3.76	3.37	1.95	2.08	1.83	1.84	2.20	1.97	2.19	2.13	2.70	1.99	2.18
Felsic/mafic ratio	21.64	33.90	42.10	38.34	35.02	24.77	10.54	10.72	5.33	4.34	9.31	9.49	13.34	7.53	29.61	6.93	7.17

A) High-calcium granites of TUREKIAN and WEDEPOHL, (1961), B) Average analysis of El-Mueilha (ZAGHLOUL ET AL., 1976), C) Leuco-granodiorite of Wadi Beizah (DIAB, 1979). D) Average analysis of granodiorite (LE MAITRE, 1976).

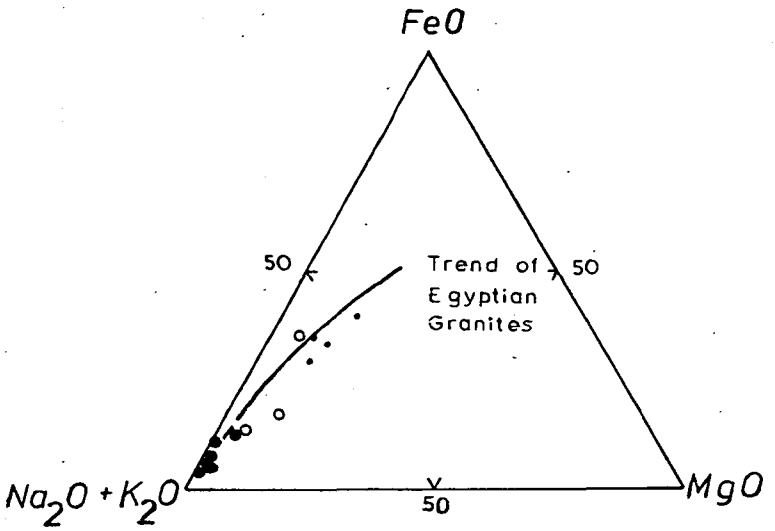

Fig. 3. AFM diagram for the studied granites. The trend of Egyptian granites is defined after HUSSEIN *et al.*, (1982), $A = K_2O + Na_2O$, $F = FeO + 0.9\ Fe_2O_3$, $M = MgO$. Symbols as in *Fig. 2.*

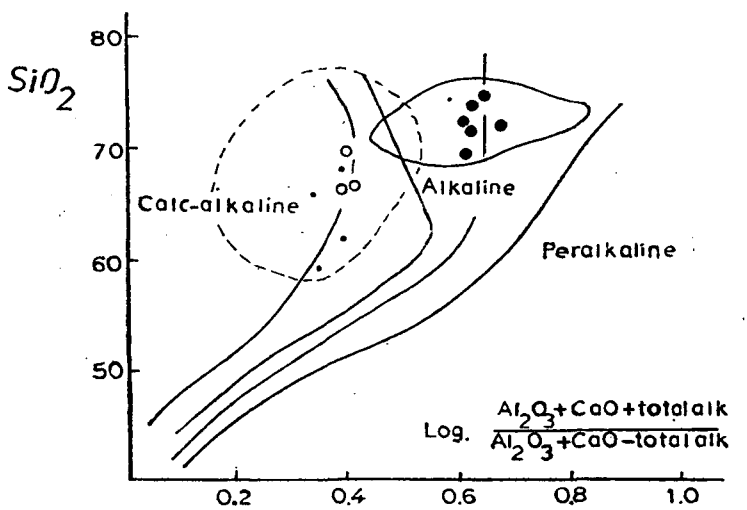

Fig. 4. Alkalinity ratio variation diagram of WRIGHT (1969) for the investigated granites. Fields of synorogenic granitoids (dashed) and late-orogenic granitoids (solid) are defined after HUSSEIN *et al.*, (1982). Symbols as in *Fig. 2.*

miaskitic types with agpaitic coefficient more or less than 1, respectively. It is evident that the investigated samples plot within the field of miaskitic nature i.e. mol. ratio of $Na_2O + K_2O/Al_2O_3$ is less than unite (hyperalkaline granites).

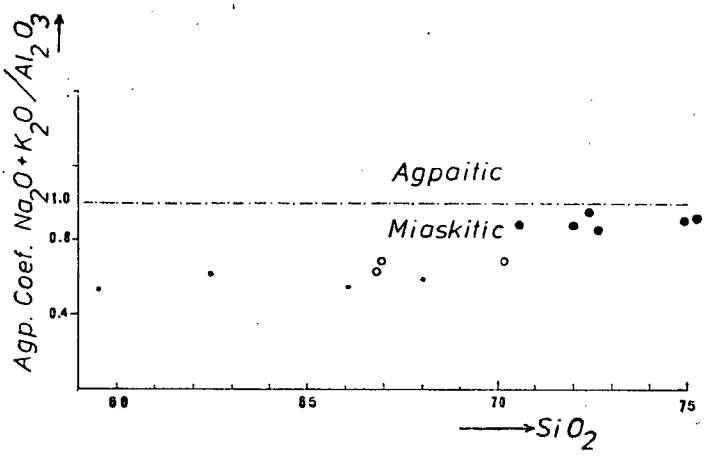

Fig. 5. Agpaitic index *versus* SiO_2 diagram. Symbols as in *Fig. 2.*

NIGGLI *values*

The calculated NIGGLI-values of the examined granitic rocks are given in Table 1. The values of *al* plotted *vs. alk* are given in *Fig. 6.* It is obvious from the figure that all samples of Um Huqab and Garf fall within the inermediate with the exception of one sample falling in the field relatively rich, (*alk*=2/3 *al*).

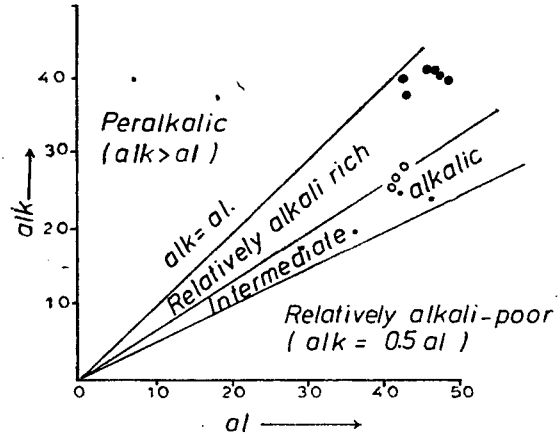

Fig. 6. Relationships of *al* and *alk* in the granitic rocks (after BURRI and NIGGLI, 1945). Symbols as in *Fig. 2.*

Norm values

The calculated norm values for the investigated granitic rocks are given in Table 2. The normative Or, Ab and An proportions of the granitic rocks are plotted in a ternary diagram *Fig. 7.* It is clear from the diagram that most of the granites of El-Mueilha fall close the field of sodic series, thus indicating their enrichment in sodium content while few samples of the examined rocks fall nearer to the field of the average

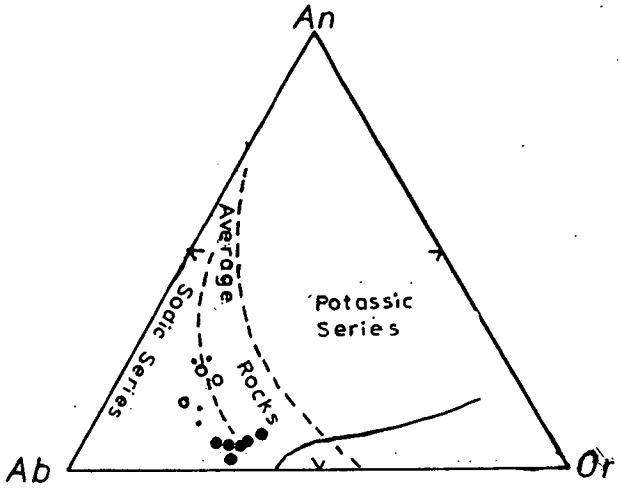

Fig. 7. An, Ab and Or normative proportions in the investigated granites. The solid line represents the two feldspar boundary curve for the quartz saturated ternary feldspar system at 1000 bars water-vapour pressure (after JAMES and HAMILTON, 1969). Sodic and potassic zones from IRVINE and BARAGAR, (1971). Symbols as in *Fig. 2.*

rocks, all plots of the examined granites follow the isobaric univariant curve, indicating that crystal-liquid equilibrium was the dominant mechanism involved in the genesis of these granites (JAMES and HAMILTON, 1969).

Chemical classification

A chemical classification of the granitic rocks of Um Huqab, Garf and El-Mueilha is attempted on the basis of their normative feldspars. *Fig. 8* shows the normative classification suggested by O'CONNOR (1965). According to this normative classification, Um Huqab and Garf granites fall within the field of granite-trondhjemite with the exception of two samples falling within the field of tonalite. All the granitic samples of El-Mueilha fall within the field of granite, with two sample falling within the field of trondhjemite.

SEGERSTROM *and* YOUNG*'s classification*

For purpose of classifying igneous rocks SEGERSTROM and YOUNG (1972) using data of average chemical composition of NOCKOLDS (1954), introduced a felsic-mafic ratio, later slightly modified by YOUNG. This ratio is expressed by SiO_2+ $+K_2O/Fe_2O_3+FeO+MgO+CaO$; values of felsic-mafic ratio are as follows:

Rock type	*Felsic-mafic ratio*
Extreme alkali granite	>50
Alkali granite (alkali rhyolite)	25—50
Granite (rhyolite)	15—25
Quartz monzonite (quartz latite)	10—15
Granodiorite (dacite)	7—10

Quartz diorite (quartz andesite)	5—7
Monzonite (latite)	3—5
Diorite (andesite)	2.1—3
Gabbro (basalt)	1.4—2.1
Ultramafics	<1.4

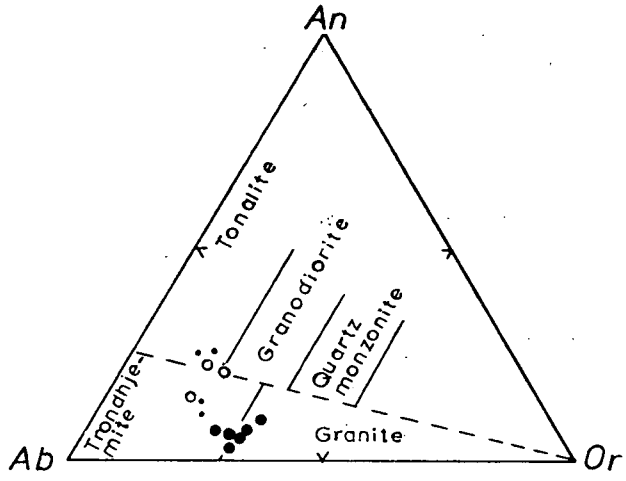

Fig. 8. Normative feldspar ratios (after O'CONNOR, 1965) Symbols as in *Fig. 2.*

In the present work felsic-mafic ratios of El-Mueilha range from 21.64—42.10 (Table 2) indicating alkaline granite and granite while Um Huqab range from 9.31—13.34 (Table 3). Accordingly the examined granitic rocks of Um Huqab are classified as granodiorite and quartz monzonite. Garf granites range from 4.34 to 10.54 indicating that Garf granites are classified as alkali granite and monzonite.

STRECKEISEN's *classification (1976)*

The normative Or, Ab and An proportions of the studied rocks are plotted in a ternary diagram introduced by STRECKEISEN (1976). It appears from the *Fig. 9.* that the granitic rocks of Um Huqab and Garf fall within the fields of granodiorites *(4)* with one sample falling in field of trondhjemite *(5)* and the other samples of El-Mueilha falling in field of syeno-granite and monzo-granite (*3a, 3b* respectively).

Petrogenesis

The normative Or, Ab and An proportions of the examined granites are plotted in a ternary diagram *Fig. 10* and the results are compared with experimental data of TUTTLE and BOWEN (1958). It is observed from this figure that the examined granitic rocks fall around the minimum melting curve of the granite system at water—vapour pressure from 500 to 10,000 bars. Most of the samples are located nearer to the high water-vapour pressure end of minimum the melting curve. This suggests that the emplacement of the examined granitic rocks was at moderate to higher water-vapour pressure (10,000 bars and in turn, at moderate to deeper depths in the crust. Also, it is observed from *Fig. 10* that the plots for Um Huqab, Garf and El-Mueilha show some scatter along the minimum melting curve at moderate to high

TABLE 3

Niggli values of the investigated granitic rocks

Granite masses	El-Mueilha Granitic Pluton						Garf Granitic Mass			Um Huqab Granitic Body			
Sample No	1	2	3	4	5	6	7	8	9	10	11	12	13
al	42.61	47.21	46.18	48.09	47.39	42.83	46.82	42.78	36.90	30.25	42.17	42.23	42.96
fm	8.62	2.16	5.43	3.12	5.57	4.71	21.00	21.23	28.37	31.99	19.62	12.68	8.67
c	8.14	9.35	6.65	8.42	5.71	14.25	7.91	10.87	15.06	19.45	11.28	19.53	19.40
alk	40.64	41.28	41.54	40.37	41.34	38.21	24.27	25.13	19.68	18.31	26.93	25.57	28.98
si	394.70	358.22	445.23	408.25	322.41	443.29	302.95	316.74	220.24	214.90	293.72	278.30	342.64
k	0.33	0.29	0.34	0.38	0.32	0.35	0.22	0.22	0.21	0.17	0.21	0.21	0.27
mg	0.47	0.18	0.45	0.11	0.07	0.19	0.28	0.48	0.41	0.40	0.21	0.50	0.35
qz	+132.14	+93.10	+179.07	+146.77	+127.05	+190.45	+105.87	+116.26	+41.52	+41.66	+86.00	+76.02	+126.72

TABLE 4

Norm values of the examined granitic rocks

Granite masses	El-Mueilha Granitic Pluton						Garf Granitic Mass			Um Huqab Granitic Body			
Sample No	1	2	3	4	5	6	7	8	9	10	11	12	13
qz	23.60	17.33	28.56	24.97	22.98	31.09	27.93	27.55	15.63	15.40	22.55	18.25	25.10
or	23.20	21.60	22.65	25.95	22.80	21.45	11.35	11.55	11.00	8.60	12.30	12.15	14.90
ab	47.05	53.85	43.15	41.65	48.30	39.70	39.40	40.00	40.75	41.45	45.70	44.95	41.30
an	1.70	5.43	3.48	6.48	4.40	3.70	6.40	8.68	17.45	16.35	11.30	18.60	13.58
c	—	—	—	—	0.32	—	6.88	3.78	2.08	—	2.05	—	—
w	1.88	1.04	—	0.02	—	2.88	—	—	—	3.64	—	0.82	1.88
en	1.40	0.14	0.78	0.12	0.14	0.28	2.46	4.16	6.10	7.08	1.78	2.82	1.18
fs	0.32	0.22	0.66	0.30	—	0.22	2.44	1.94	2.44	2.86	1.02	0.74	1.36
mt	0.62	0.21	0.12	0.29	0.60	0.48	1.34	1.05	2.58	3.29	2.63	0.78	0.29
il	0.02	0.02	0.04	0.06	0.02	0.04	1.20	0.52	1.22	0.98	0.40	0.52	0.24
ap	0.21	0.16	0.56	0.16	0.16	0.16	0.59	0.80	0.75	0.37	0.27	0.37	0.16
ht	—	—	—	—	0.28	—	—	—	—	—	—	—	—
Total	100	100	100	100	100	100	99.99	100	99.99	100	100	100	99.99
Diferentiation Index	93.85	92.78	94.37	92.59	94.09	92.24	78.68	79.10	67.38	65.46	80.55	75.35	81.30

water-vapour pressures which may indicate that the emplacement of these rocks was accompanied by a wide range of water-vapour pressure which may be interpreted in terms of multiphase origin for the examined rocks i.e. the investigated granitic rocks are formed of more than one phase.

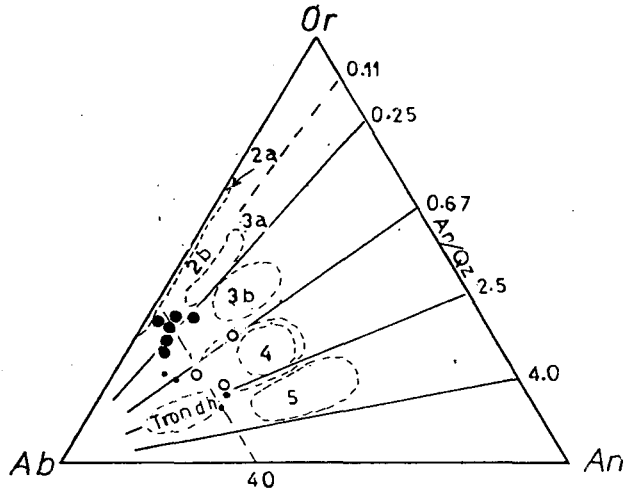

Fig. 9. Quartz-feldspar rocks (after STRECKEISEN, 1967) Symbols as in *Fig. 2.*

2a	Alkaline granite Alkali rhyolite	3b	(Monzo-)granite Rhyodacite
2b	Alkali-feldspar granite Rhyolite	4	Granodiorite Dacite
3a	(Syeno-) granite Rhyolite	5	Tonalite Plagidacite Trondhjemite

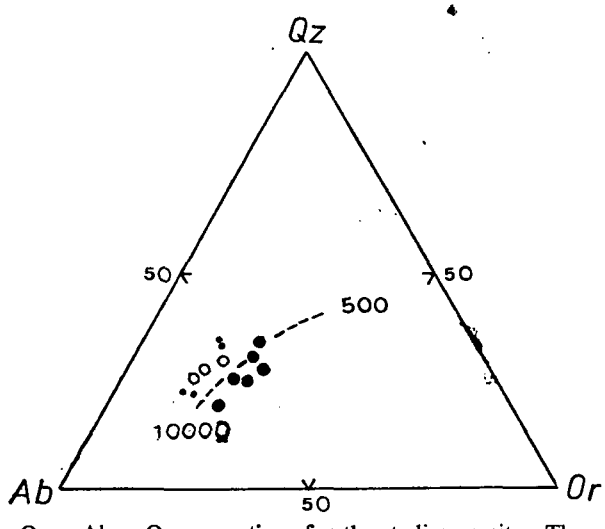

Fig. 10. Normative Qz — Ab — Or proportions for the studies granites. The solid line represents the variation in position of the minimum melting points in the granite system at water-vapour pressures from 500 to 10 000 bars (after TUTTLE and BOWEN, 1958). Symbols as in *Fig. 2.*

CONCLUSIONS

The granitic masses of El-Mueilha, Garf and Um Huqab of the Precambrian basement in the Southern part of the Central Eastern Desert of Egypt are petrochemically characterized. The examined granitic rocks are classified as synorogenic (Garf and Um Huqab) and late- to post-orogenic (El-Mueilha). The former are generally considered as belonging to the late Proterozoic intrusions "grey granites". The latter belonging to the third phase of the Gattarian granites and the muscovite-granite with the albitized types. The examined granites show a wide range of chemical composition with differentiation indices between 67.38—94.31 indicating a highly differentiated magma. Garf and Um Huqab granites range from trondhjemite to tonalite while El-Mueilha are of granite composition. The albitization of the latter is attributed to sodium metasomatism. All the examined granitic rocks are of miaskitic nature. Garf and Um Huqab granites are calc-alkali with sodic character while El-Mueilha granite has rather alkaline affinity with potassic tendency. It is argued that the examined granitic rocks are of magmatic origin. El-Mueilha granite pluton is probably derived by fractional fusion of crustal rocks. It is also suggested that the examined granitic masses are formed under compressional environments.

REFERENCES

AKAAD, M. K. and EL-RAMLY, M. F. (1960): Geological history and classification of the basement rocks of the Central Eastern Desert of Egypt. Geol. Surv. Egypt, Paper No. **9,** 24.

AKAAD, M. K. and NOWEIR, A. M. (1980) : Geology and lithostratigraphy of the Arabian Desert Orogenic belt of Egypt between latitudes 25°35′ and 26°30′ N In: P. G. GORAY and S. A. TAHOUN (editors): Evolution and mineralization of Arabian-Nubian Shield. King Abdulaziz Univ, **4,** Pergamon Press, Oxford, 127—135.

BAILY, D. K. and MACDONALD, R. (1970): Petrochemical variation among mildly peralkaline (Comendite) obsidians from the oceans and continents. Contr. Mineral and Petrol., **28,** 240—251.

BURRI, C. and NIGGLI, P. (1945): Die Jungen Eruptivgesteine des mediterranean Orogens I. Publ. Vulkaninstitut Immanuel Friedlaender No. 3.

BURRI, C. (1964): Petrochemical calculation. Basler Birkhauser Verlag, 304 pp.

DIAB, M. M. (1978): Petrological studies on some granitic rocks of Wadi Beizah, north west Urf Umm Rashid, Central Eastern Desert, Egypt: M. Sc. Thesis, Faculty of Science, Ain Shams University.

EL-GABY, S. (1975): Petrochemistry and geochemistry of some granites from Egypt. N. Jb. Miner. Abh, **124,** 2, 147—189.

EL-RAMLY, M. F. and AKAAD, M. K. (1960): The basement complex in the Central Eastern Desert of Egypt, between latitudes 24°30′ and 25°40′ N. Geol. Surv. Egypt, paper No. 9,24 pp.

EL-RAMLY, M. F. (1972): A new geological map for the basement rocks in the Eastern and South-Eastern Desert of Egypt, **2,** 1—18.

EL-SHAZLY, E. M. (1964); On the classification of the Precambrian and other rocks of magmatic affiliation in Egypt, U. A. R; Twenty second Int. Geol. Cong. India, Proc. Sec., **10,** 88—101.

FYFE, M. A. (1978): The tectonic significance of granitic liquids. Precambrian Research, Abstracts. Elsevier Scientific Publishing Company, Amsterdam.

GHAZALY, M. KH. (1984): Geological and petrochemical studies of El-Mueilha District with emphasis of the granitic rocks, Eastern Desert, Egypt. Ph. D. Assuit University.

HUSSEIN, A. A., ALI, M. M. and EL-RAMLY, M. F. (1982): A proposed new classification of the granites of Egypt. J. of Volcanology and Geothermal Research, **14,** p. 187—198.

IRVINE, T. N. and BARAGAR, W. R. A., (1971): A guide to the chemical classification of the common volcanic rocks. Canad. J. Earth. Sci., **8,** 523—548.

JAMES, R. S. and HAMILTON, D. L. (1969): Phase relations in the system $NaAlSi_3O_8$—$KAlSi_3O_8$—$CaAl_2Si_2O_8$ at 7 Kilobar water-vapour pressure. Contr. Mineral. Petrol., **21,** 11—141.

LE MAITRE, R. W. (1976): The chemical variability of some igneous rock. J. Petrol., **17,** 589—637.

NOCKOLDS, S. R. and ALLEN, R. (1953): The geochemistry of some igneous rocks series. Geochim. Cosomochin Acta, **4,** 105—142.

O'CONNOR, J. T. (1965): A classification for quartz-rich igneous rocks based on feldspar ratios. U. S: Geol. Survey Prof. Paper **525—B,** B 79— B 84

PETRO, W. L., VOGEL, T. A. and WILHAND, J. T. (1979): Major element chemistry of plutonic rocks suites from compressional and tensional plate boundaries. Chem. Geol., **26**: 217—235.

SABET, A. H. (1972): On the stratigraphy of the basement rocks Egypt. Annals of Geol. Surv., Egypt. V. **11** 97—109.

SABET, A. H., BESSONENKO, V. V., and BYKOV, B. A. (1976): The intrusive complexes of the Central Eastern Desert of Egypt. Annals of Geol. Surv., Egypt. V. **VII,** pp. 55—73

SEGERSTROM, K. and YOUNG, E. J. (1972): General geology of Hahns Peak and Farwell Mountain Quadrangles, Routt. Country, Colorado, U. S. Geol. Surv. Bull., **1349.**

SEIFERT, K. E. (1964): The genesis of plagioclase twinning in Nonewang granite. Am. Mineral, **49,** 297—320.

SILLITOE, R. H. (1979): Metallogenic consequences of late Precambrian suturing in Arabia, Egypt, Sudan and Iran. In: S. A. TAHOUN (Editor): Evolution and Mineralization of the Arabian-Nubian Shield, King Abdulaziz University, **1,** Pergamon Press, Oxford, 109—120.

SOLIMAN, M. M. (1971): Geochemical heavy mineral survey as a method of prospection for non-ferrous metal deposits in South-Eastern Desert, Egypt. M. Sc. Thesis, Cairo University, Egypt.

Soliman, M. M. (1975): Geology, geochemistry and mineralization of some younger granite masses in the Eastern Desert of Egypt. Ph. D. Thesis Mansoura University, Egypt.

STRECKEISEN, A. (1976): Classification of the common igneous rocks by means of their chemical composition. A provisional attempt. N. Jb. Miner. Monatshefte, 1—15

TUTTLE, O. F. and BOWEN, N. L. (1958): Origin of the granite in the light of experimental studies in the system $NaAlSi_3O_8$—$KAlSi_3O_8$—SiO_2—H_2O. Mem. Geol. Soc. Am., **74,** 1—153.

TUREKIAN, K. K. and WEDEPOHL, K. H. (1961): Distribution of the elements in some major units of the Earth's crust. Geol. Soc. Amer., Bull,. **72,** 175—192.

VOGEL, I. I. (1968): A Text-book of Quantitative Inorganic Analysis, 3rd Ed., Longmans, London.

WRIGHT, J. B. (1969): A simple alkalinity ratio and its application to question of non-orogenic granite genesis. Geol. Mag., **106,** 370—384.

ZAGHLOUL, Z. M., ESSAWY, M. A. and SOLIMAN, M. M. (1976): Geochemistry of some younger granite masses, South-Eastern Desert, Egypt. J. Univer. Kuwait (Sci.), **3,** 231—242.

ZAGHLOUL, Z. M., ESSAWY, M. A. and SOLIMAN, M. M. (1978): The geology of the younger granites between lat. 24° and 25° N, Eastern Desert, Egypt. J. Univer. Kuwait (Sci.), **5,** 117—128.

Manuscript received, November 5, 1984

Acta Mineralogica-Petrographica, Szeged, XXVII, 33—38, 1985

PETROCHEMICAL CHARACTER OF THE LOWER CRETACEOUS VOLCANIC ROCKS OF THE GREAT HUNGARIAN PLAIN

S. MOLNÁR*

ABSTRACT

Originally the Lower Cretaceous volcanics of the Great Plain proved to be olivine-free, pyroxene-bearing and feldspar-rich basaltic rocks. The initial magma was of tholeiitic composition. The volcanics were erupted in seawater and subsequently spilitized and auto-metasomatized. At the Lower and Upper Cretaceous boundary the rocks were uplifted and endured epigenic alteration. Their genesis is related to an early Cretaceous rift formation.

INTRODUCTION

In the region of the Great Plain considerable volcanic activity was characteristic in the Lower Cretaceous producing fairly big amounts of basaltic rocks *(Fig. 1)*. The products of this volcanic activity were revealed by hydrocarbon exploratory wells along the Kiskörös—Ebes line in a strip of 20 to 30 km width and in a depth varying between 1100 and 3100 m. Only a few publications are found on these rocks; this work has aimed to give some investigation results about these rocks.

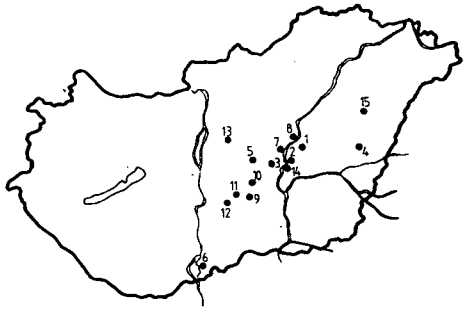

Fig. 1. The occurrence of the Lower Cretaceous volcanic rocks from hydrocarbon exploratory wells

* Department of Mineralogy, Geochemistry and Petrography Attila József University, H—6701 Szeged, Pf. 651, Hungary

ROCK TYPES OF THE LOWER CRETACEOUS VOLCANICS

Based on petrographic studies four groups of the rocks can be distinguished.

Spilitized lavas

The texture is micro-holocrystalline-porphyric, sometimes intersertal or porphyric-vitrophyric. Their main ingredients are feldspars of albite-oligoclase composition. The mafic minerals could be porphyric ingredients, their original quantity, however, might be also rather low. Recently mainly chlorite, occasionally their epidote pseudomorphs can be identified. It is conspicuous that olivine did not exist in the rocks, in their original state, as well.

Out of the auxiliary minerals leucoxene is important, apatite is subordinate.

Altered lavas

These rocks differ from the group above only in the fact that feldspars are also altered, mainly carbonatized and often transformed into clay minerals, occasionally epidotized.

Agglomerates

This types involves the pyroclastics. The clastic material does not differ from the rock types of the two foregoing groups.

Redeposited pyroclastics and volcanic alteration products

The mineral composition of these rocks could be identified only by means of X-ray and IR records. Except the low quartz content, the composition is similar to that of the groups above.

Originally, the rocks were basalts rich in feldspars and containing pyroxenes

PETROCHEMICAL CHARACTERIZATION OF THE ROCKS

Based on the results of 38 wet silicate analyses, the silica content of the rocks varies between 36 and 56%, the average being 43,5%. Out of the NIGGLI-values the average *si* amounts to −21.

The TiO_2 content is usually high, in some cases its amount exceeding 5%, as well. This is why in the thin sections so much leucoxenes are found.

The alumina content varies between 9 and 20 wt%. The occurrences of extremely high values are due to the posterior alterations.

The iron content was expressed in FeO. These values show dispersions similar to those of the alumina contents. The average proved to be 12%, this is below the value characteristic of the mafics. The low value of Fe_2O_3 of about 3% is remarkable referring to the reductive conditions of formation and alteration.

The MgO content of the rocks varies between 4 and 4.5%. This relatively low magnesium content is responsible for the fact that in this sections neither olivine nor some of its alteration product can be identified (e.g. serpentine). Magnesium is incorporated by chlorites and by the surprisingly frequent dolomite.

The average CaO content varies between 7 and 8%.

TABLE 1

Composition of rocks (diabases?) investigated

	1.	2.	3.	4.	5.	6.	7.
SiO_2	41.44	49.24	48.40	43.40	34.90	40.80	39.40
TiO_2	3.00	5.15	3.07	2.78	2.25	2.81	3.54
Al_2O_3	15.87	12.94	14.08	14.10	9.19	11.40	18.30
Fe_2O_3	2.08	3.17	2.54	2.69	5.69	5.56	3.26
FeO	13.22	7.32	8.72	9.21	1.89	3.20	2.94
MnO	0.10	0.15	0.25	0.19	0.27	0.13	0.10
MgO	7.66	7.86	4.56	8.15	2.59	5.36	1.85
Na_2O	4.56	4.00	3.62	3.21	0.76	3.04	1.86
K_2O	0.25	1.35	1.51	0.55	1.72	0.93	1.58
H_2O^+	0.53	0.63	2.74	4.78	4.32	4.47	6.23
H_2O^-	6.14	2.90	0.32	0.71	1.92	1.28	1.40
CO_2	1.23	0.89	0.73	1.18	14.10	7.67	8.73
P_2O_5	0.36	—	0.72	0.37	0.68	0.78	1.03
SO_3	0.17	—	—	—	0.26	0.33	0.21
BaO	—	—	—	—	0.26	0.33	0.21
Sum.	99.69	101.48	99.39	99.20	99.20	99.27	99.43

1. Öcsöd—2 2842—2847 m
2. Furta—4 2316—2320 m
3. Kecskemét—D—1 1401—1403 m
4. Ebes—1 1828—1830 m
5. Szandaszőlős—1 1931—1934 m
6. Szandaszőlős—1 1997—1998 m
7. Kaskantyú—1 1452—1454 m

The total amounts of the alkalies shows the characteristic values of mafics; nevertheless, the Na_2O quantity exceeds in some cases the 5%, the fact being explained by sodium metasomatism.

Some characteristic rock compositions can be seen in Table 1.

PETROGRAPHIC-PETROLOGIC QUALIFICATION OF THE ROCKS

It follows from the different instrumental (X-ray, IR, microscope) and chemical analyses that the ignous Cretaceous rocks of the Great Plain are volcanic products without exception (as to the available data, at least). The phenomenon of sodium metasomatism as well as the geological environment refer to submarine volcanism. The volcanics are mafic rocks, which originally were probably feldspar-rich basalts. This statemenet is supported by the plot of *Fig. 2.*

It is difficult to determine the character of the original magma. To decide this question one has more data available since no trace element data exist on these rocks. In spite of this some statements can be risked on the basis of main element concentrations, concerning the origin of the magma.

It has been successful to determine that the rocks were altered after their formation (seawater sodium metasomatism, autometasomatism, epigenic effects), thus only the plot could be used to the discrimination studies which do not take into account the most mobile elements. In spite of the high alkali content evidenced by the chemical analyses it can be probabilized that the original magma was of tholeiitic composition *(Figs 3* and *4).*

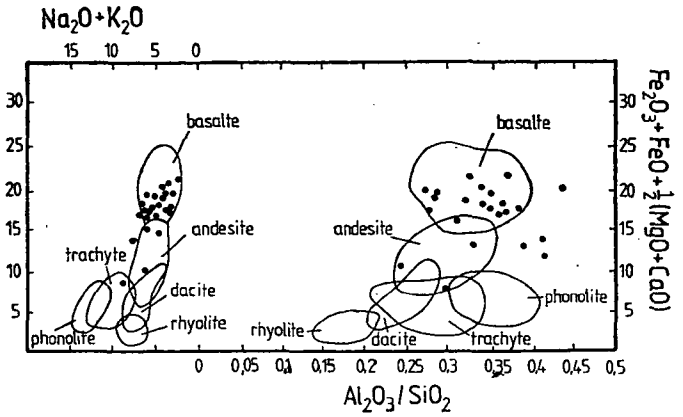

Fig. 2. The CHURCH-diagram (CHURCH, 1975)

Much more care should be applied when trying to decide the petrotectonic position, thus here only the PEARCE-plot is demonstrated *(Fig. 5)*. In this plot the points fall to the fields of continents and island arcs. In harmony with the results of thin section and analytical studies the rocks had to be generated in an enviroment where

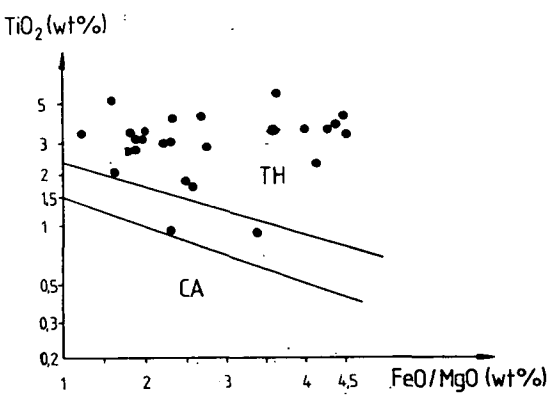

Fig. 3. The TiO_2—FeO/MgO diagram (MIYASHIRO—SHIDO, 1975)

the contamination of the originally tholeiitic magma by continental material could be possible. In the Lower Cretaceous, considerable rift formation should be most probably taken into account, this fact being supported by other geological evidences of the region (WEIN, 1978; BEÉR, 1983).

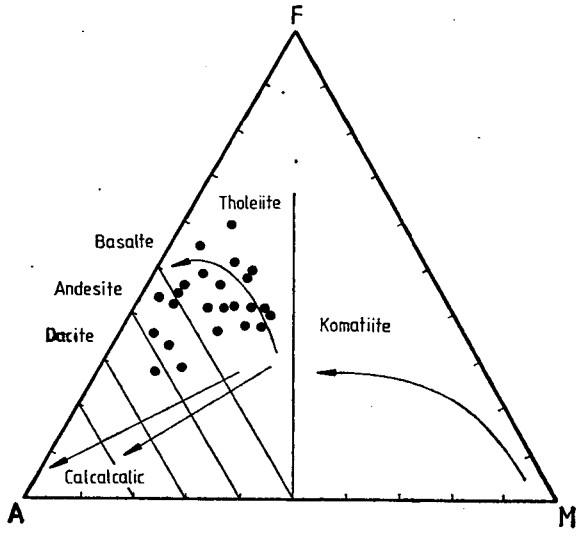

$A = Al_2O_3$ (wt%)
$F = (FeO + Fe_2O_3 + TiO_2)$ (wt%)
$M = MgO$ (wt%)

Fig. 4. The AFM diagram. (JENSEN, 1976)

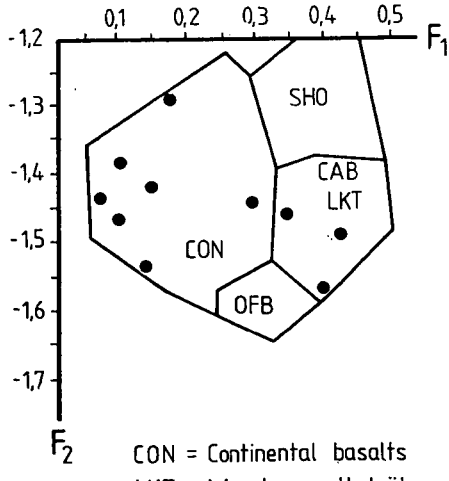

CON = Continental basalts
LKT = Island arc tholeiites
CAB = Calc-alcali basalts
SHO = Shoshonites
OFB = Ocean-floor basalts

Fig. 5. The F_1—F_2 diagram (PEARCE, 1976)

REFERENCES

AMSTUTZ, G. C. (1974): Spilites and Spilitic Rocks. Springer-Verlag Berlin, Heidelberg, New York.

BEÉR, M. A. (1983): Karpatii i Dinaridü v mezozoje. Geotektonyika **4,** 58—70.

CHURCH, B. N. (1975): Quantitative classification and chemical comparison of common volcanic rocks. Geol. Soc. Amer. Bull., **86,** 257—263.

JENSEN, L. S. (1976): A new cation plot for classifying subalcalic volcanic rocks. Ont. Div. Mines M. P.

MIYASHIRO, A., SHIDO, F. (1975): Tholeiitic and calc-alcalic series in relation to the behaviours of titanium, vanadium, chromium and nickel. Amer. J. of Sci., **274,** 265—277.

PEARCE, J. A. (1976): Statistical analysis of major element patterns in basalts. J. Petrol., **17,** 15—43.

SZEPESHÁZY, K. (1960): A Kecskemét—Szolnok közötti kréta időszaki vulkáni terület kőzetei. MÁFI Évi Jel. (1964), 525—535.

SZEPESHÁZY, K. (1977): Az Alföld mezozoós magmás képződményei. Földt. Közl. **107,** 384—397.

WEIN, GY. (1978): A Kárpát-medence kialakulásának vázlata. Ált. Földt. Szemle, **12,** 5—27.

Manuscript received, December 8, 1984

Acta Mineralogica-Petrographica, Szeged, XXVII, 39—50, 1985

XENOLITHS FROM CRETACEOUS LAMPROPHYRES OF ALCSÚTDOBOZ—2 BOREHOLE, TRANSDANUBIAN CENTRAL MOUNTAINS, HUNGARY

Cs. Szabó*

ABSTRACT

Lower Triassic sediments of Alcsútdoboz-2 borehole (30 km W of Budapest (are cross-cut by alkaline lamprophyre dykes. These dykes contain xenoliths (megacrysts, ultramafic rocks, alkaline magmatite, quartzite inclusions and carbonatic evaporites) originated from different depths. Ultramafics contain phlogopite which is characteristic for lherzolite nodules of mantle origin. The alkaline magmatite xenoliths indicate contact of the melt with an alkaline intrusion in depth, which may bear significant economic importance.

INTRODUCTION

The Scythian (Lower Triassic) sediments of Alcsútdoboz-2 borehole are cross-cut by 12 middle Cretaceous (Kubovics, 1983) magmatic dykes *(Fig. 1)*. Contacts between the magmatites and the wall-rock are sharp or brecciated, dipping 10—65°. Apparent thickness of the dykes ranges from 5 cm to 2,5 m. 30—50 vol% of dykes IV and VIII consist of xenoliths; much less are contained in dykes II, VI, III, X and XII. Size of the xenoliths ranges from 0,5 to 2,5 cm. These are of irregular shape displaying resorbed outline.

PETROLOGY OF XENOLITH-BEARING MAGMATITES

Magmatites hit by Alcsútdoboz-2 borehole — as Kubovics presented in his 1980—81 lectures at the Hungarian Geological Society — are alkaline mafic rocks. Their texture is panidiomorphic granular. Mineral composition: olivine (phenocrysts only), Ti-augite and phlogopite. The ground mass contains carbonates, partly altered glass, sanidine, analcime, opaque minerals and apatite. Occurrence of ocella is characteristic.

The rocks may be ranged as monchiquite (alkaline lamprophyre) according to Streckeisen's (1980) system, although amphiboles (kaersutite, barkevikite) are absent.

Average composition of monchiquite dykes of Alcsútdoboz-2 borehole — especially if reduced to dry rock — shows significant similarity to monchiquites of several localities on other continents. Some differences are the lower TiO_2 and higher volatile content and higher oxidation ratio.

Similar magmatites have been found in Vál-3, Budaörs-1, Zsámbék-23 and Csabdi-115 boreholes (the latter contains lamprophyre pebbles in Eocene conglomer-

* Department of Petrology and Geochemistry, L. Eötvös University, Budapest H—1088 Budapest, Múzeum krt. 4/A, Hungary

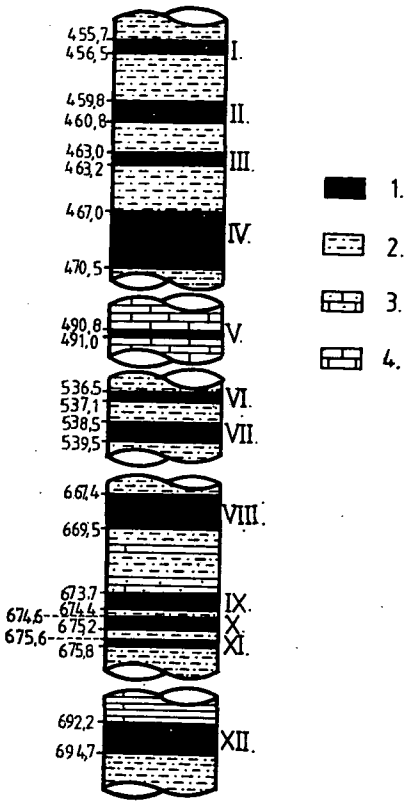

Fig. 1. Magmatites and their wall-rock in Alcsútdoboz-2 borehole (after KUBOVICS, 1981) 1 — monchiquite, 2 — aleurolite, 3 — sandstone, 4 — limestone (1 — Cretaceous, 2 to 4 — Lower Triassic)

ate only). Similar rocks have been reported by WÉBER (1962) from Nagykovácsi (Nagy-Kopasz-hegy), by HARRACH (1980) from Diósd-1 borehole and by HORVÁTH *et al.* (1983) from Sukoró-1 borehole *(Fig. 2)*.

PETROLOGY OF XENOLITHS FROM MONCHIQUITE DYKES

The following main groups were separated by microscopic examination:

A. Megacrysts (27 specimens)
B. Ultramafic xenoliths (46 specimens)
C. Alkaline rock inclusions (6 specimens)
D. Quartzite inclusions (6 specimens)
E. Calcitic evaporite (1 specimen).

A. Megacrysts

A.1. *Clinopyroxene* (21 specimens)

Most of them are black, some are dark green. Microscopically these are anhedral with tabular habit, uncoloured, having a violet tint in the thin syntaxial rim (like in clinopyroxenes of the lamprophyre). This rim often shows a saw-like form with

zonal extinction *(Fig. 3)*. Optically it is augite, having a Ti-augite rim. Some megacrysts contain rounded or elliptical calcite inclusions. Opaque minerals, euhedral phlogopite and orthopyroxene inclusions also occur. Clinopyroxenes are strongly fractured; calcitization can be observed in some places.

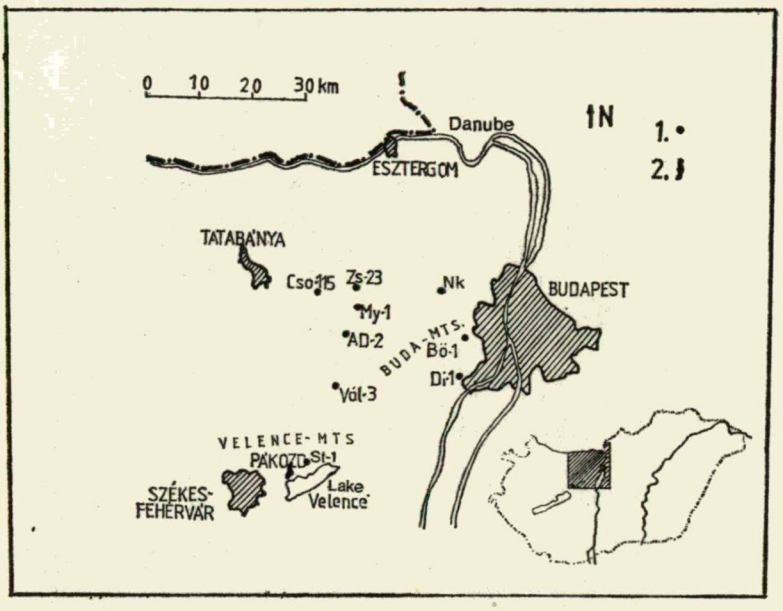

Fig. 2. Lamprophyre dyke localities in NE-Transdanubia. 1 — borehole; 2 — outcrop

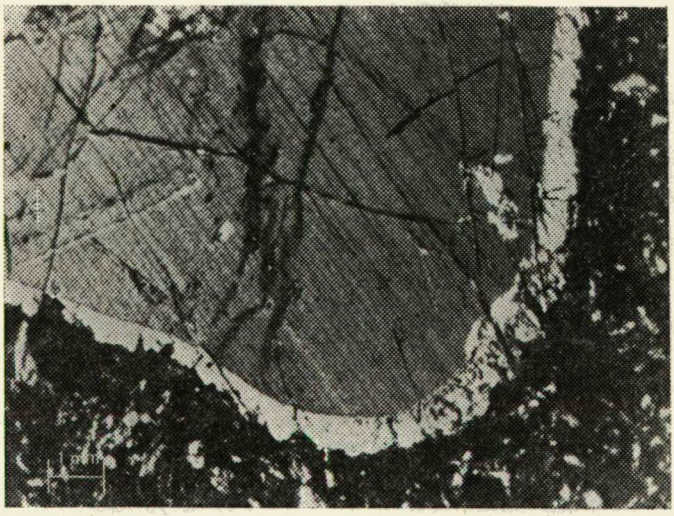

Fig. 3. Zoned clinopyroxene megacryst. +N

A.2. *Olivine* (2 specimens)

Dark green, microscopically uncoloured, anhedral, tabular forms with slightly undulatory extinction. Carbonatic alteration can be observed along rectangular cleavage planes and along the margins. Optical character is varied, so Fa-content fluctuates around 12,5%.

A.3. *Plagioclase* (2 specimens)

Rounded section with resorbed rims. Contains close twin lamellae, vanishing in the thin syntaxial rim *(Fig. 4)*. Optically the inner part is albite, the rim is potassium feldspar. The grains are fresh, cut by fissures with calcite filling.

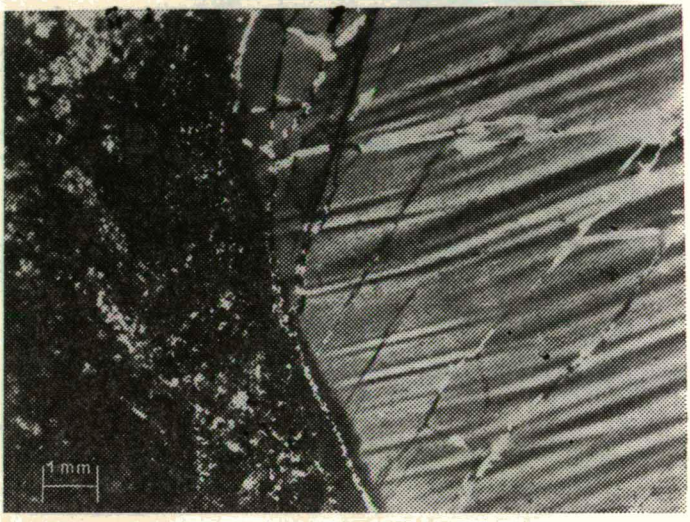

Fig. 4. Zoned plagioclase megacryst with twin lamellae. +N

A.4. *Opaque minerals* (1 specimen)

Subhedral, equate grains, probably of Ti-magnetite composition. It contains some apatite inclusions.

A.5. *Apatite* (1 specimen).

Heavily fractured, 3 mm long grain.

A.6. *Quartz* (1 specimen)

3 mm grain with resorbed rim.

B. Ultramafic xenoliths

B.1. *Classification of ultramafic xenoliths*

STRECKEISEN's classification (1974), according to modal composition, was followed. As often phlogopite occurs together with olivine, clinopyroxene and spinel, STRECKEISEN's olivine (Ol)—clinopyroxene (Cpx)—orthopyroxene (Opx) plot has

been completed by an olivine (Ol)—clinopyroxene (Cpx)—phlogopite (Phl) plot to solve classification and nomenclature problems *(Fig. 5)*. Bulk modal composition and nomenclature of xenoliths is shown in Table 1. This is partly based on STRECKEISEN's nomenclature for peridotites and pyroxenites; partly it has been deduced from his amphibole—pyroxene—olivine plot, having substituted amphibole by phlogopite and pyroxene by clinopyroxene. This modification was necessary as we couldn't find an existing special nomenclature for this relatively rare group of rocks.

Fig. 5. and Table 1 present basic characters of ultramafic xenoliths of the lamprophyre:

— clinopyroxene and olivine are dominant components in the xenoliths;
— mica can be found — even monomineralically — in all groups except clinopyroxenite;
— common occurrence of large quantities of orthopyroxene and phlogopite is not characteristic.

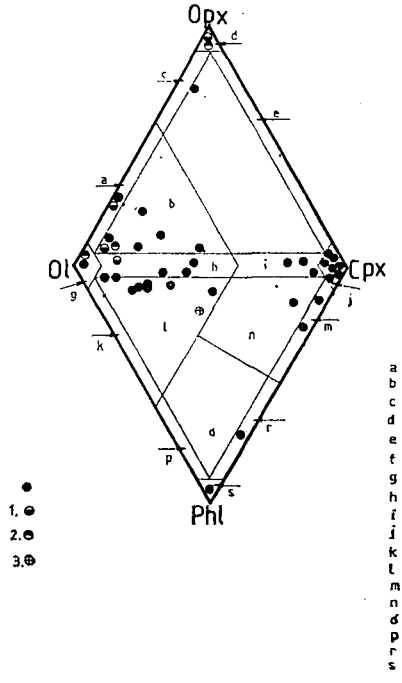

Fig. 5. Ol — Cpx — Opx and Ol — Cpx — Phl double plot of ultramafic xenoliths in dykes of Alcsútdoboz-2 borehole (Ol — Cpx — Opx plot of STRECKEISEN (1974), completed by an Ol — Cpx — Phl plot)

1 — Phl < 5 vol%
2 — Phl > 5 vol%
3 — Opx < 5 vol%

a — harzburgite, *b* — lherzolite, *c* — olivine-orthopyroxenite, *d* — orthopyroxenite, *e* — websterite, *f* — olivine-websterite, *g* — dunite, *h* — wehrlite, *i* — olivine-clinopyroxenite, *j* — clinopyroxenite, *k* — phlogopite-peridotite, *l* — pyroxene-phlogopite-peridotite, *m* — phlogopite-pyroxenite, *n* — olivine-phlogopite-clinopyroxenite, *o* — olivine-clinopyroxene-phlogopitite, *p* — olivine-phlogopitite, *r* — clinopyroxene-phlogopitite, *s* — phlogopitite

TABLE 1

Modal composition and nomenclature of ultramafic xenoliths in dykes of Alcsútdoboz-2 borehole after STRECKEISEN *(1974), slightly modified*

Minerals vol%	1	2	3	4	5	6	7	8	9	10	11	12	13	14	15
Olivine	55.3—84.3	77.7	96.5—98.0	—	—	71.5—72.6	15.8	45.5—80.6	12.5—20.4	40.8—84.9	10.3	0.0—3.1	—	—	0.0—4.0
Clinopyroxene	5.0—38.4	9.7	—	5.5	1.3	—	6.2	13.5—54.5	79.3—88.0	9.9—45.6	74.7	72.9—83.2	23.4	—	95.0—100
Orthopyroxene	4.8—24.0	6.0	0.0—1.3	91.0	67.5	23.6—23.8	75.1	0.0—3.8	—	0.0—4.0	—	—	—	—	—
Phlogopite	0.0—0.1	6.0	0.0—1.6	3.2	28.3	0.0—4.3	1.0	0.0—3.8	0.0—1.0	4.2—18.8	14.5	13.3—26.9	71.6	100	0.0—5.0
Spinel	0.2—1.2	0.6	0.6—2.0	0.3	2.9	0.4—3.8	1.9	0.0—1.2	0.3—0.5	0.0—0.7	0.5	0.2—0.4	—	—	0.0—1.0
Apatite	—	—	—	—	—	—	—	—	—	0.0—1.0	—	—	—	—	0.0—1.0

1. Lherzolite (6 specimens)
2. Phlogopite-lherzolite (1 specimen)
3. Dunite (2 specimens)
4. Orthopyroxenite (1 specimen)
5. Phlogopite-orthopyroxenite (1 specimen)
6. Harzburgite (2 specimens)
7. Olivine-websterite (1 specimen)
8. Wehrlite (4 specimens)
9. Olivine-clinopyroxenite (3 specimens)
10. Clinopyroxene-phlogopite-peridotite (3 specimens)
11. Olivine-phlogopite-clinopyroxenite (9 specimens)
12. Phlogopite-clinopyroxenite (2 specimens)
13. Clinopyroxene-phlogopitite (1 specimen)
14. Phlogopitite (1 specimen)
15. Clinopyroxenite (12 specimens)

B.2. *Components of ultramafic xenoliths in the microscope*

Olivine. Large, subhedral, tabular and small, polygonal forms can be differentiated. Both types are colourless, having a positive optical character. Some of the tabular variety show undulatory extinction and mechanical twinning. This is characteristic for some lherzolite, wehrlite and clinopyroxene-phlogopite-peridotites only. Part of the olivine grains has been altered for carbonate, iddingsite and serpentine.

Clinopyroxene. Three types can be separated in the microscope.

a) Anhedral, tabular agglomeration. Colourless or may be light green, with undulatory extinction. Besides (110) cleavage close, transversal jointing is characteristic. Inclusions are rare; carbonatization may occur along cleavage or joint planes. Occurs in a part of lherzolite, wehrlite and olivine-websterite nodules.

b) Subhedral-anhedral, tabular variety. Large, colourless crystals bearing a slight violet rim contacting the lamprophyre. Shows undulating extinction and zonality on the margins. Its composition can be taken as the same as that of the clinopyroxene megacrysts, according to optical properties. It contains phlogopite and equant opaque mineral inclusions. Heavily fractured, rarely carbonatized or chloritized. It occurs in all clinopyroxene-containing ultramafic rock groups, like olivine-websterite, orthopyroxenite and lherzolite (in which the *a* variety is missing) as epitaxial growth on orthopyroxene.

c) Anhedral, tabular variety. It is green, pleochroic, sometimes the core of the grain only as larger or smaller spots. The rim contacting the lamprophyre shows violet tint. Extinction is mosaic-like and zonal corresponding with pleochroism. The green core can be aegirine-augite, the colourless field is augite and the violet rim Ti-augite according to the optical properties. Inclusions are mostly small grains indeterminable by the microscope, but some clinopyroxenes may contain apatite and equant opaque minerals, too. This type is characteristic for olivine-barren clinopyroxenites only.

Orthopyroxene. Two varieties can be separated: a larger, subhedral, tabular one and a smaller, polygonal one. Both show positive optical character and are of enstatitic composition. The tabular grains are brown due to frequent opaque mineral inclusions. Some sections show undulatory or mosaic extinction, sometimes folding or fracturing can be observed, too *(Fig. 6)*. Inclusions are opaque minerals and phlogopite. Part of them has been totally altered to carbonate and chlorite. It is a major component of lherzolite, olivine-websterite, orthopyroxenite, phlogopite-lherzolite, phlogopite-orthopyroxenite and dunite nodules. The polygonal variety is colourless, shows normal extinction, contains no inclusions and fresh. It occurs mostly in the surroundings of tabular orthopyroxenes *(Fig. 6)*. It is present in olivine-websterite and in part of the lherzolite nodules.

Mica. Anhedral, almost equant or subhedral, tabular forms bearing resorbed rims. Pleochroism: colourless or light yellow — yellowish brown. It is surrounded by a wide, more intensively pleochroic margin near lamprophyre contacts *(Fig. 7)*. Shows undulatory extinction. It can be taken as phlogopite due to optical angle of a few degrees and weak pleochroism. Elongated carbonate grains and haematite scales can be seen along cleavage planes. Micas are fractured and folded in monomineralic phlogopitite *(Fig. 8)*.

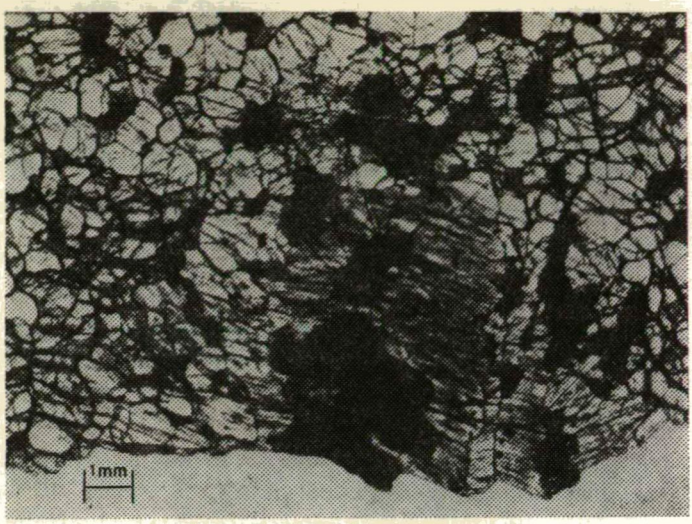

Fig. 6. Deformed, tabular and polygonal orthopyroxene (light) with clinopyroxene (dark) in lherzolite xenolith. // N

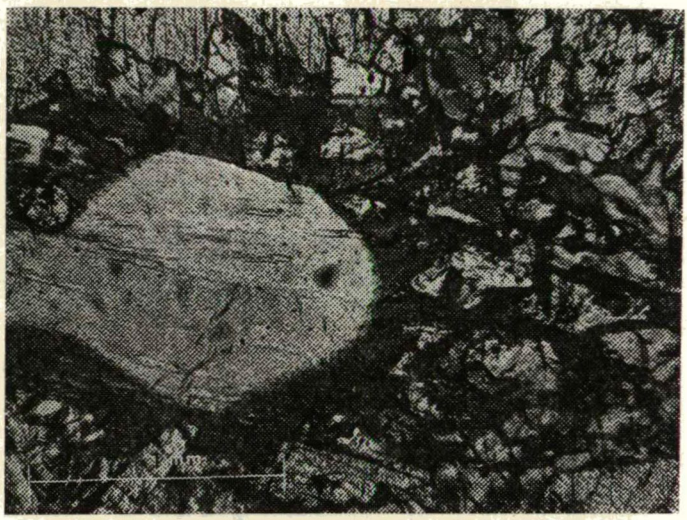

Fig. 7. Zoned phlogopite in clinopyroxene-phlogopite-peridotite. // N

Spinels occur as nearly equant grains among other components or as inclusions in pyroxenes. A variety forms agglomerations and occurs near clinopyroxenes or micas. The latter one is frequently translucent with reddish-brown tint. It is characteristic for lherzolite, phlogopite-lherzolite, phlogopite-orthopyroxenite nodules.

C. Alkaline magmatite inclusions

C.1. *Classification of alkaline magmatites* follows STRECKEISEN's (1974) system, based on modal composition (Table 2).

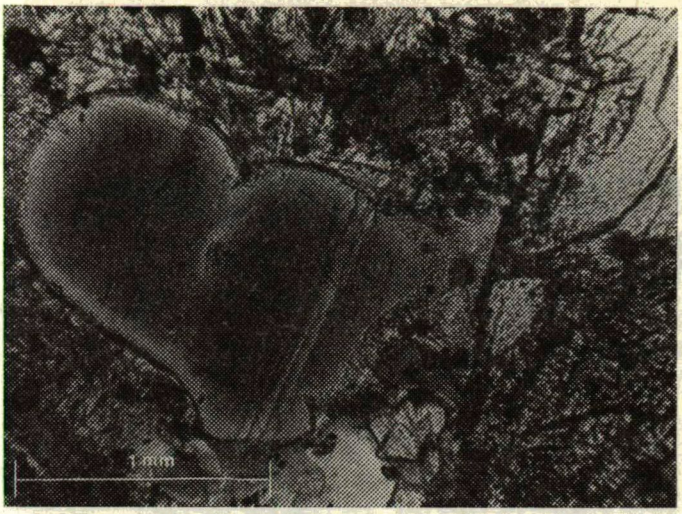

Fig. 8. Deformed, tabular phlogopite in phlogopitite xenolith. // N

TABLE 2

Modal composition of alkaline magmatite inclusions in dykes of Alcsútdoboz-2 borehole

Number of specimens	1	1	4
Rock type / Mineral vol%	Melaalkali-syenite	Leuko-alkalisyenite	Alkaligranite
Potassium feldspar	11.7	54.3	21.6—72.3
Plagioclase	—	27.6	0.0—13.0
Clinopyroxene	73.6	18.1	0.9—5.6
Quartz	—	—	26.9—59.8
Apatite	13.4	—	—
Mica	1.0	—	—
Spinel	0.3	—	—

C.2. *Alkaline magmatite components in the microscope*

Potassium feldspar. Anhedral, bears resorbed rims. Cleavage in two directions can be well observed. Sometimes undulatory extinction, negative optical character; optical angle: about 30°. Optically it can be taken as sanidine. Grains are frequently surrounded by a zone of darker interference colour which may be isotropic as well.

Plagioclase. Anhedral, resorbed grains. Birefringence larger than in potassium feldspar. Close twin lamellae, positive optical character; optical angle: about 90°. Optically it can be taken as albite. The plagioclases are usually surrounded by irregular zones of darker interference colour. Optically this may be of sanidine composition.

Clinopyroxene. Subhedral, tabular or square-build, green grains showing weak pleochroism. Negative sign of elongation, positive optical character, undulatory

extinction. Optically it can be taken as aegirine-augite. Inclusions are apatite *(Fig. 9)* and opaque minerals.

Quartz. Anhedral, resorbed, equant, colourless grains. Undulatory, sometimes mosaic like extinction. Often forms inclusions in potassium feldspar. Heavily fractured, devoid of inclusions.

Apatite. Subhedral-euhedral, square-build, columnar, fractured grains.

Mica. Anhedral, resorbed, tabular grains. Pleochroism: yellowish brown — dark greenish brown, fading towards the margins *(Fig. 9)*. It can be found in places where the lamprophyre melt penetrated xenoliths, consequently these are considered as foreign bodies.

Fig. 9. Zoned mica and apatite in clinopyroxene in alkalisyenite xenolith. // N

D. Quartzite xenolith in the microscope

Monomineralic xenolith. Quartz grains mostly form a mosaic-like order and are of similar size.

E. Carbonate evaporite in the microscope

3 mm long, ellipsoidal xenolith, formed by tabular gypsum and anhydrite, with calcite between and around them.

SIGNIFICANCE OF XENOLITHS IN THE DYKES
(Discussion)

The greatest significance is attributed to ultramafic xenoliths, alkaline magmatites and megacrysts among all inclusions.

The ultramafic xenoliths form two textural groups (besides mineral composition):

— nodules displaying deformation and recrystallization traces ("metamorphic" nodules)
— equigranular nodules displaying magmatic textures.

Sixteen ultramafic nodules display metamorphic characters based on microscopic investigations. These are positioned in the lherzolite, phlogopite-lherzolite, harzburgite, dunite, olivine-websterite, phlogopite-orthopyroxenite, orthopyroxenite, wehrlite and clinopyroxene-phlogopite-peridotite fields of *Fig. 3.* These nodules are characterized by mechanical twinning of olivine and orthopyroxene. According to MERCIER and NICOLAS (1975) this is a significant feature of nodules of upper mantle origin. These xenoliths display porphyroclastic and equigranoblastic texture (classification of HARTE, 1977). This means, that these xenoliths have suffered significant deformations and have been recrystallized. They have a "complex metamorphic record" (EMBEY-ISZTIN, 1977). Consequently, these xenoliths have been originated from the upper mantle, together with the enclosing magmatic melt.

Lherzolite nodules of similar texture have been found in Burgenland (RICHTER, 1971), in the Balaton Highlands (EMBEY-ISZTIN, 1977) and in the Nógrád—Gemer region (HOVORKA, 1978 and MOLNÁR, 1980) in Pliocene alkaline basalts of the Carpathian region. These authors have proven the upper mantle origin of the nodules by crystallization pressure and temperature values calculated from geochemical data.

However, ultramafic xenoliths from the Alcsútdoboz-2 lamprophyres show significant differences from those in Pliocene basalts in the Carpathian region, due to their phlogopite content. These xenoliths — considered as issued from the upper mantle on texture investigations — contain micas "built in" among other grains, as a primary component itself, also shown by coarse grain size (larger than 1 mm) and heavy deformation (disruption, folds, fractures) *(Fig. 8).* This means that phlogopite is a stable phase under upper mantle conditions, proven experimentally by KUSHIRO and AOKI (see RICHTER, 1971).

Few reports are known on mica-containing ultramafic xenoliths from alkaline basalt and basanite (e.g. RICHTER, 1971; SKEWES and STERN, 1979) but there is no one — as we know now — reporting them from lamprophyres. Phlogopite-bearing xenoliths of upper mantle origin are usually connected to kimberlites and carbonatites (DAWSON and Powell, 1969; DELANEY *et al.*, 1980; DAWSON, 1980; ARIMA and EDGAR, 1981).

Those ultramafic xenoliths in Alcsútdoboz-2 borehole, which show non-metamorphic, subhedral granular, rarely poikilitic texture can be taken as endogenous inclusions, together with clinopyroxene megacrysts separated from magma at great depths.

ROCK (1975) claims that ultramafic xenoliths rarely occurs in lamprophyres, since this magma does not ascend from great depths as primary melt but develops under low pressure, absorbing volatiles. High-pressure xenoliths of mantle origin become unstable under these conditions. Alkaline syenite—alkaline granite xenoliths, plagioclase, apatite and Ti-magnetite megacrysts and clinopyroxenite of aegirine-augitic composition found in Alcsútdoboz-2 borehole indicate that the lamprophyre melt "sampled" an alkaline magmatic body in depth.

Occurrence of lamprophyre and alkaline magmatic xenoliths may have economic value besides scientific importance, as similar rock sequences contain Th, REE, Nb, Ta and P deposits. The Nb, Sc, Th and U anomalies recorded by KUBOVICS (1960),

WÉBER (1962) and HORVÁTH *et al.* (1983) in Velence and Buda Mts. suggest that re-evaluation of existing data and further exploration of this region is definitely necessary.

ACKNOWLEDGEMENTS

I wish to express my sincere thanks to Professor IMRE KUBOVICS for his suggestions and advices during the investigations of this complicated and variable rock association and for the permission to present this — then unfinished — material at the Conference of Young Scientists of the Hungarian Geological Society in 1982.

REFERENCES

ARIMA, M., EDGAR, A. D. (1981): Substitution mechanisms and solubility of titanium in phlogopites from rocks of probable mantle origin. Contrib. Min. Petr., **77,** 288—295.

DAWSON, J. B. (1980): Kimberlites and their Xenoliths. Springer-Verlag, Berlin—Heidelberg—New York.

DAWSON, J. I., POWELL, D. G. (1969): Mica in the upper mantle. Contrib. Min. Petr., **22,** 233—237.

DELANEY, J. S., SMITH, J. V., CARSWELL, D. A., DAWSON, J. B. (1980): Chemistry of micas from. kimberlites and xenoliths. II. Primary- and secondary-textured micas from peridotite xenoliths. Geochim. Cosmochim. Acta., **44,** 857—872.

EMBEY-ISZTIN, A. (1977): Az alkálibazaltok peridotitzárványainak ásvány-kőzettana, eredete és összefüggése hazánk és a Massif Central nagyszerkezetével. (Mineralogy, petrology and origin of peridotite nodules in alkaline basalts; implications for the tectonics of Hungary and the Massif Central in France) (In Hungarian), Ph. D. Thesis, Hungarian Academy of Sciences, Budapest.

HARRACH, O. (1980): Dinnyés-2, Diósd-1 és Vál-3 sz. fúrások kőzettani-geokémiai vizsgálata. (Petrology and geochemistry of magmatic rocks in Dinnyés-2, Diósd-1 and Vál-3 boreholes) (In Hungarian), M. Sc. Thesis, Eötvös University, Budapest.

HARTE, B. (1977): Rock nomenclature with particular selection to deformation and recrystallization textures in olivine-bearing xenoliths. J. Geol., **85,** 279—288.

HORVÁTH, I., DARIDA-TICHY, M., ÓDOR, L. (1983): Magnesitiferous dolomitic carbonatite (beforsite) dyke rock from the Velence Mountains. Annual Report Hung. Geol. Inst. of **1981,** pp. 369—388 (in Hungarian with English abstract)

HOVORKA, D. (1978): Uzavreniny spinelových peridotitov v bazanite pri Maskovej — rezidum vrchého plasta. Mineralia Slovaca **10,** 97—112.

KUBOVICS, I. (1960): Trace element analysis of the post-magmatic formations of the Velence Mountains I. Scandium-niobium and associated traces. Földtani Közlöny, **90,** 273—292 (In Hungarian with English abstract)

KUBOVICS, I. (1980): Petrological investigation of magmatite from Alcsútdoboz-2 borehole. Manuscript. Department of Petrology and Geochemistry, Eötvös University, Budapest.

KUBOVICS, I. (1983): Petrological, geochemical and volcanological investigation of Mesozoic ultramafic, mafic and intermediate rocks from Hungary. (In Hungarian). Manuscript. Department of Petrology and Geochemistry, Eötvös University, Budapest

MOLNÁR, E. (1980): A medvesi bazalt ultrabázisos kőzet- és megakristály-zárványainak kőzettani—geokémiai vizsgálata. (Petrology and geochemistry of ultramafic nodules and megacrysts in the Pliocene basalt of Medves, N-Hungary) (In Hungarian), Manuscript, Department of Petrology and Geochemistry, Eötvös University, Budapest

RICHTER, W. (1971): Ariegite, Spinel-Peridotite und Phlogopit-Klinopiroxenite aus dem Tuff von Tobaj im südlichen Burgenland. Tscherm. Min. Petr. Mitt., **16,** 227—251.

ROCK, N. M. S. (1977): The nature and origin of lamprophyres: some definitions, distinctions, and derivations. Earth-Science Rewiews, **13,** 123—169.

SKEWES, M. A., STERN, C. R. (1979): Petrology and geochemistry of alkali basalts and ultramafic inclusions from the Palei-Aike volcanic field in Southern Chile and the origin of the Patagonian plateau lavas, J. Volc. Geotherm. Res., **6,** 3—25.

STRECKEISEN, A. (1974): Classification and nomenclature of plutonic rocks. Geol. Rundschau, **63,** 773—786.

STRECKEISEN, A. (1980): Classification and nomenclature of volcanic rocks, lamprophyres, carbonatites, and melilitic rocks: recommendations and suggestions of the IUGS Subcommission on the Systematics of Igneous Rocks. Geology **7,** 331—335.

WÉBER, B. (1962): Indications of thorium and rare earths in the Buda Mountains, Hungary. Földtani Közlöny **92,** 455—457 (In Hungarian with English abstract).

Manuscript received, February 11, 1985

Acta Mineralogica-Petrographica, Szeged, XXVII, 51—57, 1985

Rb-Sr DATING OF BASEMENT ROCKS FROM THE SOUTHERN FORELAND OF THE MECSEK MOUNTAINS, SOUTHEASTERN TRANSDANUBIA, HUNGARY

A. KOVÁCH[1], E. SVINGOR[1] and T. SZEDERKÉNYI[2]

ABSTRACT

Rb-Sr total rock and biotite age determinations have been carried out on samples from the borehole Baksa—2 disclosing sillimanite-grade metamorphic rocks of the Görcsöny Ridge (so called "Baksa Formation") at the northern margine of the Drava Basin in southeast Transdanubia.

The 331 ± 13 Ma total rock isochron age is tentatively interpreted as the time of D_1 deformation immediately coupled to the dominant staurolite — kyanite — sillimanite grades (Barrowian) first phase of metamorphism. The overprinting second progressive metamorphic episod is characterized by high T medium P effects (D_2 deformation) producing among others enstatite minerals in the ultramafics of Gyód as well as microgranitic-aplitic veins and segregations in the pelitic schists. Its age brackets of 331 and 315 Ma, followed by regional emergence and low-temperature retrograde effects probably due to prolongated uplift under low velocity conditions.

INTRODUCTION

The borehole Baksa-2 was drilled within the frames of the Reference Section Project initiated by the Hungarian Geological Bureau. The drilling was aimed at to explore the crystalline basement of the Görcsöny Ridge, located between the Western Mecsek resp. Villány Mountains. It exposed the crystalline basement formation in a total thickness of over 1100 m, with near 100% core recovery.

According to previous investigations (SZEDERKÉNYI, 1974, 1976) the crystalline of the Görcsöny Ridge overlain by a thin cover of Pannonian and Pleistocene age forms a steep, locally near-vertical turned mass, in common structural position with the basement of the Drava Basin as well as with the Papuk-Psunj-Krndija Mountains in Yugoslavia. The NW-SE striking metamorphites at the northern border of the Drava Basin together with those of the Görcsöny Ridge represent a continuous Barrowian facies series from the chlorite to the sillimanite zone with signs of anatexis and granitization.

METAMORPHIC ROCKS OF THE DRILLING BAKSA-2 AND THEIR EVOLUTION

According to the studies of SZEDERKÉNYI (1979, 1981) the drilling Baksa-2, drilled in the sillimanite zone of the Görcsöny Ridge metamorphic mass, exposed a rather heterogeneous metamorphic formation, which could be divided into the following lithostratigraphic units:

[1] Institute of Nuclear Researches, Hungarian Academy of Sciences, H-4026 Debrecen, Bem tér 18/C, Hungary

[2] Department of Mineralogy, Geochemistry and Petrography, Attila József University, H-6701 Szeged, Pf. 651, Hungary

— "upper marble" member
— chloritic two-mica gneiss member
— "lower marble" member
— garnetiferous two-mica gneiss member
— garnetiferous two-mica schist member

According to this lithostratigraphic sequence, the protolith suite consisted of rhytmically intermitting layers of mainly greywacke and pelitic type sediments, with interbedded thin layers of limestone, calcareous marl, dolomite and dolomitic marl in the upper and middle part of the exposed rock-column. The section is quite frequently interrupted by thin basic tuff layers, infrequently by small lava-beds.

The protolith rock mass of predominantly psammitic-pelitic character and of indeterminate age was subject to polyphase deformation under regional metamorphic conditions, resulting in a characteristically polymetamorphic assemblages. Besides the effect of regional metamorphism, contact phenomena have been evoked at some levels by the intrusion of small aplitic-microgranitic veins. Regional metamorphism itself has occurred in two progressive and two regressive phases.

The dominant metamorphic phase coupled to the D_1 deformation resulted in the development of crystalline schists at a temperature of 630—650 °C and 5—7 kbar pressure corresponding to the amphibolite facies and characterized by sillimanite as an index mineral. This compressional phase was followed by decompression and textural loosening, with strong lateral secretion of quartz.

The second phase of regional metamorphism having occurred at 400—410 °C and 3—4 kbar appears as an overprint, producing mineral associations corresponding to the greenschist facies (quartz-albite-epidote-biotite subfacies). The weak retrogressive phase following D_2 deformation was interrupted by the late-orogenic aplitic-microgranitic magmatism of Herzynian age, which in small zones — especially in the carbonate-rich members — led to the development of contact phenomena corresponding to the pyroxene-hornfels resp. hornblende-hornfels facies.

At some levels of the rock-column cataclastic zones younger than the aplitic-microgranitic magmatism could be observed, with a conspicuous polymetallic sulphide mineralization with a mineral association representing the highest tempered pneumatolitic resp. catathermal phase. Its development is undoubtedly connected to the rhyolitic volcanism of Early Permian age known both in the Western Mecsek resp. Villány Mountains (FAZEKAS *et al.*, 1981).

The relative succession of the individual metamorphic resp. deformational phases could be determined unambiguously, but their accurate dating — except that of the subordinate mineralization phase — raised several questions which could not be solved by geological means only. This was the main impetus for the present investigations, primarily aimed at to obtain chronological information on the deformation history of the rock mass in question.

EXPERIMENTAL METHODS AND RESULTS

The samples used in this study have been chosen so as to represent possibly all the main rock types of the metamorphic base formation, as well as to cover the whole depth range exposed by the drilling Baksa-2. The sample from the depth of 64.0 m belongs to the "upper marble" member; those from 268.0, 366.0 and 752.9 m to the chloritic two-mica member; from 856.7 m to the "lower marble" member; those from

the depth of 941.0 m and from below all belong to the garnetiferous two-mica schist member of the formation. The sample from 64.0 m is of aplitic character.

Age determinations have been carried out on total rock samples and biotites in order to obtain information both on the timing of the main phase of regional metamorphism and the uplift and cooling history of the rock mass. Biotites have been separated by conventional methods using an isodynamic magnetic separator and heavy liquids.

In the course of chemical preparation the samples were dissolved in a mixture of hydrofluoric and perchloric acids, dried and dissolved again in a small amount of 3N hydrochloric acid. Enriched ^{84}Sr and ^{87}Rb spikes used in the mass spectrometric determination of Sr resp., Rb concentration values have been added to the samples prior to dissolution.

Strontium samples for mass spectrometry have been prepared on a Dowex 50W×12, 200—400 mesh cation exchange column, and were placed into the ion source of the mass spectrometer in a nitrate form, later converted to oxide. All mass spectrometric measurements have been carried out on a modified MI 1309 type mass spectrometer equipped with a triple filament ion source. Mass discrimination effects have been corrected by normalizing to the $^{86}Sr/^{88}Sr=0.1194$ reference ratio.

To check the accuracy of the measurements, repeated measurements have been carried out on the Eimer and Amend standard strontium carbonate sample ($^{87}Sr/^{86}Sr=0.7080$). During the time of measurements reported here the average of standard measurements was $^{87}Sr/^{86}Sr=0.7079\pm0.0002$, thus no other correction was found to be necessary.

Experimental results obtained on both total rock and biotite samples are summarized in Table 1, together with the calculated model age values. All age data have been calculated using the ^{87}Rb decay constant $\lambda=1.42\cdot10^{-11}a^{-1}$. Measurement errors are in general RMS errors, whereas error estimates of individual and isochron ages correspond to a 95% probability confidence interval.

Data obtained on total rock samples are shown in *Fig. 1* in a conventional sochron diagram. Irrespective of their petrographical character, the data points can

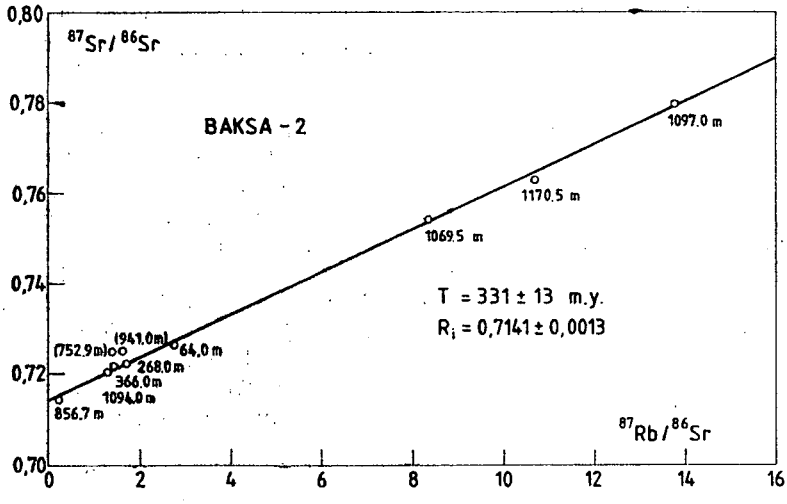

Fig. 1. Analytical data obtained on total rock samples from the borehole Baksa-2, shown in an isochron diagram

be interpolated with a single straight line, corresponding to an isochron age of 331 ± 13 Ma and an initial Sr isotopic ratio $R_i = 0.7141 \pm 0.0013$ (the errors include the analytical errors of the data points and correspond to a 95% confidence interval). The data for the samples taken from the depths of 752.9 and 941.0 meters have been omitted in calculating the isochron age, because theerespective points plot off the isochron well outside analytical errors as ascertained by several repeated measurements.

TABLE 1

Compilation of analytical data obtained on samples from drilling Baksa-2

Depth (m)	87_{Rb} µg/g	Rb µg/g	86_{Sr} µg/g	Sr µg/g	$87_{Rb}/86_{Sr}$ (atomic ratio)	$87_{Sr}/86_{Sr}$ (atomic ratio)	Age (Ma)
Total rock samples							
64.0 m	39.95	143.6	14.17	146.8	2.787	0.7264 ± 0.0012	
268.0 m	37.57	133.5	21.82	225.9	1.702	0.7223 ± 0.0007	
366.0 m	32.64	117.3	22.28	230.8	1.448	0.7218 ± 0.0008	331 ± 13
752.9 m	34.26	123.1	24.13	249.9	1.403	0.7250 ± 0.0011	(iso-
856.7 m	9.09	32.7	40.11	415.1	0.224	0.7144 ± 0.0007	chron
941.0 m	39.24	141.0	23.82	246.7	1.628	0.7252 ± 0.0011	age)
1069.5 m	59.32	213.1	7.01	72.9	8.360	0.7543 ± 0.0015	
1094.0 m	29.74	106.8	22.60	234.0	1.301	0.7210 ± 0.0009	
1097.0 m	83.74	300.9	6.01	62.6	13.766	0.7797 ± 0.0021	
1170.5 m	62.69	225.2	5.81	60.3	10.675	0.7629 ± 0.0012	
Biotites							
268.0 m	101.50	364.7	6.665	69.33	15.054	0.7676 ± 0.0012	239 ± 9
366.0 m	96.22	345.7	3.276	34.34	29.034	0.8467 ± 0.0009	318 ± 4
752.9 m	86.64	311.3	3.167	33.17	27.043	0.8386 ± 0.0016	311 ± 5
941.0 m	82.85	297.8	4.623	48.24	17.715	0.8001 ± 0.0020	327 ± 10
1069.5 m	80.11	287.8	4.461	46.53	17.751	0.7961 ± 0.0025	313 ± 22
1094.0 m	89.42	321.3	2.154	22.70	41.036	0.9004 ± 0.0012	317 ± 9
1097.0 m	92.93	333.9	4.239	44.30	21.671	0.8148 ± 0.0015	312 ± 23
1170.5 m	108.53	390.0	2.326	24.55	46.123	0.9198 ± 0.0015	311 ± 4
					Weighted average of biotite model ages:		315 ± 4

Biotite individual model ages calculated with reference to the corresponding total rock samples are concordant with a weighted average of 315 ± 3 Ma except the biotite sample from depth of 268.0 m, yielding a model age of 239 ± 9 Ma, evidently attributable to the local effect of a Permian disturbance. No systematic dependence of the biotite ages on sampling depth could be ascertained.

A controll of Rb/Sr age determinations was carried out by the laboratory of Padova University on a sample of Baksa-2 metamorphics (from 1095,50 m). The age calculated from the next chemical data is 328 ± 5 m.y. (whole rock — biotite isochron) which is the age of the biotite. Biotite: Rb=364 ppm, Sr=6,8 ppm. $^{87}Rb/^{86}Sr = 168.15$, $^{87}Sr/^{86}Sr = 1.005$. Whole rcok: Rb=139 ppm, Sr=221 ppm, $^{87}Rb/^{86}Sr = 1.82$, $^{87}Sr/^{86}Sr = 0.7248$. It looks like a fairly similar radioactive age to that of Table 1.

DISCUSSION

The 331±13 Ma total rock isochron age, as well as the 315±3 Ma average biotite age are directly comparable with the results of K/Ar measurements carried out by BALOGH *et al.* (1983) on white micas and biotites from the rock column of the Baksa-2 borehole. The average K/Ar muscovite age of 306±6 Ma and the 288±10 Ma average K/Ar biotite age when compared with the data presented here point equivocally to a prolonged Herzynian thermal history of the crystalline in question, the different ages obtained by different methods being in the proper order according to their different blocking temperatures. A detailed analysis of the thermal and uplift history of the Görcsöny Ridge will follow elsewhere, but without going into details one can safely conclude that the time span indicated by the radiochronological data gives an appropriate time frame for a polyphase metamorphic-deformational development during the Herzynian. Previous assumptions (*cf.* LELKES—FELVÁRI *et al.*, 1981) declared the metamorphic development to be partly pre-Herzynian, a possibility still maintained by ÁRKAI (1984) based on petrological investigations on basement rocks from the Drava Basin with results pointing to an analoguous sequence of metamorphic events in the chlorite zone of a facies series belonging to another tectonic unit.

The 331±13 Ma total rock isochron age, however, makes it highly probable that even the oldest metamorphic-deformational phase detectable by petrographical petrological means occurred during the Herzynian. The blocking temperature of the total rock Rb-Sr system on a regional scale is sufficiently high even in the presence of a considerable amount of fluids circulating over the rock column as implied by the Barrowian character of metamorphism, and is in the order of the temperature conditions attributed to the dominant first phase of metamorphism. Even if we assume, that this datum corresponds already to the (incipient) thermal decline of the first metamorphic event, there is no reason to assume that temperatures of about 600 °C under Barrowian conditions could have been maintained over a prolonged period of time all the more because the strong deformation points to the dynamic behaviour of the system during metamorphism. Even if we assume, that the amphibolite grade metamorphism has occurred (somewhat) prior to the 331±13 Ma datum, we feel convinced that this value gives a reliable age for the deformation D_1, during which conditions inappropriate for isotopic equilibration over a km-scale became manifest. This interpretation might be supported by additional evidences obtained on the anatectic granodiorites of the Mecsek Mountains, adjoining the Görcsöny Ridge metamorphic basement. Rb-Sr studies (SVINGOR and KOVÁCH, 1981) bracket the development of the anatectic mass between the age limits of 400 to 270 Ma with concordant Rb-Sr *(loc. cit.)* and K-Ar (BALOGH *et al.*, 1983) evidence for a prominent event at around 334 Ma. As this concordant datum has been obtained on biotites, it points to the rapid uplift of the anatectic mass, taking into account the 337+18 average K-Ar obtained on amphiboles from the immediate cover. Although a direct link between the Görcsöny Ridge metamorphites and the Mecsek granodiorites could not have been ascertained up till now, the increase of metamorphic grade towards the granitized mass of the Western Mecsek Mountains supports the interpretation that the D_1 deformation might have been synchronous with the emergence of the anatectic mass nearby. If this parallelization is correct, the zircon concordia age of 365±8 Ma quoted by BALOGH *et al.* (1983) for the Mecsek anatectites might serve as additional evidence for the peak of metamorphism in the area under study, in support of placing the main phase of metamorphism into the Late Devonian-Early Carboniferous, i.e. into Herzynian times.

The timing of the second metamorphic-deformational overprint is bracketed by the total rock isochron age and the 315±3 Ma average biotite Rb-Sr age, the blocking temperature of the biotite Rb/Sr system (PURDY and JÄGER, 1976) being definitely lower than possible temperatures assigned to this metamorphic episode. A more accurate positioning in time of this metamorphic event might be possible in the course of a detailed analysis of the thermal history of the rock unit.

The present data allow no conclusion with respect to the age of the subordinate dyke intrusions interrupting the decline of the second metamorphic event. The aplitic sample from the depth of 64.0 m fits into the isochron picture and does not seem to represent a definitely different source for the late dyke intrusions. It rather points to the possibility, that most of the late aplitic dykes represent paraautochtonous mobilizates of the basement. It should be mentioned, however, that Rb-Sr data obtained on highly differentiated microgranitic dyke rocks from the Mecsek Mountain area supply evidence for dyke intrusions appearing locally in the final stage of uplift of the anatectic region, too (SVINGOR and KOVÁCH, 1981).

The only discordant biotite age of 238±9 Ma obtained on a sample from the depth of 268.0 m is in agreement with the 243+15 Ma total rock isochron age obtained on Permian rhyolites from the Villány Mountains nearby, supporting the interpretation of FAZEKAS *et al.*, (1981) on the locally appearing late stage disturbances.

As shown by the data in Table 1 as well as by the K-Ar data of BALOGH *et al.* (1983) already quoted, no distinct Alpine effects could be ascertained by radiochronological means. This fact might be in favour of the interpretation, that the low-temperature retrograde effects shown by ÁRKAI (1984) in metamorphites of the Drava Basin might be evoked mainly during the continuous, low-velocity uplift of the metamorphic mass.

CONCLUSIONS

Based on the discussion above, the following tentative timing sequence for the individual metamorphic-deformational events might be given for the metamorphic rocks of the Görcsöny Ridge, considered as the southern foreland of the Mecsek Mountains in the Southeastern part of the Transdanubian region in Hungary:

- 1st phase of metamorphism: (365) ... 331±13 Ma
- D_1 deformation: 331±13 Ma (Devonian/Carboniferous boundary)
- 2nd phase of metamorphism and D_2 deformation: about 315 Ma (Early/Late Carboniferous boundary)
- Continuing emergence and low-temperature retrograde alteration: 315 to about 280 Ma
- Local disturbances: about 240 Ma (Permian).

REFERENCES

ÁRKAI, P. (1984): Polymetamorphism of the crystalline basement of the Somogy—Drava basin (Southwestern Transdanubia, Hungary). Acta Miner: Petr., Szeged, **26**, 129—153

BALOGH, K., ÁRVA-SOÓS, E., BUDA, GY. (1983): Chronology of granitoid and metamorphic rocks of Transdanubia (Hungary). Anarul Inst. Geol. si Geofiz. (Bucuresti) **61**, 359—364

FAZEKAS, V., MAJOROS, GY., SZEDERKÉNYI, T. (1981): Late Paleozoic subsequent volcanism of Hungary. IGCP No. 5 Newsletter **3**, 61—69

KOVÁCH, A., SVINGOR, E. (1977): A Rb-Sr geochronological study of Permian quartz-porphyries from the Transdanubian region. Manuscript, Hungarian Geological Survey (in Hungarian).

LELKES-FELVÁRI, GY., SASSI, F., *et al.* (1981): Outlines of the pre-Alpine metamorphism in Hungary. IGCP No. 5 Newsletter **3,** 87—99
PURDY, F. W., JÄGER, E. (1976): K-Ar ages on rock-forming minerals from the Central Alps. Mem. Inst. Geol. Min. Univ, Padova, **30,** 1—31
SVINGOR, E., KOVÁCH, A. (1981): Rb-Sr isotopic studies on granodioritic rocks from the Mecsek Mountains, Hungary. Acta Geol. Acad. Sci. Hung., **24,** 295—307
SZEDERKÉNYI, T.: (1974): Palaeozoic magmatism and tectogenesis in Southeast Transdanubia. Acta Geol. Acad. Sci. Hung., **18,** 305—313
SZEDERKÉNYI, T. (1976): Barrow type metamorphism in the crystalline basement of Southeast Transdanubia. Acta Geol. Acad. Sci. Hung., **20,** 47—61
SZEDERKÉNYI, T. (1979): Complex geological investigations of Old-Palaeozoic-Precambrian main profiles in the Mecsek Mountains, II. Manuscript, Hungarian Geological Survey (in Hungarian)
SZEDERKÉNYI, T. (1981): Character of metamorphism of Görcsöny Hill crystallins (SE Transdanubia, Hungary) based on the Baksa-2 deep drilling. Acta Geol. Acad. Sci. Hung., (in press).

Manuscript received, April 29, 1985

Acta Mineralogica-Petrographica, Szeged, XXVII, 59—70, 1985

EARLY CALEDONIAN EVENT IN THE PRE-ALPINE METAMORPHIC SEQUENCES OF THE ROMANIAN CARPATHIANS

RADU DIMITRESCU*

ABSTRACT

An Early Caledonian event is to be recognized in the Romanian Carpathians, its evidence being based on palynological data, radiometric ages and structural unconformities. The main proof consists in the break of sedimentation, post-dating an older metamorphism of formations belonging to the lower structural stage occurring at some point during the Ordovician.

INTRODUCTION

The Carpathian-Balkan mountain belt of South-Eastern Europe, of Alpine age, displays an intricate nappe structure, less complicated admittedly than the Alps themselves. In this belt, almost all the pre-Late Carboniferous deposits are more or less intensively metamorphosed; even a part of the Mesozoic deposits were subjected to a slight metamorphism. The metamorphic piles, together with their Mesozoic sedimentary cover, are involved in the nappe structure. This intensive fragmentation by the nappes — and by younger fault systems — together with the multiplicity of the superposed structural and metamorphic events within the crystalline sequences themselves, lead to the fact that the recognition of an Early Paleozoic tectonic cycle was highly difficult in these regions.

Evidence on the presence of an Early Caledonian (Finnmarkian) event within the metamorphic piles exposed in South-Eastern Europe is based on palynological data, on radiometric ages and on structural unconformities.

STRUCTURAL FRAMEWORK

The main structural units including metamorphic rocks of Late Proterozoic-Early Paleozoic age are the following (SĂNDULESCU, 1984).

1) Internal Dacides (northern Apuseni Mountains), with their north-western prolongation, the Tatric, Veporic and Gemeride nappes of the West Carpathians (Ostalpin) in Slovakia.

2) Median Dacides of the East and South Carpathians, including the Central East Carpathian nappes, the Supragetic and Getic nappes, with their southern prolongation into Serbia (north-eastern Yugoslavia) and Sredna Gora (Bulgaria). The Serbo-Macedonian massif could perhaps be considered as included in the Supragetic nappes or could rather have a higher, more internal position.

3) Marginal Dacides of the South Carpathians (Lower and Upper Danubian units), together with the Stara Planina Unit in the Balkans (Bulgaria).

* University "Al. I. Cuza", Calea 23 August 20 A, Iaşi, Romania.

In contrast with other structural units (Pienides, Moldavides), the Dacides have in common the Late Cretaceous age of their tectogenesis. They are made up of superposed nappes advancing from the interior of the Carpathian-Balkan belt towards its exterior (northwards, eastwards or southwards).

GENERAL STRUCTURAL EVOLUTION OF THE CRYSTALLINE SCHISTS

Geological research undertaken during the last three decades in the metamorphic basement of the Carpathian-Balkan ranges (South-Eastern Europe) has shown that the pre-Upper Carboniferous crystalline schists building up the cores of these mountains have to be divided into three major supergroups.

The uppermost one may be called Variscan Supergroup. Its main characteristics may be summarized as follows: low-grade metamorphism; frequent appearance of metaconglomerates at different levels, and of massive limestones and dolomites in the upper parts; presence of basic metavolcanic formations, sometimes (bimodal magmatism) associated with acid ones; only a few granitic bodies emplaced. Sporo-protistologic research resulted in according an Ordovician-Lower Carboniferous age to this group. K/Ar ages of rocks included in this group were exclusively Variscan ($\leqq$350 m.y.).

The median supergroup was called "Marisian" by KRÄUTNER (1980). Its main characteristics are: low to medium-grade metamorphism (epidote-amphibolite facies, almandine zone) followed by a retrogressive chlorite event; extensive presence of a basic metavolcanic formation, followed by an acid one; widespread granitie intrusive activity in many regions. Microfloristic research yielded Upper Proterozoic-Cambrian palynomorphs; geochronologic studies gave a series of 400—500 m.y. K-Ar ages, besides a large number of Variscan ones.

The lower supergroup was called "Carpian" by KRÄUTNER (1980). Medium- to high-grade metamorphism was accompanied locally by migmatization; pegmatites are frequent. Almost no K-Ar ages from 600 m.y. upwards were obtained. Mycrophytological research is unconclusive. Opinions differ widely regarding this supergroup: basement of the Marisian, the two being separated by a structural and metamorphic discordance; lateral or downward gradual transition from the former.

The purpose of the present paper is to analyze the relations between the Variscan and the Marisian supergroups, leading to the conclusion that this very important and conspicuous discordance represents an Early Caledonian (Finnmarkian) event.

General features of the Marisian (Vendian-Cambrian)

In the Alpine territory of South-Eastern Europe dated Cambrian formations are known only from the Carpathians and the Balkans. All formations assigned to the Cambrian consist of low-grade metamorphic rocks (greenschist facies), down to the almandine isograd. Rocks of higher metamorphic degree have systematically been regarded as Precambrian in age, although, as already supposed by ANDRUSOV 1968), some metamorphic rocks from areas subjected to intense Variscan diastrophism (basement of the Tatro-Veporids) might be Lower Paleozoic in age. An abundant granitic magmatism was emplaced in the Marisian formations.

The Cambrian age assigned to several "epimetamorphic" formations of the Carpathians and the Balkans is mainly supported by palynological evidence. The only Cambrian macrofossils so far reported are Archeocyathids found near the

Dubocane village, in eastern Serbia (KALENIĆ, 1966). Some of the listed assemblages of palynomorphs from the "epimetamorphic" formations of the Carpathians are claimed to be of diagnostic value for the Upper Precambrian or Riphean *(sensu lato)*, others — either for the Lower Cambrian or for the Middle-Upper Cambrian. Many forms have a uniform distribution throughout the Upper Proterozoic and the Lower Cambrian.

An increase in the frequency and diversity of the Acritarchs from the Holmia Zone onwards, as well as the explosion of Ellipsoidomorphids in the Middle Cambrian seem actually to be the most reliable microfloristic changes to be used in biochronologic correlation.

General features of the Variscan

Variscan piles of metamorphic rocks constituting fairly well established lithostratigraphic sequences which, together, build up an upper structural stage of the crystalline basement, are known from almost all the structural units of the Carpathians and the Balkans. Their metamorphism was low-grade (or even very low-anchizonal). Metapsephites are frequent in lithologic sequences, mainly at the basis of the transgressive ones. Granitic intrusions crossing the Variscan formations are scarce in some regions, sometimes they are definitely absent (but in Slovakia they seem to be well represented). Radiometric ages of these formations are exclusively Variscan.

In contradistinction to the Alps, where the boundary between the "Altkristallin" and the "Jungkristallin" divides the Alpine structural stage from the Variscan and the Pre-Variscan, in the Carpathians and the Balkans the former includes only the Pre-Variscan (*i.e.* Caledonian and possibly earlier structural stages) whilst the latter is built up of Variscan and, when present, Alpine metamorphites.

The purpose of the present paper being the analysis of the Caledonian event in the Romanian Carpathians, the description of the Variscan will include only the lowest lithostratigraphic units and those assigned to the "Caledonian Era", the Ordovician, Silurian or the basis of the Devonian.

I MARGINAL DACIDES

1) Danubian

a) Marisian. In the Stara Planina Zone of the Balkans, a Late Precambrian (Riphaean) to Early Cambrian age has been assigned to the so-called Diabase-Phyllitoid Formation (DPF), which consists of mafic rocks, metakeratophyres, basic tuffogenic and tuffitogenic phyllites, metagreywackes and arkosic metasandstones (VRÎBLENSKI *et al.*, 1963). The stromatolitic marbles outcropping in the Bela Reka antiform of the Poréc Zone are considered to represent the upper member of this formation. It is from the top of the stromatolitic marbles that Archaeocyathids listed as Ajacicyathus ex. gr. anabarensis (Vologdin) have been recorded (KALENIĆ, 1966).

Through the Poréc Zone of eastern Serbia, the Stara Planina Zone extends northwards, across the Danube, into the Danubian of the South Carpathians.

A highly controversial problem is represented by the existence, or the inexistence, of a "green" Vendian-Cambrian lithostratigraphic unit in the Danubian Realm.

Just north of the Danube, a mafic "Corbu formation" was thought to be an equivalent of the DPF: chlorite-albite-epidote, actinolite, quartz-chlorite-sericite-

graphite, quartz-albite-sericite and muscovite-garnet schists, with porphyroids and carbonatic lenticular intercalations (CODARCEA, CODARCEA—DESSILA, 1968). Recent research (MĂRUNȚIU, SEGHEDI, 1983; STAN, 1984) has shown that these rocks do not represent a distinct lithostratigraphic unit, being in fact plagiogneisses and micaschists with staurolitic and andalusite, amphibolites and amphibole gneiss of another Carpian Group (Neamțu), intensively retrogressed along an overthrust line of Early Caledonian age.

Further north, in the Vulcan, Parîng and Retezat Mountains, another "green" series (Clastic series, MANOLESCU, 1937; Upper Drăgșanu "Series", PAVELESCU, 1953; Vulcan "Series", SAVU *et al.*, 1978) had been separated, consisting of sericite-chlorite-epidote, chlorite-albite, actinolite and garnet-muscovite schists, porphyroids and limestones; their age should have been Cambrian. The same rocks are considered by BERZA (1975) as resulted by a Paleozoic retrogression from the Precambrian Drăgșanu Amphibolite Group.

In the northern part of the Retezat-Petreanu Mountains, the Zeicani Formation (GHERASI, DIMITRESCU 1968; GHERASI *et al.*, 1968) was also considered as Cambrian. It consists of a lower member of amphibole- and chlorite-albite-epidote-calcite-muscovite ± biotite schists (basic metatuffs), with sills of metagabbros and serpentinites, a median member of muscovite gneisses (metagreywackes) and an upper member of basic tuffogenic greenschists and metakeratophyric porphyroids (GHERASI, ZIMMERMANN, unpublished data). The Early Cambrian age assigned to the lower member is claimed to be supported by Protomycterosphaeridium marmoratum, occurring together with long ranging palynomorphs (GHERASI *et al.*, 1973), whereas the sporomorph assemblage of the upper member with Ellipsoidomorphids such as Acanthodiacrodium and Trachyzonodiacrodium (VISARION, SOLOMON, 1974) points to a Middle-Late Cambrian age.

All Danubian pre-Variscan formations are intruded by a great number of granitoid plutons the radiometric ages of which span between the Late Precambrian and the Lower Paleozoic.

b) Variscan (Tulișa Group). The Carpian highly metamorphic basement of the South Vulcan-Culmea Cernei Mountains is transgressively overlain by the Valea Izvorului Formation. A stratigraphic and metamorphic discordance is conspicuous at the basis of quartzites and sericitic metaconglomerates, followed by chlorite-, sericite- and graphite-phyllites. The first and only macrofauna of metamorphic rocks from Romania was discovered at Cloșani (STĂNOIU, 1971); it includes: *Favosites* sp., *Halysites* sp., *Cyathophyllum* sp., *Fenestella?* sp., *Plectorthinae, Dalmanellidae, Dolerorthis* sp., *Eoplectodonta* sp., *Ygerodiscus aff. undulatus, Leptaena* sp., *Leangella* sp., *Atrypina aff. barrandei, Atrypa cf. reticularis, Coelospira aff. hemisphaerica, Enricnurus* sp., *Flexicalymene* sp., *Caleidocrinus aff. artifex*. Conspicuously absent are the Spiriferida and Productida. According to this macrofauna the Valea Izvorului Formation has to be ascribed to the Upper Ordovician, grading perhaps into the Lower Silurian.

The basement of the Valea Izvorului Formation has a palynological assemblage including *Protoleiosphaeridium cambriense* and *Tyloligotriletum asper* (STĂNOIU, 1972). Its top is overlain by the transgressive Tusu Formation, which frequently overlies directly the Carpian basement. It is built up of metaconglomerates, quartzites and graphite- or chloritoid-phyllites. According to palaeofloral forms (STĂNOIU, 1980), the Tusu Formation is ascribed to the Devonian.

In the southern-eastern Banat an Ordovician-Silurian age is ascribed to the volcano-sedimentary Rîul Alb Formation (metaconglomerates, metasandstones, sericite-chlorite-quartz phyllites, metabasites and basic metatuffs; total thickness 1300 m) (NĂSTĂSEANU, 1975).

2) Getic Realm

a) Marisian. In the Kucaj Zone of eastern Serbia, Ordovician sandstones and phyllites are unconformably underlain by a metamorphic formation assumed to be an equivalent of the DPF of Bulgaria, and Riphaean-Early Cambrian in age.

North of the Danube, in different regions belonging to the Getic Realm (southern Semenic Mountains, southern Poiana Ruscă, northern Sebeş Mountains, eastern Cibin Mountains), the subjacent highly metamorphic Carpian Lotru Group is covered in discordance by the Cibin Group. It lithostratigraphic sequence was synthesized by KRÄUTNER (1980 *b*) as follows: 1) basic volcano-sedimentary formation, with a lower amphibolitic member and an upper metapryoclastic or metaterrigenic member; 2) carbonatic formation with graphitic schists; 3) blastodetrital formation. In different areas of the South Carpathians, this Group was described as Miniş-Buceava Series (CODARCEA, 1940; STRECKEISEN, 1934; SAVU, 1973), Dăbîca Series (MAIER *et al.*, 1975), Căpîlna-Cărpiniş Series (CHIVU, 1970, 1979) and Sibişel Series (CODARCEA—DESSILA, 1965). All the mentioned sequences have been metamorphosed in greenschist facies (almandine zone) and display a Variscan retrogression. Their palynomorph assemblages include mainly ultramicrospores and Sphaeromorphids ranging from the Late Proterozoic to the Cambrian, together with *Protoleiosphaeridium cambriense, Trachydiacrodium* and *Protomycterosphaeridium marmoratum* (DESSILA—CODARCEA, ILIESCU, 1967), allowing to assign at least the top of the Cibin Group to the Cambrian.

There are no Variscan formations overlying the Cibin Group.

The Miniş-Buceava "Series", together with its Carpian basement (Lotru Group) are intruded by the Sichevița-Poniasca pluton.

3) Supragetic Realm

Western Supragetic Unit (Banat)

a) Marisian. In the inner part of the Serbo-Macedonian massif there are several "epimetamorphic" rock sequences considered to be Late Precambrian to Early Cambrian in age. On of them is the Vlasina "Complex" from the central part of the Morava Zone.

b) Variscan. In the same Morava Zone, the next younger formation, transgressive over the Vlasina Formation or the DPF, is built up of sericite-quartz phyllites and green metasandstones, with intercalated metaspilites, metadiabases and metagabbros. A Tremadocian fauna includes *Obolus feistmanteli* or *O. barrandei, O. complexus* or *Orbiculoidea* sp.

In the western Banat, the Locva Formation may be divided into two members. The lower member consists of muscovite-chlorite (±microcline) gneisses predominating over chlorite-muscovite-albite, quartz- and actinolite-schists. The upper member includes muscovite-chlorite schists with albite porphyroblasts interbedded with albite-chlorite-calcite, actinolite-chlorite-epidote schists and quartzites (Maier, 1974).

The palynologic assemblage of this formation (MAIER, VISARION, 1976) includes *Leiosphaeridae, Pseudozonosphaeridiae, Lophosphaeridium* sp., *Acanthodiacrodium* sp., *Leiofusa* sp., *Veryhachium* sp., *Schizmatosphaeridium* sp., *Navifusa* sp., as well as Chitinozoans *(Conochitina, Clathrochitina, Desmochitina);* its age seems accord-

ingly to be Ordovician (supposedly raising to the Silurian, but possibly beginning in the Cambrian).

The origin of the Locva Formation has to be sought in a terrigene material, of greywacke nature mixed with basic tuffs. The first metamorphism, of medium grade and Caledonian in age, produced oligoclase, garnet and biotite; it was followed by a Variscan retrogression, transforming the above minerals in albite, chlorite, sericite and calcite.

The Locva Formation is overlain by the Leşcoviţa Formation (MAIER, 1974) beginning with leptynites, metadacitic porphyroids, epidote-chlorite-actinolite-albite schists (basic metatuffs), metadolerites and terrigenic quartz-muscovite schists. The palynological assemblage includes Acritarchs, Scolenodonts, Chitinozoans *(Lagenochitina, Conochitina, Angochitina), Verrucosisporites grandis, Punctatisporites* sp., *Stenozonotriletes* sp., and points to an Early-Medium Devonian age (MAIER, VISARION, 1976).

Eastern Supragetic Unit
Făgăraş-Ezer-Leaota Mountains)

a) Marisian. The Vendian and perhaps a part of the Cambrian are probably included în the Lereşti Formation (1500—3000 m). It consists mainly of muscovite-chlorite schists with albite porphyroblasts, of probable greywackean origin, with intercalations of chlorite-albite greenschists (basic metatuffs), amphibolites, graphite schists and dolomites. An upper member of the Lereşti Formation consists of quartz-albite (±microcline) schists, with a few muscovite and chlorite flakes. The metamorphism of the Lereşti Formation developed in the greenschist facies, partly in the almandine zone and partly in the chlorite zone. The sedimentation age is not directly known, but by lithologic comparison with the Biharia Formation it may be inferred as Upper Proterozoic (DIMITRESCU, 1978).

b) Variscan. In the eastern part of the Făgăraş Massif (Păpuşa Mountains) the Lereşti Formation is overlain by the probably transgressive Căluşu Formation (chlorite-sericite-albite, chlorite-actinolite-albite, sericite-quartz and graphite schists, scarce acid metatuffs) which yields Palaeozoic (up to Lower Carboniferous) microspores.

No granitic rocks intrude the Căluşu Formation. The Lereşti Formation, by contrast, is intruded by vein-like bodies of red Lalu Granite, the age of which is still unclear. In the basement of the Lereşti Formation sills of Albeşti Granites are known, with three K-Ar ages of 464, 475 and 477 m.y. (DIMITRESCU, 1978; POPOVICI, 1978).

4) Eastern Carpathians: Bucovinian nappe system

a) Marisian. In the East Carpathians, the main lithostratigraphic unit is represented by the Marisian Tulgheş Group. It consists of five formations: Tg_1 Blastodetrital-Quartzitic Formation; Tg_2 Graphite-Metalyditic Formation; Tg_3 Volcano-Sedimentary Metarhyolitic Formation; Tg_4 Blastodetrital-Phyllitic Formation; Tg_5 Graphitic-Greenschist-Carbonatic Formation. The whole group was metamorphosed in the greenschist facies, reaching locally the biotite zone (BERCIA *et al.*, 1976).

Four types of palynomorph assemblages were recognized in the Tulgheş Group: 1) Acritarchs of the types *Baltisphaeridium, Cymatiosphaerea* and *Veryhachium*, considered to make their first appearance in the Cambrian; 2) Acritarchs characteristic of the Lower Cambrian *(Granomarginata vulgaris, Acantosphaera cambriensis,*

Microconcentrica atava, Spumosata prima; 3) Sphaeromorpha common to the Vendian and Lower Cambrian: *Archaeopsophosphaera asperata, Archaeosacculina* sp., *Granomarginata cf. squamacea, Trachypsophosphaera exilis, Trachysphaeridium incrassatum, T. atenuatum;* 4) Sphaeromorphs covering most of the Middle and Late Proterozoic and declining in the Lower Cambrian *(Protosphaeridium flexuosum, P. acis, P. tuberculiferum, P. laccatum, Orygmatosphaeridium distributum, Asperatopsophosphaera* sp., *Archaeofavosina* sp., *Podoliella irregulare)* (ILIESCU *et al.*, 1983).

The Tg_1 Formation represents, according to ILIESCU, MURESAN (1972), ILIESCU *et al.* (1983) the Lower Cambrian and possibly also the Upper Vendian. For the upper part of the Tulgheş Group (Tg_4 and Tg_5 formations), a Middle Cambrian age at least may be supposed, but the Upper Cambrian and possibly the Lowest Ordovician may also be included in the sequence (ILIESCU *et al.*, 1983), especially according to the forms *Leiomesotriletes, Stenomesotriletes* found by ONICEANU *et al.* (1977).

The available radiometric ages of rocks constituting the Tulgheş Group are the following: U-Pb zircon ages of 560—640 m.y. (BOIKO *et al.*, 1974), Pb-Pb ages 540—600 m.y. on syngenetic stratiform ores in the Tg_3 Formation (VÎJDEA, ANASTASE in MÎNZATU *et al.*, 1975 and unpublished data; POPESCU, unpublished data), K/Ar whole rock and sericite ages with maximal values of 475 m.y. (K/Ar isochrone age of 505 ± 5 m.y., KRÄUTNER *et al.*, 1976).

b) Variscan. In the western Rodna Mountains, the Carpian Bretila Group is overlain in transgression by the Repedea Formation (KRÄUTNER, 1968). It consists of a lower member Rp_1 with greenschists (basic metatuffs) and sericite-chlorite-chloritoid schists and an upper member Rp_2 built up of metaconglomerates, graphitic quartzites, sericite-chlorite schists and limestones. The age is Late Ordovician-Silurian, according to the palynologic assemblage of the Rp_2 member *(Bursachitina* sp., *Lagenochitina macrostoma, Desmochitina congulata, Sphaerochitina* sp., *Chonochitina lagenomorpha, Leiotriletes* sp., *Retusotriletes* sp.*)*, characteristic of the Ludlovian.

A slight Late Caledonian premetamorphic discordance separates the Repedea Formation from the overlying Cimpoiasa Formation (Devonian, according to its palynomorph assemblage; ILIESCU, KRÄUTNER, 1976).

In the eastern Rodna Mountains, the place of the Repedea Formation is taken by the Rusaia Formation. Beginning with metaconglomerates, limestones and quartzites, it continues with chlorite schists, the top being built up of dolomites and carbonatic schists. Besides common Silurian-Devonian forms *(Bursachitina cf. urna, Leiotriletes* sp., *Leptotriletes* sp., *Achantotriletes* sp., *Archaeozonotriletes* sp., *Pterospumopsis* sp., *Protosphaeridium cf. microgunifer, Multiplicisphaeridium* sp., *M. cf. lobezum),* the palynomorph assemblage (ILIESCU, KRÄUTNER, 1978) includes *Lophosphaeridium* sp., *Baltisphaeridium* sp., *Synsphaeridium* sp., *S. conglutinatum, Zonosphaeridium* sp., *Leiosphaeridium* sp., *Trachysphaeridium* sp., which do not transgress the Silurian-Devonian boundary; the age has accordingly to be ascribed to the Silurian (including perhaps the Late Ordovician).

There are no granitic intrusions either in the Variscan or in the Marisian of the East Carpathians.

III INTERNAL DACIDES

5) Apuseni Mountains

a) Marisian. The Bihor Autochthon of the Northern Apuseni Mountains has a very large sole of crystalline schists, the upper part of which is built up of the Arada Formation (3000 m) (DIMITRESCU, 1966). It consists mainly of sericite-chlorite

schists in which persistent intercalations are represented by sericite-chlorite-albite, chlorite-epidote and albite-actinolite-epidote schists (basic metatuffs±metagraywackes), porphyroids (metarhyolitic welded tuffs), hälleflinta (acid metatuffs), graphite quartzites (metalydites) and a single layer of crystalline dolomitic limestone.

The polynomorph assemblage of the Arada Formation includes common Vendian-Lower Cambrian forms *(Protosphaeridium* sp., *Pr. cf. acis, Kildinella* sp., *Laminarites* sp., *Favososphaeridium* sp., *Orygmatosphaeridium* sp., *Pseudozonosphaeridium* sp., *Asperatopsophosphaera* sp., *Leiospshaeridia* sp., *Synsphaeridium* sp., and in addition *Pr. flexuosum (M. marmoratum)* (Cambrian) (VISARION, DIMITRESCU, 1971; VISARION, unpublished data).

The metamorphism of the Arada Formation corresponds to the low-grade or to the greenschist facies. A biotite (+oligoclase) and a chlorite isograd have been traced. However, the formation is polymetamorphic, the retrogression being evident in the biotite zone only, by the chloritization of biotites and amphiboles. Both the Someş and the Arada formations are intruded by the Muntele Mare granitic massif, which yielded, besides Alpine and Variscan ages, on K-Ar age of 522 m.y.

The Bihor "Autochthon" underlies the Codru Nappe System covered itself by the Biharia Nappe System. The crystalline basement of the latter consists of the Biharia and the Muncel formations.

The Biharia Formation (1000 m) is mainly built up of chlorite-albite, chlorite-epidote-calcite and actinolite-epidote-albite schists (basic metavolcanogenic rocks), alternating with muscovite-chlorite-quartz-albite schists; two thin intercalations of dolomitic limestone are known (DIMITRESCU, 1976). Another characteristic element is represented by small bodies of orthoamphibolites (metagabbros, metadiorites, metadolerites). Locally metatrondhjemites are associated. Its metamorphism is generally of lowgrade (greenschist facies) in the chlorite zone, but occasionally biotite and garnet appear (epidote-amphibolite subfacies).

The palynomorph assemblage of the Biharia Formation *(Protosphaeridium* sp., *Pr. flexuosum, Pr. cf. acis, Kildinella* sp., *Laminarites* sp., *Favososphaeridium* sp., *Orygmatosphaeridium* sp., *Pseudozonosphaeridium* sp., *Ps. cf. populosum, Asperatopsophosphaera* sp., *Leiosphaeridia* sp., *Synsphaeridium* sp.*)* supports only a Late Proterozoic (Vendian) age.

The Biharia Formation grades upwards into the Muncel Formation (1500 m). The lower member of the latter (200—500 m), considered by some as an upper member of the Biharia Formation, consists of sericite-chlorite, sericite-albite, chlorite-albite and quartz-albite schists (DIMITRESCU, 1976). Its palynomorph assemblage includes *Protosphaeridium flexuosum (M. marmoratum), Uniporata nitidus, Spumosata nova, Polyporata verrucosa, Margaporata glabella,* common Vendian-Early Cambrian forms, along with *Veryhachium balticum, Polyedrixium prituli, Archaeohystrichosphaeridium pungens,* allowing its ascribing to the Lower-Middle Cambrian (VISARION, DIMITRESCU, 1971; SOLOMON *et al.*, 1984). The middle member of the Muncel Formation (300—1000 m) consists of sericite schists with intercalations of metarhyolitic porphyroids and of augen gneisses. The upper member (500—700 m) begins with graphite quartzites and continues with biotite-sericite schists, biotite paragneisses, amphibole schists and metarhyolitic biotite porphyroids. The palynological assemblage (VISARION, DIMITRESCU, 1971; VISARION, unpublished data) including *Leiosphaeridia cf. dehisca, Cymatiosphaera* sp., *Acanthodiacrodium* sp., *Trachydiacrodium cf. signatum, Baltisphaeridium* sp., *B. cf. papillosum, Lagenochitina* sp., *Scolecodonta* sp., is more definite Cambrian in age, including the Upper Cambrian and perhaps even a part of the Ordovician.

The metamorphism of the Muncel Formation is low-grade (chlorite isograde), excepting the upper part that overpasses the biotite and even the almandine isograde.

Comparing the lithostratigraphic sequences in the Bihor "Autochthon" and in the nappes, a close affinity may be observed between the Arada Formation on the one hand and the Biharia and Muncel Formations on the other hand. In both realms, an acid magmatism follows or is associated to a basic one. The palynological contents are similar.

b) Variscan. In the Codru and Biharia Nappe Systems of the northern Apuseni Mountains, the Biharia Formation is transgressively overlain by the Păiuşeni Formation. The lower member of the latter is built up of sericite-metaconglomerates, quartzites, sericite-chlorite schists, scarce limestones; in the upper member, chlorite-albite schists, actinolite schists, metakeratophyric porphyroids and carbonatic schists predominate. The palynologic assemblage of the lower member includes, in the Highiş Mountains (VISARION, in ISTOCESCU, 1971), *Stenozonotriletes simplicissimus, Leiotriletes microrugosus, Zonotriletes cf. auritus,* pointing to a Late Devonian age (the upper member being proved as Early Carboniferous).

The Păiuşeni Formation is intruded by the Variscan Highiş Granite.

CONCLUSIONS

Similarly to the Alps, a Caledonian event has to be recognized in the Carpathians. This does not mean that a direct link with the Caledonides of Scandinavia has already been demonstrated.

The main proof of the Caledonian event consists in the break of sedimentation, post-dating an older metamorphism of formations belonging to the lower structural stage, occurring at some point during the Ordovician, thus dividing the Variscan from the Marisian. The Valea Isvorului, Leşcoviţa, Repedea-Rusaia and Păiuşeni formations overlie a basement built up sometimes of Carpian and sometimes of Marisian formations. The proved Cambrian (—Early Ordovician?) age of the latter diminishes the time-gap between themselves and the basis of the Variscan transgression, taking place at the earliest moment in the Late Ordovician.

Between the two groups, as seen from the previous descriptions, there is almost always a difference in metamorphic degree, the Variscan being naturally less metamorphosed. Metaconglomerates are very frequent at the basis of the Variscan pile.

A granitoid plutonism, conspicuously absent from the Variscan (with the exception of the Apuseni Mts) intrudes the Carpian and its Marisian cover: Muntele Mare massif in the Apuseni Mts, Sicheviţa-Poniasca massif in the Banat, Danubian. The isotopic ages of some of these granites are Caledonian.

In the Carpian formations themselves (older elements within the Caledonian) a number of 40—50 radiometric ages between 400—500 m.y. suggest an Early Caledonian thermal event.

Structural analysis of Marisian rocks yielded a last deformation phase F_3 attributed to the Variscan. By contrast, the structural analysis of the Variscan formations revealed less metamorphic episodes.

A basic (ophiolitic?) suite is recognizable almost everywhere within the Marisian, as a prelude of the Caledonian event. By contrast, there is no clear separation between an acidic volcanism postdating this event and a basic volcanism, which can be considered as initiating the Variscan orogeny.

Later Caledonian events (*e.g.* the slight discordance of the Devonian Cimpoiasa overlying the Repedea Formation) are devoid of metamorphic phenomena, having thus a minor importance.

REFERENCES

ANDRUSOV, D. (1968): Grundriss der Tektonik der nördlichen Karpaten. VEDA, Ed. S. A. V., p. 1—188, Bratislava.

BERCIA, I., KRÄUTNER, H., MUREŞAN, M. (1976): Pre-Mesozoic Metamorphites of the East Carpathians. An. Inst. Geol. Geofiz., **50,** p. 37—70, Bucureşti.

BERZA, T. (1975): „Seria clastică" şi cîteva probleme de stratigrafie şi metamorfism ale formaţiunilor cristalofiliene din partea externă a Autohtonului Danubian. Stud. cerc. geol., **20/2,** p. 179—186, Bucureşti.

BOIKO, A., BARNIŢKII, E., ELISEEVA, G., KAZANŢEVA, A., LEVKOVSKAIA, N., OVSIENOV, TEREŢ, G. (1975): Rezultatî pervoga isledovaniia po ţirkonovii hronologhii kristalliceskoga iada vostocinîh Karpat. Gheologiceskii Jurnal **34/2,** p. 112—116, Kiev.

CHIVU, C. (1970): Contribuţii la cunoaşterea petrografiei şi tectonicii părţii de nord-est a munţilor Sebeş. D. S. Inst. geol. geofiz., **56/5,** p. 41—56, Bucureşti.

CHIVU, C. (1979): Contribuţii la cunoaşterea geologiei şi metalogenezei părţii de N a munţilor Sebeş. D. S. Inst. geol. geofiz. **64/2,** p. 37—55, Bucureşti.

CODARCEA, AL. (1940): Vues nouvelles sur la tectonique du Banat méridional et du Plateau de Mehedinţi. An. Inst. Geol. Rom., **20,** p. 1—74, Bucureşti.

CODARCEA, AL., DESSILA-CODARCEA, M. (1968): Consideraţii asupra paleolitologiei şi paleotectonicii zonelor de şisturi cristaline din partea de SE a Banatului. Stud. cerc. geol., **13/1,** p. 17—24, Bucureşti.

DESSILA-CODARCEA, M. (1965): Studiul geologic şi petrografic al regiunii Răşinari-Cisnădioara-Sadu, Mem. Inst. geol., **6,** p. 1—96, Bucureşti.

DESSILA-CODARCEA, M., ILIESCU, V. (1967): Asupra prezenţei depozitelor metamorfozate ale paleozoicului inferior în Carpaţii Meridionali centrali. Stud. cerc. geol., **12/2,** p. 311—319, Bucureşti.

DIMITRESCU, R. (1966): Muntele Mare. Studiu geologic şi petrografic. An. Com. geol., **35,** p. 165—239, Bucureşti.

DIMITRESCU, R. (1976): Les terrains métamorphiques des Monts Apuseni. I. Formations préhercyniennes. Geol. Zbor.-Geol. Carp., **27/2,** p. 347—354, Bratislava.

DIMITRESCU, R. (1978): Structure géologique du massif cristallin Făgăraş-Ezer-Leaota. Rev. Roum. Géol., **22,** p. 43—51, Bucureşti.

GHERASI, N., DIMITRESCU, R. (1968): Contribuţiuni la structura cristalinului în partea nordică a munţilor Retezat şi Petreanu. An. St. Univ. „Al. I. Cuza", Secţ. II b (Geol.-Geogr.), **14,** p. 29—38, Iaşi.

GHERASI, N., ZIMMERMANN, V., ZIMMERMANN, P. (1968): Structura şi petrografia şisturilor cristaline din partea de N a munţilor Tarcu. D. S. Inst. geol., **54/1,** p. 55—80, Bucureşti.

GHERASI, N., VISARION, A., ZIMMERMANN, P. (1973): Consideraţii asupra vîrstei unor şisturi cristaline şi depozite sedimentare din autohtonul danubian, situate la marginea de nord a munţilor Godeanu. Stud. cerc. geol., **18/2,** p. 303—310, Bucureşti.

GRÜNENFELDER, M., POPESCU, G., SOROIU, M., ARSENESCU, V., BERZA, T. (1983); K-Ar and U-Pb dating of the metamorphic formations and the associated igneous bodies of the central South Carpathians. An. Inst. geol. geofiz., **61,** p. 37—45, Bucureşti.

IANOVICI, V., BORCOŞ, M., BLEAHU, M., PATRULIUS, D., LUPU, M., DIMITRESCU, R., SAVU, H. (1976): Geologia Munţilor Apuseni. Edit. Academiei R. S. R., p. 1—632, Bucureşti.

ILIESCU, V., KRÄUTNER, H. (1976): Precizarea vîrstei seriei de Repedea s. s. din munţii Rodnei, pe baza unor asociaţii palinologice. D. S. Inst. geol. geofiz., **62/4,** p. 3—10, Bucureşti.

ILIESCU, V., KRÄUTNER, H. (1978): Contribuţii la cunoaşterea vîrstei seriei de Rusaia. D. S. Inst. geol. geofiz., **64/4,** p. 7—15, Bucureşti.

ILIESCU, V., KRÄUTNER, H., KRÄUTNER, F., HANN, H. (1983): New palynological proofs on the Cambrian age of the Tulgheş Series. An. Inst. geol. geofiz., **59,** p. 7—11, Bucureşti.

ILIESCU, V., MUREŞAN, M. (1972): Asupra prezenţei Cambrianului inferior în Carpaţii Orientali — seria epimetamorfică de Tulgheş. D. S. Inst. geol., **58/4,** p. 23—38, Bucureşti.

ISTOCESCU, D. (1971): Studiul geologic al sectorului vestic al bazinului Crişului Alb şi al ramei munţilor Codru şi Highiş. Inst. Geol., St. tehn. econ., Ser. T, **8,** p. 1—201, Bucureşti.

KALENIC, M. (1966): First record of Lower Cambrian in Eastern Serbia. Spisan. Bulg. geol. druz. 1966, p. 216—219, Sofia.

KRÄUTNER, H. (1968): Vederi noi asupra masivului cristalin al Rodnei. Stud. cerc. geol., **13/2,** p. 337—355, Bucureşti.
KRÄUTNER, H. (1980): Lithostratigraphic correlation of Precambrian in the Romanian Carpathians. An. Inst. geol. geofiz., **57,** p. 229—296, Bucureşti.
KRÄUTNER, H., KRÄUTNER, F., TĂNĂSESCU, A., NEACŞU, V. (1976): Interprétation des âge radiometriques K-Ar pour les roches métamorphiques régénérées. Un exemple-les Carpates Orientales. An. Inst. geol. geofiz., **50,** p. 167—229, Bucureşti.
MAIER, O. (1974): Studiu geologic şi petrografic al masivului Locva. St. tehn. econ., I **5,** p. 9—173, Bucureşti.
MAIER, O., SOLOMON, I., ZIMMERMANN, P., ZIMMERMANN, V. (1979): Studiul geologic şi petrografic al cristalinului din partea sudică a munţilor Poiana Ruscă. An. Inst. geol. geofiz., **43,** p. 65—189, Bucureşti
MAIER, O., VISARION, A. (1976): Vîrsta formaţiunilor cristalofiliene din masivul Locva. D. S. Inst. geol., **62/4,** p. 11—22, Bucureşti.
MANOLESCU, G. (1937): Etude géologique et pétrographique dans les Munţii Vulcan. An. Inst. Geol. Rom., **18,** p. 79—112, Bucureşti.
MĂRUNŢIU, M., SEGHEDI. A. (1983): New data concerning the metamorphic rocks and metamorphic processes in the Eastern Almaj Mountains. Rev. Roum. Géol., **27,** p. 29—35, Bucureşti.
MÎNZATU, S., LEMNE, M., TIEPAC, I., COLIOS, E. (1974): Données géochronologiques concernant les massif granitoides de l'Autochthene Danubien situé au nord du Danube. Rev. Roum. Geol., **18,** p. 9—17, Bucureşti.
MÎNZATU, S., LEMNE, M., VÎJDEA, E., TĂNĂSESCU, A., IONCICĂ, M., TIEPAC, I. (1975): Date geocronologice obţinute pentru formaţiuni cristalofiliene şi masive eruptive din România. D. S. Inst. geol. geofiz., **61/5,** p. 85—111, Bucureşti.
MUREŞAN, M., TĂNĂSESCU, A., IONCICĂ, M. (1975): Concordanţa de vîrstă între metamorfismul regional proterozoic al granitoidelor de Hăghimaş şi cel al seriei de Bretila-Rarău. D. S. Inst. geol. geofiz., **61/5,** p. 135—149, Bucureşti.
NĂSTĂSEANU, S. (1975): General outlook on the Paleozoic of the Danubian Autochthonous. An. Inst. geol. geofiz., **46,** p. 191—218, Bucureşti.
ONICEANU, M., OLARU, L., ERHAN, V. (1977): An. St. Univ. „Al. I. Cuza", Secţ. II b (Geol.-Geogr.), **23,** p. 23—28, Iaşi.
PAVELESCU, L. (1953): Studiul geologic şi petrografic al regiunii centrale şi de sud-est a munţilor. Retezat. An. Com. Geol., **25,** p. 119—210, Bucureşti.
POPOVICI, I. (1978): Contribuţii la orizontarea litostratigrafică şi stabilirea vîrstei metamorfitelor din munţii Iezer-Păpuşa şi Leaota. D. S. Inst. geol. geofiz. **64/5,** p. 123—139, Bucureşti.
SAVU, H. (1973): Stratigrafia, tectonica şi metamorfismul formaţiunilor din etajul superior al Precambrianului mediu din regiunea Bozovici. Stud. cerc. geol., **18/1,** p. 13—28, Bucureşti.
SAVU, H., MAIER, O., BERCIA, I., BERZA, T. (1978): Assyntic metamorphosed formations in the South Carpathians. Rev. Roum. Géol., **22,** p. 7—17, Bucureşti.
SĂNDULESCU, M. (1984): Geotectonica României. Ed. Tehnică, p. 1—336, Bucureşti.
SOLOMON, I., MOŢOI, A., MĂRGĂRIT, M., MĂRGĂRIT, G. (1984): Cercetări geologice pe versantul estic al munţilor Gilău. D. S. Inst. geol. geofiz., **68/5,** p. 115—139, Bucureşti.
SOROIU, M., POPESCU, GH., KASPER, U., DIMITRESCU, R. (1969): Contributions préliminaires à la géochronologie des massif cristallins des Monts Apuseni. An. St. Univ. „Sl. I. Cuza'., Secţ. II b (Geol.), **15,** p. 25—33, Iaşi.
SOROIU, M., POPESCU, GH., GHERASI, N., ARSENESCU, V., ZIMMERMANN, P. (1970): K-Ar dating by neutron activation of some igneous and metamorphic rocks from the southern branch of the Romanian Carpathians. Ecl. Geol. Helv., **63/1,** p. 323—334, Basel.
STAN, N. (1984): Polimetamorfismul şisturilor cristaline situate în partea de est a masivului granitoid de Cherbelezu (munţii Almăj). D. S. Inst. geol. geofiz., **68/1,** p. 293—300, Bucureşti.
STĂNOIU, I. (1971): Notă preliminară asupra prezenţei Silurianului fosilifer în Carpaţii Meridionali. D. S. Inst. Geol., **57/4,** p. 5—15, Bucureşti.
STĂNOIU, I. (1972): Incercare de reconstituire a succesiunii Paleozoicului din partea externă a autohtonului danubian, cu privire specială asupra regiunii de la obîrşia văii Motru. D. S. Inst. Geol., **58/4,** p. 57—71, Bucureşti.
STĂNOIU, I. (1980): Prezenţa unor asociaţii macrofloristice în cadrul şisturilor cristaline ale formaţiunii de Tusu. D. S. Inst. geol. geofiz., **67/3,** p. 167—172, Bucureşti.
STRECKEISEN, A. (1934): Sur la tectonique des Carpates Méridionales. An. Inst. Geol. Rom., **16,** p. 327—418, Bucureşti.
VISARION, A., DIMITRESCU, R. (1971): Contribuţii la determinarea vîrstei unor şisturi cristaline din Munţii Apuseni. An. şt. Univ. "Al. I. Cuza", Secţ. II b (Geol.), **17,** p. 1—13, Iaşi.

VISARION, A., SOLOMON, I. (1974): Asupra prezenței Cambrianului epimetamorfic în munții Retezat. D. S. Inst. geol., **60/4**, p. 19—23, București.

VRÎBLEANSKI, B., VÎLOVA, G., GRAȘEVA, N., KOLCEVA, K., KOSTADINOV, T., NEDEALKOVA, S., IARANOV, B. (1963): Formațiunea diabazo-filitică în partea occidentală a regiunii Stara Planina. K. B. G. A., Congr. VI, **2**, p. 251—260, București.

Manuscript received, June 5, 1985

Acta Mineralogica-Petrographica, Szeged, XXVII., 71—88, 1985

TEXTURAL CHARACTERISTICS OF THE NILE DELTA COASTAL SANDS: AN APPLICATION IN RECONSTRUCTING THE DEPOSITIONAL ENVIRONMENTS

N. M. EL FISHAWI*

ABSTRACT

The textural characteristics of the Nile Delta coastal sands from the nearshore zone, breaker zone, beach, backshore zone, coastal dunes and River Nile were studied. A consistent difference exists between the coastal environments from the point of view of the bivariant scatter plots, the shape of log-probability curves and CM diagrams. This information has been used as an aid in determining the depositional environments of some unknown borehole sand deposits. The study of the vertical change for each unit of borehole sediments can be considered as a tool for reconstructing the depositional history and shoreline changes of the Nile Delta coast. It is indicated that the shoreline of the central part of the Nile Delta coast has advanced and marine sediments (nearshore zone, breaker zone, beach) with a thickness of 22 m have been laid over the backshore flat area. The false impression of many studies may be connected with the comparison of unknown sediments from one area with known sediments from another area.

INTRODUCTION

For many years sedimentary petrographers have attempted to use grain size to determine sedimentary environments. A survey of the extensive literature on this subject illustrates the steady progress that has been made toward this goal. Many excellent contributions have been published during the past twenty to thirty years, each providing new approaches and insights into the nature and significance of grain size distributions. One of the major problems of the analysis of grain size distributions is that the same sedimentary processes occur within a number of environments, and the consequent textural response is similar. Now that there are many physical criteria available to identify specific depositional environments, the textural studies do not need to stand alone, but can provide a separate line of evidence to aid in interpreting clastic deposits of unknown origin.

Several methods of treating the grain size distribution of sands were evaluated for their ability to discriminate between depositional environments of the Nile Delta coast. The following techniques were applied to sediment samples:

A. Technique of MASON—FOLK *(1958) and* FRIEDMAN *(1961, 1963):*

The basis of this technique depends on the relation between the grain size statistical parameters in the form of scatter plots. When the parameters are effective in differentiating between two environments, a boundary line is drawn that splits the fields best.

* Institute of Coastal Protection, Alexandria, Abu Qir, Egypt

B. Technique of VISHER *(1965, 1969):*

The shape of log-probability grain size distribution curves is used for environmental analysis. Analysis is based on recognizing rolling, saltation and suspension populations within a grain size distribution. The sorting, size range, number, degree of mixing and the points of truncation of these populations vary systematically in relation to sedimentary environments.

C. Technique of PASSEGA *(1957, 1962, 1964):*

A CM diagram is constructed by plotting the one percentile particle diameter in μm (C) versus the fifty percentile particle diameter in μm (M) on bilogarithmic paper. PASSEGA argued that the texture of a clastic sediment represented in this way is characteristic of the depositional agent. The transport mechanism that built up the deposit can be suggested on the basis of the shape and the arrangement of the pattern of the sample points in a CM diagram.

Petrographic characteristics of recent sands of the Nile Delta coast from nearshore, breaker zone, beach, backshore, coastal dune and river environments have been studied, to determine if there are textural characteristics which will permit diagnosis of the depositional environment. By using different techniques, the study shows that depositional environments can be recognized from grain size data. These techniques were applied in order to investigate the origin of deposition in subsurface sediments.

SAMPLING AND METHODS OF STUDY

Samples were collected along the Nile Delta coast between Rosetta and Damietta *(Fig. 1)*. During July, 1978, the coast was surveyed and samples were collected at 3 km intervals. The sample net consisted of 49 transects at right angles to the coast.

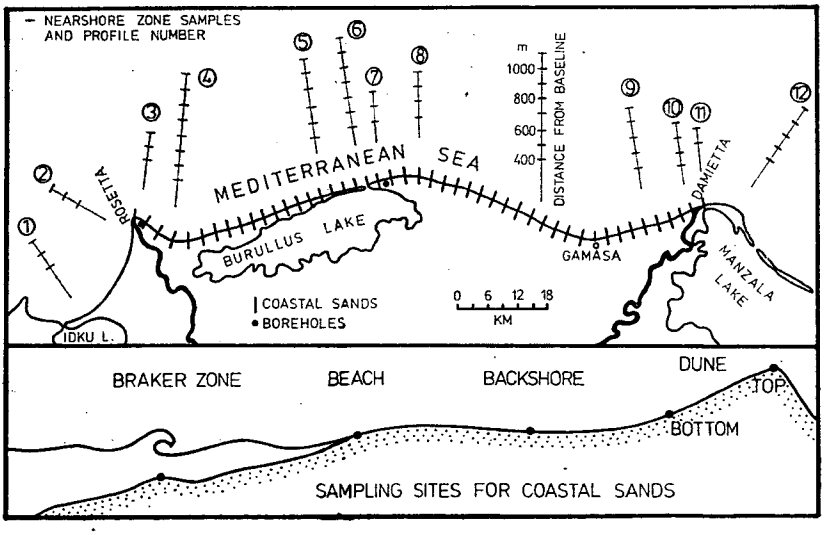

Fig. 1. Location map and sampling sites for the recent environments of the Nile Delta coast

Samples were collected from the shallow water where the waves break at the 1.00—1.25 m depth below the sea level (breaker zone samples), on the surf zone of the beach (beach samples), on the flat area at the back of the beach (backshore zone samples) and from the bottom and top of the coastal dunes (dune samples). In sampling, care was taken not to collect any special concentrate represented by unusual conditions. In general, the samples were taken from the top 5 cm of each environmental deposit.

In addition, samples from the nearshore zone, the River Nile and borehole sediments were obtained from the Institute of Coastal Research, Alexandria. Twelve nearshore profiles were selected and samples were collected every 100 m until a depth of 6 m below sea level was reached *(Fig. 1)*. Two boreholes with a depth of 30 m were selected at Rosetta and Burullus headlands for comparative studies. Borehole samples were secured every 1 m.

Since the sands under investigation are friable, no disaggregation was found necessary. All the samples collected were washed, dried and split. Mechanical analysis was carried out by the conventional sieving method, with screens placed at one-phi intervals. It is planned to use the half-phi intervals in between 3—4 phi sets because they give more accurate cumulative curves. About 100 g of materials was taken for analysis, using a mechanical shaker with a sieving time of 20 minutes. The sieve meshes give the class intervals 2000, 1000, 500, 250, 125, 90, 63 and 37 μm. These correspond to the phi classes of −1, 0, 1, 2, 3, 3.5, 4 and 5, respectively.

The data were plotted as cumulative curves on probability paper to ensure maximum accuracy in determining the grain size parameters by the graphical method (FOLK, 1968). Statistical measures proposed by FOLK and WARD (1957) for median diameter, sorting, skewness and kurtosis were then obtained from values intercepted at specific percentiles in these curves.

GRAIN SIZE VARIATION OF THE COASTAL SANDS

The grain size variation of the Nile Delta coastal environments was analysed along 49 profiles normal to the shoreline over a distance of 144 km *(Fig. 1)*. Each profile covers the nearshore zone, breaker zone, beach, backshore and dune sands. River Nile sands were also represented.

Figure 2 shows the average cumulative percentages and histograms for each environment; Table 1 illustrates the data. A visual inspection of the modal classes and tails on the histograms can be used as a preliminary interpretation of the energy conditions within each environment. The coastal sands are unimodal, but differ in the modal class and tails. Nearshore zone sands have a modal class of 3—4Φ units. In moving through the breaker zone to the beach sands, there is a shift in the modal class to the coarser size of 2—3Φ. The breaker zone retains a higher percentage of coarser fractions than does the beach sands. This indicates an increase in the energy level from the nearshore to the breaker zone, and then a slight decrease to the beach. Backshore sands keep the same feature, but their coarse tail is slightly more pronounced than the beach one. The bottom of the dune sands has the mode in the 1—2Φ unit class, while the top sands once again display a mode in the 2—3Φ unit class. Therefore, it can be said that the bottom of the dune receives more energy than the backshore, and the energy level slightly decreases from the bottom to the top of dunes. On the other hand, the River Nile sands show distinctive tails in the coarse fractions with a modal class of 2—3Φ units.

TABLE 1

Average wt. % of fractions and statistical parameters for the Nile Delta coastal environmental sands

Environment	Wt. % of fractions in Φ units								Statistical parameters			
	—2 to —1	—1 to 0	0 to 1	1 to 2	2 to 3	3 to 4	4 to 4	Pan	D_{50}	σ_I	Sk_I	K_G
Nearshore	—	0.16	0.84	2.02	17.04	68.32	8.56	3.06	3.35	0.53	+.22	1.64
Breaker zone	0.63	1.68	7.74	18.88	56.76	14.10	0.33	0.16	2.28	0.57	−.10	1.12
Beach	—	0.11	2.12	19.36	65.92	12.32	0.17	0.08	2.40	0.44	−0.1	1.04
Backshore	—	—	3.47	22.28	60.73	12.22	0.82	0.48	2.36	0.51	+0.4	1.09
Dune bottom	—	—	5.10	45.81	44.25	4.50	0.18	0.16	1.98	0.55	+0.6	1.01
Dune top	—	—	0.84	32.70	58.50	7.21	0.27	0.46	2.22	0.48	+.11	1.01
River Nile	1.58	4.10	14.36	27.08	44.50	7.44	0.67	0.26	1.86	0.74	−.03	1.11

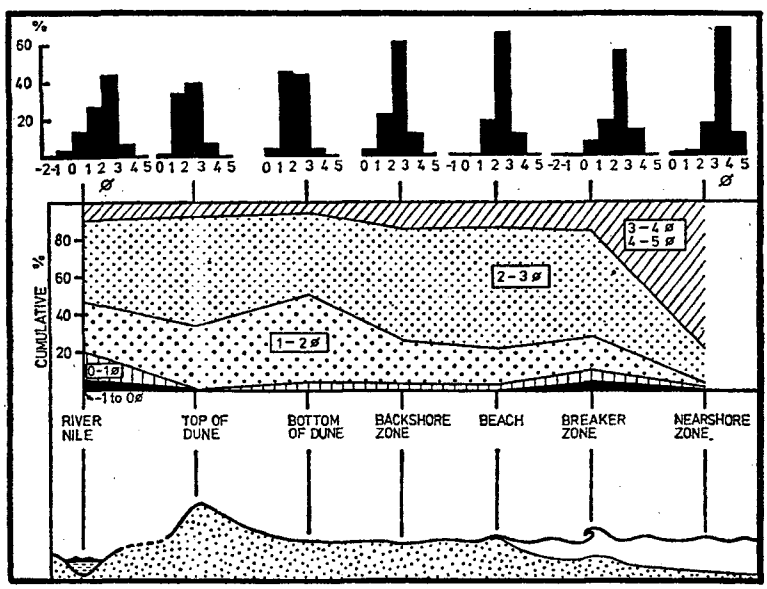

Fig. 2. Variation of cumulative percentages and histograms normal to the shoreline

BIVARIANT PLOT TECHNIQUE

The area along the Nile Delta coast was chosen as a testing ground to determine if there exists a statistically significant difference in grain size properties between the sands of the various environments. The textural evidence for environmental identification has been pursued during the last two decades; the most significant are the studies by MASON and FOLK (1958), FRIEDMAN (1961, 1967), MARTINS (1965), MOIOLA and WEISER (1968), HAILS (1967), HAILS and HOYT (1969) and EL FISHAWI *et al.* (1976). These authors found that the statistical parameters are environmentally sensitive, and combinations of these parameters permit distinction between different depositional environments. EL FISHAWI (1977) and GINDY *et al.* (1982) demonstrated

that bivariant plots of skewness *versus* grain diameter gave the best differentiation between the sands of the nearshore, beach and coastal dune. On the other hand, scatter plots of grain size parameters fail to distinguish reliably between environments, as shown by SHEPARD and YOUNG (1961) and SOLOHUB and KLOVAN (1970).

Most authors plotted only two environments at a time in their graphs, and thus decided easily where to place the line that splits the fields best. MASON and FOLK (1958) plot three environments in one graph, but FRIEDMAN (1961, 1967) does not, nor do MOIOLA and WEISER (1968). The range of values of the statistical parameters of the coastal sands is wide, but many environmental sands overlap and all fields could not be shown separately. Therefore, the nearshore, beach, dune and River Nile sands can be represented in one graph, while the breaker zone and backshore can be shown in another one.

The statistical parameters generally used may not be the best means of describing most grain size distributions. However, it may be possible to determine which pair of parameters yields an optimum discrimination between environments. The properties of the Nile Delta coastal sands have been compared in 3 effective scatter plots as shown in *Figs. 3—5.*

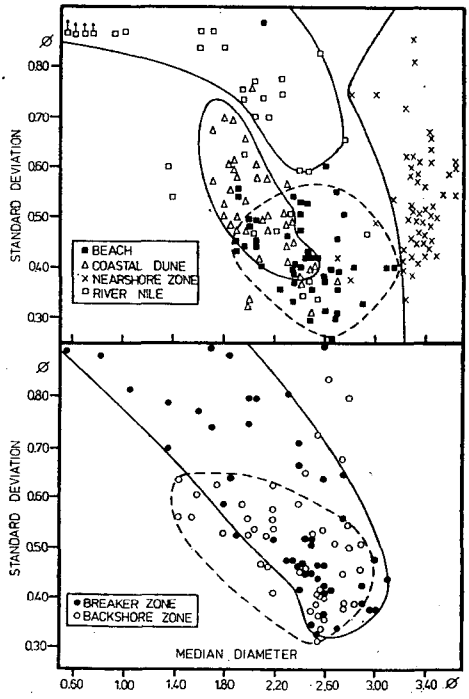

Fig. 3. Bivariate plot of median size *versus* standard deviation

Median diameter vs. standard deviation

In *Fig. 3* the median diameter is plotted against the standard deviation for sands from various environments. It results a nearly complete separation of distinct fields, although some overlap is exhibited. The River Nile sands have the worst standard

deviation values and the coarsest median diameter. The nearshore sands are the finest ones and show a median size finer than 3.20Φ; the majority of the standard deviation values lie in the ranges of well and moderately well sorted. The beach sands are better sorted and relatively finer than the dune sands, although a narrow mixed area is exhibited between them. The breaker zone sands scatter in a significant trend, where the distribution field is long and narrow. Coarse, poorly-sorted sands and fine, well-sorted sands occur together within the breaker zone, indicating the wide change of the breaker heights. In general, the backshore zone sands are finer, well sorted and restricted better in their field than the breaker zone sands.

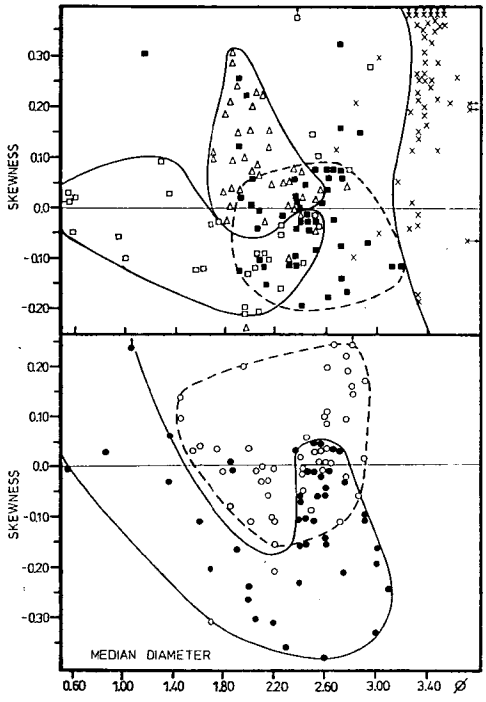

Fig. 4. Bivariate plot of median size *versus* skewness. Symboles as in *Fig. 3*.

A strong negative correlation appears to exist between the median size and the standard deviation, with the exception of the nearshore sands. The standard deviation is practically dependent on the median size: the coarser sands are less sorted than the finer ones. MASON and FOLK (1958) found no correlation between the median size and the standard deviation, which may be connected with the small range of their parameters.

Median diameter vs. skewness

Separation into environmentally designated fields is possible by plotting median size *versus* skewness *(Fig. 4)*. In this diagram, the best differentiation of the samples is accomplished with the aid of the skewness. Both nearshore and dune sands are

for the most part highly positively skewed, but the latter are coarser. The River Nile sands are coarser than the beach ones; they show both negative and positive skewness, with a considerable difference; they contain percentages of negative skewness samples of 53% and 68%, respectively. The breaker zone and backshore sands fall into distinct groupings, separating the plot of *Fig. 4* into two environmental fields. The breaker zone sands are for the most part negatively skewed (72%) with high values. The backshore sands are generally positively skewed (61%) and the remainder give symmetrical or nearly symmetrical curves. No predictable correlation could be determined between the median size and the skewness.

Median diameter vs. first percentile

In *Fig. 5,* the first percentile is plotted *versus* the median size in phi units for all coastal sands, and shows a good separation into environmental fields. The River Nile sands have the coarsest maximum size in the first percentile range. The 1% range of the dune sands is relatively coarser than that of the beach sands. Nearshore sands have the finest size in this range. The backshore sands are finer in both the 1% and 50% ranges than the breaker zone sands, which show wide scattering toward the coarse end. In general, the separation owes more to the 1% range than to the median size; the 1% range correlates well with the environment.

In conclusion, of the different statistical parameters used, bivariant plots of median size *versus* standard deviation, skewness and first percentile gave the best sepa-

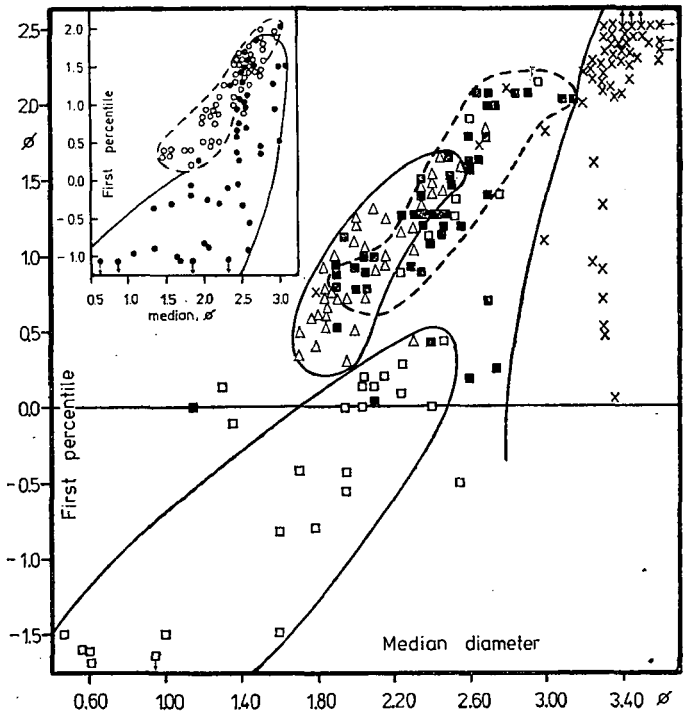

Fig. 5. Bivariate plot of median size *versus* the first percentile. Symboles as in *Fig. 3.*

ration between the sands of the coastal environments. On the other hand, the combinations of kurtosis *versus* median and skewness are ineffective, and complete overlap is exhibited between the sands of different depositional environments.

LOG-PROBABILITY CURVE TECHNIQUE

One of the most significant papers relating sedimentation dynamics to texture was published by INMAN (1949). He recognized that there are three fundamental modes of transport; surface creep, saltation and suspension. Many authors, including SINDOWSKI (1958), FULLER (1961), SPENCER (1963) and VISHER (1965, 1969), used the grain size distribution curves drawn on probability paper for environmental analysis. For these curves, the truncation points between traction, saltation and suspension transport may reflect the physical conditions at the time of deposition, and hence give the true limiting value of grain size for each mode of transport. The most important aspect in the analysis of textural patterns is the recognition of separate log-normal populations which relate to the position of truncation points and the degree of mixing between these population. Moreover, it is valuable to depend upon the degree of sorting as indicated by the slope of each population to characterize the environmental deposits.

Figure 6 shows the grain size distribution curves for the Nile Delta coastal environments. The analysis revealed that there are several different fundamental curve shapes and many differences appear.

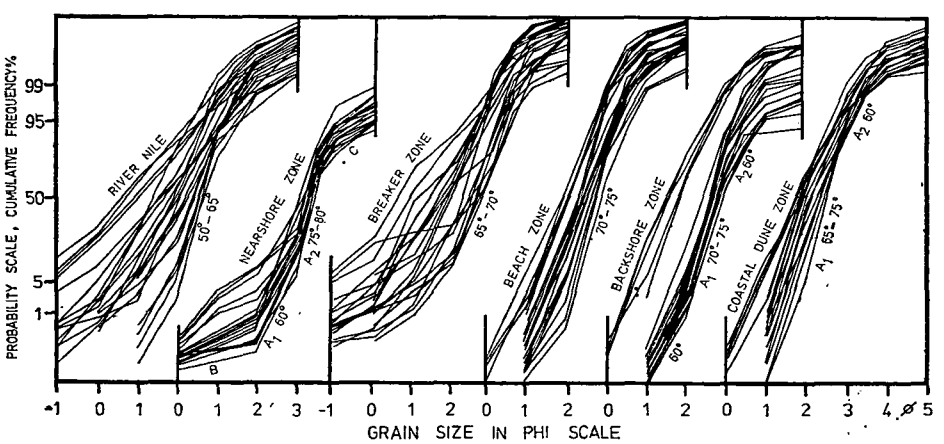

Fig. 6. Grain size distribution curves, probability scale, for the Nile Delta coastal environments. B: rolling, A_1: coarse saltation, A_2: fine saltation, C: suspension.

River Nile sands

Of special significance is the fact that the samples are characterized by high percentages of sediment in the coarse and very coarse rolling population. Size distribution curves show the three population modes of transport with a high degree of mixing. The positions of the coarse truncation points are highly variable and the range is between 0—2Φ (1—30%) of the distribution. The saltation population has a

size range between 2—3Φ (5—95%). It is clearly observed that mixing occurs between rolling and saltation populations. A suspension population has been defined; it represents less than 1% of the distribution. In general, the River Nile sands have poorly sorted populations, usually with a slope between 50° and 65°.

Nearshore sands

The rolling population in the nearshore samples is more pronounced, without mixing, than that in the Nile samples. The truncation point lies at 2Φ with values less than 5%. Of most significance is the development of two saltation populations with different slopes. The coarse saltation population extends between 2—3Φ (7—30%), with a slope of 60°. The fine saltation is better sorted than the coarser one (75°—80°) and has a size range between 3.0—3.5Φ (5—80%). The suspension population is well defined and ranges between 70—99% of the distribution.

Breaker zone sands

The grain size distribution curves for breaker zone sands appear to be fundamentally different from those described for the Nile sands, but some similarities do exist. These sands reflect the characteristic features of the breaker waves. They have a well-developed rolling population, relatively smaller in amount and less sorted than that in the Nile sands. This population joins the saltation population without mixing between 1—2Φ. The saltation population has a size range between 5—95% and is truncated well at the fine end to contain the suspension population near 3.5Φ. The slope of the saltation population ranges between 65° and 70°, and therefore it is better sorted than that in Nile sands.

Beach sands

The grain size distribution curves for the beach sands appear to be related to the action of waves on the beach sands, with a distinctive pattern. The absence of a rolling population characterizes the majority of beach sands. It may be true that the rolling and saltation populations are completely mixed together, with the same degree of slope. The development of a well sorted saltation population with a slope between 70° and 75° is the distinguishing characteristic of the beach sands. This population represents 99% of the size distribution. The suspension population is defined well and is truncated at 3.5Φ with an amount of 1%.

Backshore sands

The backshore zone curves are different from those developed in other environments. In the majority of the samples, the main difference lies in the presence of a somewhat mixed rolling population and two well developed saltation populations. The rolling population occurs between 1—2Φ (1—10%), with a slope of 60°. The coarse saltation population is better sorted than the finer one. The slope of the coarse saltation population ranges between 70° and 75°, with a maximum value of 90% (2—3Φ), while the finer one ranges between 60—90% (3—4Φ), with a slope

of 60°. A well-developed suspension population occurs between 4—5Φ, with a variable amount of very fine sand and silt, which ranges between 95—99.90% of the distribution.

Coastal dune sands

The rolling population is absent from the coastal dune sands. The lack of this population in the beach and dune, and its weakness in the backshore sands appears to characterize the inland coastal deposits. Two saltation populations can be observed. The coarser one extends between 0—3Φ and is better sorted (65°—75°) than the finer one (60°), which extends between 3—4Φ. The amount of the suspension appears to be less than 1%.

CM DIAGRAM TECHNIQUE

PASSEGA (1957, 1962, 1964) proposed a combination on a bilogarithmic diagram of two parameters of a cumulative grain size distribution; the coarsest one percentile value C, and the median diameter M in μm. He argued that the texture of a clastic sediment represented in this way is characteristic of the depositional agent. The transport mechanism that built up the deposit can be suggested on the basis of the shape and the arrangement of the pattern of the sample points in a CM diagram. The position of sample points in a CM pattern depends on the mode and agent of transport. The change from a pattern parallel to the CM line (graded suspension) to a pattern parallel to the C-axis (rolling, suspension) corresponds to a difference in mode of deposition. The maximum value of C in the pattern is an indication of maximum turbulence caused by dynamic forces in each environment.

This subject is an attempt to establish the relationships between the textures of sediments and coastal environments. The sediments of each environment are represented in a CM pattern as shown in *Fig. 7*. Each pattern is formed by 32—53 samples.

Nearshore zone pattern

The CM pattern of the nearshore sands is generally narrow and long. It can be subdivided into 2 groups *(Fig. 7A)*. The first group is a pattern of concentrated points on the finer lower side with C values of 125—270 μm and M values of 55—125 μm. The upper coarser group is long, narrow and parallel to the C-axis; the C values are limited to 300—2000 μm, while the M values range between 95—160 μm. During periods of strong wave activity, there are many indications that the waves can cause some movement toward the nearshore zone. TRASK (1955) observed that at a depth of about 14 m, the passing waves disturbed the bottom sediments. The tractive currents generated by surface waves can roll coarser sand grains with C values of 300—2000 μm, to form fairly poorly sorted deposits. Finer grains with maximum C values of 270 μm are kept in suspension; they are generally better sorted and form the fine groups of the pattern. In quiet conditions within 6 m depth, these sediments settle together and give their characteristic pattern to the nearshore sediments.

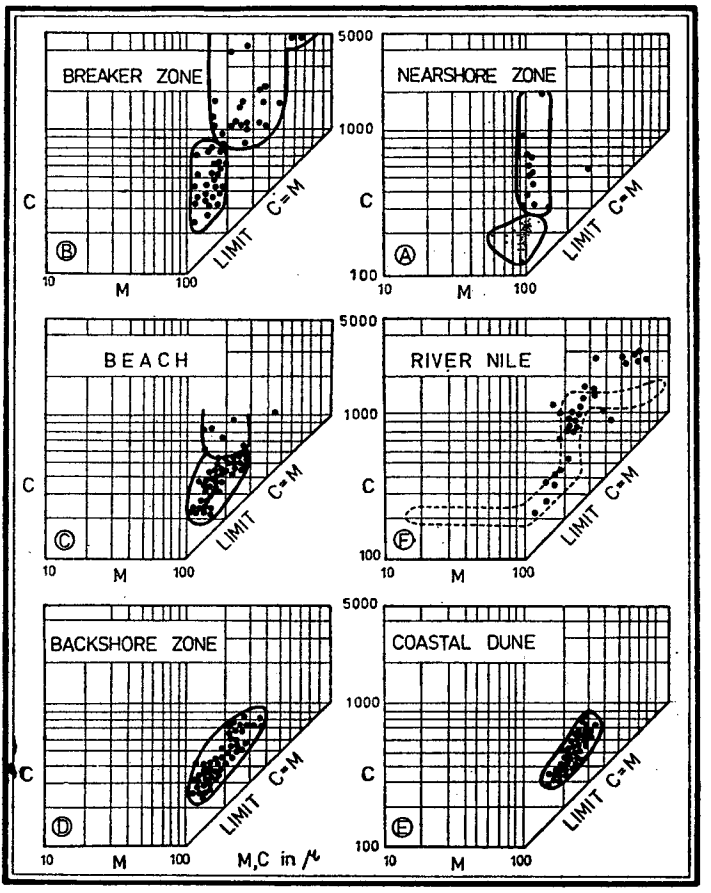

Fig. 7. CM diagrams for the Nile Delta coastal environments

Breaker zone pattern

The CM pattern of the breaker zone sands is the widest and longest pattern among the coastal environments. Two parts can be observed, depending on the spreading C with relation to the M values *(Fig. 7B)*. The upper part is formed essentially by particles with C values of 850—5000 μm and M values of 170—700 μm. The lower part is finer, with C values of 250—800 μm and M values of 100—200 μm. Therefore, the breaker zone sands are characterized by a restricted variation of the M values whilst the C values are more scattered, resulting in a CM pattern elongated and parallel to the C-axis. If the M values are not too strongly varying, the coarse grains in sediments may be responsible for the rolling pattern of these sediments by spreading the C values as in the breaker zone. The approaching breakers carry all available sediments; the coarser part can be transported by rolling under the action of vigorous waves, while the finer one can also be transported by rolling when the conditions became weaker. The breaker zone sands are often poorly sorted because, when the coarse sands settle, a large amount of fine sand generally settles with them and the pattern tends to be distant from the limit C=M.

Beach zone pattern

The distribution of the points in the CM pattern gives a broad shape *(Fig. 7C)*. The points are concentrated in the finer lower part and scattered in the coarser upper one. The lower part is limited by C values of 200—600 μm and M values of 100—300 μm. The sediment points are distributed parallel to the limit C=M, indicating an area of good sorting. It is observed that C is subjected to marked variations, while M varies proportionally. The upper part of the pattern consists of scattered coarser sands, where C ranges between 600—1000 μm and M between 130—450 μm. These sediments are poorly sorted, because their points are situated at a considerable distance from the limit C=M. The action of the tractive current caused by the waves is reflected in the CM pattern of the beach sands. The approaching waves keep the finer materials in suspension, while the coarser ones can be transported by means of rolling.

Backshore and coastal dune pattern

The backshore and dune sands have the same distribution points, but the field of the dune is more condensed *(Fig. 7D* and *E)*. These sediments are characterized by their elongation parallel to the limit C=M, where C and M are directly covariant. The backshore pattern is limited by C values of 220—850 μm and M values of 120—350 μm, while the dune pattern is limited by C values of 280—850 μm and M values of 150—380 μm. These sediment are well sorted, because the wind is responsible for their transport. Dry winds with an onshore directional component actively deflate the beach and carry its sediment to the backshore and dune zones. The aeolian sediments may be transported as a graded suspension in air; the coarse grains are transported close to the ground, while the finer ones are blown far up into the air.

River Nile pattern

The River Nile sands are sufficiently coarse and fine to form a more complete CM pattern than for the other environmental deposits. The CM pattern of the sands *(Fig. 7F)* shows that the fine sands are transported as graded suspensions, the medium sands by rolling and as suspensions, and the coarsest ones by rolling.

The deposit formed from a graded suspension when turbulence decreases is characterized by a value of C proportional to the value of M. It is observed from *Fig. 7* that the relationship between C and M becomes very close on passing from the breaker zone through the beach and backshore and up to the coastal dune sands. At the same time the sorting improves. The strict proportionality between C and M indicates one origin for the coastal sands, which may arise from offshore drift. When the waves disturb the bottom sediments, the coarsest part of the suspension, which tends to stay in the bottom water, moves shoreward, while finer particles will move seaward (KING, 1972). This selective transportation keeps the coarses materials in the breaker zone, whereas most of the fine and very fine materials go back and deposit in the nearshore zone. As might be expected from the interpretation of the CM patterns, some of the coastal sands are deposited by a single transport mechanism, while the other are subjected to more complicated ones. It is generally possible to differentiate between coastal environments with the criteria given by the CM pattern.

Following the finding that a consistent difference exists between the Nile Delta coastal environments from the point of view of the shape of the log-probability curves, bivariant plots and CM diagrams, this information has been used as an aid in determining the depositional environments of some unknown sand deposits. Two borehole samples to a depth of 30 m were chosen at Rosetta and Burullus. Table 2 illustrates the grain size parameters.

To get a better idea of the depositional history of the subsurface sediments, samples from known depositional environments must be studied and compared with the subsurface sediments at the same area. The false impression of many studies may be connected with the comparison of unknown sediments from one area with known sediments from another area. Therefore, the shape of the grain size distribution curves, bivariant plots and CM diagrams of the Nile Delta coastal environments have been used to predict the depositional environments of the subsurface sands of the Nile Delta coast at Rosetta and Burullus. The study of the vertical change for each unit of the borehole sediments can be considered a tool for the depositional history and shoreline changes of the Nile Delta coast.

Log-probability curves of borehole sands

A comparison of log-probability curve shapes between known depositional environments and subsurface sequences will be available for interpreting the origin of the borehole sands. Log-probability curves for borehole sands were plotted, and those showing similar features were grouped together in one unit according to their depth. The next step was to compare each unit with *Fig. 6* to predict the environment of deposition.

For Rosetta borehole, three units can be recognized *(Fig. 8A)*. The following depths reveal the origin of each unit:

a) 29—19 m depth: backshore zone. It is followed by a 10 m thickness of silty clay deposits which may be derived from Rosetta branch.
b) 8—5 m depth: nearshore zone.
c) 4—1 m depth: beach zone.

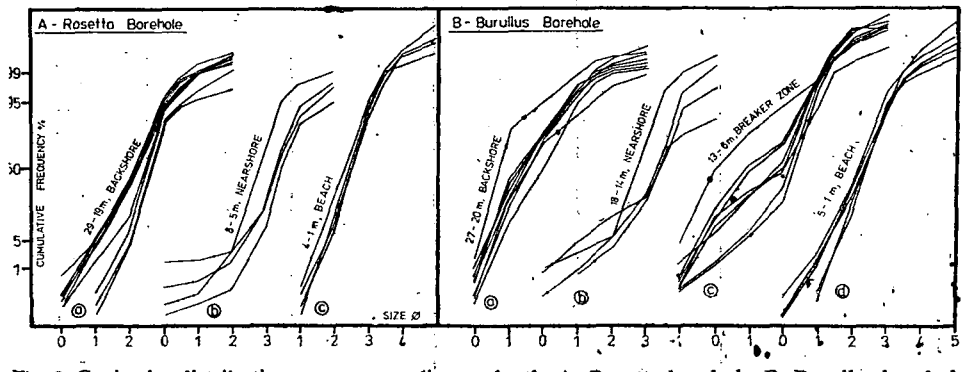

Fig. 8. Grain size distribution curves according to depth. A: Rosetta borehole, B: Burullus borehole

TABLE 2

Grain size parameters of borehole sands

A. Rosetta borehole, BH 6:

Depth m	D_{50}	σ_I	SK_I	K_G	C μm	M μm
1	2.50	0.36	0.13	1.14	342	177
2	2.30	0.46	—.02	1.06	435	203
3	2.55	0.42	0.02	1.08	380	171
4	2.50	0.42	0.02	1.08	406	177
5	2.85	0.43	—.05	0.99	320	140
6	3.50	0.49	0.21	1.26	196	88
7	3.50	0.59	—.12	1.64	1000	88
8	3.35	0.44	0.13	1.39	287	98
9	2.40	0.35	—.02	0.94	380	190
19	2.25	0.61	—.11	1.15	660	210
20	2.15	0.62	—.09	1.08	683	225
21	2.20	0.61	—.09	1.08	637	218
22	2.15	0.60	—.16	1.02	683	225
24	2.45	0.43	—.10	1.31	555	183
25	2.50	0.39	0.04	1.27	380	177
26	2.60	0.42	0.16	1.46	330	165
27	2.60	0.44	0.19	1.43	320	165
28	2.15	0.56	—.10	1.04	933	225
29	2.60	0.43	0.16	1.19	354	165

B. Burullus borehole, BH 3:

Depth m	D_{50}	σ_I	SK_I	K_G	C μm	M μm
1	2.20	0.51	0.00	1.07	518	218
2	2.30	0.54	—.05	1.05	536	203
3	2.35	0.43	0.05	1.08	392	196
4	2.40	0.41	—.04	1.15	420	190
5	2.20	0.50	—.17	1.07	637	218
6	1.85	0.90	—.37	0.91	2144	277
7	2.15	0.58	—.31	1.26	1150	225
8	2.30	0.60	—.32	1.80	1000	203
9	2.00	0.94	—.48	0.95	1570	250
10	1.10	0.97	0.12	0.78	1626	467
11	0.95	1.04	0.12	0.72	1803	518
12	0.05	0.91	0.32	1.12	2640	966
13	2.05	1.13	—.43	0.77	1625	242
14	2.70	0.43	—.05	0.99	933	154
15	3.25	0.61	—.33	1.36	484	105
16	3.30	1.27	0.54	2.30	435	102
18	3.35	0.85	—.37	1.90	707	98
20	1.55	0.90	0.28	1.07	871	342
21	1.55	0.66	0.19	1.06	785	342
22	1.45	0.65	0.18	0.93	841	366
23	1.40	0.71	0.11	1.01	966	380
24	0.80	0.49	0.10	1.73	1036	574
25	1.30	0.71	0.19	0.90	933	406
26	1.25	0.73	0.27	0.98	901	420
27	1.90	0.68	0.01	0.93	707	268

For Burullus borehole, four units were observed *(Fig. 8B)*. The following depths reveal the origin of each unit:

a) 27—20 m depth: backshore zone.
b) 18—14 m depth: nearshore zone.
c) 13—6 m depth: breaker zone.
d) 5—1 m depth: beach zone.

Bivariant plots of borehole sands

The preliminary origins of the subsurface units, as suggested by the shape of the grain size distribution curves, should be examined by plotting their data in bivariant plots of known fields. A plot of median diameter against skewness *(Fig. 4)* provides the best menas for distinguishing beach, backshore, nearshore and breaker zone sands. By replotting the boundary of these environments, the depositional environments of the borehole units can be predicted as shown in *Fig. 9*.

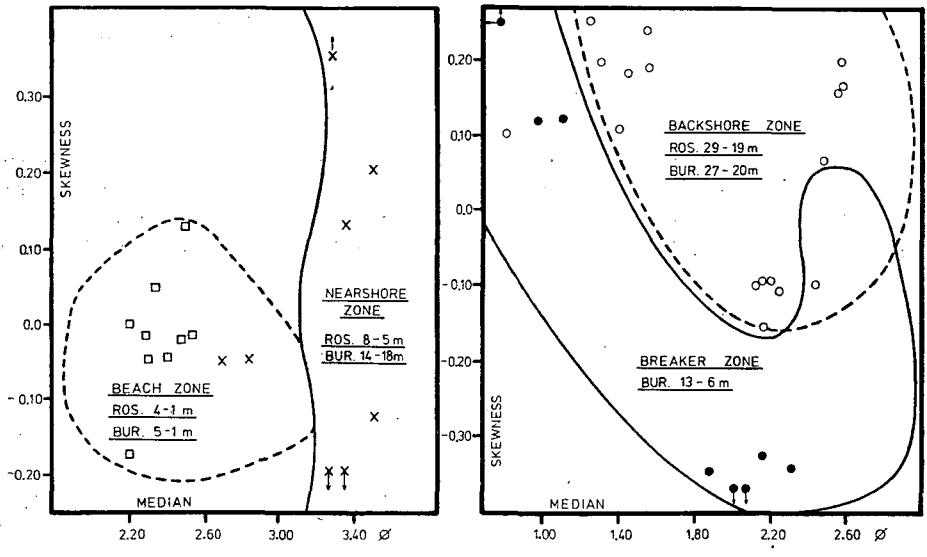

Fig. 9. The origin of Rosetta and Burullus borehole sands as indicated by the relation between median size and skewness. The boundaries are from *Fig. 4*.

In Rosetta and Burullus boreholes, the sediments of the upper 5 m thickness lie in a given position of the beach sands. Rosetta sediments between 8—5 m depth, and Burullus sediments between 18—14 m depth, were found to be nearshore. Burullus sands between 13—6 m depth lie within the breaker zone field. Rosetta sands between 29—19 m depth, and Burullus sands between 27—20 m depth, were found to be backshore. As shown before, the same results were obtained by using the shape of the curves and the bivariant plots for the prediction of the subsurface units.

CM pattern of borehole sands

The boundaries of the environments were replotted from the CM patterns in *Fig. 7*. The data of the subsurface units were plotted for the suggested environmental fields to test the degree of fitness *(Fig. 10)*. The examined samples from the

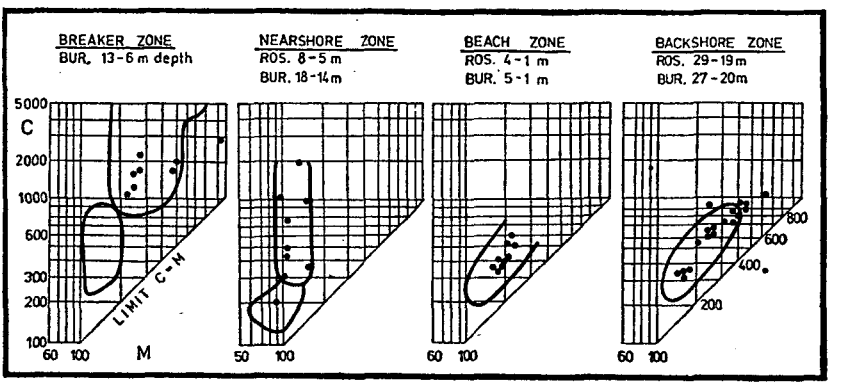

Fig. 10. CM patterns for Rosetta and Burullus borehole sands.

breaker zone, nearshore and beach lay inside each given field. The majority of the backshore samples were found to be inside the given field; some samples were located outside, but near the boundary. Thus, the application of the CM pattern for the subsurface units gave the same results as in the distribution curves and bivariant plots.

Shoreline changes: a result

Distinguishing subsurface coastal sediments may serve as a tool to reconstruct the historical geology and the approximate position of the shoreline in a stratigraphic sequence. The results obtained in this study are summarized in *Fig. 11*.

The position of the Rosetta borehole was located at a wide backshore flat, as indicated by the lower 29—19 m depth sediments. This unit was followed by a 10 m thickness of silty clay deposits, maybe from Rosetta branch. A transgression was observed, and as a result the location of the borehole was situated in the nearshore zone, as represented by the sediments of 8—5 m depth. The shoreline began to retreat gradually and then stopped near the present shoreline, leaving the upper 4 m thickness unit as a beach zone.

The position of the Burullus borehole was located at the backshore flat. The shoreline advanced and a 5 m thickness of nearshore deposits was laid over the 8 m thickness of the backshore deposits. A little regression of the shoreline was observed in that the position of the borehole was located in the breaker zone. After an 8 m thickness of breaker zone sands, the shoreline retreated again, to stop near the present shoreline, as indicated by the upper 5 m thickness of beach sediments.

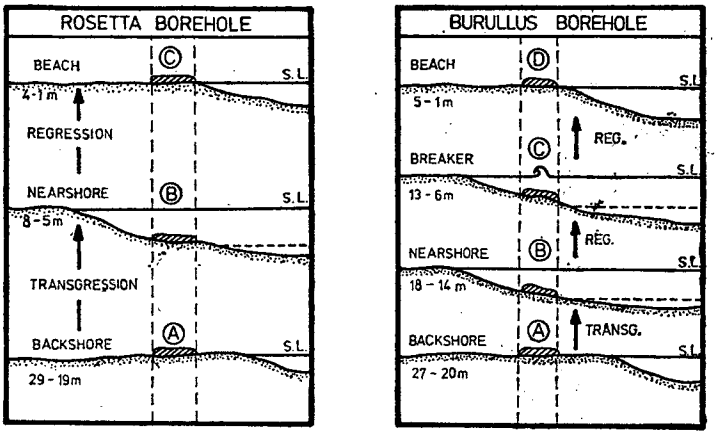

Fig. 11. Transgression and regression of shoreline at Rosetta and Burullus

CONCLUSIONS

1. It is possible to demonstrate some changes in sand textures normal to the shoreline. The breaker zone receives more coarse and very coarse sands than does the beach zone. The median diameter decreases, the sorting improves and the skewness trends from negative to positive as one progresses from the breaker zone across the beach and backshore and up to the dune sands.

2. Several methods of treating the grain size distribution of coastal sands were evaluated for their ability to discriminate between the depositional environments. Of the different scatter plots used, bivariant plots of median diameter versus standard deviation, skewness and first percentile gave the best discriminations between the sands of the River Nile, nearshore, breaker zone, beach, backshore and coastal dune.

3. The analysis of log-probability grain size distribution curves was found to be a good method for distinguishing between the depositional environments. The most important aspect in the analysis of textural patterns is the recognition of separate log-normal populations which are related to the position of truncation points and the degree of mixing between these populations. It is also valuable to make use of the degree of sorting and the extension of coarse and fine tails.

4. The mechanism of the transport that built up the deposit can be suggested on the basis of the shape and arrangement of the pattern of the sample points in a CM diagram. The position of the points in a CM pattern depends on the mode and agent of transport. This method permitted distinction between the Nile Delta coastal environments.

5. After the discovery that a consistent difference exists between the Nile Delta coastal environments from the point of view of the bivariant plots, the shape of the log-probability curves and the CM diagrams, this information is used as an aid in determining the depositional environments of borehole samples on Rosetta and Burullus. The false impression of many studies may be connected with the comparison of unknown sediments from one area with known sediments from another area.

6. The study of the vertical change for each unit of the borehole sediments can be considered a tool for the depositional history and shoreline changes of the Nile

Delta coast. Distinguishing subsurface sediments of the Burullus headland indicates that the position of the borehole was located at the backshore flat. The shoreline has advanced and a 5 m thickness of nearshore zone deposite has been laid over the backshore sands. A slight regression of the shoreline happened in that the position of the borehole was located in the breaker zone. After an 8 m thickness of breaker zone deposits, the shoreline continued to retreat again and stopped near the present shoreline, as indicated by the upper 5 m thickness of the beach sands.

REFERENCES

EL FISHAWI, N. M. (1977): Sedimentological studies of the present Nile Delta sediments on some accretional and erosional areas between Burullus and Gamasa. M. Sc. thesis, Alexandria Univ., 143 p.

EL FISHAWI, N. M., SESTINI, G., FAHMY, M. and SHAWKI, A. (1976): Grain size of the Nile Delta beach sands. In: Proc. Sem. on Nile Delta Sed., Alex., Oct., 1975, p. 79—94.

FOLK, R. L. (1968): Petrology of sedimentary rocks. Hemphill's, Texas, 170 p.

FOLK, R. L. and WARD, W. C. (1957): Brazos River bar, a study in the significance of grain size parameters. Jour. Sed. Petr., V. **27**, p. 3—27.

FRIEDMAN, G. M. (1961): Distinction between dune, beach and river sands from their textural characteristics. Jour. Sed. Petr., V. **31**, p. 514—529.

FRIEDMAN, G. M. (1967): Dynamic processes and statistical parameters compared for size frequency distributions of beach and river sands. Jour. Sed. Petr., V. **37**, p. 327—354.

FULLER, A. O. (1961): Size characteristics of shallow marine sands from Cape of Good Hope, South Africa,. Jour. Sed. Petr., V. **31**, p. 256—261.

GINDY, A. R., EL ASKARY, M. A. and EL FISHAWI, N. M. (1982): The skewness — median environmental discriminator for some recent and ancient sediments from Egypt. N. Jb. Geol. Paläont. Mh., Stuttgart, H. **12**, p. 705—722.

HAILS, J. R. (1967): Significance of statistical parameters for distinguishing sedimentary environments in New South Wales, Australia. Jour. Sed. Petr., V. **37**, p. 1059—1069.

HAILS, J. R. and HOYT, J. H. (1969): The significance and limitations of statistical parameters for distinguishing ancient and modern sedimentary environments of the lower Georgia coastal plain. Jour. Sed. Petr., V. **39**, p. 559—580.

INMAN, D. L. (1949): Sorting of sediments in the light of fluid mechanics. Jour. Sed. Petr., V. **19**, p. 51—70.

KING, C. A. M. (1972): Beaches and coasts. 2nd ed., Edward Arnold Ltd., London, 570 p.

MARTINS, L. R. (1965): Significance of skewness and kurtosis in environmental interpretation. Jour. Sed. Petr., V. **35**, p. 768—770.

MASON, C. C. and FOLK, R. L. (1958): Differentiation of beach, dune and aeolian flat environments by size analysis, Mustang Island, Texas, Jour. Sed. Petr., V. **28**, p. 211—226.

MOIOLA, R. J. and WEISER, D. (1968): Textural parameters: an evaluation. Jour. Sed. Petr., V. **38**, p. 45—53.

PASSEGA, R. (1957): Texture as characteristic of clastic deposition. Am. Assoc. Petr. Geol. Bull., V. **41**, p. 1952—1984.

PASSEGA, R. (1962): Problem of comparing ancient with recent sedimentary deposit. Am. Assoc. Petr., Geol. Bull., V. **46**, p. 114—118.

PASSEGA, R. (1964): Grain size representation by CM patterns as a geological tool. Jour. Sed. Petr., V. **34**, p. 830—847.

SHEPARD, F. P. and YOUNG, R. (1961): Distinguishing between beach and dune sands. Jour. Sed. Petr., V. **31**, p. 196—214.

SINDOWSKI, F. K. H. (1958): Die synoptische Methode des Kornkurven-Vergleiches zur Ausdeutung fossiler Sedimentationsräume. Geol. Jahrb., V. **73**, p. 235—275.

SOLOHUB, J. T. and KLOVAN, J. E. (1970): Evaluation of grain size parameters in lacustrine environments, Jour. Sed. Petr., V. **40**, p. 81—101.

SPENCER, D. W. (1963): The interpretation of grain size distribution curves of clastic sediments. Jour. Sed. Petr., V. **33**, p. 180—190.

TRASK, P. D. (1955): Movement around southern California promontories. U. S. Army Corps Eng., B. .E. B., Tech. Memo. 76.

VISHER, G. S. (1965): Fluvial processes as interpreted from ancient and Recent fluvial deposits. In: Middelton, G. V., ed., Primary sedimentary structures and their hydrodynamic interpretation. Soc. Econ. Paleo. Miner., sp. pub. no. **12**, p. 116—132.

VISHER, G. S. (1969): Grain size distributions and depositional processes. Jour. Sed. Petr., V. **39**, p. 1074—1106.

Manuscript received, July 5, 1984

Acta Mineralogica-Petrographica, Szeged, XXVII., 89—100, 1985

MINERALOGICAL RELATIONSHIPS BETWEEN THE NILE DELTA COASTAL SANDS

N. M. EL FISHAWI[1] and B. MOLNÁR[2]

ABSTRACT

The mineralogy of the Nile Delta coastal sediments has been examined. This study summarizes the results of mineralogical examinations of 13 profiles collected along the coast. Each profile contains breaker zone, beach, backshore zone and dune samples. The distribution of the translucent heavy minerals in the coastal environmental sands suggests that there are four characteristic suites among the four provinces, generated by the hydrodynamic forces affecting the coast. The interconnections between hornblende and both garnet+ZTR reveal negative correlations. These relationships can be used to differentiate between coastal environments. Three explanations are offered for the higher concentration of the heaviest minerals in the Burullus beach sands than in the beaches near Rosetta and Damietta: *a)* contributions from offshore old sediments of classic Nile branches rather than the present Nile, *b)* contributions from the land itself, and *c)* minerals have a good chance of being concentrated during coastal erosion.

INTRODUCTION

Published geological information on the heavy minerals of the Nile Delta coastal sands is still scarce. Studies include those of SHUKRI (1950), NAKHLA (1958), RITTMAN and NAKHLA (1958), MASHREF (1962), ANWAR and EL BOUSIELY (1970) and FRIHY (1975). Coastal Erosion Studies (1973, 1976) measured the percentages of magnetite on some stretches along the coast. These studies were concerned with more local effects than the present study. Further, the data of the present study and those of the previous ones are not entirely comparable, because most of the previous studies were concerned with total mineralogy rather than the mineralogy of the size fractions.

During July, 1978, the Nile Delta coast was surveyed between Rosetta and Damietta. The sample net consisted of 13 profiles at 12 km intervals *(Fig. 1A)*. Each profile contains breaker zone, beach, backshore zone and dune samples *(Fig. 1B)*.

The objectives of the present study were:

1. To investigate the distribution of the heavy minerals.
2. To show the changes in profiles normal to the shoreline.
2. To differentiate between coastal environments.
4. To evaluate the action of the hydrodynamic forces in the distribution of the heavy minerals.
5. To detect the direction of sediment transport and source areas.

[1] Institute of Coastal Protection, Alexandria, Abu Qir, Egypt
[2] Department of Geology, Attila József University, H-6722 Szeged, Egyetem u. 2—6, Hungary

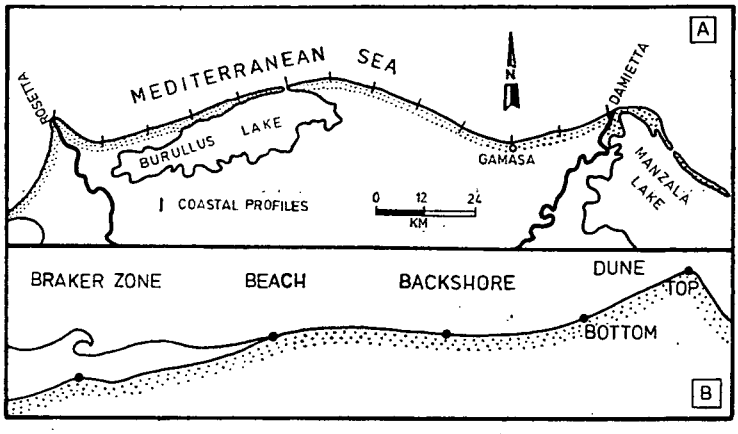

Fig. 1. Location map showing the coastal profiles (A) and sampling sites (B)

The following properties of the heavy residues were used:

1. The quantity (weight percentage) of heavy residue.
2. The number frequency of opaque and non-opaque minerals.
3. Amphibole/opaque ratio.

METHODS OF STUDY

The examined number of samples was 46 and two fractions were selected for each sample. The choice of grain sizes for heavy mineral analysis is of great importance. This choice must be based on the mechanical composition of the sediment in question. The modal size (the size having the highest frequency) and the two successively finer sizes have the greatest significance (SINDOWSKI, 1949). In the present study, the modal size (250—125 μm fraction) and the successively finer size (125—90 μm fraction) were selected for each sample.

Samples under investigation were quartered using a sample splitter, to obtain a representative sample for each locality. Fractions lying between 250 μm and 90 μm were used for this study. The heavy minerals were separated using the well-known bromoform (sp. gr. = 2.89) separation technique, taking into consideration the precautions given by CARVER (1971) in order to obtain a satisfactory separation. After the separation, the heavy fractions were washed with carbon-tetrachloride, dried and weighed. Portions of heavy fractions were mounted in Canada Balsam on glass slides and identified under the polarizing microscope. Mineral frequency was obtained by a line-counting method and about 500 grains were counted for each slide.

Quantity of heavy residue

Figure 2 shows the distribution of the weight percentages of the heavy fractions along the coast and across the different environments; Table 1 illustrates the data. The amount of heavy residue by weight in 250—125 μm fraction of the coastal sands ranges between 4.11% and 30.23%, with an average of 15.05%. In the 125—90 μm

fraction it ranges between 37% and 91.23%, with an average of 65.33%. Therefore, the greater quantity of heavy residue usually occurs in the finer fraction investigated.

On the basis of the relative percentage of heavy residue along the coast, it has been possible to subdivide the Delta coast into 3 stretches. The area between Rosetta and Burullus is characterized by a steady decrease in heavy residue. The greatest concentration is observed in the area between Burullus and Gamasa. The area between Gamasa and Damietta shows the lowest amount of heavy residue.

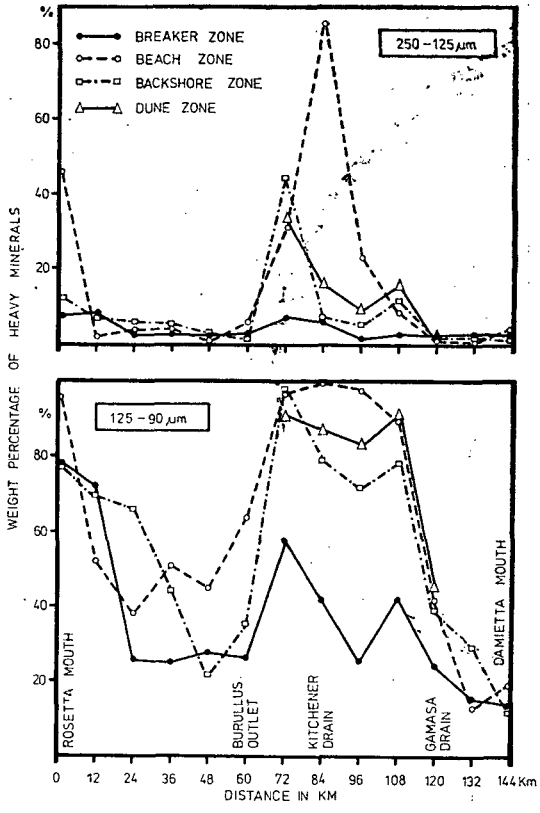

Fig. 2. Quantity of heavy minerals along the Nile Delta coast

Mineralogy of the coastal sands

The main mineral constituents of the heavy fractions are: opaques, amphiboles, pyroxenes, epidotes and garnet. Zircon, tourmaline, rutile, apatite, kyanite, monazite, staurolite, biotite and chlorite are present in subordinate amounts. Weathered minerals are also recorded. The opaque minerals were not studied in detail but were counted together as "opaques", because this was not an objective of the present study. *Figure 3* shows the frequency of various minerals observed within each coastal environmental sands, and the lateral variations along the coast. In compiling mineral frequencies, certain varieties were grouped to simplify illustrations. Hornblende

TABLE 1

Weight percentages of heavy fractions on the coastal sands

Distance in km	Breaker zone		Beach		Backshore		Bottom of dune		Top of dune	
	250—125 μm	125—90 μm	250—125 μm	125—90 μm	250—125 μm	125—90 μm	250—125 μm	125—90 μm	250—125 μm	125—90 μm
0.0	7.49	78.60	26.20	96.49	12.39	78.57				
12	8.63	72.00	1.73	51.73	8.42	69.97				
24	2.60	25.96	2.80	38.46	5.63	65.76				
36	3.22	25.16	3.93	50.79	4.92	44.27				
48	2.50	28.20	0.83	45.07	3.04	22.19				
60	2.83	27.09	6.16	63.88	2.21	36.11				
72	7.35	57.90	30.65	96.94	43.86	97.88	33.93	91.82	32.15	94.96
84	6.00	42.17	86.96	99.43	7.24	78.79	16.48	88.57	28.30	87.50
96	1.49	26.07	22.58	98.45	5.44	72.62	8.90	83.97		
108	2.72	42.11	8.71	89.75	12.64	78.49	15.98	91.51		
120	3.25	25.34	1.99	42.67	2.58	39.45	2.33	46.53		
132	2.71	16.07	1.58	13.34	2.14	29.67				
144	2.58	14.35	3.37	19.31	1.99	13.04				
Average	4.11	37.00	16.73	62.02	8.65	55.91	15.52	80.48	30.23	91.23

and actinolite-tremolite are grouped under the heading of amphiboles. Zircon, tourmaline and rutile (ZTR) are grouped together, etc. From the graphs of *Fig. 3* it is interesting to note that the central part of the coast is characterized by the maximum concentration of the heaviest minerals, while Rosetta and Damietta sands contain lower frequencies of these minerals. It is noticeable that the heaviest minerals are concentrated and have higher frequencies in the 125—90 μm than in the 250—125 μm size fraction. Between Rosetta and Burullus the opaques in the two size fractions tend to behave separately, where they increase in the coarse fraction and decrease in the finer one.

Variation normal to the shoreline

Figure 4 shows the total variation of the heavy residue and number frequencies of heavy minerals normal to the shoreline; Table 2 illustrates the data. The percentage of the heavy residues increases from the breaker zone to the beach, and then decreases slightly to the backshore zone. The percentage progressively increases from the bottom to the top of the dune, where it attains the maximum values. The opaques and translucent heavy minerals vary significantly normal to the coast. In the 250—125 μm fraction, opaques decrease while garnet, pyroxenes and amphiboles increase between the breaker zone and dune sands. On the other hand, in the 125—90 μm fraction opaques and ZTR increase, while amphiboles and pyroxenes decrease.

A sedimentary petrological province is defined as a group of sediments which constitute a natural unit by age, origin and distribution. A province is best defined when it contains minerals that do not occur in significant amounts in any of the other provinces in the same region. Table 2 shows that the translucent heavy minerals of the Nile Delta coastal sands comprise an amphibole-pyroxene-epidote-garnet-ZTR suite. The distribution of these minerals in the breaker zone, beach, backshore and

dune provinces, as indicated by the mean values, suggests that there are four characteristic suites among the four provinces: an amphibole-pyroxene-epidote suite in the breaker zone, an amphibole-pyroxene-garnet suite in the beach, an amphibole-pyroxene-garnet (or epidote) suite in the backshore, and an amphibole-pyroxene-

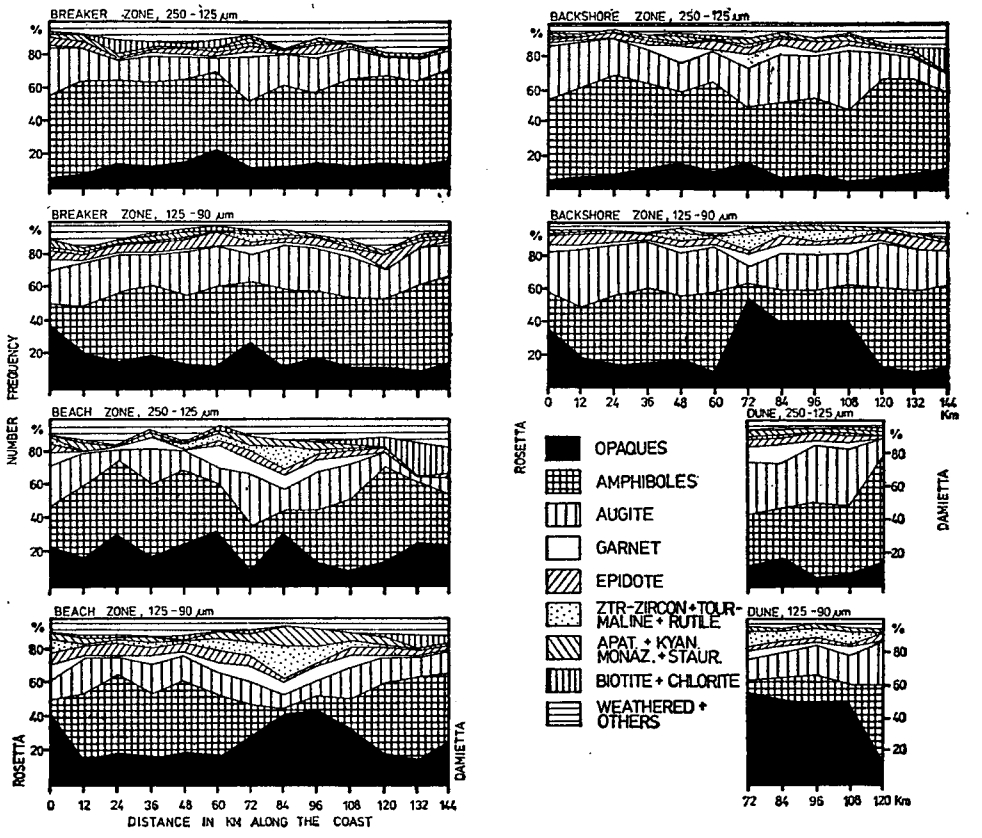

Fig. 3. Distribution of number frequency of heavy minerals along the Nile Delta coast

garnet (or ZTR) suite in the dune. The distribution of opaque heavies also varies by province, as shown in *Fig. 4.*

The analysis indicates that these four provinces correspond to four well-defined grain size provinces generated by the contrasting hydraulic regimes of the breaker zone, surf zone and wind action. Onshore-offshore transport and differentiation of sediments play an important role in the generation of the heavy mineral suites across the coastal environments. SWIFT *et al.* (1971) found three heavy mineral provinces in the beach, nearshore and offshore. They suggested that the variation had been hydraulically induced by an onshore-offshore differentiation of sea-floor sands. The sensitivity of heavy mineral suites to the local hydraulic regime has long been known (RUBY, 1933; RITTENHOUSE, 1943; BRIGGS, 1965).

The breaker zone sediments reveal a higher content of amphiboles and augite and a lower content of opaques, garnet and ZTR than in the beach sediments. This

sorting may be related to the action of breakers, which tend to concentrate the less heavies with the coarse sands. In the natural separation, the heaviest minerals (opaques, garnet, ZTR) were left on the beach surface due to the action of waves on the surf zone. SWIFT *et al.* (1971) found that the content of garnet in beach sands is essentially higher than that in nearshore sands.

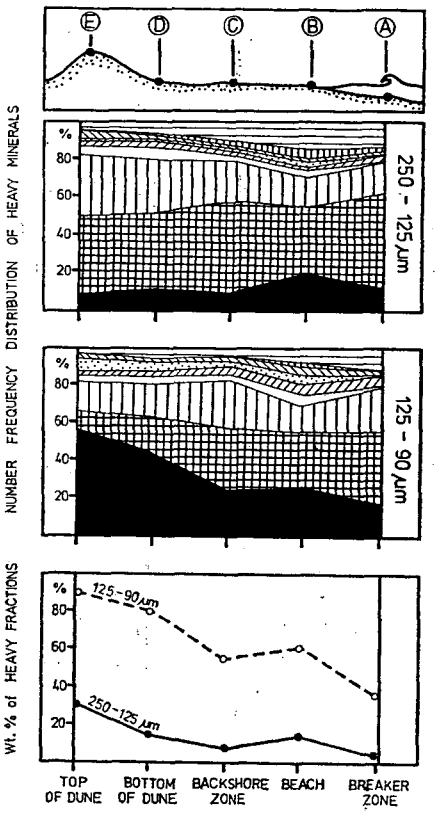

Fig. 4. Heavy mineral variations normal to the shoreline. Legend as in *Fig. 3.*

It is desirable to compare beach zone mineral concentration anomalies with the concentrations of the same minerals in the nearby dune. The dune sands have higher contents of the heavy residue, opaques, garnet and ZTR than those of the beach sands. The explanation is that the heavy minerals may represent the lag concentrate, due to wind working over the dunes more than the beaches, where wetness prevents much wind action. During this reworking, the wind picks up the light minerals, which may be largely removed, leaving the heavies behind on the dunes. This result agress in general with the findings of VON ENGELHARDT (1940), STEWART (1956), BRADSSLEY (1957), SHEPARD and YOUNG (1961) and GILES and PILKEY (1965).

TABLE 2

Average frequency distribution of heavy minerals on the coastal sands

Environment / Mineral	250—125 μm fraction					125—90 μm fraction				
	Breaker zone	Beach zone	Backshore zone	Bottom of dune	Top of dune	Breaker zone	Beach zone	Backshore zone	Bottom of dune	Top of dune
Opaques	13.52	20.88	9.36	11.42	6.98	16.66	25.31	24.37	43.30	54.54
Hornblende	45.40	30.02	47.80	40.28	40.57	38.06	26.60	31.76	18.85	11.61
Tre.—Act.	4.90	6.01	2.17	0.93	2.62	2.06	4.13	2.31	0.84	0.36
Augite	17.06	15.78	21.84	27.74	32.81	21.81	13.42	24.01	17.59	15.59
Epidote	3.13	1.69	3.27	3.79	3.12	4.57	5.16	4.22	2.77	2.80
Garnet	0.99	4.43	3.29	6.03	4.76	2.23	5.47	2.76	4.00	2.75
Zircon	0.08	1.12	0.06	—	—	0.27	2.07	0.90	3.26	3.77
Tourmaline	0.20	0.53	0.25	0.25	0.51	0.25	0.52	0.22	0.21	0.23
Rutile	0.12	0.65	0.17	0.49	0.25	0.36	2.39	1.32	2.60	2.93
Apatite	0.66	0.64	0.53	0.89	0.88	1.08	1.77	1.41	0.94	1.00
Kyanite	—	0.58	0.07	0.73	1.02	0.09	0.37	—	0.41	0.36
Monazite	—	0.12	0.34	0.35	0.12	0.31	1.56	0.69	0.78	0.91
Staurolite	0.27	0.79	0.72	1.08	3.01	0.06	0.71	0.29	—	0.23
Biotite	1.77	3.16	1.67	1.27	0.51	0.48	1.06	0.13	0.47	—
Chlorite	0.05	1.12	0.10	—	—	0.11	0.39	—	—	—
Weathered	6.19	10.21	5.11	1.87	1.49	5.04	4.84	3.12	2.51	1.48
Others	5.63	1.92	3.31	1.68	1.37	6.00	4.23	2.32	1.56	1.46

Variations along the shoreline

In order to see if coastwise transport plays a significant role, the lateral variation of some selected heavy minerals has been considered through the various provinces. It was found that the opaques, garnet+ZTR and amphiboles of the 125—90 μm fraction vary significantly in a down-drift direction, as shown in *Fig. 5.*

The opaques heavies of the Nile Delta coast reveal a considerable trend. In all provinces between Rosetta and Burullus, opaques decreased most rapidly at first and more slowly later. A rapid increase in opaques was found between Burullus and Gamasa and then a sharp decrease eastwards. Garnet+ZTR reveal the same behaviour as the opaques. The distribution of amphiboles shows a reverse behaviour, in a down-drift direction. There is a rapid increase east of Rosetta and then a slow rise to the Burullus coast. Between Burullus and Gamasa, the amphiboles sharply decrease at first and then tend to increase to Damietta.

Mineralogically, the Nile Delta coast can be subdivided into three stretches, based on opaques and transparent minerals:

1. Rosetta—Burullus stretch: the sediments in this area are characterized by a decrease in opaques and garnet+ZTR, and an increase in amphibole.

2. Burullus—Gamasa stretch: this area shows the greatest content of opaques and garnet+ZTR, and the lowest content of amphibole.

3. Gamasa—Damietta stretch: the sediments are characterized by an abundance of amphibole, and a reduced amount of opaques and garnet+ZTR.

A similar trend of decreasing garnet and increasing amphibols in a down-drift direction has been reported by many authors (PETTIJOHN and RIDGE, 1933; MCMASTER, 1960; LANGFELDER *et al.*, 1968). The previous studies on the Nile Delta coast

have shown a characteristic decrease in percentage of heavy minerals eastward and westward of the Rosetta headland (RITTMAN and NAKHLA, 1958; MASHREF, 1962). FRIHY (1975) showed that opaques, zircon and garnet decrease, while amphiboles and pyroxenes increase westward of Rosetta mouth. Such trends could be the result of selective down-drift sorting, whereby the heavier mineral grains have a higher probability of being selected for permanent deposition during their intermittent down-drift journey. As regards river sands, the results reported by RUSSELL (1937) for the Mississippi River and by POLLCAK (1961) for the South Canadian River show no significant change in the percentage of heavy minerals downstream.

Amphibole/opaque ratio

The ratio of stable to unstable heavy minerals is a convenient measure of the maturity of recent sands (BULLARD, 1942). Directions by which the sediments moved along the beaches may be indicated by systematic changes in the ratio of certain unstable and stable mineral species. The amphibole/opaque ratio was calculated along the Nile Delta beach sands to represent the unstable/stable ratio.

The features recognized along the beaches have significantly different ratios *(Fig. 6)*. Rosetta sands are comparatively immature, with an average amphibole/

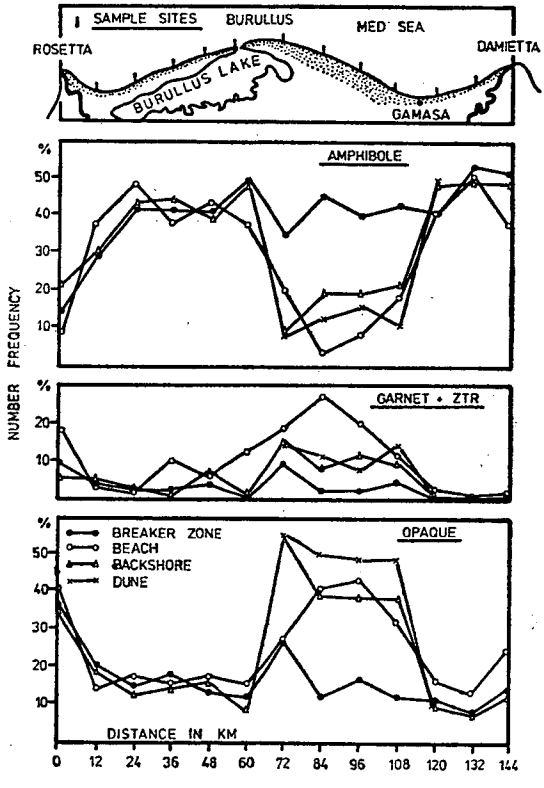

Fig. 5. Lateral variation of opaque, garnet+ZTR and amphibole along the coast for 125—90 μm size grade

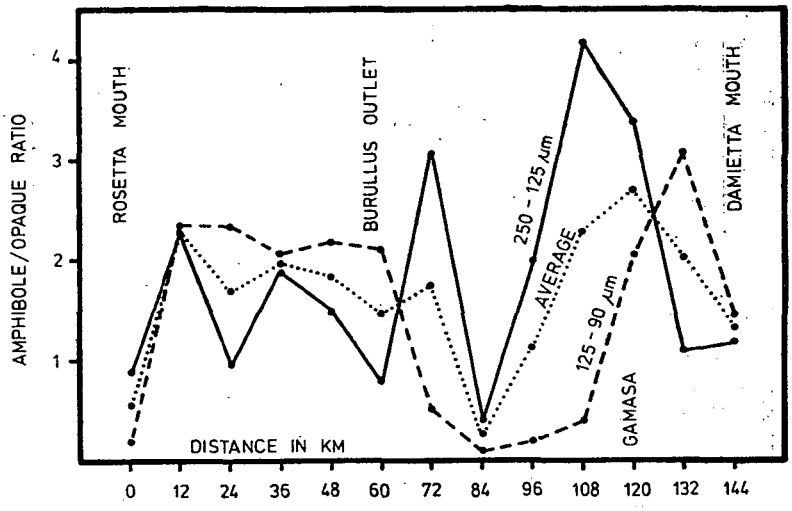

Fig. 6. Amphibole/opaque ratio along the Nile Delta beach sands

opaque ratio of 0.55. The ratio increases between Rosetta and Burullus, and the average value ranges between 1.5 and 2.2. This means that the sediments become mature in a down-drift direction. Between Burullus outlet and location 84 km, the amphibole/opaque ratio decreases and the sediments become immature, with an average ratio of 0.40, as a result of dilution with opaque association from some sources. East of location 84 km the sediments tend to be strongly mature, with an average ratio of 2.70. Near Damietta mouth, the sediments become intermediate in maturity, with an average of 1.30, due to tilution with opaques from Damietta mouth. In conclusion, it can be said that the amphibole/opaque ratio may be used as an indicator to trace the direction of sediment movement along the beaches. The central part of the Nile Delta coast is largely of local origin, formed by reworking and dispersal of older deposits present in the coastal zone itself or in the immediate vicinity on the continental shelf.

Mineralogical relationships between coastal sands

There has been comparatively little work on the heavy minerals of the coastal environments, and publications are seldom encountered except relating to beach sands. So far, there has been no attempt to differentiate between the various coastal sands by heavy mineral analysis.

The relationship between opaques and hornblende, as well as that between garnet+ZTR and hornblende, are shown in *Fig. 7* for the 250—125 μm and 125—90 μm size fractions. The association between the values reveals negative correlations; the higher the hornblende content, the lower the opaque and garnet+ZTR contents.

The Nile Delta coastal environments can be differentiated by heavy mineral analysis. The 250—150 μm size fraction gives a better differentiation than the 125—90 μm one, as shown in *Fig. 7*. For the 250—125 μm size fraction, boundary lines have been drawn and separated fields resulted for each environment.

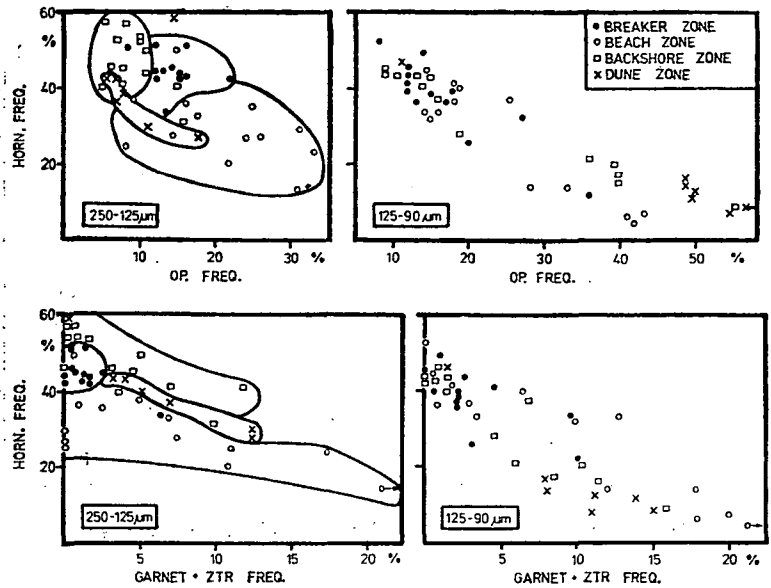

Fig. 7. Relationships between opaque and hornblende and that between garnet + ZTR and hornblende for coastal sands

Source of beach minerals

A comparison of beach mineralogy along the Nile Delta coast indicates that the beaches near Rosetta and Damietta contain lower percentages of heavy residue than along Burullus headland. On this basis it can be assumed that Rosetta and Damietta Rivers are not important contributors to the present-day beach sediments.

If longshore drift in an eastward direction is the principal mechanism of sediment supply, an eastward increase in amphibole and decrease in garnet and opaques should be expected. This is apparently the case in the areas between Rosetta and Burullus and west of Gamasa, but not for Burullus headland. The increase of heavy mineral suites and contents in Burullus suggests that the shelf on this part of the coast is the source of sediments. The evidence relating to the source of sediments is based on comparisons between the high opaque, garnet and ZTR contents of Burullus sands and the corresponding low contents of these minerals near Rosetta and Damietta mouths. Therefore, the sediments of the Burullus coast may be derived from outcropping ancient sediments on the shelf formed by the ancient Sebennitic branch during times of a lowered sea level, when sediments from old rivers were carried directly downslope across the exposed shelf to deep water.

To sum up, three explanations are offered for the higher concentration of the heaviest minerals in the Burullus beach:

1. Contributions from offshore old sediments of classis Nile branches, rather than the present Nile, where the heaviest minerals are more abundant in Burullus beaches than in both Rosetta and Damietta beaches. Unfortunately, there is very little information in the literature concerning the detailed mineralogy of the offshore and shelf sediments.

2. Contributions from the land itself, where the backshore flat and coastal dunes contain a high amount of opaques and a considerable amount of garnet and ZTR. It is important to mention that the preferential mechanical concentration of ZTR plays an effective role because of their hydraulic properties.

3. Coastal Erosion Studies (1973) reported that the best conditions for the concentration of the heaviest minerals are where the shore is retreating, especially where there is a reworking of beach sands. Minerals do not have much chance to be concentrated if the coast is actively advancing. In fact, the Burullus headland is retreating due to severe erosion, and as a result it may lead to some concentration of the heavy minerals.

CONCLUSIONS

1. The translucent heavy minerals of the Nile Delta coastal sands comprise an amphibole-pyroxene-epidote-garnet-ZTR suite. The distribution of these minerals in the breaker zone, beach, backshore and coastal dune sands suggests that there are four characteristic suites among the four provinces, generated by the contrasting hydraulic regimes of the breaker zone, surf zone and wind action.

2. The heavy mineral variations normal to the shoreline show a significant trend. In general, the heavy residues, opaques, garnet and ZTR markedly increase, while amphiboles and pyroxenes decrease in moving from the breaker zone across the beach and backshore and up to the dune. The breaker zone sands reveal a higher content of amphiboles and pyroxenes and a lower content of opaques, garnet and ZTR than the beach sands. The reason may be related to the action of the breakers in concentrating the less heavies with the coarse sands, while in the natural separation the heaviest minerals are left on the beach surface due to the wave action. The dune sands have higher contents of the heavy residues and heaviest minerals than the beach sands. The explanation is that the heavy minerals may represent a lag concentrate due to the wind working over the dune more than the beaches, where the wetness prevents much wind action. Therefore, the wind picks up the light minerals, leaving the heavies behind on the dunes.

3. The associations between hornblende and both opaques and garnet+ZTR reveal negative correlations; the higher the hornblende content, the lower the opaque and garnet+ZTR contents. These relationships in the 250—125 μm size grade can be used to differentiate between coastal environments.

4. The coastwise variation in heavy minerals indicates that the beaches near Rosetta and Damietta contain relatively lower percentages of heavy residues and other heavies than the Burullus headland coast. If longshore drift in an eastward direction is the principal mechanism of sediment supply, an eastward increase in amphibole and a decrease in opaques and garnet+ZTR should be expected. This is apparently the case in the Rosetta—Burullus stretch and west of Gamasa, but not for the Burullus headland coast.

5. Three explanations are offered for the high concentration of the heaviest minerals in the Burullus beach sediments:

a) Contributions from offshore old sediments of classis Nile branches rather than the present Nile.

b) Contributions from the land itself, where the backshore and dunes contain considerable amount of these minerals.

c) These minerals have a good chance of being concentrated during coastal erosion.

REFERENCES

ANWAR, Y. M. and EL BOUSEILY, A. M. (1970): Subsurface studies of the black sand deposits at Rosetta Nile mouth, Egypt. Part II: mineralogical analysis. Bull. Fac. Sci. Alex. Univ., V. **10**, p. 141—150.

BRADLEY, J. S. (1957): Differentiation of marine and subaerial sedimentary environments by volume percentage of heavy minerals, Mustang Island, Texas, Jour. Sed. Petr., V. **27**, p. 116—125.

BRIGGS, L. I. (1965): Heavy mineral correlations and provenances. Jour. Sed. Petr., V. **35**, p. 939—955.

BULLARD, F. M. (1942): Source of beach and river sands on the Gulf Coast of Texas. Geol. Soc. Am, Bull., V. **53**, p. 1021—1043.

CARVER, R. E. (1971): Heavy mineral separation. In: Carver, R. E., ed., Procedures in sedimentary petrology, Wiley — Interscience, New York, p. 427—452.

COASTAL EROSION STUDIES (1973): Detailed Technical Report. Project 70/581, UNESCO (ASRT) UNDP, Alex., 259 p.

COASTAL EROSION STUDIES (1976): Detailed Technical Report on Coastal Geomorphology and Marine Geology, Nile Delta. Project 73/063, UNESCO (ASTR) UNDP, Alex., 175 p.

FRIHY, O. E. (1975): Geological study of Quaternary deposits between Abu Quir and Rashid. M. Sc. thesis, Fac. Sci. Alex. Univ.

GILES, R. T. and PILKEY, O. H. (1965): Atlantic beach and dune sediments of the southern U. S. Jour. Sed. Petr., V. **35**, p. 900—910.

LANGFELDER, J., STAFFORD, D. and AMEIN, M. (1968): A reconnaissance of coastal erosion in North Carolina. Dept. of Civil Eng., North Carolina State Univ., Raleigh, 172 p.

MASHREF, W. M. (1962): Mineralogical and radiometric study for some black sand deposits on the Mediterranean coast. M. Sc. thesis, Fac. Sci. Ain Shams Univ.

MCMASTER, R. L. (1960): Mineralogy as an indicator of beach sand movement along the Rhode Island shore. Jour. Sed. Petr., V. **30**, p. 404—413.

NAKHLA, F. A. (1958): Mineralogy of Egyptian black sands and its application. Egyptian Jour. Geol. V. **2**, no. 1.

PETTIJOHN, F. J. and RIDGE, J. D. (1933): A mineral variation series of beach sands from Cedar Point, Ohio. Jour. Sed. Petr., V. **3**, p. 92—94.

POLLACK, J. M. (1961): Significance of compositional and textural properties of South Canadian river channel sands, New Mexico, Texas and Oklahoma. Jour. Sed. Petr., V. **31**, p. 15—37.

RITTENHOUSE, G. (1943): Transportation and deposition of heavy minerals. Geol. Soc. Am. Bull., V. **54**, p. 403—413.

RITTMAN, A. and NAKHLA, F. A. (1958): Contribution to the study of Egyptian black sands. Egyptian Jour. Chem., V. **1**, p. 127—135.

RUBEY, W. W. (1933): The size distribution of heavy minerals within a water-laid sandstone. Jour. Sed. Petr., V. **3**, p. 3—29.

RUSSELL, R. D. (1937): Mineral composition of Mississippi River sands. Geol. Soc. Am. Bull., V. **48**, p. 1307—1348.

SHEPARD, F. P. and YOUNG, R. (1961): Distinguishing between beach and dune sands. Jour. Sed. Petr., V. **31**, p. 196—214.

SHUKRI, N. M. (1950): The mineralogy of some Nile sediments. Quart. Jour. Geol. Soc. London, V. **105**, p. 511—534.

SINDOWSKI, F. K. H. (1949): Results and problems of heavy mineral analysis in Germany: A rewiev of sedimentary-petrological papers, 1936—1948. Jour. Sed. Petr., V. **19**, p. 3—25.

STEWART, H. B. (1956): Sediments and the environments of deposition in a coastal lagoon. Ph. D. thesis, Univ. Calif., 355 p.

SWIFT, D. J. P., DILL, C. E. and MCHOME, J. (1971): Hydraulic fractionation of heavy mineral suites on an unconsolidated retreating coast. Jour. Sed. Petr., V. **41**, p. 683—690.

VON ENGELHARDT, W. (1940): Unterscheidung wasser-und windsortierter Sande auf Grund der Korngrössenverteilung ihrer leichten und schweren Gemengteile. Chemie der Erde, V. **12**, p. 445—465.

Manuscript received, July 5, 1984

Acta Mineralogica-Petrographica, Szeged, XXVII, 101—116, 1985

SEDIMENTOLOGY OF SINJAR LIMESTONE FORMATION, SULAIMANIAN AREA, NORTHEASTERN IRAQ

KHALIL AHMED MALLICK[1] and BASIM J. AL-QAYEM[2]

ABSTRACT

Sinjar Limestone Formation of Eocene age is composed of allochthonous and autochthonous limestones. Petrographic and geochemical characteristics of the rocks of this Formation show the occurrence of phosphatic rocks in two horizons which are separated by 43 feet thick nonphosphatic limestone beds.

The study also reveals that the phosphatic rocks are recycled sedimentary deposits from the near-by source. No effects of phosphatization was observed in the associated rocks.

Five phases of sedimentation representing different physicochemical controls have been established on the basis of petrography, chemistry and the fossils present in them.

INTRODUCTION

The present article deals with the sedimentological investigation of Sinjar Limestone Formation exposed in Kinjinnah, Bazyan and Dukan areas of Sulaimaniah county in northeastern Iraq (*Fig. 1*). Attempt has been made to reconstruct the depositional environment of the formation which is composed of allochthonous and autochthonous limestones. The investigation also seems to ascertain the degree of mineralogical correspondence between Sinjar Limestones and the intertonguing Kolosh Formation on the basis of clastics.

Besides the studies of the physical properties, field relationships, structural continuity of Sinjar Limestones and the associated rocks, the petrographic invetigation of the samples collected and the quantitative estimation of the acid insolubles were also made. The petrographic evidences and acid insolubles are expected to help in the determination of the degree of mineralogical correspondence between the beds of Sinjar Limestone Formation intertonguing with the associated Kolosh Formation. Efforts have also been made to trace the possible provenance of the clastics present in the rocks and to study the diagenetic changes. Chemical analysis of the representative samples of the Sinjar Limestone Formation has been made to study the variations in Ca and Mg concentrations of the beds under varying geochemical conditions of the depositional basin.

GENERAL GEOLOGY OF THE AREA

Reference to the geology of Sinjar Limestone Formation is found in the reconnaissance geological reports since 1959 but no attention was paid to the petrographic investigations of this formation which is composed of varieties of limestones. Studies

[1] Department of Geology, University of Karachi, Karachi, Pakistan.
[2] Department of Geology, University of Salahuddin, Arbil, Iraq.

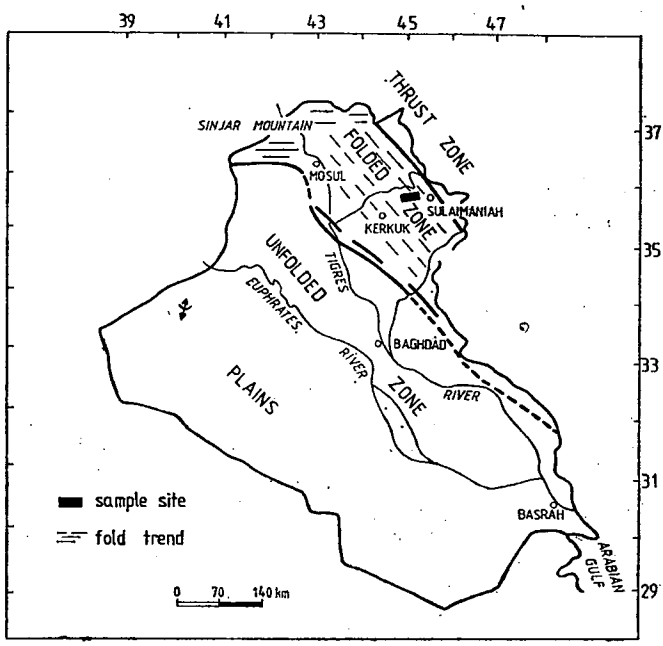

Fig. 1. Tectonic map of Iraq showing location of sample site

on the stratigraphic aspects and the microfacies of Sinjar Limestone Formation has been made by AL-SIDDIQI (1968). AL-KUFAISHI (1977) made a geochemical study of some of the core samples from Sinjar Formation and concluded that no relationship exists between the microfacies of the formation and the trace elements concentration. The author could also establish non-reefal origin of the facies and decreasing effects of dolomitization with depth on the basis of Ca/Mg ratio and the strontium contents.

The formations exposed in Kinjinnah, Bazyan and Dukan areas are Sheranish, Tanjero clastic, Sinjar and Kolosh, and the Gercus of Upper Cretaceous, Paleocene and Miocene ages respectively (VAN BELLEN, 1956). Tanjero Clastic Formation is contemporaneous of Sheranish Formation and Kolosh Clastic Formation intertongues with Sinjar Limestone Formation.

Sheranish Formation is composed of blue marl at the upper part and thinly bedded marly limestone at the bottom. Fresh surface of the marl looks dark blue but on weathering the colour changes to a typical pale blue. The rocks are considered to be of transgressive sequence of Upper Campanian age.

Tanjero Clastic Formation is contemporaneous of Sheranish Formation and underlies Sinjar Limestone Formation in the areas of present investigation. It is composed of silty marls, siltstones, sandstones, conglomerates and sandy or silty organic reef and shoal types of limestones. The non-calcareous clastics are dominated by chert and green rock detritus. The clastics comprise the pebbles and fine grained detritus of different Mesozoic limestones, green rock fragments and radiolarian cherts.

Sinjar Limestone Formation of Paleocene/Eocene age is well exposed in the type locality near the village of Mamissa in the Sinjar Mountains at Latitude 36°22'33"

N and Long. 41°41′23″ E after which the formation is named. In the type locality the formation is 577 ft. thick limestone showing elements of algal reefal facies, a lagoonal miliolid facies and a shoal nummulitic facies. It is usually recrystallized hard and yellow in colour. It overlies the Sheranish Formation unconformably and is marked by a complete faunal and facies changes. In this locality Jaddalah Formation overlies the Sinjar Limestone Formation unconformably and is marked by ravinement and glauconite concentration.

In other localities such as Kin-Jinnah, Bazyan and Dukan which are under the present study, Sinjar Limestone Formation underlies Gercus Formation unconformably instead of Jaddalah Formation and overlies the Tanjero Clastic Formation. The rocks of Sinjar Limestone Formation are composed of varities of limestones which differ in texture from coarse friable to fine dense hard and compact states with varying contents of fossils. Generally the microfossils are more abundant in the upper part of this formation. The colour varies from light grey to brown yellow and mottled. The effects of physical and chemical weathering are non-uniform. Some of the beds which are compact and hard stand out in relief with steep escarpments, while others which are brown yellow or mottled show intense effects of physical and chemical weathering probably due to their higher argillaceous contents which make them soft and give different colours in presence of organic matter and iron oxides.

Kolosh Clastic Formation interfingering with Sinjar Limestone is composed of shales, coarse and fine sandstones of dark and green colours. Thin layers of marl are also found. The formation is highly heterogenous in lithology and is rapidly variable both horizontally and vertically. It is deposited by turbidity currents (BANAT *et al.*, 1981).

Gercus Formation of Miocene age is contemporaneous of Jaddalah Formation. It is composed of reddish brown maroon coloured shale and sandstones of different grades. It overlies the Sinjar Limestone Formation in the area of study instead of Jaddalah Formation.

Structurally the area forms a flank of a major anticline trending NW and SE in the Zagros folded mountain belt of Iraq. The main highway connecting Sulaimaniah and Baghdad is across the strike of the beds in the western flank of the major anticline. The topography of the area is moderately rugged because of variable lithological characteristics of the limestones, shales and sandstones of different formations present in the area. Gentle to steep escarpment slopes with interstream highs are common features in this area.

METHOD AND MATERIAL

The localities mentioned earlier were selected for detailed sampling of Sinjar Limestone Formation, the top of the underlying Tanjero Clastic Formation and the bottom of the overlying Gercus Formation. Samples were also collected from Kolosh Clastic Formation which interfingers with Sinjar Limestone Formation. The samples collection was based on the differences in colour, texture, structure, algal characters, compactness, thickness of beds, types of weathering, response to acid test and other characteristics observable in the field, in order to get proper representation of the varying conditions during deposition of the rocks. To facilitate the study of the degree of correspondence between the beds of Sinjar Limestone Formation, special consideration was given to the study of samples collected from the contact zones of

the beds. Qualitative estimation of insoluble residues has been made to facilitate the study of the degree of correspondence with the associated rocks.

The limestone beds of Sinjar Formation show variable thicknesses and shades in colours on the weathered and fresh surfaces. In hand specimens light grey, yellow and brown are the dominating colours with patches and streaks of reddish brown, pink, white and black (Table 1). In some of the beds, the effects of argillaceous content and organic matters are well pronounced. Mottled appearance is more pronounced in phosphatic beds which have been discovered by the senior author of the present paper. The details of the phosphorite is discussed in a separate paper already published (MALLICK and AL-FADHLI, 1980).

TABLE 1

Lithostratigraphic details on a section from Sinjar Limestone Formation, Sulaimaniah area, Iraq

Bed №	Thickness of bed in ft.	Lithology
SK—22	19	Mottled (brown and white) coarsely crystalline limestone.
SK—21	17	Light brown crystalline limestone.
SK—20	12	Light brown hard and massive limestone with white streaks.
SK—19	39	Light brown massive limestone with black specks.
SK—18	13	Light green, dense and massive limestone.
SK—17	37	Dark brown argillaceous limestone showing recrystallization effects.
SK—16	51	Light grey with pink streaks dense and hard limestone.
SK—15	17	Mottled hard and massive argillaceous limestone.
SK—14	20	Mottled clastic argillaceous limestone.
SK—13	18	Reddish brown hard and compact clastic limestone.
SK—12	19	Yellow clastic argillaceous limestone.
SK—11	8	Light brown dense and hard limestone.
SK—10	17	Dark brown massive limestone with sub-conchoidal fracture.
SK—9	16	Mottled clastic hard limestone.
SK—8	2	Light brown and banded hard limestone.
SK—7	5	Reddish brown hard clastic limestone.
SK—6	10	Mottled argillaceous fossiliferous limestone.
SK—5	21	Light brown argillaceous clastic limestone.
SK—4	6	Mottled argillaceous clastic limestone.
SK—3	6	Light grey hard argillaceous clastic limestone.
SK—2	10	Light grey hard clastic limestone with argillaceous patches of brown colour.
SK—1	7	Light grey argillaceous limestone with black specks.

The development of weathering features like honeycomb, spongy and plain surfaces are common in Sinjar Limestone Formation, signifying non-uniform condition during deposition with respect to sedimentation and tectonism in the area. The Formation is more argillaceous in the lower part than the upper. Honeycomb and spongy weathering is quite common. Uneven development of escarpments and escarpment slopes as common features are probably due to variable lithology and compactness of the rocks in the beds, wide range of textural varieties are observable in hand specimens and the thin sections of the rocks.

The limestones are mainly allochthonous and, therefore, the textural variations seem to be very much related to lithology of the limestones of this formation. The variation in autochthonous limestones of this formation is not very much. Banded algal structures are quite pronounced both in hand specimens and the thin sections of the limestones.

The thim sections from the rock samples of the overlying Gercus and the underlying Tanjero Formations were examined to study the similarities in the shapes of the grains and the mineralogy of the non-carbonate contents of Sinjar Limestone beds. Special attention was paid to the study of similar and oissimilar non-calcarlous minerals in the beds of the limestones in relation to the associated beds. Due emphasis was given to the study of the samples collected from the contact of the consecutive beds to facilitate the study of non-carbonate minerals present due to transition or intermixing, if they were laid down in the same cycle of deposition with some degree of fluctuations in the depositional basin or there were some pronounced changing conditions of deposition due to inter-play between tectonism and sedimentation.

PETROGRAPHY

In megascopic study the shales, marls, siltstones and the sandstones of Tanjero Formation appear greenish grey in colour. The texture is fine to medium. In this sections, quartz grains and grains of limestone fragments which are generally crystalline are common. Relatively fresh grains of alkali feldspars and the flakes of muscovite and biotite are also present. The grains of the minerals in the limestone are angular to subrounded in shape. Fossils are not common in the upper part of Tanjero Formation which has unconformable contact with Sinjar Limestone Formation. Perhaps the provenance of Tanjero clastics was not far from the depositional basin and the sedimentation rate was relatively higher than the sinking of the basin of deposition which helped in preserving the morphology of the grains without much modifications.

The lowermost bed of Sinjar Limestone Formation in unconformable contact with the top of Tanjero clastics is fine grained, massive and fairly hard to break. Black specks probably of organic matter are common.

The thin section of the rock reveals an aggregate of argillaceous pellets and fragments embedded in calcareous matrix. The pellets range in size from 1 mm to 3 mm and amount to about 15%. The argillaceous fragments are angular to subrounded, 1 to 5 mm in diameter and their amount is about 20%, obliterated microfossils showing micritization are also present. Some of the fossils although micritized can be seen with partly preserved characters. Micritization and presence of sparry calcite in matrix and concretions having cluster of argillaceous pellets and fragments are easily observable in thin sections *(Fig. 2)*. The pelleted argillaceous limestone beds are repeated in the sequence. The effects of micritization and the cluster of calcite grains are not uniform in all the argillaceous limestones. Fossils are rare and algal structures are observable. Argillaceous patches can also be seen. The mud supported limestones both the ooids and the massive with irregular patches of sparry calcite show variable degree of micritization and appear quite different from the pelleted limestone beds. The fossils are not visible in the mud supported limestones *(Fig. 2d)*. Perhaps the sparites are the fossil fragments which have been completely replaced and recrystallized.

Where ever the ooids have developed into larger sizes of 0.6 mm to 1.0 cm, the sparites in association with them are also larger in sizes and more in abundance. Micritization and sparry calcite can also be seen within concritions producing concentric pattern due to the presence of organic and argillaceous matters at the time of deposition of the rocks. The non-pelleted limestones appear relatively less argillaceous

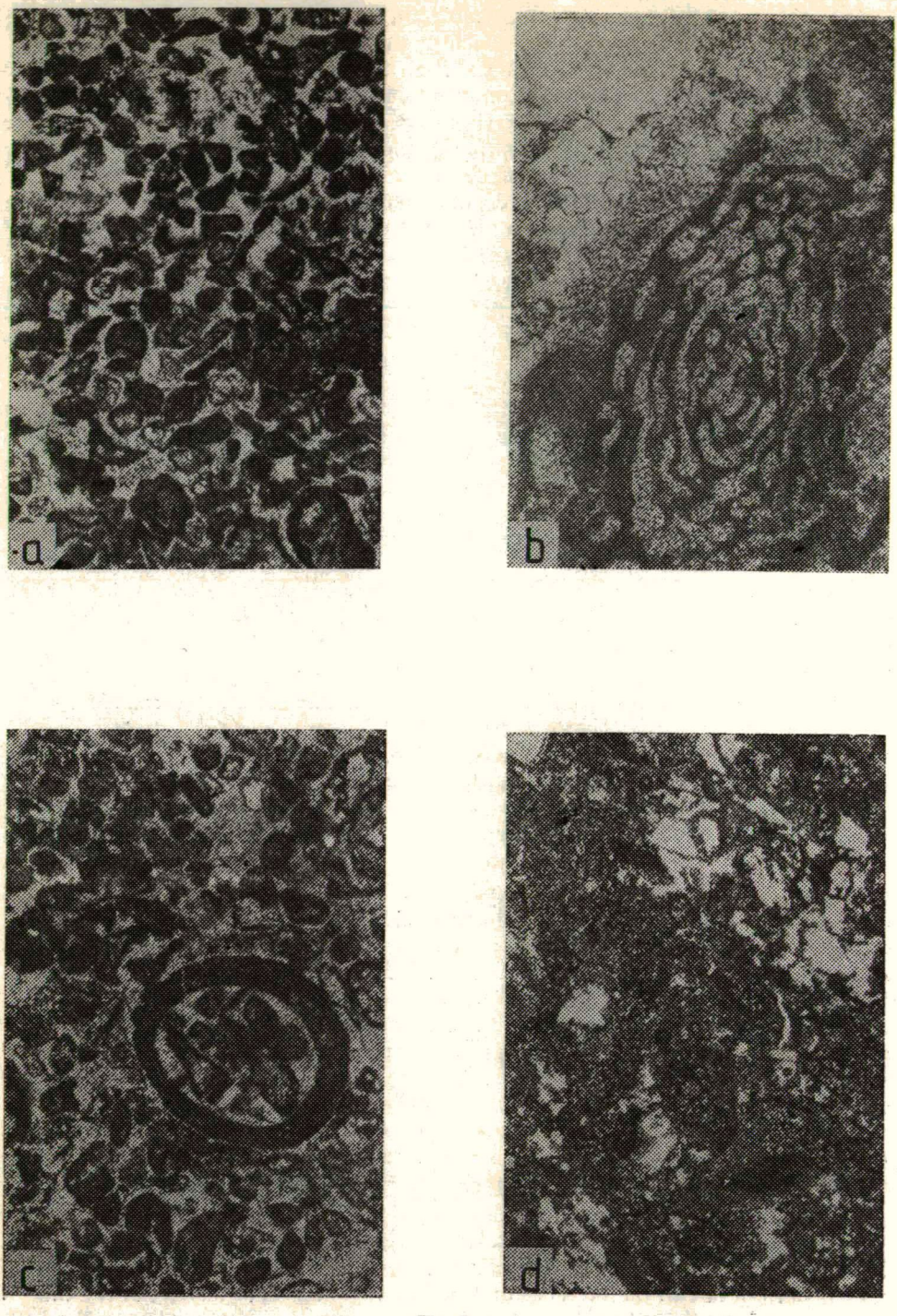

Fig. 2

and contain fragments of fossils, angular grains of quartz, calcites and few argillaceous fragments showing micritization effects. Some of the thin sections of the rocks from Sinjar Limestone Formation show an aggregate of well packed uneven grains of variable mineralogical compositions.

The bed overlying the lowermost bed of Sinjar Limestone Formation appears more algal and argillaceous and contains rounded to subrounded grains of limestones. The grains show varying degree of recrystallization with seggregation of argillaceous and organic matters within their bodies. Smaller fragments appearing as sparry calcite in the algal matrix are common *(Fig. 3)*.

The upper part of Sinjar Limestone Formation is relatively more fossiliferous and the fossils are well preserved in their outlines and internal structures. Tubular larger fragments of fossils in association with the smallers in the calcareous matrix are common. The smaller fragments are mostly replaced by calcite and appear as fragments of calcite in argillaceous matrix *(Fig. 4)*. The larger fragments of fossils also show diagenetic effects, and therefore, they appear to be composed of sparry calcite with black specks of argillaceous matter but the structure of the fossils is recognizable.

The occurrence of tube like structures with pelloids, argillaceous angular fragments and sparry calcite probably indicates that mud feeding animals were present in the shallow depositional basin. The outer wall of the tube gives indications of micritization and the presence of sparites. In such types of rocks the percentage of pellets is about 2 and the matrix is calcareous. No effects of dolomitization could be observed in these rocks. The rocks with calcareous matrix, well preserved fossils and algal lumps of variable sizes occur in all over the area under present study.

The overlying bed of the same formation shows a marked change in the matrix from calcareous to argillaceous in which well preserved microfossils and fossil fragments are present. The effects of replacement in the fossils and fossil fragments are well pronounced but the internal structures are not disturbed.

The top of Sinjar Limestone Formation in contact with the bottom of the overlying Gercus Formation is hard lithic limestone. The thin section reveals the presence of lumps, pellets and intraclasts embedded in calcaro-ferruginous matrix. Micritization is well pronounced both in the lumps and the intraclasts.

The bottom of Gercus Formation in immediate contact with the top of Sinjar Limestone Formation is highly ferruginous and clastic. In thin section of the rock, rounded to subrounded grains of orthoclase, microcline, perthite, limestone, and quartz are identifiable. Mostly the grains range in size from 0.5 to 2.0 mm. Fine grains of quartz are also observable in the matrix.

Fig. 2. Photomicrographs from phosphorite deposits, Sulaimaniah area, North Eastern Iraq. a) An aggregate of argillaceous intraclasts, pellets and microfossils embedded in calcareous matrix. Micritization observable specially in the central parts of the microfossils. Pressure solution effects are also visible. ×50.4, polarized light. b) Ooid showing concentric structure with micrites, sparry calcite, collophane and dahllite, visible. Sparry calcite developed due to pressure solution effects is also observable. ×50.4, polarized light. c) Lump, intraclast and pelloids embedded in calcareous matrix. Micritization prominent. Collophane and dahllite and pressure solution effects can be seen. ×50.4, polarized light. d) Lathic limestone containing peloids and intraclasts. The intraclasts probably of fossil fragments are completely recrystallized and firmly embedded in calcaro-argillaceous matrix. ×50.4, polarized light

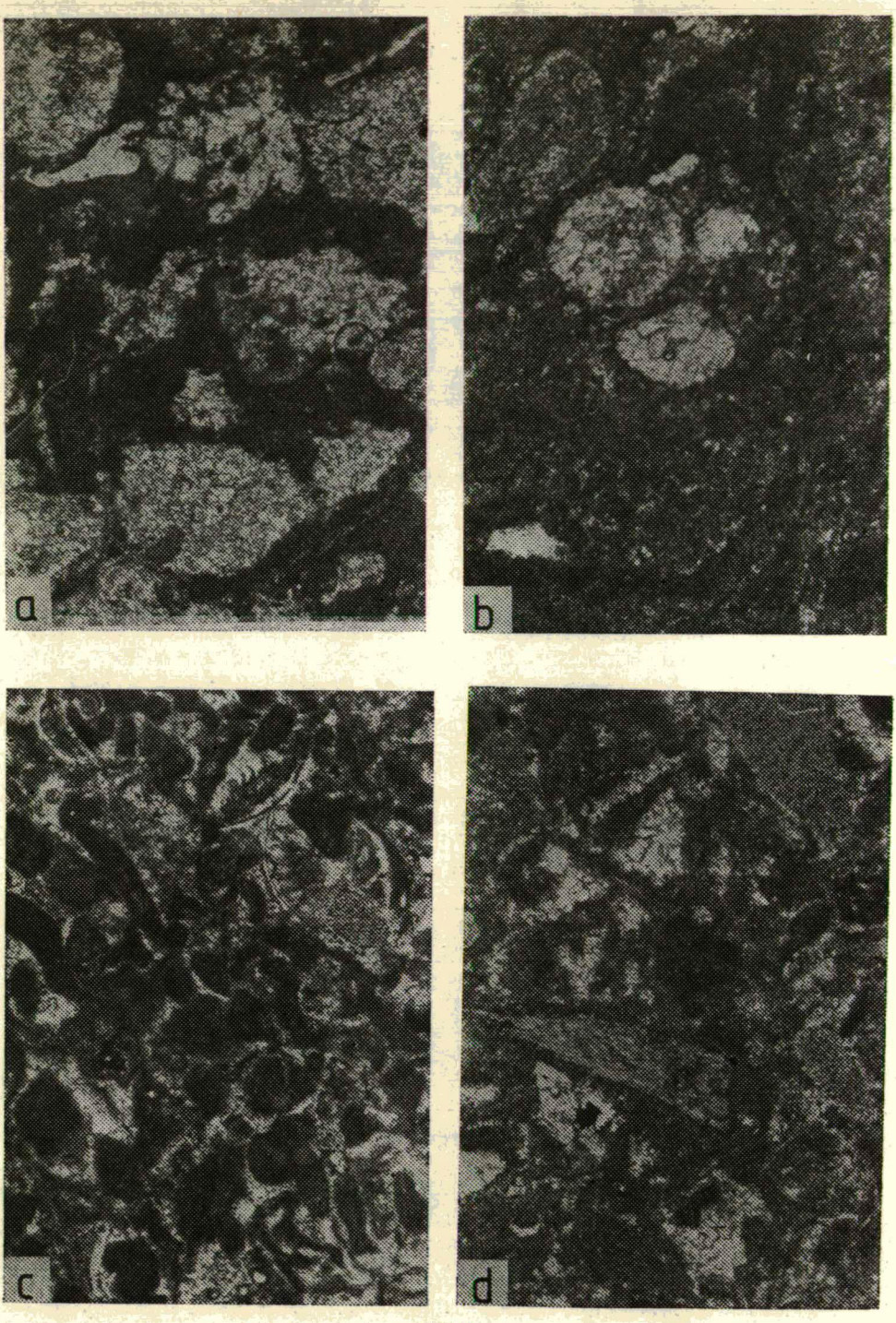

Fig. 3

MAJOR CHEMICAL CONSTITUENTS OF THE ROCKS

Quantitative estimations of calcium, magnesium, silicon, phosphorous and acid insolubles were made to study their relative concentrations in the beds of Sinjar Limestone Formation which appear different in physical and compositional characteristics. The graphs have been plotted with the assumption that the magnesium concentration in the nearshore water or in shallow seas is more as compared to the offshore deep-sea water and reverse is true for Ca. Any change or abnormal concentration of either of the elements would be an indication of varying physico-chemical conditions giving rise to enrichment or depletion of the elements through replacement and diagenesis. This assumption may not be rigorously true in all cases due to complexity in the local condition of the region during deposition and diagenesis but it would be helpful in over all appraisal of the conditions fairly satisfactorily.

The concentration of phosphorous, silica and acid insolubles were determined to describe the degree of correspondance if any, between the major constituents of the rocks. The graphs plotted represent a cross section of the major chemical constituents of the rocks of this formation in the area.

The plots of concentrations for Ca and Mg appear to show antipathic relationship with each other except in sample Nos. 9, 14 and 15 *(Fig. 5)*, and their concentrations appear in accordance with the assumption described earlier. It is inferred from the graphs that geochemical conditions in the depositional basin were not consistent and caused an appreciable range of variation in the concentration of Ca and Mg or the beds during deposition.

The plot of Ca/Mg ratio versus Mg concentration shows a fairly good inverse relationship in general *(Fig. 6)* but it is not possible to conclude any sytematic change in the depth condition of the basin of deposition from the bottom to the top of the formation or *vice versa*. The cluster of points definitely indicates two different populations characterized by low and high ratios. The population having higher Ca/Mg ratio represents the deeper marine condition than that which has lower concentration. The Ca/Mg ratios between 13.5 to 16.5 appear to separate the population of shallower and relatively deeper marine water deposits or at least it shows fluctuations or possibly break in the depositional cycle.

Since the numbers with the points indicate to the beds of Sinjar Limestone Formation in ascending order i.e. from bottom to top, it is hard to interpret gradual increase or decrease in the depth conditions. The random enrichment and depletion of Ca and Mg in the beds of the formation may be because of the interplay of tectonics and sedimentation at the time of depositions. As the area is not far from the subduction zone of Afro-Arabian and Iranian plates which were very active during Paleocene, the above interpretation appears quite logical. The possibilities of heterogenous concentration of Ca and Mg in the beds of the formation due to selective diagenesis under changing geochemical conditions in the depositional basin and afterwards cannot be ignored.

Fig. 3. Photomicrographs from non-phosphatic beds of Kinjinnah and Bazyan areas, North-eastern Iraq. a) Intraclasts in ferro-calcareous matrix. Micritization prominent in intraclasts probably due to recrystallization of the calcareous fragments. ×50.4, crossed Nicols. b) Banded algal structure with ooids and fine shell fragments. Micritization prominent. Matrix calcaro-carbonaceous. ×50.4, polarized light. c) Ferro-argillaceous pellets, intraclasts, fossils and fossil fragments in calcareous matrix. Fossils and fossil fragments are micritized. Pressure solution filled the intergranular spaces with sparite. ×50.4, crossed Nicols. d) Skeletal limestone with argillaceous intraclasts. Effects of micritization and pressure solution prominent. Sparry calcite is also present. Matrix argillo-calcareous. ×50.4, polarized light

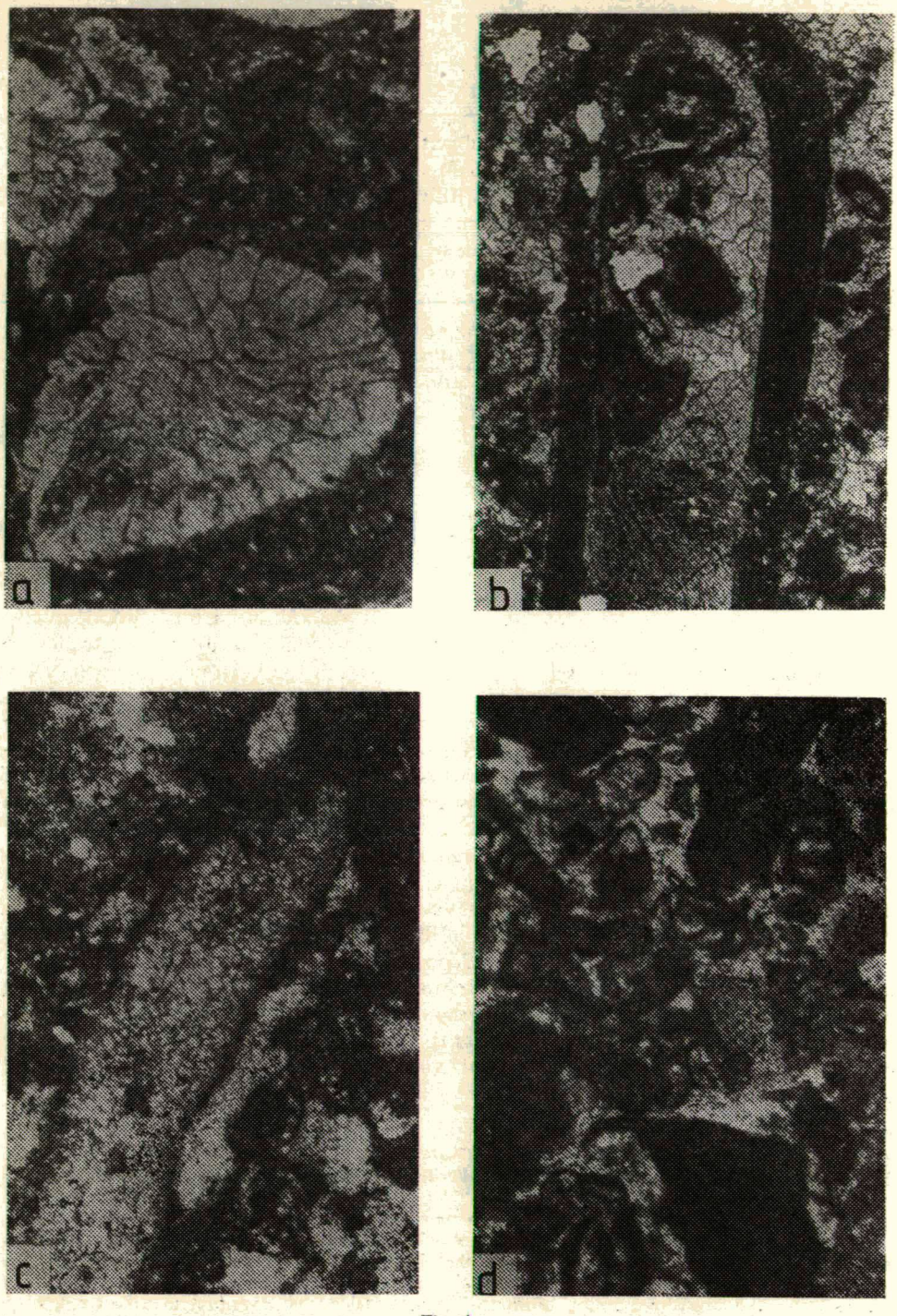

Fig. 4

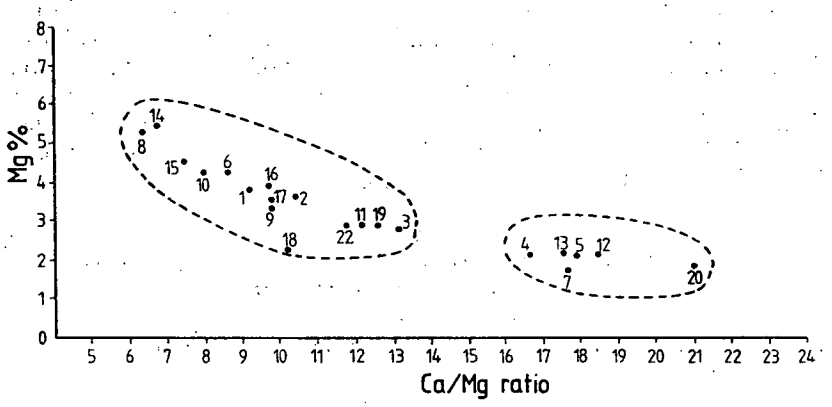

Fig. 5. Enrichment and depletion of calcium and magnesium in the rocks of Sinjar Limestone Formation

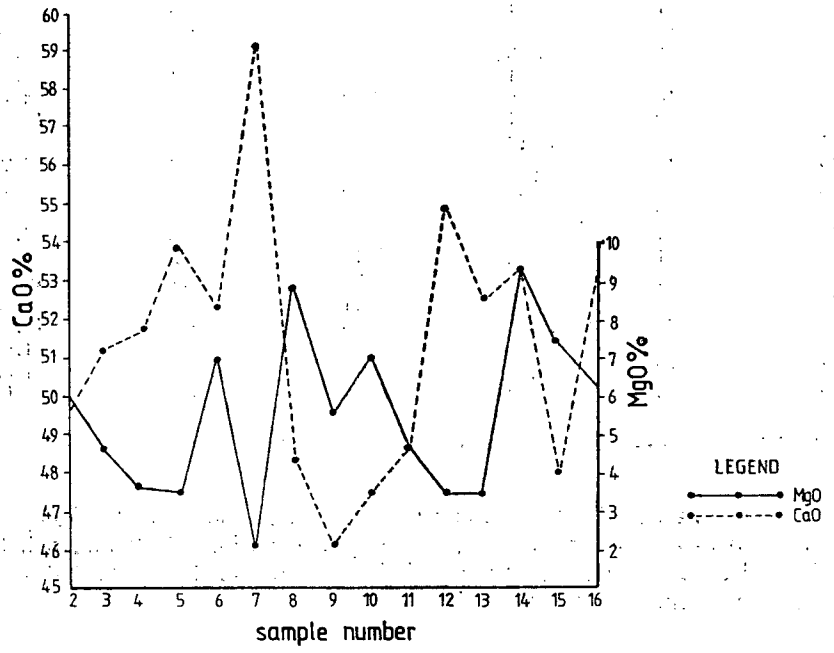

Fig. 6. Variation of Mg with Ca/Mg ratio in the rocks of Sinjar Limestone Formation

---

Fig. 4. Photomicrographs from non-phosphatic beds associated with the phosphorite beds, Sulaimaniah area, Iraq. a) Fossils and fossil fragments embedded in argillo-calcareous matrix. Peloids as black speeks and micrites in the ground mass. ×50.4, crossed Nicols. b) Argillaceous pellets, intraclasts and fossil fragments within tubicular part of a mud-feeding organism and around it. Micritization and pressure solution effects prominent. Sparry calcite and dolomite observeable. ×50.4, crossed Nicols. c) Micritized obliterated fossils and intraclasts in argillo-calcareous matrix. Primary pores filled with sparry calcite due to pressure solution effects. ×50.4, crossed Nicols. d) Lathic intraclasts fossils and fossil fragments in calcareous matrix. Micritization more prominent in fossil fragments than in the intraclasts. ×50.4, crossed Nicols.

The cluster of points showing to the population with higher Ca/Mg ratio represents to phosphatic limestone beds of Sinjar Limestone Formation with the exception of samples No. 14 and 2 which are in the cluster of the other population representing non-phosphatic rocks. No relationship could be observed in the concentration of silica and phosphorous. The contents of acid insolubles and phosphorous in the phosphatic beds suggest some positive correspondence which may be because of argillaceous contents of the rocks (Table 2).

TABLE 2

Chemical characteristics of the beds of Sinjar Limestone Formation Kanijinnah section Sulaimaniah area, Northeast Iraq

Bed №.	Thickness in ft.	Ca/Mg ratio	SiO_2%	P_2O_5%	AIR %
SK—1	7	9.26	1.24	ND	3.80
SK—2	10	10.44	3.80	ND	4.10
SK—3	6	13.12	2.37	1.77	5.4
SK—4	6	16.89	1.22	3.60	5.61
SK—5	21	17.91	2.93	4.60	7.79
SK—6	10	8.79	0.33	ND	3.82
SK—7	5	37.90	0.49	1.46	2.95
SK—8	2	6.41	0.69	ND	1.73
SK—9	16	9.89	1.64	ND	4.98
SK—10	17	8.01	5.39	ND	15.30
SK—11	8	12.19	0.27	ND	3.04
SK—12	19	18.46	0.98	2.29	4.59
SK—13	18	17.67	0.85	3.17	4.82
SK—14	20	6.89	0.33	5.95	6.38
SK—15	17	7.58	3.56	1.36	7.30
SK—16	51	9.76	0.19	ND	1.35
SK—17	37	9.89	3.78	ND	10.60
SK—18	13	10.23	0.31	ND	2.20
SK—19	39	12.64	2.29	ND	16.24
SK—20	12	20.89	1.69	ND	1.84
SK—21	17	64.32	0.29	ND	1.21
SK—22	19	11.82	0.98	ND	2.13

N.B: AIR stands for Acid Insoluble Residues and ND for non detectable.

The concentration of P_2O_5 shows positive correspondence with MgO in those samples which have angular to subangular argillaceous intraclasts and pellets embedded in calcareous matrix. This relationship has developed most probably due to dolomitization of the calcareous matrix.

ACID INSOLUBLE RESIDUES

Quantitative estimation of insoluble residues was made according to the procedure described by IRELAND (1936). The clay fraction was amonge the major components of the acid insoluble residue. The non-clay minerals in the insoluble residue were gypsum, anhydrite, quartz and grains of alkali feldspars. The grains were angular to subangular with sharp edges. No relationship could be found between the percentage of insoluble residue, the thickness of the beds and the concentration of CaO and MgO of Sinjar Limestone Formation. However, the concentration percentage of insoluble residue shows radical variation from one bed to the other proba-

bly due to pronounced fluctuation in the source of supply of the clastics or due to varying turbidity conditions in the basin of deposition (Table 2). It is also possible that the energy conditions responsible for contributing clastics were inconsistent. The intertonguing of Kolosh Clastic Formation with Sinjar Limestone Formation also reveals inconsistency either in the energy condition responsible for the deposition of clastics or fluctuation in depth of the basin of deposition which caused present geometry of Kolosh Clastic Formation and Sinjar Limestone formation. Perhaps the basins of deposition of these contemporaneous formations were separated by barriers and so whenever the energy conditions were changed and the depth of the basins were affected they gave rise to interfingering of the two formations having clastic and nonclastic characteristics. The radical variation in the percentage of the insoluble residues of the beds may be attributed to the same conditions. The ratios of Ca/Mg in the beds of Sinjar Limestone Formation also confirm the tendency of increase and decrease in depth of the basin of deposition. No correspondence could be established between the concentration of insoluble residues and the enrichment or depletion of Ca and Mg (Table 2).

DISCUSSIONS

The occurrence of angular to subangular grains of limestones, quartz and relatively fresh grains of alkali feldspars in Tanjero Clastics of Upper Cretaceous age lying below Sinjar Limestone Formation indicates the condition of more supply of sediments from near-by source and slower rate of subsidence of the basin of deposition.

In view of the characteristics observed it is concluded that the sedimentological cycle, physico-chemical conditions and the environments of deposition were changing during the deposition of Sinjar Limestone Formation of Paleocene age. The occurrence of varying percentages of clay fraction and the non-clay fraction in insoluble residues having minerals like quartz, alkali feldspars, anhydrite, gypsum etc. in the beds of Sinjar Limestones Formation show some degree of similarities with Tanjero Clastic Formation. Most probably the supply of sediments which formed Tanjero Clastic Formation did not stop completely but it was very slow and non-uniform. It is considered that the weak energy condition helped mixing the clastics into the sea water which was enriched with calcium to precipitate limestones along with variable contents of fine clastics, algal material and fossils of fossil fragments. The presence of algal material, fossils and fossil fragments indicate shallow warm water condition of deposition of the limestones.

It is hard to think about restricted shallow basin and the reworking of the upper part of Tanjero Formation to be the source of insolubles in the beds of Sinjar Limestone Formation because the constituents of the insolubles are not limited only in the lower beds of the Formation but are present in all the beds from lower to the upper part of the formation in varying percentages. No relationship could be found between the thickness of the beds and the contents of insolubles. Thus it appears reasonable to conclude that the supply of clastic was independent of the conditions in the depositional basin and the amount changed with respect to tectonic conditions and the rate of weathering in the source area.

The presence of micropellets of variable sizes with characters of reworking and argillaceous angular to sub-angular fragments in micritic matrix are sufficient indications of shallow basin of deposition, getting supply of argillaceous matter from the near-by source through weak energy condition. The absence of any orientation

in the long axis of the elliptical pellets does not encourage to think about the diagenetic origin of the pellets in the limestone beds. On the contrary the association of lumps with randomly oriented pellets help in interpreting shallow turbid water condition in the basin of deposition. Thus it appears reasonable to describe the origin of the pellets as a result of coagulation of clays from turbid water of the basin and deposited with the limestone. Differential aggradation of clays both during sedimentation and diagenetic stages resulted in variable sizes of the pellets.

The algal structures in the limestones with fossils and fossil fragments and the clastics indicate warm and shallow water conditions possibly littoral or shoal conditions, having intrabasinal barriers wich gave rise to contemporaneous deposit of Kolosh Clastic Formation, mainly composed of marls, siltstones and carbonaceous shales. The possibilities of contribution of clays and clastics from the provenance of Kolosh Clastic Formation due to fluctuation in depth of the depositional basin and the height of the intrabasinal barriers at the time of deposition of the two formations cannot be neglected. The intermixing of the sediments across the barriers due to fluctuations in the depth of depositional basins appears reasonable explanation in favour of the observation made during the present investigation.

Relative abundance of microfossils like nummulites, miliolids and less percentage of argillaceous matter in the upper part of Sinjar Limestone Formation indicates a period of relative stability in depositional basin with respect to turbidity and favourable ecological conditions for the growth of life in clear water. Corals are found in the lower part of Sinjar Limestone Formation where argillaceous matter, clastics and pellets are common. Fossils and fossil fragments are obliterated and replaced due to the processes of diagenesis. However, some of the fossils are preserved with internal structures and their characteristics but micritized.

The presence of micro-pellets with some degree of orientation in aragonite and calcite matrix is an indication of diagenetic changes in loose textured and moderately hard limestones. Calcareous intraclasts with pellets having obliterated outlines are good indications of diagenesis. Selective micritization in the fossil fragment further confirm to the differential effects of diagenesis. Micritization of ooids has resulted concentric internal structure pattern probably due calcareous and organo-argillaceous composition of the ooids.

The clastics and the ooids embedded in lithic and organic matrix show no effects of solution pressure but indicate highly porous texture of the limestones. The calcitic fragments irregularly distributed in the rock samples are present as angular or rounded grains and are probably the remains of fossil fragments subjected to diagenesis. The aggregate of recrystallized clastics and fossil fragments along with non-crystalline sediments of argillaceous nature indicate that the diagenetic forces were active on aragonitic components quite prominantly.

Sparry calcite fillings in micro-fossils and mud-feeding animals are the results of diagenesis in the limestones. The phosphatic limestones show pronounced effects of diagenesis in the matrix and not in the pellets probably due the presence of collophane and dahllite which are not very sensitive to the diagenetic forces.

Variable contents of acid insolubles in different beds of the Formation irrespective of thickness and top and bottom further support the hypothesis of fluctuation in the depositional basin and the barriers which gave rise to the lithosomes of Kolosh elastics and Sinjar Limestones. Likewise, variable Ca/Mg ratio in the beds of Sinjar Limestone is also an indication of periodic changes in the geochemical and tectonic conditions mainly of epirogenic origin during deposition.

The absence of facies like Aaliji Limestone Formation and Jeddala Formation from the areas of present study further supports the hypothesis that the depositional basin trending northwest and southeast was having barriers and non uniformities with respect to depth conditions, energy conditions responsible for the supply of clastics and the rate of subsidence of Zagros Basin in which contemporaneous formations of different lithologic characteristics were deposited. The reasons could also be attributed to the tectonic frame work of this region during Upper Cretaceous, Paleocene and Miocene ages, beeause during these periods the regions was facing uplift from the north-east and sinking of the basin in the south-west along the margin of the Arabian shield which resulted the present Zagros Mountains (SAMIMI, 1977). The active slow subduction of the Arabian Shield along the northwest and southeast margins of the Zagros Mountains and the presence of Arabian Gulf as a remain of Zagros Basin are satisfactory proves to confirm the above arguments.

In view of the characteristics observable in the rocks of the Formation, it appears reasonable to conclude that there were at least five phases of sedimentation with varying physico-chemical conditions. These phases of sedimentation from bottom to top of the Formation were *i)* deposition of sugary limestone with very little percentage of fossils, *ii)* deposition of phosphatic beds, *iii)* deposition of non-phosphatic clastic limestones with fossils, *iv)* deposition of phosphatic beds, *v)* deposition of highly fossiliferous limestones.

ACKNOWLEDGEMENTS

We are thankful to the President of the University Salahuddin for providing facilities to carry out field work and laboratory investigations for the completion of the research.

The assistance of MISS NEGAR ABDUL AZIZ of the Department of Soil Science during the determination of phosphorous and MR. NIZAR AL-DYNI in making quantitative estimation of insoluble residues are acknowledged with thanks.

REFERENCES

AL-KUFAISHI, F. A. M. (1977): A geochemical study of on Sinjar Limestone in a subsurface section (K-16). Jour. Geol. Soc. Iraq, Vol. X p. 47—51.

AL-SAIGH, A. Y. and AL-OMARI, F. S. (1977): General Geology. p. 377, University of Mosul Press, Mosul, Iraq.

AL-SIDDIQI, A. A. M. (1968): Stratigraphy and Microfacies of Sinjar Formation. Unpub. M. Sc. Thesis, Baghdad University, Baghdad, Iraq.

AMES, L. L. Jr. (1959): The genesis of Carbonate Apatites. Econ. Geol. vol. **54**, p. 829—841.

ARRHENIUS, G. (1963): "Pelagic sediments". In the sea and observations on progress on the study of the sea. Edited by M. N. HILL, N. Y. Interscience Publishers, Inc. pp. 655—727.

BATHURST, R. G. C. (1976): Carbonate sediments and their diagenesis. Elsevier Scientific Publishing Company, N. Y. pp. 77—90.

BANAK, K. M. *et al.* (1981): Sedimentology of the Paleocene Flysch of the Kolosh formation Northeast Iraq. Sixth Iraqi Geological Congress, Abstract p. 41.

BROMLEY, R. G. (1967): Marine phosphorites as depth indicators. Marine Geol., Vol. **7**, pp. 503—509.

BUSHINSKY, G. I. (1935): Structure and origin of the phosphorites of the USSR. Jour. Sed. Petrol., vol. **5**, pp 81—92.

— — (1964): On shallow water origin of phosphorite sediments. Development in Sedimentology vol. 1, Edited by L. M. J. U. VAN STRAATEN, Elsevier Publishing Co. N. Y.

CAYEUX, L. (1939): Phosphate sedimentaries et bacteries. Compt. Rend., vol. **203**, pp. 1198—1200.

CONSULTANTS of USSR & IRAQI GEOLOGISTS (1965): Report on geological prospecting and investigation into phosphate deposits of Rutba and Akashat areas. Open file report, Geol. Min. Surv. Div. Baghdad, Iraq.

DEGENS, E. T. (1965): Geochemistry of sediments. pp. 144—146, Prentice Hall, Inc. N. Y.
DIETZ, R. S., EMERY, K. O. and SHEAPARD, F. P. (1942): Phosphorite deposits on the sea floor off southern California. Bull. Geol. Soc. Am., vol. **53**, pp. 815—810.
IBRAHIM, M. W. (1979): Shifting Depositional Axes of Iraq: An outline of Geosynclinal History, Jour. Petrol. Geol., vol. **2**, pp. 181—197
GOLDBERG, E. D. and PARKER, R. H. (1960): Phosphatized wood from the Pacific sea floor. Bull. Geol. Soc. Am., vol. **71**, pp. 631—633.
GULBRANDSEN, R. A. (1966): Chemical composition of phosphorites of the Phosphoria Formation. Geochem. Cosmochim. Acta, vol. **30**, No. 8, pp. 769—778.
KAZAKOV, A. V. (1937): The phosphorite facies and the genesis of phosphorites. Trans. Sc. Inst. of Fertilizers and insect Fungicides, Moscow, Vol. **142**, P. 95—113.
— — (1950): Fluorapatite system equililibria under conditions of formation of sedimentary rocks. Akad. Nauk., **114**, Geol. Ser. No. 40, pp. 1—21.
MALLICK, K. A. & AL-FADBLI, I. (1980): Phosphorites in Sinjar Formation of Sulaimaniah Area, Iraq. Acta Miner. Petrographica, vol. **XXIV**, No—2, p 219—233.
MC. KELVEY, V. E., SWANSON, R. W. & SHELDON, R. P. (1953): The Permian phosphorite deposits of western United States. 19th Int. Geol. Congr. Algiers, Compt. Rend., **XI**, pp. 45—64.
MALLICK, K. A. and AL-FADBLI, I. (1980): Phosphorites in Sinjar Formation Sulaimaniah Area, Iraq and its tectonic significance. 26th Inter. Geol. Congr. France, Abstract vol. **11**, Section 6, p. 493.
NOTHOLT, A. J. G. (editor) (1977): Phosphate rock in CENTO Region, CENTO press, Ankara, Turkey.
— — (1965): Discussion on exploration for phosphorite in Turkey. Econ. Geol., vol. **60**, No. 4 pp. 822—823.
SAMIMI, M & GHASEMIPOUR, R. (1977): Phosphate deposits in Iran, phosphate rock in CENTO Region. Edited by NOTHOLT, A. J. G. pp. 1—40, Ankara, Turkey.
SHAPIRO, L. (1952): Simple field method for the determination of phosphate rocks. Am. Miner., Vol. **27**, No. 3, pp. 341—343.
SHELDON, R. P. (1964): Exploration for phosphorite in Turkey. Econ. Geol., Vol. **59**, No. 6, pp. 1159—1175.
— — (1964): Paleolatitudinal and paleogeographical distribution of phosphorite. Prof. Pap. No. **501—C**, USGS Bull. pp. 106—113.
SMITH, J. S. (1954): Radioactive anomalies in the western part of the Republic of Iraq on the Syrian Desert. Open file report, Geol. and Mineral Surv. Division, Baghdad, Iraq.
VAN BELLEN, R. C. (1956): Lexique Stratigraphique International, vol. **111**, ASIE, Fascicule 100, pp. 108—112, 155—157, 274—285.
YOUSEF, M. I. (1965): Genesis of bedded phosphates. Econ. Geol., vol. **60**, No. 3, pp. 590—600.

Manuscript received, December 4, 1983

Acta Mineralogica-Petrographica, Szeged, XXVII, 117—130 1985

ZIRCON IN GRANITOIDS FROM SINAI, EGYPT AND ITS GENETIC SIGNIFICANCE

MOHAMED A. HEIKAL[1], ABDEL-KARIM A. SALEM[2] and YOUSSEF A. EL-SHESHTAWI[1]

ABSTRACT

The granitic plutonism in the area around Wadi El-Sheikh, southwestern Sinai, Egypt is mainly represented by the Older and Younger Granitoid Rocks. The younger granitic rocks comprise in turn, two granitic phases, distinguished on field basis.

Morphological characters of zircon concentrates from the examined rocks have been statistically studied. Zircon populations in the Older Granitoids contain a wide variety of crystal shapes while in those of the younger granitic rocks, zircon crystals become prograssively more uniform in morphology. Distinction between zircons of the Older and Younger Granitoids is based mainly on their dimensional parameters. Similarity of the dimensional parameters of zirkons in the younger granitic phases renders their separation difficult. The significance of zircon as a guide to the petrogenesis of Wadi El-Sheikh granitoids is ascertained.

INTRODUCTION

Studies of zircon have generally emphasized that genetic relationships can be established for chemically similar igneous rocks on the basis that similar zircon populations are derivatives of one magma while dissimilar zircon populations are derived from different magma sources (LARSEN and POLDERVAART, 1957; ALPER and POLDERVAART, 1957; TAUBENECK, 1957; HALL and ECKELMANN, 1961; LARSEN and POLDERVAART, 1961; CLIFFORD *et al.*, 1962; SPOTTS, 1962; KARNER and HELGESEN, 1970). Recent studies have shown that the alumina/alkaline ratio and the temperature of the crystallization medium are the main factors controlling the growth of zircon typology (PUPIN and TURCO, 1972, 1975; PUPIN, 1976). In accordance, a genetic relationship is considered between a granite's zircon populations and its magma type. According to PUPIN (1980), the zircon populations in rocks reflect very accurately the origin of the magma, regardless of post-magmatic geochemical variations induced locally by deuteric processes.

Studies on zircon from Egyptian granites in the Eastern Desert of Egypt have been carried out by ZAGHLOUL and KHAFFAGY (1965), RAGAB (1971) and HEIKAL (1973). No study of zircon has ever been published pertaining to the extensive Precambrian granitoids of Southwest Sinai.

The present study encompasses the morphological characters of zircon and its dimensional parameters with the aim to ascertain the origin of the granitic rocks in Wadi El-Sheikh area *(Fig. 1)*. Moreover the study attempts to reveal whether the granitic rocks have been derived from the same or closely related magma or else

[1] Geology Dept., Al-Azhar Univ., Cairo, Egypt.
[2] Earth Sciences Lab., National Research Centre, Cairo, Egypt.

differentiated, on the basis of zircon characteristics as morphology and elongation trends. The examined zircon crystals are believed to be representative of the granitic rocks around Wadi El-Sheikh.

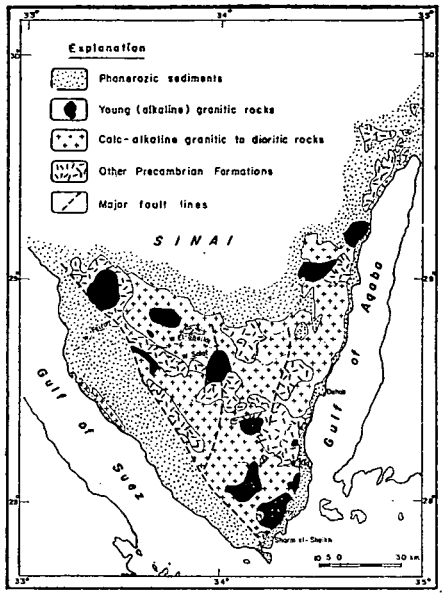

Fig. 1. Geological map of Sinai showing location of Wadi El-Sheikh area (simplified after SHIMRON' 1980).

GENERAL FEATURES OF WADI EL-SHEIKH GRANITOIDS

Two plutonic cycles are responsible for the formation of the granitic rocks in the area around Wadi El-Sheikh: *(1)* an old cycle that provided the Older Granitoid Rocks, and *(2)* a younger cycle that provided the Younger Granitoid Rocks. The younger granitoid rocks comprise in turn, two main granitic phases, distinguished on field basis, and corresponding to the second and third phases of the Younger Granitoids of the Eastern Desert of Egypt (SABET *et al.*, 1976).

The Older Granitoids of Wadi El-Sheikh area are two feldspar observed in subordinate amounts. Coloured minerals are represented by biotite and hornblende. Sphene is often abundant together with zircon and apatite. On the other hand, the Younger Granitoids are leucocratic, subsolvous rocks rich in K-feldspar, plagioclase and quartz. Biotite is the sole ferromagnesian mineral detected in these rocks.

Model classification (STRECKEISEN, 1976) of the Older Granitoids show that they are mainly represented by quartzdiorite, quartz-monzodiorite, tonalite and granodiorite. Granite and granodiorite are the two main rock units recognized among the granitic rocks of the second phase. Granitic rocks of the third phase are only represented by granite. The average modes of the studied granitic rocks are given in Table 1. Details of field relations and petrographic characters of the examined rocks are described by EL-SHESHTAWI (1984).

TABLE 1

Average modes (in volume %) and average zirconium contents (ppm) of the examined granitoids

	Older Granitoids	Younger Granitoids	
		Phase II	Phase III
Plagioclase	56.0	35.6	18.8
K-feldspar	9.1	30.3	48.8
Quartz	16.6	29.2	31.0
Muscovite	—	0.1	0.1
Biotite	8.1	3.5	0.7
Hornblende	7.6	0.1	—
Opaques and accessories	2.6	1.2	0.6
Total	100.0	100.0	100.0
Zirconium content	153.0	124.9	106.8

DISTRIBUTION OF ZIRCON

The random distribution of the small number of minute zircon crystals in various host minerals, renders the study of thin sections of limited value. However, thin section study reveals that zircon crystals are preferentially associated with ferromagnesian minerals *(Fig. 2a)* but they are also enclosed in quartz and feldspars. *(Fig. 2b, c)*. It is argued that zircon in Wadi El-Sheikh granitic rocks has crystallized early and continued up to the end of the magmatic stage. In support of this conclusion, the works of KÖHLER (1970); and PUPIN *et al.*, (1979) show that in magmas defficient in water, zircon crystallizes during an early magmatic stages. In water-rich magmas, zircon crystallisation begins early in the magmatic period and continues up to the end with the development of hydrozircon rich in some trace elements such as U, Th and Y.

Chemical studies on Wadi El-Sheikh granitic rocks (EL-SHESHTAWI, 1984 show that the zirconium content decreases from the Older to the Younger Granitoids *(Fig. 3)*.

A similar trend of zirconium descent has been detected by GREENBERG (1981) for the Younger Granitoids of the Fastern Desert of Egypt. The partial melting of the mantle which was invoked by HUSSEIN *et al.* (1982) to account for the calc-alkaline magma of the Older Granitoids of Egypt is also capable of concentrating appreciable quantity of zirconium inasmuch as this element is normally present in noticeable quantity in basic magmas (CHAO and FLEISCHER, 1960; PUPIN, 1980).

MORPHOLOGICAL AND STATISTICAL VARIATIONS IN ZIRCON

Preparation and measurement of zircon samples

Sample size is approximately 250 to 300 grams. After fine crushing, all the crushed material is passed through a 60-mesh U.S. Standard sieve (0.25 mm opening), caught on a 100-mesh sieve (0.149 mm opening). Thus two size fractions (−60+ 100 mesh and −100 mesh) of crushed material are obtained. The crushed samples

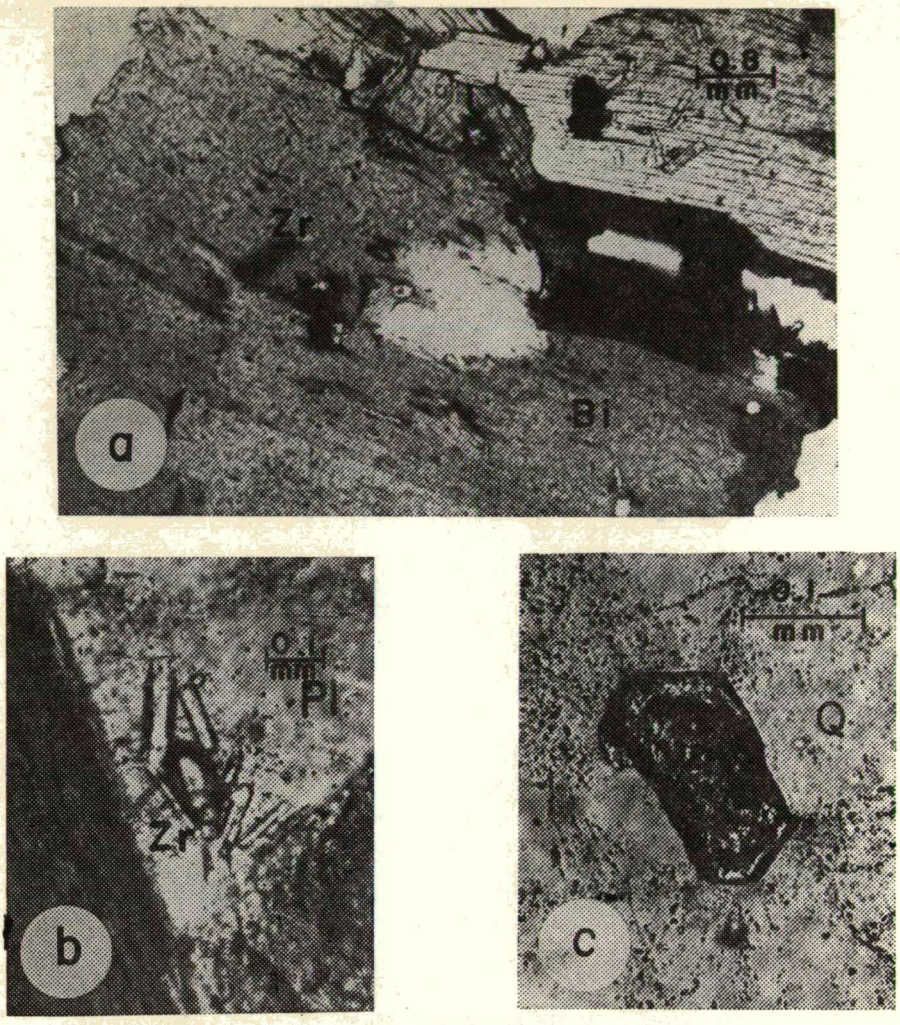

Fig. 2. a) Textural association of zircon (Zr) with biotite (Bi). Note pleochroic haloes surrounding the zircon crystals due to their content of radioactive elements, plane polarized light *b)* and *c)* Zircon (Zr) enclosed in plagioclase (Pl) and quartz (Q), plane polarized light

are individually separated with bromoform (sp. gr. 3.3). Mineral fractions with densities greater than 3.3 were purified by passing through a Frantz Isodynamic Separator following directions given by ROSENBLUM (1958). Side tilt at 15°, forming tilt at 25° with the magnet set at 1.7 amps. are the best extractions conditions. Permanent mounts of the entire nonmagnetic residues of each sample are prepared. Both coarse and fine fractions of each sample are prepared and mounted separately.

Zircon is most abundant in the −100 mesh fraction. The predominance of doubly terminated crystals in most samples suggests only minor breakage during crushing. A mechanical stage is used in measuring and counting unbroken zircon crystals observed along regularly spaced intervals. 100 doubly terminated zircon crystals are measured at high magnification (×250) with an ocular micrometer.

Description of zircon in concentrates

The morphological characters of zircon crystals are focussed on colour, shape, form, habit, elongation, zoning, inclusions, outgrowths, overgrowths and coincidence of crystal length and *c*-axis. Representative zircon crystals as well as some of the less common types are pictured in *Fig. 4.*

Study of zircon concentrates revealed that zircon of the Older Granitoids is predominantly colourless to pale green. Pale pink and pale yellow crystals are uncommonly encountered. Zircon of the second phase granitic rocks shows similar colours. In addition, metamict zircon is rarely observed. On the other hand, zircon of the third phase granitic rocks is predominantly brown, with a relatively higher percentage of metamict varieties *(Fig. 4v, w).*

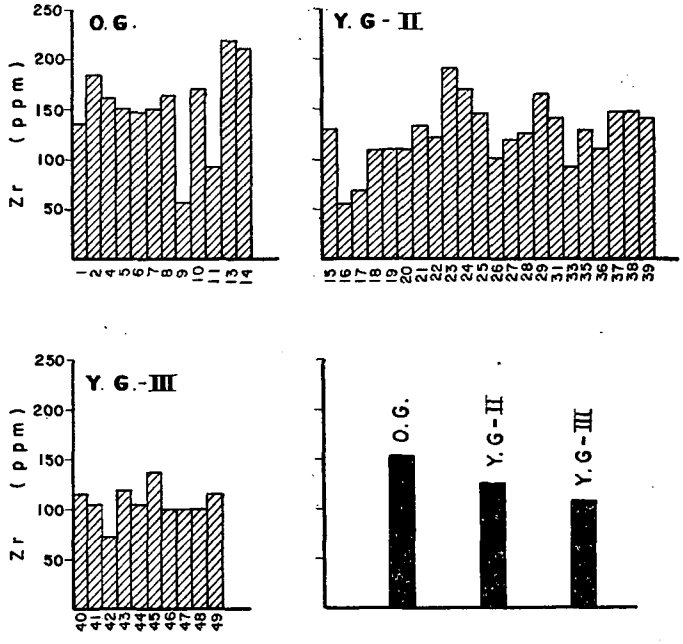

Fig. 3. Frequency histograms showing distribution of zirconium in Wadi El-Sheikh granitoids. O. G.: Older Granitoids; Y. G. — II: Younger Granitoids of the second phase, Y. G. — III: Younger Granitoids of the third phase

Nearly, all the crystals examined are euhedral *(Fig. 4b, c, p, w).* Less than 5% show slight to moderate rounding of crystal edges and terminations *(Fig. 4f, s).* Rounded zircons (rounded terminations) rarely occur *(Fig. 4k, l, o)*, most probably due to magmatic resorptions. SPOTTS (1962, p. 1228) proposed that such zircons may have produced during the cooling of magma.

The microscopic examination of zircon crystals proves the frequent occurrence of the following forms: tetragonal prism, tetragonal bipyramid and basal pinacoid. These forms are combined in different ways giving rise to different crystal habits *(Fig. 4d, e, i, t, u).* Rare complex forms of zircon showing many crystal faces are rarely encountered *(Fig. 4q).* The relative development of the prism with respect

to the bipyramid is found to vary considerably *(Fig. 4a, j, t)*. Hemimorphic crystals are also detected.

Zoning predominates in the studied zircon. Although a detailed analysis of zoning is not attempted, several groups of zoned crystals are recognized: *1*—zircons with uniform zoning throughout *(Fig. 4q)*, *2*—zoned zircons enclosing an unzoned central area *(Fig. 4u, x)*, *3*—zoned zircons with unzoned periphery *(Fig. 4b)*. In most cases, zoning runs parallel to the periphery of the crystal *(Fig. 4u)*. In some cases, irregularities have been observed e.g. zones are shifted from the centre of the crystal.

Generally, zircon of the Younger Granitoids is poor in inclusions, while inclusions in zircon of the Older Granitoids are numerous and diverse. Commonly, inclusions are of apparently random distribution *(Fig. 4j, n)*. However, inclusions oriented parallel to the c-axis *(Fig. 4c)* or to the bipyramidal faces *(Fig. 4t)* are rarely observed. Concerning the composition of these inclusions, several kinds of zircon inclusions are distinguished. Some of the inclusions are possibly transparent acicular rutile (?) *(Fig. 4j)* and others are typically irregular opaque matter *(Fig. 4h, j)*. Opaque inclusions are observed *(Fig. 4b, j, g, u)* mainly in zircon of the Older Granitoids. Transparent colourless to light brown fluid inclusions are observed, being of a spherical bubble-like *(Fig. 4f)* or tubular form *(Fig. 4i, p)*. A final group consists of small zircon inclusions (euhedral, rounded or both) *(Fig. 4g, h, s)*. AUGUSTITHIS (1973) considered the central rounded zircons as representing a sedimentogenic phase and the overgroths as representing a later generation under the influences and conditions of granitisation. In contrast, *Fig. 4g* shows an euhedral zircon inclusion representing the first zircon generation. A sedimentary origin could not be invoked for the explanation of such euhedral crystals. However, the rounded zircon inclusions, are suggested by the present authors to represent the first zircon generation, which was later corroded by magmatic corrosion and the overgrowths represent a second generation formed in the same magmatic phase of crystallization.

Zircon with outgrowths are very rare, not exceeding fraction of a percent. Outgrowths may have a spherical shape *(Fig. 4o)* or a rectangular form attached with its base to the bipyramid face *(Fig. 4v)*. Outgrowths with irregular shapes have been rarely detected *(Fig. 4n)*. These outgrowth when met with, are identical in properties and appearance with their supporting zircon grains *(Fig. 4v)*.

Parallel growth is quite rare in the examined zircons *(Fig. 4r)*. The formation of parallel growth suggests that zircon crystals crystallized early from a melt of low viscosity permitting the movement and collision of growing zircons (JOCELYN and PIDGEON, 1974).

The coincidence of the crystal length with *c*-axis in all the crystals studied is very clear.

Zircon elongation studies

Statistical investigations of zircon elongation are made on 11 samples by measurement of length and breadth of euhedral (unbroken) crystals in each sample. The length and breadth frequencies of zircon are given in Table 2. The elongation frequencies of zircon are given in Table 2. The elongation frequencies are given in Table 3. Length and breadth are represented graphically by frequency curves of length, breadth and elongation *(Fig. 5)*. *Fig. 6* illustrates the dimensional differences between the Older and Younger Granitoids. An attempt to correlate the dimen-

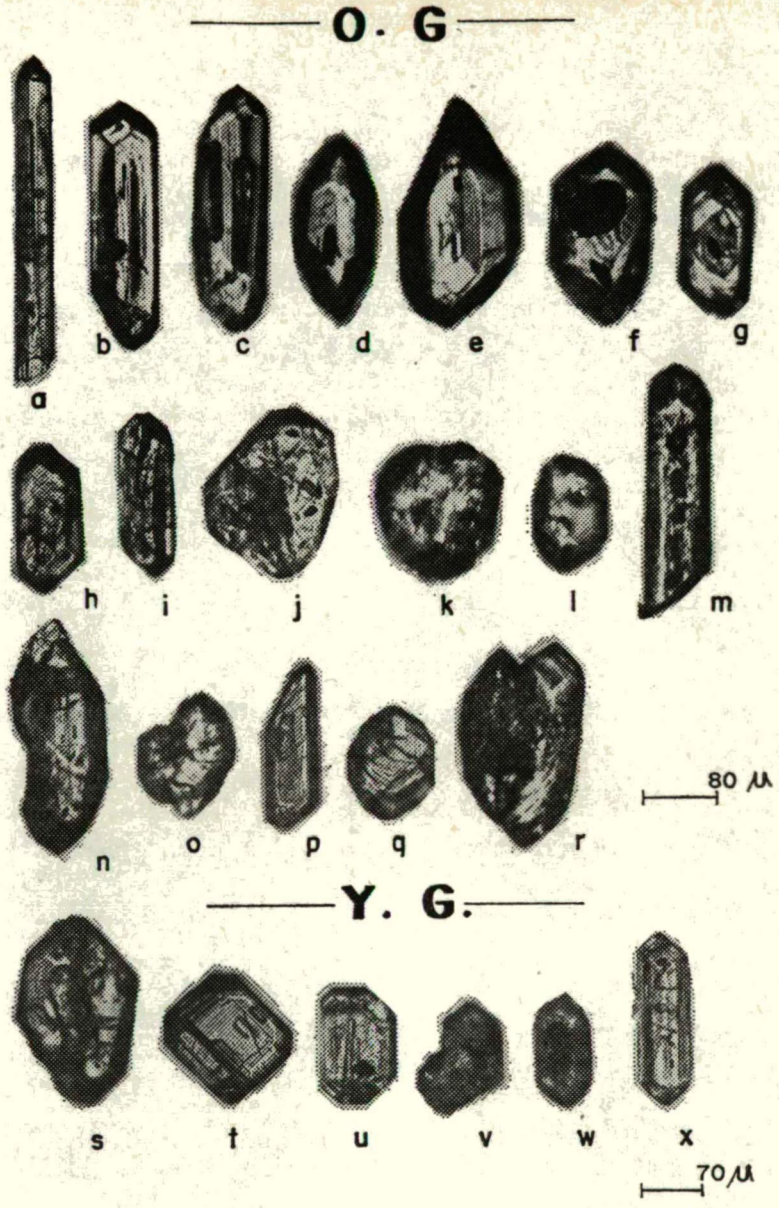

Fig. 4. Zircon crystals from Wadi El-Sheikh granitoids. (Details in the text)

sional parameters of the second and third phases of the Younger Granitoids, is shown on the same graph.

Of the dimensional parameters, the width of zircon crystals varies far less than their length. The mean width of zircon in the studied granitic rocks falls in the narrow range 0.06—0.08 mm. The mean length falls in the range 0.10—0.21 mm. Zir-

cons in the Older Granitoids are typical longer than those in the Younger Granitoids. Zircon crystals in the second phase granites are slightly longer than those in the third phase. The mean elongation ranges from 1.57 to 2.63. Zircon crystals in the third phase granite have a majority of short stubby crystals, while normal prismatic crystals characterize the zircon populations in the other granitic rocks.

Results of the statistical parameters $\bar{x}$ (mean of x), $\bar{y}$ (mean of y), S_x (standard deviation of x), S_y (standard deviation of y), r (correlation coefficient) and Dd (correlation of relative dispersion about RMA) or zircon of various granitic samples

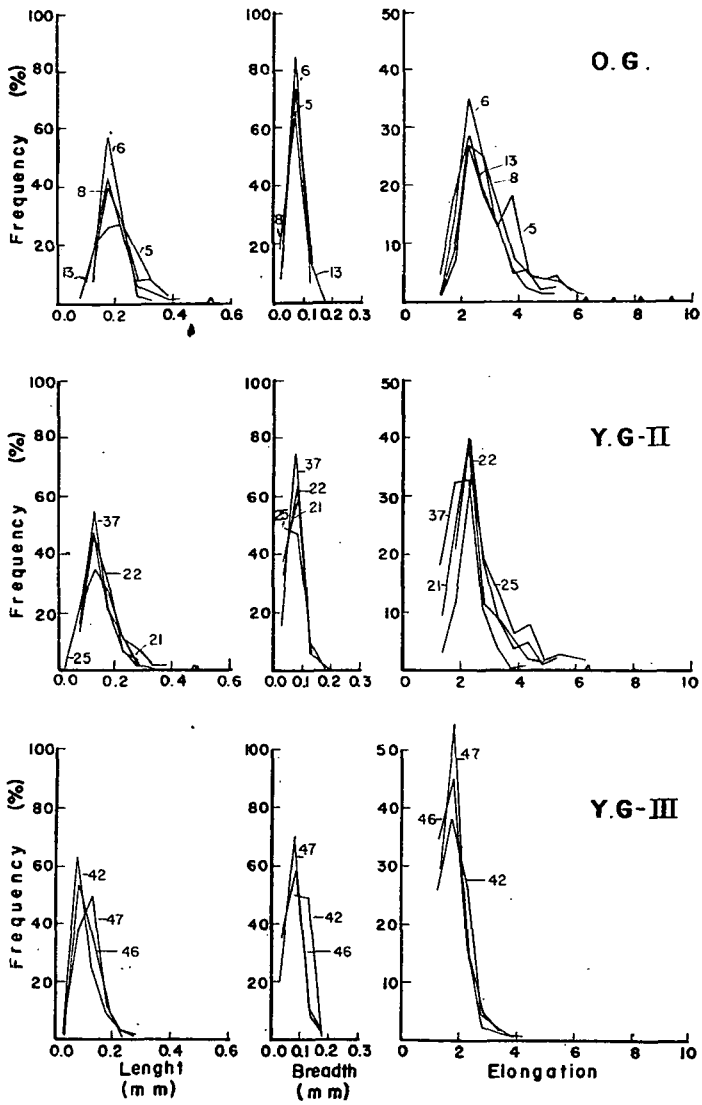

Fig. 5. Size frequency curves for zircon in the examined granitoids

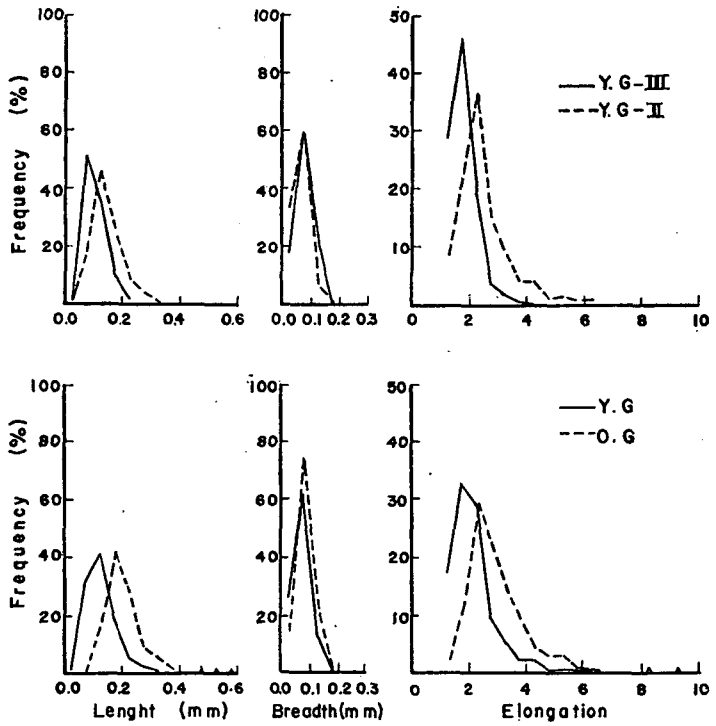

Fig. 6. Frequency curves for mean lengths, widths and elongation values for zircon populations in Wadi El-Sheikh granitoids

are given in Table 4. Reduced major axes of zircons are plotted in *Fig. 7*, where a distinction between the Older and Younger Granitoids is marked. The axis of the older granitoids have a longer length than that of the younger granitic rocks. Furthermore, their point for mean length *versus* mean breadth plots to the right of that of the Younger Granitoid Rocks.

DISCUSSION AND CONCLUSION

It is well established that granites of magmatic origin have a majority of euhedral zircons, in contrast to detrital zircon suites which usually contain a high percentage of rounded zircon (POLDERVAART, 1955, 1956). The high percentage of sharply bounded, euhedral zircons in Wadi El-Sheikh granitic rocks suggests their magmatic origin. The enclosure of zircon in early and late constituent minerals suggests that zircon has crystallized early and continued up to the end of the magmatic stage.

With respect to the criterion of the coincidence of crystal length and *c*-axis, it is resonable to predict that during sedimentary transport, some elongate zircons will tend to break at angles other than 90° to their long axes, leading to the formation of rounded segments whose long axes does not concide with the *c*-axis (extinction position) of the original crystal. MURTHY and SIDDIQUIE (1964) found that well rounded zircons from some Indian metasedimentary rocks possess angles between

TABLE 2

Length and breadth frequencies of euhedral zircon in Wadi El-Sheikh Granitoids
(frequencies are given as percentages)

Sample №		0.00—0.05	0.05—0.10	0.10—0.15	0.15—0.20	0.20—0.25	0.25—0.30	0.30—0.35	0.35—0.40	0.40—0.45	>0.45
5*	x	—	—	20.5	26.0	27.0	16.5	7.0	2.5	—	0.5
	y	16.0	72.0	12.0	—	—	—	—	—	—	—
6	x	—	—	7.5	57.5	31.5	2.5	1.0	—	—	—
	y	8.5	85.0	6.5	—	—	—	—	—	—	—
8	x	–	–	15.0	40.0	28.0	8.5	8.5	—	—	—
	y	20.0	67.5	12.5	—	—	—	—	—	—	—
13	x	—	1.0	19.0	43.5	24.0	6.0	3.5	1.5	1.5	—
	y	12.0	73.5	14.0	0.5	—	—	—	—	—	—
O.G.	$\bar{x}$	—	0.1	15.5	41.8	27.6	8.4	5.0	1.0	0.4	0.1
	$\bar{y}$	14.1	74.5	11.3	0.1	—	—	—	—	—	—
21	x	—	21.0	46.5	19.5	10.5	1.5	0.5	—	—	0.5
	y	36.0	58.0	5.5	0.5	—	—	—	—	—	—
22	x	—	12.5	46.5	30.5	6.5	3.5	—	—	—	0.5
	y	32.0	63.0	5.0	—	—	—	—	—	—	—
25	x	0.5	21.5	34.5	25.5	9.5	6.5	1.0	1.0	—	—
	y	48.5	46.5	5.0	—	—	—	—	—	—	—
37	x	—	15.5	55.0	21.0	7.0	1.5	—	—	—	—
	y	15.5	74.5	9.5	0.5	—	—	—	—	—	—
	$\bar{x}$	0.1	17.6	45.6	24.1	8.4	3.3	0.4	0.3	—	0.2
	$\bar{y}$	33.0	60.5	6.3	0.3	—	—	—	—	—	—
42	x	1.6	62.5	23.4	8.6	3.1	0.8	—	—	—	—
	y	—	50.0	49.2	0.8	—	—	—	—	—	—
46	x	1.0	54.0	34.5	10.0	0.5	—	—	—	—	—
	y	34.0	58.0	7.5	0.5	—	—	—	—	—	—
47	x	1.0	36.5	49.0	11.0	2.0	0.5	—	—	—	—
	y	19.5	69.5	10.5	0.5	—	—	—	—	—	—
	$\bar{x}$	1.2	51.0	35.6	9.9	1.9	0.4	—	—	—	—
	$\bar{y}$	17.8	59.2	22.4	0.6	—	—	—	—	—	—
Y.G	$\bar{x}$	0.6	31.9	41.3	18.0	5.6	2.0	0.2	0.1	—	0.2
	$\bar{y}$	26.5	59.9	13.2	0.4	—	—	—	—	—	—

* Older Granitoids: 5—13; Younger Granitoids (Second phase): 21—37; Younger Granitoids (third phase): 42—47

TABLE 3

Elongation frequencies of euhedral zircon in Wadi El-Sheikh Granitoids
...(frequencies are given in percentages)

Sample No.	100—14.9	1.50—1.99	2.00—2.49	2.50—2.99	3.00—3.49	3.50—3.99	4.0—4.49	4.50—4.99	5.0—5.49	5.50—5.99	6.0—6.49	<6.49
5	1.0	9.0	26.5	18.0	12.5	18.0	4.5	3.5	4.0	1.5	1.0	0.5
6	1.0	13.0	35.5	25.5	13.5	6.0	2.5	1.5	1.5	—	—	—
8	1.0	7.0	27.0	25.0	17.0	7.5	4.5	4.0	3.5	2.0	1.0	0.5
13	4.5	18.5	29.0	19.0	13.0	4.5	5.5	2.0	2.5	—	0.5	1.0
Mean (O.G.)	1.9	11.9	29.5	21.9	14.0	9.0	4.3	2.8	2.9	0.9	0.6	0.5
21	8.5	25.0	38.5	11.0	8.5	5.0	1.5	1.0	—	—	1.0	—
22	3.5	20.5	39.5	17.5	8.0	3.5	4.5	1.0	2.0	—	—	—
25	3.0	11.5	33.5	18.5	12.5	6.0	7.5	1.5	2.5	2.0	1.5	—
37	18.0	32.5	3.3	11.0	0.5	1.0	—	—	—	—	—	—
Mean	8.3	22.4	36.1	14.5	8.3	3.8	3.6	0.9	1.1	0.5	0.6	—
42	25.8	38.3	27.3	4.7	2.3	0.8	0.8	—	—	—	—	—
46	34.5	45.0	15.0	4.0	1.5	—	—	—	—	—	—	—
47	26.5	54.5	15.5	2.0	1.0	0.5	—	—	—	—	—	—
Mean	28.9	45.9	19.3	3.6	1.6	0.4	0.3	—	—	—	—	—
Mean (Y.G.)	17.1	32.5	28.9	9.8	5.4	2.3	2.2	0.5	0.6	0.3	0.4	—

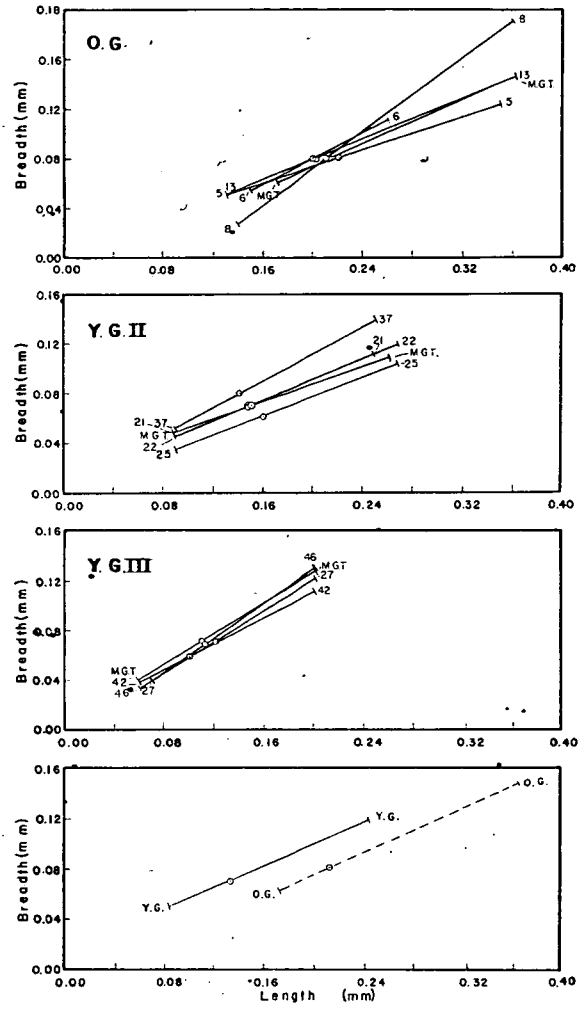

Fig. 7. Reduced major axes of zircon samples from Wadi El-Sheikh granitoids. MGT: mean growth trend of a zircon population

their length and *c*-axis in the range 13.28°—21.10°. Igneous rocks which have not been transported in the sedimentary cycle should exhibit a coincidence of crystal length and *c*-axis. This is true for all the studied suites.

The zircon percentage in the examined granitic rocks decreases from the older to the younger rocks. The distinction between the zircon populations in the two granitic groups is based mainly on their dimensional parameters. The populations in the Older Granitoids contain a wide variety of crystal shapes while those of younger granites become progressively more uniform in morphology. The RMA plots clearly show such distinction. In addition, inclusions in zircon of the older granitic rocks are abundant and diverse while zircons of the younger granites are inclusions poor. According to PUPIN (1980) zircons of the sialic origin granites are inclusions poor

TABLE 4

Dimensional zircon data for Wadi El-Sheikh Granitoids

Sample No.	x (mm)	y (mm)	S_x (mm)	S_y (mm)	a	r	Dd
5	0.22	0.08	0.0681	0.0231	0.3392	0.4586	31.74
6	0.20	0.08	0.0326	0.0167	0.5123	0.1319	22.41
8	0.21	0.08	0.0576	0.0264	0.4583	0.4489	29.60
13	0.20	0.08	0.0602	0.0241	0.4003	0.3123	35.30
MGT* (O. G.)	0.21	0.08	0.0546	0.0226	0.4275	0.3379	29.76
21	0.15	0.07	0.0603	0.0250	0.4146	0.6347	33.46
22	0.15	0.07	0.0495	0.0207	0.4182	0.5237	31.75
25	0.16	0.06	0.0611	0.0244	0.3993	0.6028	34.32
37	0.14	0.08	0.0411	0.0220	0.5353	0.4848	29.35
MGT	0.15	0.07	0.0530	0.0230	0.4419	0.5615	32.22
42	0.10	0.06	0.0443	0.0232	0.5237	0.7293	31.55
46	0.11	0.07	0.0339	0.0240	0.7080	0.7489	22.58
47	0.12	0.07	0.0357	0.0227	0.6359	0.7961	19.44
MGT	0.11	0.07	0.0380	0.0226	0.6225	0.7581	24.52
MGT (Y. G.)	0.13	0.07	0.0466	0.0231	0.5193	0.5551	28.92

* MGT: Mean growth trend

while inclusions in zircons of granite of crustal and mantle origin are numerous and diversified. The partial melting of the mantle as proposed by HUSSEIN *et al.* (1982) for the origin of the Egyptian Older Granitoids, may account for this criterion.

The similarity of the dimensional parameters of zircons in the younger granitic phases of Wadi El-Sheikh area renders their separation difficult. However, elongation values change gradually from the second to the third phase granithes. In addition, colour of zircon changes (from colourless or pale green to brown and nearly black). The observed colour changes are probably due to progressively higher uranium and thorium contents, which could be correlated to the stage of differentiation of the Younger Granitoids of Wadi El-Sheikh area.

REFERENCES

ALPER, A. M. and A. POLDERVAART (1957): Zircons from the Animas Stock and associated rocks, New Mexico. Econ. Geol., **52,** 952—971.

AUGUSTITHIS, S. S. (1973): Atlas of the textural patterns of granites, gneisses and associated rock types. Elsevier, Amsterdam.

CHAO, E. C. T. and M. FLEISCHER (1960): Abundance of zirconium in igneous rocks. 21th Int. Geol. Congr. Report, **1,** 106—131.

CLIFFORD, T. N., L. O. NICOLAJSEN and A. J. BURGER (1962): Petrology and age of the Pre-Otavi Basement granites of Franzfontein, Northern South-West Africa. J. Petrology, **3,** 244—279.

EL-SHESHTAWI, Y. A. (1984): Petrographical and geochemical studies of the granitic rocks around Wadi EL-SHEIKH, southwestern Sinai, Egypt. Ph. D. Thesis, Al-Azhar Univ., Cairo, Egypt.

GREENBERG, J. K. (1981): Characteristics and origin of Egyptian Younger Granites: Summary. Geol. Soc. Amer. Bull., **1,** 224—232.

HALL, B. A. and F. D. ECKELMANN (1961): Significance of variations in abundance of zircon and statistical parameters of zircon populations in a granodiorite dyke, Bradford, Rhode Island. Am. J. Sci., **259,** 622—634.

HEIKAL, M. A. (1973): Petrographical and petrochemical studies of G. El Ineigi granitic rocks, Eastern Desert, Egypt. Ph. D. Thesis, Cairo Univ., Egypt.

HUSSEIN, A. A., M. M. ALI, and M. F. EL RAMLY (1982): A proposed new classification of the granites of Egypt. J. Volcan. and Geother. Research, **14,** 187—198.
JOCELYN, J. and R. T. PIDGEON (1974): Examples of twinning and parallel growth in zircons from some Precambrian granites and gneisses. Mineral. Mag., **39,** 587—594.
KARNER, F. R. and J. O. HELGESEN (1970): Petrologic significance of zircon variation in the Tunk Lake Granite, southeastern Maine. J. Geol., **78,** 480—497.
KÖHLER, H. (1970) Die Änderung der Zirkonmorphologie mit dem Differentiationsgrad eines Granits. Neues Jahrb. Mineral., **9,** 405—420.
LARSEN, L. H. and POLDERVAART A. (1957): Measurement and distribution of zircon in some granitic rocks of magmatic origin. Mineral. Mag., **31,** 544—564.
LARSEN, L. H. and A. POLDERVAART (1961): Petrologic study of Bald Rock Batholith, near Bidwell Bar, California, Geol. Soc. Am. Bull., **72,** 1, 69—92.
MURTHY, M. V. N. and H. N. SIDDIQUIE (1964): Studies on zircons from some garnetiferous sillimanite gneisses (Khondalites) from Orissa and Andhra Pradesh, India. J. Geol., **72,** 123—127.
POLDERVAART, A. (1955): Zircon in rocks, 1, Sedimentary rocks. Am. J. Sci., **253,** 433—461.
POLDERVAART, A. (1956): Zircon in rocks 2, Igneous rocks. Am. J. Sci., **254,** 521—554.
PUPIN, J. P. (1976): Signification des charactéres morphologiques du zircon commun des roches en pétrologie. Base de la méthode typologique. Applications. Thése Doct. Etat., Univ. Nice, France.
PUPIN, J. P. (1980): Zircon and granite petrology. Contrib. Mineral. Petrol, **73,** 207—220.
PUPIN, J. P., B. BONIN, M. TESSLER, and G. TURCO (1979): Role de l'eau sur les charactéres morphologiques et la cristallisation du zircon dans les granites. Bull. Soc. Géol. Fr., **20,** 5, 721—725.
PUPIN, J. P. and G. TURCO (1972): Le zircon accessoire en géothermométrie. C. R. Acad. Sci. Paris, **274,(D),** 2121—2124.
PUPIN, J. P. and G. TURCO (1975): Typologie de zircon accessoire dans les roches plutoniques dioritiques, granitiques et syéniques. Facteurs essentiels déterminant les variations typologiques. Petrologie **1,** 2, 139—156.
RAGAB, A. I. (1971): Geology of Gebel El Atawi Area, Eastern Desert, Egypt. Ph. D. Thesis, Ain Shams Univ. Egypt.
ROSENBLUM, S. (1958): Magnetic susceptibilities of minerals in the Frantz Isodynamic Magnetic Separator. Am. Mineral., **43,** 170—173.
SABET, A. H., BESSONENKO, V. V. and BYKOV, B. A. (1976): The intrusive complexes of the Central Eastern Desert of Egypt. Annals. Geol. Surv. Egypt., **6,** 53—73.
SHIMRON, A. F. (1990): Proterozoic island arc volcanism and sedimentation in Sinai. Precam. Res., **12,** 437—458.
SPOTTS, J. H. (1962): Zircon and other accessory minerals. Coast Range Batholith, California. Geol. Soc. Am. Bull., **73,** 1221—1240.
STRECKEISEN, A. (1976): To each plutonic rock its proper name. Earth-Sci. Rev., **12,** 1—33.
TAUBENECK, W. H. (1957): Geology of Elkhorn Mountains, Northeastern Oregon; Bald Mountain batholith. Geol. Soc. Am. Bull., **68,** 181—238.
ZAGHLOUL, Z. M. and M. B. KHAFFAGY (1965): Zircon in the granites of Aswan Upper Egypt, U. A. R. Bulla. Sci Tech., **8,** 129—141.

Manuscript received, June 24, 1984

Acta Mineralogica-Petrographica, Szeged, XXVII, 131—138, 1985

DISTRIBUTION AND PROPERTIES OF PLACER ILMENITE IN DAMIETTA — PORT SAID BEACH SANDS, EGYPT

S. N. WASSEF* and N. S. HAMMOUD*

ABSTRACT

This work deals with a comprehensive study of ilmenite distribution in the sands of Damietta-Port Said beach which is a part of the African Coast on Mediterranean Sea. This area extends for about 36 km to the east of Damietta Nile branch estuary, and of about 11 km².

The sands come out of the estuary and subjected to northwesterly winds, and a current parallel to the beach line from west to east. These conditions cause the accumulation of heavy minerals bearing ilmenite on the eastern side of Damietta estuary.

Systematic withdrawal of 116 auger samples distributed regularly on the beach stretch have been analyzed for ilmenite. The tenor of ilmenite was found to vary between 5.82% and 15.328% and concentrates in three main locations. The upper meter showed a reserve of about 1.23 million dry tons of ilmenite.

Ilmenite is characterized by the presence of hematite, rutile, magnetite as exsolutions and decomposition into different alteration products is recorded.

The presence of ilmenite besides zircon and rutile is suggesting the Precambrian and basic plutonic rocks provenances drained by the highlands of the River Nile in Africa. The high chromium content in ilmenite relates its origin to the basaltic rocks in Ethiopia, Sudan and Upper Egypt.

INTRODUCTION

The ilmenite content was estimated in 116 auger samples in the area between Damietta and Port Said beach sands *(Fig. 1)*. This area extends for about 36 km east of Damietta mouth eastwards to Port Said, and represents about 11 km². This area is the second important one after east Rosetta. The heavy minerals come down the River Nile and passed through Damietta mouth to the outlet in Mediterranean Sea. Because of the long shore currents which forms the horizontal component of the waves initiated by the prevailing north-westerly winds, the sediments travel eastwards to deposit on the area between Damietta mouth and Port Said on the beach stretch.

HILMY (1951) divided the coast of Egypt arbitrarily into three parts based mainly on the general difference in topography and lithology. These parts are: (1) Western part west of Rosetta, (2) Middle part between Rosetta and Damietta, and (3) Eastern part east of Damietta. This study revealed that these beach sands are mostly derived from the Ethiopian volcanic highland with minor addition from Sudan and Upper Egypt. The minerals are reported to occur in fresh state and to have a medium size ranging from 0.25 to 0.63 mm in diameter, and well sorted (So=1.1—1.56), and well rounded. Also HILMY (1951) stated his belief that these sands represent waterborne sediments transported mechanically by the River Nile.

* Nuclear Materials Corporation, Cairo, Egypt

Damietta beach is characterized by relative unstability of sedimentation conditions due to the subjection of different climatic conditions and frequent high tide periods.

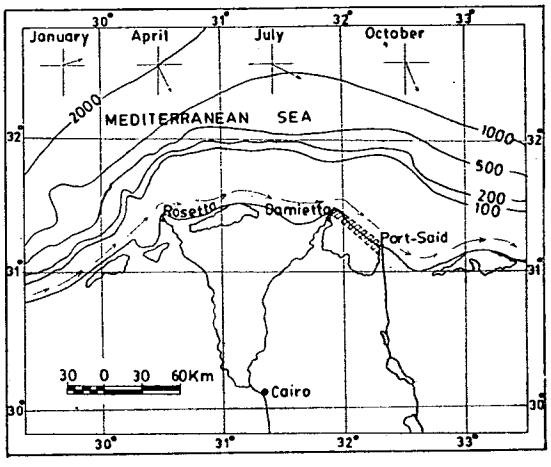

Fig. 1. Location map showing the depth contours, the direction of water current and the prevailing wind in Damietta

It is known that there have been old branches of the Nile between Damietta and Port Said (BALL, 1942). According to HERODOTUS map, 450 B.C. *(Fig. 2)* these branches were called; Mendesian mouth which was 13 km to the south-east of the actual Damietta mouth, and Saitic mouth which was 10 km to the west-north of Port Said. These old branches may be responsible for the present crenulations of the beach as a result of their openings into the Mediterranean Sea (WASSEF, 1964). The Bucolic mouth was mostly in the same site of the actual Damietta mouth. The Pelusiac mouth was mostly east of Port Said by not less than of 20 km.

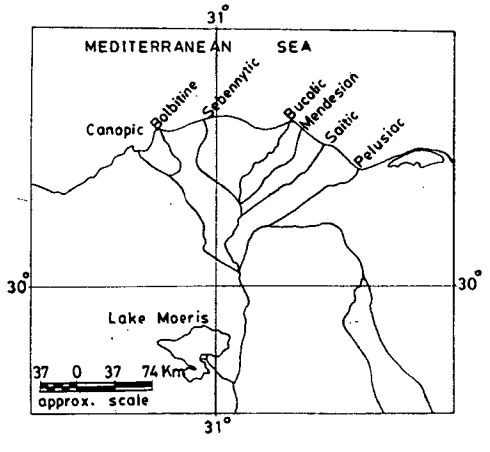

Fig. 2. Map showing the extinct Nile branches between Damietta and Port Said, after HERODOTUS 450 B. C. (BALL, 1942)

EL-SHAZLY (1966) estimated the reserve of the economic minerals on the beach from Abu Quir to Port Said. This study showed the presence of 6.922.300 t of total economic minerals in the upper meter.

MELEIK *et al.* (1978) compared the aerial and ground radiometric surveys. The result obtained by different methods particularly aeroradiometry distinguished six zones of rich minerals content, either directly on the beach or inland. Three of these zones can be related to the former branches of the River Nile, the Bucolic, Mendesian and Saitic branches mentioned by BALL (1942). The study revealed that there is a general direct correlation between aerial data and that from ground radiometry and zircon and monazite contents.

The mineralogy as well as the petrography of ilmenite is studied by: BASTA (1953, 1959*a*, 1959*b*, 1960), RITTMAN and NAKHLA (1958), EL-GORESY (1962), EL-HINNAWI (1964), BOCTOR (1966), HAMMOUD (1966).

Morphology of the area

The beach of Damietta is sufficiently narrow in order to permit the high tide sea water to drop in Lake Manzalah especially in winter and stormy conditions. The crop of the heavy minerals is denser in Damietta than in Rosetta due to the higher deposition rate in winter and flood time. The reworking process of these crops by sea water takes place in summer and a wave-cut ridge appears close to the berm (WASSEF, 1964, 1973).

The building of the coast takes place by accretion in longitudinal portions each of which is being formed by an off-shore submarine spit or bar. The alluvial advance of the coast is attributed to the fact that spits were built infront of the shore, separated from it by swales which filled up and formed a part of the solid land. The long shore current is responsible for the distribution of the materials along the foreshore area. The sediments of the bars are gently well sorted and if black sand placers are found they are always only on the seaward side of the bar. This is supported by the presence of numerous elongated islands in Lake Manzalah running parallel to the sea coast. Thus the Damietta beach is actually a compound bar that have grown seawards by building of secondary bars and the silting of the lagoons trapped behind (SAID, 1958).

The pattern of Damietta beach is gentle slope, flat, smooth and regular. The effect of the gentle slope is to absorb nearly all the energy approaching from offshore, so there are no strong waves acting on the beach except when abnormal stormy conditions are present. No rock structures are present on Damietta-Port Said beach, therefore all the deposits present are maintained by water, not including disintigrated grains of rocks as a result of wave action. It was found that from the shore to about 60 km in sea water the depth of the shelf ranged between 0 and 100 m *(Fig. 1)*.

There are no sand dunes in this area, except some spots of wind-blown quartz sand not more than 20 cm thick overlying the shore sand. The nature of the waves acting on the beach along the year in the normal climatic conditions is low amplitude waves (low crest), or gentle waves because the subsurface topography is gentle and simple. The prevailing wind to Damietta beach is in NW-SE direction with a small angle to the east at months from April to December *(Fig. 1)*. Thus causes the waves created to strike the beach obliquely at the same angle as the prevailing wind. In July the angle of wind changes to a more westerly direction, hence the angle of striking of the waves is changed, and a drift of deposit to the east takes place.

The mechanical analysis of the beach sands of Damietta showed an average median diameter equals 0.114 mm which is finer than those of Rosetta sands which equals 0.163 mm. The sorting coefficients in both areas are the same and equal 1.27.

METHODS APPLIED

Field sampling method

The samples were collected in sequence along the beach line every 400 m using the auger drill representing the upper one meter. In the wide locations another sample is collected towards the mainland perpendicular to the beach line and separates 200 m from the first sample. Since Damietta beach is a narrow stretch no more than three samples in the column all over the area. The first sample was collected always within the berm close to the beach line. The auger sampler is hummered twice per one sample.

Laboratory work

1. The dry original sample is quartered carefully down to about 75 gm.
2. The sample is then washed to remove the clay by decantation. The organic matter is removed by addition of few cc. of conc. hydrogen peroxide with hot water. After about half an hour, the sample is washed by distilled water and dried in an oven at about 60 °C until complete dryness.
3. The clean sample is divided into two halves, one for the mechanical analysis and the other one for the mineral separation.
4. Magnetite is removed simply by using a small natural magnet according to the method explained by RITTMAN (1957) and NAKHLA (1958).
5. Frantz isodynamic separator is used for magnetic fractionation of the magnetite-free samples. This separator is used twice, once to concentrate the magnetic heavy minerals in the magnetic fraction, and the other one to separate ilmenite from this fraction.

For the concentration of the heavy minerals, the working conditions were 20° side slope, current of 1.5 amp., and tilt 3°. This magnetic fraction contains nearly all the economic minerals and green silicates, while the non-magnetic fraction contains mainly quartz and the non-magnetic zircon and some rutile.

The working conditions of the separator are changed to perform a suitable field for ilmenite separation from the previous magnetic fraction. The tilt is changed into 4°, the current into 0.3 amp., and the slope is maintained with 20°, with moderate vibration rate. In these conditions the magnetic fraction obtained is very rich in ilmenite which represents about 98% of the total ilmenite present in the sample. The exact percentage of ilmenite is defined by checking the fraction under the microscope by using the grain counting technique (WASSEF, 1981).

The ilmenite is the most major one among the economic minerals of the black sands. The rest of minerals are; magnetite, hematite, monazite, zircon, rutile, and garnet. Ilmenite and magnetite are of $FeO—Fe_2O_3—TiO_2$ system.

RESULTS

Ilmenite distribution

The distribution of ilmenite in East Damietta area *(Fig. 3)* concentrates in three main locations, A, B, and C. The area A is the most rich location in ilmenite, and the concentration is declined eastwards in locations B and C.

The modal class of ilmenite is ranged between 6 and 8% which reached a frequency of 56.05% of the total distribution *(Fig. 4)*. The average value of ilmenite ($\bar{X}$) showed an order of 8.277%. The minimum percentage is 5.852%, and the maximum reached 15.328%.

The calculation of ilmenite reserve revealed the presence of about 1.23 millions dry tons as a proven reserve in the upper meter. If the continuation of the heavy minerals is until 20 m depth, and if the upper meter unit is repeated, a probable reserve of order 24.6 millions dry tons can be considered.

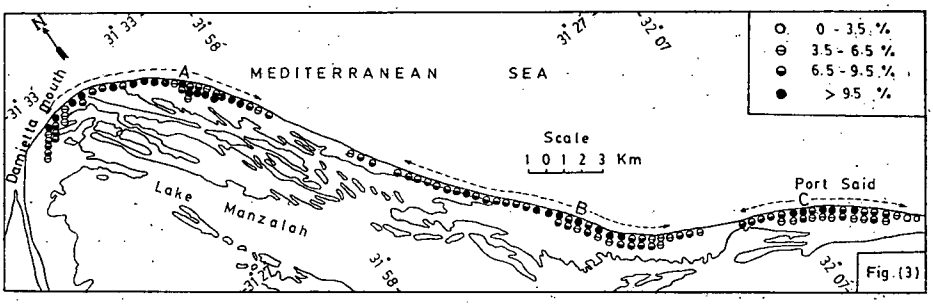

Fig. 3. Distribution of ilmenite along Damietta beach

Properties of ilmenite

Ilmenite is mostly black with bluish or violet tint. Some altered grains are dull black. Most of ilmenite grains are irregular in shape; angular to subangular and some grains are rounded. The ilmenite grains show the L/B (Length—Breadth) ratio between 2:1, among them the majority have L/B ratio between 1:1 and 2:1 (MIKHAIL, 1971). Twinning is a common feature, twin lamellae exist in one or two directions parallel to *(10$\bar{1}$1)* planes of ilmenite.

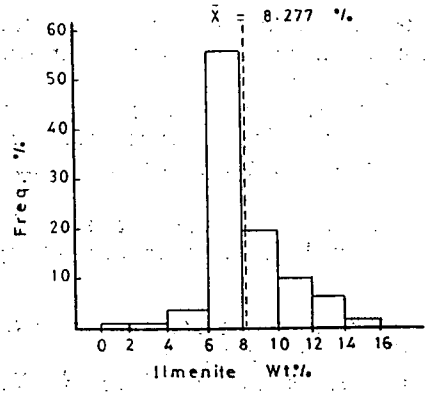

Fig. 4. Statistical distribution of ilmenite

Exsolutions

A- Hematite

At high temperature ilmenite and hematite form a continuous solid solution series. On moderately slow cooling unmixing takes place into two solid solutions, ferri-ilmenite and titanhematite. However BASTA (1953, 1959*b*) found that at normal temperature ferri-ilmenite with 18% Fe_2O_3 and titanhematite with 10% TiO_2 in solid solution exist in nature.

B- Rutile

There is limited solid solution between rutile and ilmenite which does not exceed 6% TiO_2 at about 1050 °C. The exsolution of rutile in ilmenite is not common in comparison with those of titanhematite and is found as fine lamellae in six directions parallel to *(hh$\bar{2}$hl)* directions of ilmenite (BASTA, 1959*b*).

C- Magnetite

RAMDOHR (1955, 1956) explained that at high temperature there is a limited solid solution between magnetite and ilmenite, possibly not more than 5—10% of Fe_3O_4.

In some twinned ilmenite grains, few relatively coarse tabular lamellae or fine grains of magnetite are developed inside the twin lamellae (BOCTOR, 1966).

Ilmenite is occasionaly decomposed to different alteration products of variable composition. Two types of alteration are recorded: high temperature alteration represented by rutile-hematite and rutile-magnetite intergrowth, and low temperature alteration represented by rutile-anatase intergrowths (BOCTOR, 1966).

BAILEY *et al.* (1956) explained that the alteration of ilmenite takes place in 3 stages:

1. Ilmenite is partially altered to greyish amorphous phase.
2. Complete alteration of ilmenite to this phase forming an amorphous iron-titanium oxides as an end product.
3. Development of leucoxene on the expense of this amorphous material.

The composition of this leucoxene was questionable and described by many authors as follows:

1. Oriented aggregates of finely crystalline rutile or brookite (BAILEY *et al.*, 1956).
2. Amorphous iron-titanium oxide as crystalline mixture of anatase, brookite, sphene and rutile (ALLEN, 1956).
3. Rutile with subordinate anatase (BAILEY and CAMERON, 1957).
4. A mixture of hematite, pseudobrookite and rutile in an average molar ratio of approximately 1:5:7 as in the brown leucoxene from Quilon (KARKHANAVALA *et al.*, 1959).
5. Development of leucoxene on the expense of amorphous iron-titanium oxide. The leucoxene results in higher titanium content together with high oxidation of iron (HAMMOUD, 1966).

The ilmenite can be recovered in the isodynamic separator as maximum at 0.3 amp., 4° tilt, and 20° as side slope (WASSEF, 1981).

The chemical difference between the strongly and weak magnetic ilmenite showed that the strongly one contains 46.32% TiO_2, 0.34% Cr_2O_3, and 0.12% V_2O_5.

The weak magnetic ilmenite contains 47.52% TiO_2, 0.12% Cr_2O_3, and 0.05% V_2O_5. The chemical composition of highly purified dry ilmenite sample analyzed chemically and by *X*-ray fluorescence spectroscopy was found to be composed of as follows: 18.63% Fe_2O_3, 31.18% FeO, 46.24% TiO_2, 1.35% MnO, 0.64% MgO, 0.87% Al_2O_3, 0.28% Cr_2O_3, 0.14% V_2O_5, 0.12% CaO, 0.32% SiO_2, 0.04% P_2O_5, 0.03% S and traces of Nb, Co, Ni, Zn, Mo and Zr (HAMMOUD, 1966, 1975).

CONCLUSIONS

Ilmenite showed the presence of considerable reserve reaches 1.23 millions dry tons. The presence of ilmenite besides zircon and rutile is suggesting the Precambrian and basic plutonic rocks provenances drained by highlands of the River Nile in Africa. The high chromium content in ilmenite relates its origin to the basaltic rocks in Ethiopia, Sudan and Upper Egypt.

REFERENCES

ALLEN, V. T. (1956): Is leucoxene always finely crystalline rutile?: a discussion. Economic Geology **51,** p. 830.

BAILEY, S. W., CAMERON, E. N., SPEDDEN, H. R., and WEEGE, R. I. (1956): The alteration of ilmenite in beach sands: Economic Geology, **51,** p. 263.

BAILEY, S. W., and CAMERON, E. N. (1957): Is leucoxene always finely crystalline rutile? a reply: Economic Geology, **52,** p. 712.

BALL, J. (1942): Egypt in the classical Geographers: Survey and Mines Dept. Cairo, Egypt.

BASTA, E. Z. (1953): Mineralogical aspects of system FeO-Fe_2O_3-TiO_2: Ph. D. thesis. Bristol.

— — (1959*a*): Some mineralogical relationship in the system Fe_2O_3-Fe_3O_4 and the composition of titanomagnetite: Economic Geology, **54,** p. 698.

— — (1959*b*): New data on the system Fe_2O_3-$FeTiO_3$-TiO_2 (Ferri-ilmenite and titanomagnetites): Proc. Egypt. Acad. Science, **14,** p. 1.

— — (1960): Natural and synthetic titanomagnetites (the system Fe_2O_3-Fe_2TiO_4-$FeTiO_3$): N. Jb. Min. Abh., **94,** p. 1017.

BOCTOR, N. Z. (1966): Ore microscopic studies of the opaque minerals in Rosetta-Damietta black sands: M. Sc. thesis, Cairo University.

EL-GORESY, A. A. (1962): Mineragraphic study of ilmenite and magnetite from the Egyptian black sands: Cairo Central Laboratories for Mineral Research, Internal report.

EL-HINNAWI, E. E. (1964): Mineralogical and geochemical studies on Egyptian (U. A. R.) black sands: Beiträge zur Mineralogie und Petrographie, **9,** p. 519.

EL-SHAZLY, E. M. (1966): Thorium resources and their utilization in the U. A. R.: Vienna panel on thorium utilization in reactors, I. A. E. A., p. 186.

HAMMOUD, N. S. (1966): Concentration of monazite from Egyptian black sands, employing industrial technique: M. Sc. thesis, Cairo University, Egypt.

— — (1975): A process for recovery low-chromium high grade ilmenite from North Egyptian beach deposits: Proc. of 11*th* International Mineral Processing Congress. Regione Autonome Della Sardegne, Italy.

HILMY, M. E. (1951): Beach sands of Mediterranean Coast of Egypt: J. Sed. Pet., **21,** p. 109.

KARKHANAVALA, M. D., MOMIR, A. C., and REGE, S. G. (1959): An x-ray study of leucoxene from Quilon, India: Economic Geology, **54,** p. 913.

MELEIK, M. L. FOUAD, K. M., WASSEF, S. N., AMMAR, A. A., and DABBOUR, G. A., (1978): Aerial and ground radiometry in relation to the sedimentation of radioactive minerals of the Damietta beach sands, Egypt: Economic Geology, **73,** p. 1738.

MIKHAIL, M. A. (1971): Distribution and sedimentation of ilmenite in black sands west of Rosetta: M. Sc. thesis, Faculty of Science, Cairo University.

NAKHLA, F. M. (1958): Mineralogy of the Egyptian black sands and its application: Egyptian Jour. Geol., **2,** p. 1.

RAMDOHR, P. (1955): Die Erzmineralien und ihre Verwachsungen: Akademie Verlag. Berlin.

— — (1956): Die Beziehungen von Fe-Ti Erzen aus magmatischen Gesteinen: Bull. Comm. Geol. Finland, Helsinki No **173,** p. 3.

RITTMAN, A. (1957): Preliminary remarks on the methods of determination of quantitative mineralogical composition of black sands: Internal report N. C. R., Cairo, Egypt.
RITTMAN, A., and NAKHLA, F. M. (1958): Contribution to the study of Egyptian black sands: Egypt. Jour. Chem., **1**, p. 127.
SAID, R. (1958): Remarks on the geomorphology of the deltaic coastal plain between Rosetta and Port Said: Soc. Geographie d'Egypt, Bull., **31**, p. 116.
WASSEF, S. N. (1964): Correlation of the sedimentation conditions of the Mediterranean beach east of Damietta to Suez Canal by heavy minerals and isotopes application: M. Sc. thesis, Faculty of Sci. Ein Shams University, Cairo, Egypt.
— — (1973): Distribution of monazite in the black sands of Rosetta and Damietta and its conditions of sedimentation: Ph. D. thesis, Faculty of Sci. Ein Shams University, Cairo, Egypt.
— — (1981): Distribution and properties of placer ilmenite in east Rosetta beach sands, Egypt: Mineralium Deposita, **16**, p. 259.

Manuscript received, June 21, 1984

Acta Mineralogica-Petrographica, Szeged, XXVII, 139—144, 1985

CRYPTOPSEUDOMORPHISM: A NEW PSEUDOMORPHIC TYPE

A. A. EL SOKKARY[1] and G. M. SALLOUM[2]

ABSTRACT

A new pseudomorphic phenomenon, the so-called cryptopseudomorphism, is discussed here to the first time. This phenomenon is checked against the known types and found that it can not be paramorphic, replacement (substitution) or incrustation pseudomorphism. It is different as well from alteration pseudomorphism because: (1) The new pseudomorphic type is an occult or hidden phenomenon which can not be detected easily except by a combination of several techniques including x-ray diffraction, microscopic examination and chemical analysis. (2) While alteration pseudomorphism is the result of alteration of minerals at mild and more localized environment, the new pseudomorphic phenomenon requires more severe conditions like metamorphism or metasomatism acting on a more or less regional scale.

Three examples are given to illustrate this new phenomenon, the most important and most frequent of which is the albitization of basic oligoclase. Studying pseudomorphism of some uranium compounds revealed the presence of a special type called here radioactive pseudomorphism.

INTRODUCTION

The phenomenon of pseudomorphism of minerals is one which did not receive enough recent studies. However, this phenomenon is important in mineralogical studies as it allows to give an insight into mineral paragenesis and into chemical reactions involved in the formation of minerals. In this connection, DANA (1949) stated that: The chemical processes involved in such changes open a wide and important field for investigation. Their study has served to throw much light on the chemical constitution of mineral species and the conditions under which they have been formed.

The present work is essentially a contribution to the study of the phenomenon of pseudomorphism of minerals. It exposes a new type of pseudomorphism other than the well known four types, named by the authors cryptopseudomorphism. This new type so-called because it is not readily distinguished by the naked eye, rather it needs for its manifestation a combination of several methods including X-ray diffraction, optical study and chemical analysis, hence the prefix crypto-denoting a hidden or occult type of pseudomorphism. The term aphanopseudomorphism can alternatively be used as well on the basis that the Greek *aphanos* means unseen, but aphanite is a dense fine grained diabase with a compact texture. To avoid misuse and misunderstanding the term cryptopseudomorphism is more preferable.

[1] Nuclear Materials Corporation, Cairo, Egypt
[2] Al Azhar University, Cairo, Egypt

DEFINITION AND TYPES OF KNOWN PSEUDOMORPHS

The phenomenon of pseudomorphism has long been under study. Different authors defined the phenomenon in somewhat different ways. Thus, KRAUS *et al.* (1959) said that crystals alter in such a way that the external form of the original specimen is retained, such altered crystals are called pseudomorphous. DANA (1959) mentioned that if a crystal of a mineral is altered so that the internal structure is changed but the external form is preserved, it is called a pseudomorphous or false-form. The same author adds that the chemical composition and structure of a pseudomorph belong to one mineral species whereas the crystal outline corresponds to another.

MASON and BERRY (1967) defined pseudomorphism as follows: when a mineral can be replaced by another mineral without any change in the external form. BETEKHTIN (1968) discussed the phenomenon of pseudomorphism as replacement of crystal by a certain constituent in such a way that the resulting mineral retains not only the external shape but sometimes also the peculiar internal structure of the original mineral.

SINKANKAS (1969) defined the phenomenon as when a crystal changes chemically or structurally, yet keeps the shape of the original, it is called a pseudomorph, or false form, it looks like a crystal of one species but is composed of another. On the other hand READ (1973) states that pseudomorphism is the assumption by a mineral of a form other than that which really belongs to it.

It is clear that the previous authors agree that pseudomorphism implies both chemical and structural changes of a mineral species, while the external outline is kept unchanged.

Concerning the various types of pseudomorphs, most authors agree upon four main types despite the fact that they might classify them differently. KRAUS *et al.* (1959) referred to four types which are paramorphous, alteration, substitution and incrustation pseudomorphs. On the other hand, DANA (1959) recognised: substitution, incrustation, alteration and paramorphic pseudomorphism. MASON and BERRY (1967) mentioned that there are two types of pseudomorphism, one in which no change of substance occurs, the other in which there is addition of some element or elements and removal of others.

SINKANKAS (1969) claimed that there are two types of changes which are mainly chemical and structural. He adds as well the replacement type of pseudomorphism. READ (1973) tabulated the following four types of pseudomorphism: incrustation, infilteration, replacement (substitution) and alteration. This author mentioned that pseudomorphism may often be recognized by a want of sharpness in the edges of the crystals, whilst their surfaces usually present a dull and somewhat granular or earthy aspect.

DEFINITION OF THE NEW PSEUDOMORPHIC TYPE

A new pseudomorphic phenomenon is recorded here to the first time. In this type, the crystal has underwent chemical changes involving removal and addition of certain elements with the production of a new but closely related phase, at the same time the structural state of the new mineral is either modified or kept without change, the outer rims are still showing optical properties of the previous mineral. It should be emphasized once again that such mineral pseudomorph is occult and can not be recognised easily. As stated in the introduction, the authors propose the

name cryptopseudomorphism for this kind of pseudomorphs and suggest that it would be added as a fifth type to the previously mentioned list including four pseudomorphic types.

EXAMPLES ON THE NEW PSEUDOMORPHIC TYPE

Three examples are given here illustrating the new phenomenon of pseudomorphism, the so-called cryptopseudomorphism, they are partly taken from the first author's experimental work on feldspars and carbonates and partly taken from available literature.

1) The albitization of more basic plagioclase: EL SOKKARY (1970) reported the case of a plagioclase feldspar separated from Shaitian granite which is a special type of granitic rocks occurring in the south Eastern Desert of Egypt and found from optical determination and norm calculations that this plagioclase is basic oligoclase with 25% An, while the diffraction pattern identifies it as albite with not more than 10% An. This discrepancy between the two determinations of the plagioclase was attributed to a later albitization process of the more basic plagioclase.

EL SHAZLY, EL SOKKARY and KHALIL (1977) discussed in some detail the phenomenon of albitization of plagioclases. These authors stated that albitization of the more basic plagioclase can take place and results in the formation of albite and some other minor minerals. DICKINSON (1962) on studying the diagenesis of some andesites mentioned that the plagioclase was largely decomposed to albite plus one or more of several hydrous Ca-bearing minerals of which pumpellyite is the most abundant, although prehnite, laumontite and minor calcite also occur. SCHULZE and EL HINNAWY (1967) on studying the alteration of some basic sills and dykes pointed towards the albitization of plagioclase feldspars. They mentioned that KORSHINSKI (1963) indicated that the albitization of basic plagioclases could be regarded as a metamorphic process which took place at great depths.

EL SHAZLY *et al.* (1977) are inclined to the opinion that both albitization (and sericitization) of the feldspars of Shaitian granites are indications of a sort of Na and K-metasomatism accompanying metamorphism of the retrogressive type which occurred to these granites after their emplacement. It seems that the introduction of K in sericitization expelled Na which helped later in albitization of certain members of the same Shaitian rocks in a process of Na-autometasomatism.

Thus both KORSHINSKI (1963) and EL SHAZLY *et al.*, (1977) agree that the albitization of basic plagioclases is either a metamorphic process or a process of Na-metasomatism accompanying metamorphism.

DEER *et al.* (1972) mentioned that in matters of detail the structures of plagioclases are complex and vary according to chemical composition, conditions of crystallization and thermal history. As in the case of albite, so also for the whole plagioclase series, there are high-, low- and intermediate-temperature structural states.

Since the conversion of oligoclase to albite in the studied pseudomorphic type is essentially a chemical change from a feldspar with oligoclase composition (An_{10-30}) to a feldspar with albite composition (An_{0-10}), according to DEER *et al.* (1972) statement this should be accompanied by a structural change of the newly formed mineral. Moreover, the newly formed albite under metasomatic conditions is believed to be a high-temperature form when compared with the original low-oligoclase formed (together with the enclosing granite) under plutonic conditions of somewhat lower temperature of formation.

Thus in the studied pseudomorphic type, the formation of albite in place of oligoclase is accompanied by a structural change between the two mineral phases composing the pseudomorph.

2) Pseudomorphism of iron oxides and calcite after ferroan dolomite: EL SOKKARY (1981) studied the mineralogy and chemistry of a peculiar carbonate mineral occurring in a metamorphic zone at Wadi Um Kabu, South-Eastern Desert of Egypt. On the basis of X-ray diffraction and chemical analyses, this mineral proved to be a mixture of dolomite, hydrated ferric oxide mostly amorphous goethite, and calcite while its very coarse and brownish crystals give the impression that it is just only a dolomite mineral.

It seems that the original ferroan dolomite mineral started to break under metamorphic environment giving rise to minor colloidal goethite, calcite plus possible free magnesia phase, but still keeps the original ideal rhombohedral form.

It is argued that the present dolomite has acquired the structure of its predecessor: ferroan dolomite because the diffraction lines of the former do not accord precisely with those of dolomites of ASTM cards, rather they show certain limited displacements reflecting substitution in the unit cell, a matter which might reflect that the newly formed dolomite is pseudomorphous after ferroan dolomite.

It is worthy to note that EL SOKKARY (1977) mentioned that the schists of Wadi Um Kabu (the country rocks of the present carbonate mineral) were the place of certain chemical mobility under thermal metamorphic environment, the main elements that were mostly affected by differential mobilization in the present case are Ca, Fe and Mg. It is now possible to say that this type of pseudomorphism is the result of metamorphism.

3) Pseudomorphism of uranium compounds: GOLDSCHMIDT (1962, p. 564) mentioned that the composition of the pitchblende from certain veins corresponds more or less to that of U_3O_8, but gives X-ray interference diagrams of the fluorite lattice of UO_2.

KRAUSKOPF (1967) mentioned that the chief primary compound of uranium in vein deposits is the dioxide, UO_2, which occurs in the well crystallized variety uraninite and the microcrystalline form pitchblende. Incipient oxidation and loss of uranium by radioactive decay may increase the oxygen—uranium ratio, so that uraninite and pitchblende seldom show precisely the composition UO_2, often approaching a composition symbolized by U_3O_8.

Thus in the example given by GOLDSCHMIDT there is chemical change involving transformation of UO_2 to U_3O_8 but the original structure of UO_2 is retained. Here again is a peculiar type of pseudomorphs which deserves more study, but because radiation is the main initiating factor, it can be called radioactive pseudomorphism.

Despite that the processes responsible for chemical changes of the mentioned uranium compounds (incipient oxidation and loss of U by radioactive decay) are quite different from those responsible for chemical changes given in the previous two examples (metasomatism and/or metamorphism), yet pseudomorphs of uranium compounds, like the other two examples, are occult and could not be revealed except by chemical analysis combined with X-ray diffraction analysis.

DISCUSSION

On comparing the present type of pseudomorphs with the four known types, it can be said that the present pseudomorphic type can not belong to the paramorphic, the replacement (substitution) or incrustation types, the only known type which

may approach the present case is alteration pseudomorphism. DANA (1959) defined this kind of pseudomorphism as including a partial addition of new material or a partial removal of the original material, a case in which the unaltered mineral may be found in such pseudomorphous mineral. The common given examples are those of alteration of potash feldspars into kaolinite and the alteration of galena (PbS) to anglesite ($PbSO_4$). In the first example, there is removal of K and addition of H_2O, but the anionic silicate group is unchanged, while in the second example the cation (Pb) did not change and the anionic group has changed from S^{2-} to SO_4^{2-}.

In the new pseudomorphic case, there is both partial removal and addition of cations, while the anionic group remains unchanged, however the structural state of the new mineral has underwent in some cases a certain degree of change.

Nevertheless, the new type of pseudomorphism is different from alteration pseudomorphism, the most important differences are as follows. In the first place alteration pseudomorphism in all the given examples is a phenomenon which can be easily recognised by the naked eye *e.g.* kaolinization of feldspar but the new pseudomorph is an occult phenomenon which can not be easily detected except by a combination of several techniques including X-ray diffraction, microscopic examination and chemical analysis.

In the second place alteration pseudomorphism is the result of alteration of minerals occurring at mild and more localized environment, but the new type of pseudomorphism requires more severe conditions like metamorphism or metasomatism accompanying metamorphism acting on a more or less regional scale as seen from the example of albitization of basic oligoclase.

In the third place and in cryptopseudomorphism the newly formed mineral is closely related from a chemical point of view to the original mineral, this is again illustrated from albite pseudomorph after oligoclase.

On these grounds, the authors suggest that the present type of pseudomorphism is different from alteration pseudomorphism and deserves to be considered as a new type of pseudomorphs to be added to the other known types.

REFERENCES

BETEKHTIN, A. (1968): A course of mineralogy. Peace Publishers, Moscow.

DANA, E. S. (1949): A textbook of mineralogy. Revised by: W. E. FORD, 4th ed., 12th printing, John Wiley and Sons, Inc., New York.

DANA, E. S. (1959): Dana's manual of mineralogy. John Wiley and Sons, Inc., New York.

DEER, W. A., HOWIE, R. A. and ZUSSMAN, J. (1972): An introduction to the rock-forming minerals. Longman.

DICKINSON, W. R. (1962): Petrology and diagenesis of Jurassic andesitic strata in central Oregon. Am. J. Sci., Vol., **260,** p. 481—500.

EL SHAZLY, E. M., EL SOKKARY, A. A. and KHALIL, S. O. (1977): Petrography and geochemistry of some altered granite pebbles from Atud area, Eastern Desert. Egypt. J. Geol., Vol. **18,** No. 2, p. 105—114.

EL SOKKARY, A. A. (1970): Geochemical studies of some granites in Egypt, U. A. R. Ph. D. Thesis, Alexandria Univ.

EL SOKKARY, A. A. (1977): Mineralogical and chemical studies on anthophyllite-actinolite schist from Wadi Um Kabu, south Eastern Desert, Egypt. Acta Miner. Petr., Szeged, Vol. **23/1,** p. 71—76.

EL SOKKARY, A. A. (1981): An unusual carbonate mineral from the schists of Wadi Um Kabu, south Eastern Desert, Egypt. Under publication.

GOLDSCHMIDT, V. M. (1962): Geochemistry. Oxford, At the Clarendon Press.

KRAUS, E. H., HUNT, W. F. and RAMSDELL, L. S. (1959): Mineralogy. McGraw-Hill Book Co., Inc., New York.

KRAUSKOPF, K. B. (1967): Introduction to geochemistry. McGraw-Hill Book Co., New York.
MASON, B. and BERRY, L. G. (1967): Elements of mineralogy. Freeman and Co., San Francisco.
READ, H. H. (1973); Rutley's elements of mineralogy. Thomas Murby and Co., London.
SCHULZE, E. G. and EL HINNAWI, E. F. (1967): Petrography and geochemistry of some basic sills and dykes from southern Rhenish Schiefergebirge. Geol. Mag., Vol. **104**, p. 35.
SINKANKAS, J. (1969): Mineralogy. Van Nostrand Reinhold Co.

Manuscript received, December 12, 1984

Acta Mineralogica-Petrographica, Szeged, XXVII, 145—152, 1985

ORGANIC GEOCHEMICAL FEATURES OF THE MAAR-TYPE OIL SHALES OF HUNGARY

M. HETÉNYI*

ABSTRACT

In the last decade several so-called maar-type oil shales were discovered in Hungary, this type being infrequent on a world scale, as well. These were deposited in the enclosed lakes formed in volcanic rings. The composition of the biomass serving as precursor of the organic matter of the oil shales proved to be different in each bed.

The organic matter of the three beds generated under the same geological but somewhat differing biological conditions is different both from qualitative and quantitative points of view. In the Pula locality the favourable environmental conditions allowed the accumulation of the algal material, its good preservation, thus the formation of type I kerogen. The organic matter of the Várkesző and Gérce oil shales is heterogeneous, the precursors of the kerogens of type I and III are mixed in them. The kerogen of Várkesző is of type II due to the higher proportions of the humic substance. The kerogen of Gérce is transitional between the types I and II.

The organic matter content, the genetic potential, the HI, OI, T_{max} values measured by Rock-Eval pyrolysis, as well as the H/C atomic ratios and diagenesis coefficients (C_R/C_T) of the oil shales support the classification mentioned above. To express quantitatively the type-differences the PC/TOC ratio seems to be suitable. Its value in the order of Pula, Gérce, Várkesző is as follows: 65, 47 and 38%. Taking the same sequence, the quantity of bitumen of the oil shales, formed during the natural evolution of the oil shales, is increasing, i. e. the activation energy of kerogen is decreasing.

INTRODUCTION

In the last decade several oil shale beds were discovered in Hungary, their dimensions being rather small. These beds can be fundamentally divided into two groups. The first group is represented by the accumulations of the former intramontane lagoons. The second group involves the maar-type oil shales being curious also on a world scale and only of geological interest.

The maar-type oil shales of Pula, Gérce and Várkesző were deposited in the enclosed lakes developed in basalt craters of Western Hungary, Transdanubia (BENCE, JÁMBOR, PARTÉNYI, 1979; JÁMBOR and SOLTI, 1975, 1976). In the course of the final basalt volcanism of the Carpathian Basin, as a result of a strong eruption happening once isometric tuff-rings were developed. Their age is 3.05—5.34± ±0.93 ma (JÁMBOR, RAVASZ and SOLTI, 1982). In the oligohaline water (about 3‰ salt content) of the lakes formed in the tuff rings, the intense weathering of the basalt tuff produced favourable conditions to the growth of planctonic algae, first of all of the Botryococcus braunii. The accumulation of the organic matter was promoted by the warm-temperate climate during sedimentation (NAGY, 1976; HAJÓS, 1976) and by the anaerobic conditions prevailing in the lower horizon of the

* Department of Mineralogy, Geochemistry and Petrography, Attila József University, H-6701 Szeged, Pf. 651, Hungary

lakes (RAVASZ, 1976). Simultaneously, the dense vegetation at the crater margins prevented the coarse detritus to get the water.

In some strata the Pula oil shale is of excellent, but on the average of medium quality, the oil shales of Várkesző and Gérce are of medium to poor quality. The qualitative differences between the beds of the same type can probably be attributed to the fact that in the Pula crater the water of the crater lake was warmed periodically by the uprushing hot water produced by the post-volcanic activity (SOLTI, 1981). The hot water produced favourable conditions first of all to the algae, promoting thus the formation of sediment more abundant in organic matter and, of oil shale of better quality. In the composition of the biomass serving as precursor of the organic matter of the bed qualitative differences can also be observed in addition to the quantitative ones. In the Gérce oil shale the pollen analyses identified coalified vascular tissue remnants in addition to the amorphous organic matter of huge quantity (KEDVES, personal communication). In some strata of the Várkesző oil shale the coalified remnants of higher terrestrial plants can be observed macroscopically, as well. Thus, the composition of the original biomass of the beds accumulated under the same geological conditions and to be compared below slightly differs from one another. Further, as proved by the pollen analyses, the biological activities of the afore-mentioned sedimentary basins was also different (KEDVES, 1983; HETÉNYI *et al.*, 1982; HETÉNYI, 1983). The state of preservation of the Botryococcus algae and sporpmorphs of the Pula oil shale refers to biologically inactive sedimentation environment. The Várkesző bed could develop under conditions of special biological activity: the Botryococcus algae are destructed, the sporomorphs, however, being fairly well preserved. In the Gérce oil shale the quantity of Botryococcus is small and, based on the remnant composition, the deposition took place in a biologically active, probably alkaline environment (KEDVES, personal communication).

In this paper the organic geochemical features of three maar-type oil shales of Hungary (Pula, Gérce, Várkesző) will be compared, the oil shales being formed under the same geological but somewhat different biological conditions. It could be assumed that due to the somewhat different character of the sedimentation environment, the organic matter of the beds would differ from one another both from the qualitative and from the quantitative points of view.

EXPERIMENTAL

The oil shale samples were ground to the grain size of 0.05—0.15 mm, the bitumen was extracted in a Soxhlet extractor in two steps: first by chloroform (Bit-A), then by benzene-acetone-methanol mixture of 70:15:15 ratio (BAM-bitumen).

Kerogen was enriched first by specific gravity differences, the remaining mineral components were destroyed by means of chemical procedures.

The determination of the C_{org} content was carried out at 1000 °C under intense oxygen flow, by means of combusting in a Carmhograph-8 equipment.

The H and C contents were measured in CHN-analysator.

The determination of the maximal hydrocarbon generation temperature (T_{max}), of the genetic potential (S_1+S_2), of the H- and O-indices was performed by Rock-Eval pyrolysis (ESPITALIE *et al.*, 1977).

The C_R/C_T ratio was measured on the basis of the ASTM standard (CUMMINS *et al.*, 1972).

RESULTS

As it has been usual, the characterization of the organic matter was made according to the organic carbon content. The quantity of the organic carbon is extremely high in the Pula bed, especially in some strata where the above-mentioned conditions favoured the accumulation and preservation of the algal material. The average organic carbon content of the samples between 4.5 and 39.5 m (sampling

TABLE 1

Quantitative characterization of the organic matter of the maar-type oil shales

Characteristics	Locality		
	Pula	Gérce	Várkeszö
Depth (m)	4.5—39.5	4.0—68.3	55.0—70.5
Organic carbon content (%)	0.3—45.7	0.1—15.5	3.2—18.7
Soluble organic matter (%)	2.47	3.50	4.79
Bit-A (%)	1.78	2.54	3.30
BAM-Bit (%)	0.69	0.96	1.49
β-coefficient (%)	18.4	53.0	36.8

Bit-A = soluble organic matter extracted by chloroform
BAM-Bit = soluble organic matter extracted by benzol: acetone: metanol = 70:15:15
β-coefficient = 100 × soluble organic matter/organic carbon content

interval 0.5 to 1.0 m) is 13.4% (Table 1). In some layers (*e.g.* 24.5—26.0 m and 14.0—17.0 m) the organic carbon content is as high as 30 to 50% (HETÉNYI *et al.*, 1977). This periodicity can be most probably attributed to the hydrochemical changes, to the periodical geyser activity. In harmony with the sedimentation, the organic carbon content of the Gérce and Várkeszö oil shales is much lower than in the Pula oil shale, i.e. 15.5 and 18.7%, respectively.

Based on the genetic potential being the most important quantitative index from the hydrocarbon genetic point of view, the Pula oil shale can be fairly well distinguished from that of Gérce and Várkeszö. In case of the Pula oil shale the genetic potential is 70—80 kg HC/t rock on the average, the extreme values being 40 and 260 kg HC/t rock. The genetic potential of the Gérce and Várkeszö oil shales is 40—60 and 40—50 kg HC/t rock, the extreme values being 10 and 115 kg HC/t rock in the Gérce, 10 and 88 kg HC/t rock in the Várkeszö oil shales.

The determination of the primordial feature of the organic matter, i.e. of the type, bear great possibility of error. In most measurement methods a peculiarity is traced which changes as a function of the type and maturity stage of the organic matter. Considering the fact that the organic matter of the oil shale is in the initial stage of evolution and thus samples of the same evolution stage are compared, the value of the indices will depend unambiguously on the type. The mineral components, however, mean further problems. The inorganic ingredients constituting the major part of the sedimentary rocks impede the determination of the adjoining organic matter. When isolating the kerogen the following circumstance should be taken into account: a part of kerogen will be lost; certain chemical changes will follow in

the organic matter in the course of isolation. These error possibilities thought to be decreased by making measurements both in the oil shales and in the kerogens isolated from them.

Some samples representing the average of the three beds were chosen and Rock-Eval pyrolysis were made. The most important data measured in this manner are shown in Table 2. In addition to the differences in the genetic potential, the type I and II can be distinguished also after the H- and O-indices, and the transition between the two types can be observed, respectively *(Fig. 1)*. When plotting the H-index as a function of the maximal hydrocarbon generation temperature the type and evolution state of the organic matter can be determined together (ESPITALIE *et al.*, 1977). As it is seen in *Fig. 2,* the organic matter of the Pula oil shale is assigned unambiguously to the type I, that of the Várkesző oil shale to the type II. The organic matter of the Gérce oil shale shows values usually characteristic of the type II, but in certain layers it approches the type I on the basis of all the characteristics. As a whole, it can be considered to be transitional between the types I and II.

To characterize the type differences the PC/TOC ratio seems to be suitable describing the pyrolysable part of the organic carbon content of the samples under definite experimental conditions (the measurement of PC was carried out by Rock-Eval pyrolysis). Based on the average values of the ratio the organic matter of type I (PC/TOC=65%) and of type II (PC/TOC=38%) can be fairly well distinguished, and the transitional character of the Gérce oil shale (PC/TOC=47%) can also be demonstrated, as well (Table 3). The PC/TOC seems to be useful not only to distin-

TABLE 2

Characterization of the organic matter of the maar-type oil shales by Rock-Eval pyrolysis

Depth (m)	T_{max} (°C)	S_1+S_2 kg HC/t oil shale	S_2/S_3	HI mg HC/g TOC	OI mg CO_2/g TOC
		PULA			
9.5—10.0	440	40.08	8.18	556	67
10.0—10.5	440	81.13	10.44	671	64
16.0—16.5	437	71.63	8.79	560	63
19.5—20.0	439	77.22	14.89	749	50
25.0—25.5	440	258.53	22.21	840	37
		GÉRCE			
14.0—14.5	434	39.40	9.18	407	44
21.0—22.0	436	45.74	9.66	598	61
34.0—35.0	425	35.34	6.95	372	53
43.0—44.0	432	69.57	10.94	646	59
58.0—59.0	426	57.39	7.01	426	60
		VÁRKESZŐ			
55.0—56.0	421	47.94	7.74	397	51
58.0—59.0	434	48.62	5.02	354	70
69.0—69.5	422	43.65	4.61	330	71
70.0—70.5	431	88.12	8.42	461	54

TABLE 3

Quantitative characterization of the different types of oil shale kerogen

Pula		Gérce		Várkesző	
Depth (m)	PC/TOC %	Depth (m)	PC/TOC %	Depth (m)	PC/TOC %
9.5—10.0	60	14.0—14.5	39	55.0—56.0	42
10.0—10.5	51	21.0—22.0	54	58.0—59.0	33
16.0—16.5	77	34.0—35.0	38	69.0—69.5	35
19.5—20.0	65	43.0—44.0	63	70.0—70.5	43
25.0—25.5	72	58.0—59.0	42		
Average:	65		47		38

guish the type but to make distinction between the sub-types. This ability is shown by the fact that the value of this ratio proved to be between 30 and 40% in case of other three oil shales generated under different geological conditions and containing organic matter of type II. At the same time, the sediments of organic matter of type

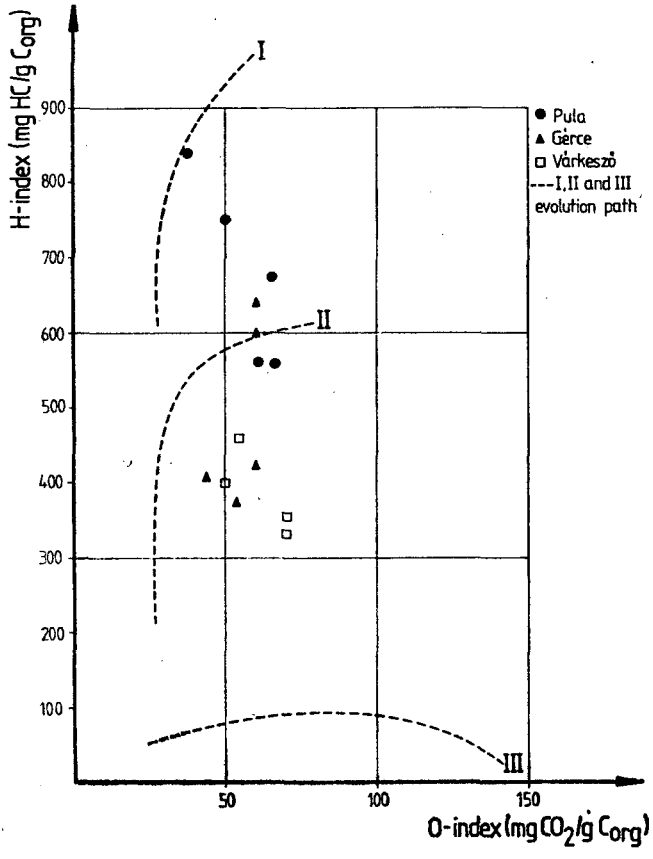

Fig. 1. Classification of the kerogens of the different Hungarian oil shales in a hydrogen index/oxygen index diagram

III and of the same evolution state could be characterized by PC/TOC values of 12 to 13% (HETÉNYI, unpublished data).

As it has been shown by the measurement data, there are considerable differences between the organic matter of the three oil shale beds accumulated in the same geological environment. It is highly probable that these differences can be attributed to the composition of the initial biomass. The differences between the organic matter of the Pula and Várkesző oil shales can be attributed to the different ratio of mixing of the algal material constituting the biomass and of the higher terrestrial plants. In the organic matter of the Várkesző oil shale the latter is of higher proportion. This biopolymer being the precursor of the organic matter of type III of somewhat greater quantity produced an essentially heterogeneous organic matter having mixed with the kerogen of type I.

In order to demonstrate the type-modifying effect of the higher terrestrial plants samples were chosen from the Várkesző oil shale which showed proportions of the plant remnant higher than the average. In case of all the three oil shales, isolation was carried out from the strata most abundant in organic matter. The organic geochemical characteristics of kerogens (Table 4) fairly reflect the type difference which was generated by the biomass of different composition under the same geological conditions. Based on their H/C atomic ratios the Pula kerogen of type I and the Gérce kerogen representing the transition between types I and II differ from each other only to small extent. More remarkable is the difference when taking the C_R/C_T and T_{max} values. All features of the kerogen isolated from the Várkesző oil shale of highest terrestrial plant remnant quantity considerably differ from the same values of the two other kerogens (Table 4). The difference is much greater than in case of comparing the averages of the beds (Tables 2 and 3).

This type-modifying effect of the humic matter can be proved by the comparison of the kerogens and of their humin-free forms. The differences occurring in the oxidation features of the Pula and Várkesző kerogens referring to the type differences, cannot be observed in the course of oxidation of the humin-free organic matter (HETÉNYI, 1983).

The activation energy of the evolution process, thus the quantity of the degradation products of the organic matter (under the same external conditions) is closely related to the type of kerogen. The organic matter of the oil shales to be compared here is in a maturity state preceding the oil generation zone. In the course of the natural evolution different gaseous (*e.g.* CO_2, H_2S) products and bitumen were formed. The bitumen — oil transformation is insignificant yet, i.e. the end product

TABLE 4

Characterization of kerogen isolated from Hungarian maar-type oil shales

	H/C	C_R/C_T	PC/TOC (%)	S_1+S_2 kg HC/t kerogen	S_2/S_3	T_{max} (°C)
Pula	1.72	<0.10	77	697	25.7	444
Gérce	1.68	0.20	78	687	25.8	430
Várkesző	1.33	0.43	56	445	10.5	426

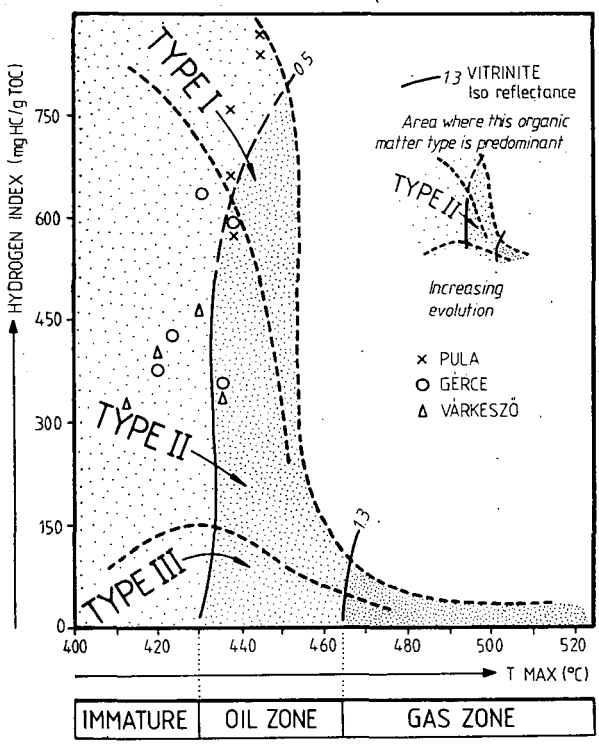

Fig. 2. Classification of the kerogens of the different Hungarian oil shales and characterization of their degree of evolution

of the process is the soluble organic matter in this stage. Thus, the fact that the quantity of the organic solvent soluble organic matter (bitumen) of the three oil shale beds increase in the order Pula—Gérce—Várkesző (Table 1) refers to the decreasing activation of kerogens in the same sequence. The smallest quantity of bitumen was generated in the course of natural evolution of the kerogen of type I requiring the greatest activation energy, and most considerable evolution intermediary product was formed from the Várkesző sample requiring the lowest activation energy.

REFERENCES

Bence, G., Jámbor, Á. and ParténYi, Z. (1979): Exploration of alginite (oil-shale) and bentonite deposits between Várkesző and Malomsok (Transdanubia, W. Hungary). Annual Report of the Hungarian Geological Institute of 1977., Budapest, p. 257—268.

Cummins, J. J. and Robinson, W. E. (1972): Thermal degradation of Green River kerogen at 150° to 350 °C. U. S. Bur. Mines. Rep. Invest. **7620**, 15.

Hajós, M. (1976): Diatom flora in Upper Pannonian sediments of borehole Put-3 at Pula village (Transdanubia, Hungary). Annual Report of the Hungarian Geological Institute of 1974, Budapest, p. 263—286.

Hetényi, M., Maitz, K. and Tóth É. (1977): Contributions to the knowledge of the Hungarian oil shale kerogen I. Preliminary report on the results of the pyrolysis and selective oxidation. Acta Miner. Petr., Szeged, **XXIII/1**, 165—175.

HETÉNYI, M., TÓTH, J. and MILLEY, GY. (1982): On the role of temperature and pressure in the artifical evolution of organic matter of the Pula oil shale (Hungary). Acta Miner. Petr., Szeged, **XXV/2,** 131—146.

HETÉNYI, M. (1983): Experimental evolution of oil shales and kerogens isolated from them. Acta Miner. Petr., Szeged, **XXVI/1,** 73—85.

JÁMBOR, Á., RAVASZ, CS. and SOLTI, G. (1982): Geological and lithological characteristics of oil shale deposits in Hungary. 3rd All Union Meeting on the Geochemistry of Oil Shales, Tallinn.

JÁMBOR, Á., SOLTI, G. (1975): Geological conditions of the Upper Pannonian oil-shale deposit recovered in the Balaton Highland and at Kemeneshát. Acta Miner. Petr. Szeged, **XXII,** 9—28.

JÁMBOR, Á. and SOLTI, G. (1976): Geological conditions of the Upper Pannonian oil shale deposit recovered in the Balaton Highland and at Kemeneshát (Transdanubia Hungary). Annual Report of the Hungarian Geological Institute of 1974, Budapest, p. 193—220.

KEDVES, M. (1983): Étude paléobotanique sur les schistes pétroliféres du tertiaire supérieur de Hongrie. Revue de Micropaléontologie, **26/1,** p. 48—53.

NAGY, E. (1976): Palynological investigation of Transdanubian oil shale exploratory boreholes. Annual Report of the Hungarian Geological Institute of 1974, Budapest, p. 247—262.

RAVASZ, Cs. (1976): Petrographic examinations of oil shale at Pula and Gérce (Transdanubia, Hungary).
Annual Report of the Hungarian Geological Institute of 1974,. Budapest, p. 221—246.

SOLTI, G. (1981): The geyserite of Pula. Annual Report of the Hungarian Geological Institute of 1979, Budapest, p. 241—247.

Manuscript received, May 10, 1984

Acta Mineralogica-Petrographica, Szeged, XXVII, 153—164, 1985

SIMULATED MATURATION PROCESS OF THE BITUMENS OF THE PULA OIL SHALE, HUNGARY

L. PÁPAY

ABSTRACT

Maturation processes were carried out between 200 and 500 °C in the bitumens of the Pula oil shales, the alteration was traced partly by the thermal residue, partly by the IR and C—H analyses of the organic condensate.

It was stated that the relatively high oxygen content of the Bit—A and BAM-bitumen is gradually lost by the release of compounds of different oxygen contents (carboxylic acids, ketons etc.) and by their decomposition, respectively. Above 400 °C no oxygen-bearing compound could be identified in the thermal residue.

In case of both bitumens considerable part of the long paraffin chain and alicyclic skeleton is preserved up to 400 °C. At 450 °C the thermal residue contains very small quantities of paraffinic part in case of Bit—A, at the same temperature more paraffinic compounds survive the thermal effect in case of the BAM-bitumen. At 500 °C the difference between their thermal resistivity is manifested by the coke-like thermal residue of Bit—A and by the product of BAM-bitumen being similar to that of 450 °C.

At lower temperatures the condensates are characterized by large quantities of oxygen-bearing compounds. The amount of these compounds is decreasing as a function of increasing temperature and mainly above 400 °C this value becomes ever lower, but the compounds can be detected even at 500 °C. The quantity of terminal olefines increases parallel with the temperature.

In the course of the simulated maturation processes the changes followed in the bitumen structure of the Pula oil shale show considerable similarities to those described in the thermal investigations of kerogens.

INTRODUCTION

The methods used in the research of insoluble organic matter (kerogen) are applied in the investigations of bitumens, too. So the artificial diagenesis of soluble esters isolated from the chloroform extract of brown coals (BROOKS and SMITH, 1969) as well as the solid phase functional group extraction for bitumens and kerogens (COSTA NETA *et al.*, 1978) were studied.

Due to the high organic matter content, out of the sedimentary rocks the oil especially suitable to yield kerogen concentrate or after extraction to produce greater quantities of bitumen, since a part of them bears bitumen content of percentual order of magnitude (YEN, 1976). Nevertheless, formations with extremely high bitumen content also exist, *e.g.* coorongite. The solubility of coorongite in common organic solvents likewise varies from over 50% when reasonably young to less than 15% for old material (CANE, 1969).

In the Transdanubian Central Mountains (Hungary) in the vicinity of Pula, Upper Pannonian oil shale was found as filling of a basalt crater (JÁMBOR, SOLTI,

* Department of Mineralogy, Geochemistry and Petrography, Attila József University, H-6701 Szeged, Pf. 651, Hungary

1975). Its biological precursor proved to be the *Botryococcus braunii* KÜTZ. alga (NAGY, 1976).

Since this discovery in 1973, several oil shale beds were found in Hungary (JÁMBOR, 1980), the studies of the oil shale of Pula and of the kerogen isolated from it, however, are most complete (GRASSELLY *et al.*, 1978; HETÉNYI *et al.*, 1977, 1978, 1982; HETÉNYI, 1979, 1980). Since the investigations needed the isolation of kerogen from year to year, the first step of this process being the extraction of the soluble matter of the oil shale, the possibility has been provided to carry out the simulated evolution experiments also with the bitumens. These investigations aimed to determine the thermal features of the bitumens as intermediary products of kerogen decomposition under the conditions when due to the lack of mineral matrix neither their catalytic, nor their retention effects should be taken into account.

EXPERIMENTAL

The starting material was obtained by long extraction from the Pula oil shale, by chloroform in Soxhlet extractor (Bit-A) and subsequently by the mixture of benzene-acetone-methanol of 70:15:15 ratio (BAM-bitumen).

The thermal treatment was carried in a Heraeus-type furnace in oxygen-free nitrogen flow. Out of the experiments of different durations only the samples are discussed which underwent five hours thermal treatment Bitumens were put in a boat made from Pyrex glass and this was put in the heating tube consisting of the same material, and the trap at its end collected the condensates, *i.e.* the brownish-black fat-like organic part and water. The organic matter was separated from water in a filler by means of chloroform, the organic solvent was evaporated at 60 °C in a drying chamber.

Analyses were carried out partly on the thermal residue remained in the glass-boat, partly on the organic condensates. These materials were characterized by IR spectra and C—H analyses.

The IR spectra of the original bitumens and thermal residues were recorded by the Specord 75 IR (Carl Zeiss, Jena), in the wavenumber range of 4000 to 400 cm^{-1} using the KBr disc method, except the thermal residues of Bit-A of 375 and 400 °C, since their spectra could be recorded only by means of film techniques because of the sticky state of the material.

In addition to the qualitative evaluation, by means of the base-line method the extinction ratios of the carbonyl group (1710 and 1720—40 cm^{-1}) and of the methylene group (1460 cm^{-1}) of the corresponding compounds were calculated. These indices can be fairly well applied to characterize genetically the bitumens (GLEBOVSKAYA, 1971), and in addition to other indices these are used in the studies of hydrocarbon generation (BRUKNER-WEIN and VETŐ, 1981), as well as when qualifying the organic matter of core samples (BRUKNER-WEIN and SZÜCS, 1982).

The hydrogen and carbon contents were determined by CHN—1 analysator. In case of some samples of high carbon content, the determination of carbon was carried out by Carmhograph 8 (Wösthoff) in oxygen flow at 1000 °C.

The nitrogen determination was carried out by the Kjeldahl-method. Measurements were carried out after destruction in concentrated sulfuric acid in form of ammonium ion, using ion-selective electrodes in an equipment of OP—264 type.

RESULTS

The data of elementary analyses of starting bitumens as well as the extinction ratios of carbonyl and methylene groups of the corresponding compounds measured at the given wavenumber are shown in Table 1, the data concerning the C, H and S contents were published earlier (PÁPAY, 1979).

Based on the IR spectra of the thermal residues of Bit-A *(Fig. 1)* it can be stated that the long unbranched alkyl-chain (strong aliphatic C—H absorption bands at 2920, 2860 and 1460 cm^{-1}, moderate absorption at 1370 and 720 cm^{-1}) and the cycloparaffin skeleton (965 cm^{-1}) are mostly preserved up to 400 °C, the major part of the oxygen-bearing functional groups is broken off, while at higher temperatures being absent.

TABLE 1

The data of elementary analyses and extinction ratios of carbonyl and methylene groups of the corresponding compounds measured at the given wavenumber of starting bitumens

	C %	H %	N %	S %	O (diff.) %	$\frac{E_{1710}}{E_{1460}}$	$\frac{E_{1720-40}}{E_{1460}}$
Bit-A	72.9	11.8	0.05	0.14	15.09	0.92	0.86
BAM-bitumen	72.6	11.2	0.07	0.17	15.96	1.08	1.02

It is to be noted that when interpreting the band at about 970 cm^{-1} the other part of the spectrum should also be taken into account, since the bands at 965 cm^{-1} (DOUGLAS *et al.*, 1970) and at 978 cm^{-1} (CANE and ALBION, 1973) were interpreted as trans-olefines, the band at 970 cm^{-1} (GLEBOVSKAYA, 1971) as naphthenic structure. In case of the Pula bitumens the presence of trans-olefines cannot be unambiguously excluded, but the NMR studies of the Pula paraffin oils revealed large amounts of cycloparaffins (PÁPAY, 1982), thus the IR-band of 965 cm^{-1} is believed to be produced by cycloparaffin skeletons.

At 450 °C the overwhelming majority of the paraffin chains was broken off. At 500 °C the spectrum indicates strongly coaly (coke-like) state. Out of the oxygen-bearing compounds a small quantity of alcohol-type matter is preserved at 200 °C (3450 cm^{-1}) while out of the esters representing the major part (1720—40 cm^{-1}) the ketons are more resistive to temperature. The thermal effect of 400 °C is endured only by a few keton-types out of the oxygen-bearing compounds, the quantity of esters becomes minimal already after the thermal treatment at 375 °C.

It is characteristic of the thermal residues of BAM-bitumens (*Fig. 2*) that at 450 °C a part of the unbranched long paraffins and of the alicyclic skeletons is preserved. The functional groups with oxygen content are broken off above 400 °C. The residue obtained at 500 °C is not coke, but similar to the spectrum of Bit-A at 450 °C.

In case of both bitumens (Bit-A and BAM), especially at 375 °C and above, the spectra of the thermal residues show a small band at 1600 cm^{-1} which is usually attributed to aromatic structures. Though in the course of the former IR and NMR analyses no aromatic structure could be identified in the Bit-A and BAM bitumens, the fact cannot be excluded that small quantity of aromatic compounds occurs in the starting bitumens, since palynological studies revealed pollens of higher plants

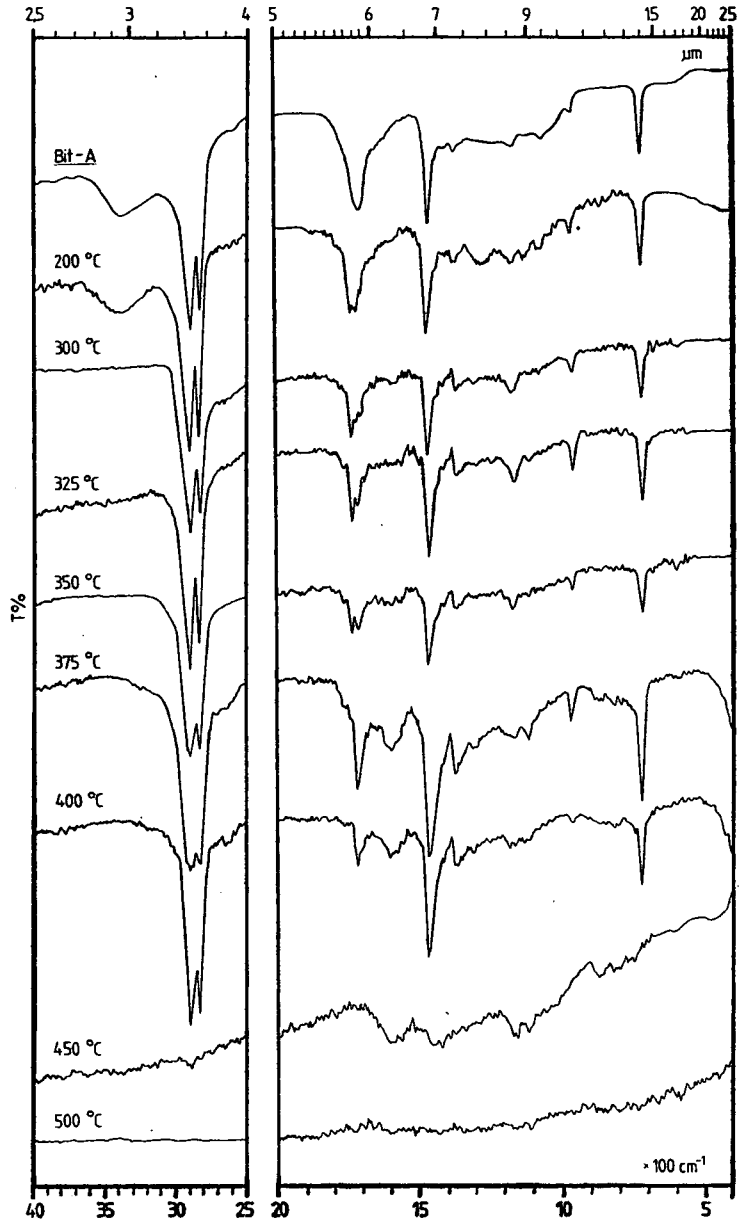

Fig. 1. The IR spectra of starting and thermal residues of Bit-A

(pines and deciduous trees), in addition to the predominancy of *Botrycoccus braunii* KÜTZ. algae (NAGY, 1976). It is to be taken into consideration, however, that due to the thermal effect in case of Bit-A a relative concentration increase of a factor of two (375 °C) and of twenty (450 °C), in case of the BAM-bitumen that of ten (450 °C) followed as a result of coalification, as compared to the initial state. More-

over, the spectra of Bit-A were made by film-technique at 375 and 450 °C, thus in case of these records the material quantity is greater than in case of the KBr disc records.

Based on the C—H analyses the maturation (coalification) processes can also be followed (Table 2). In the thermal residues of Bit-A, the thermal treatment at

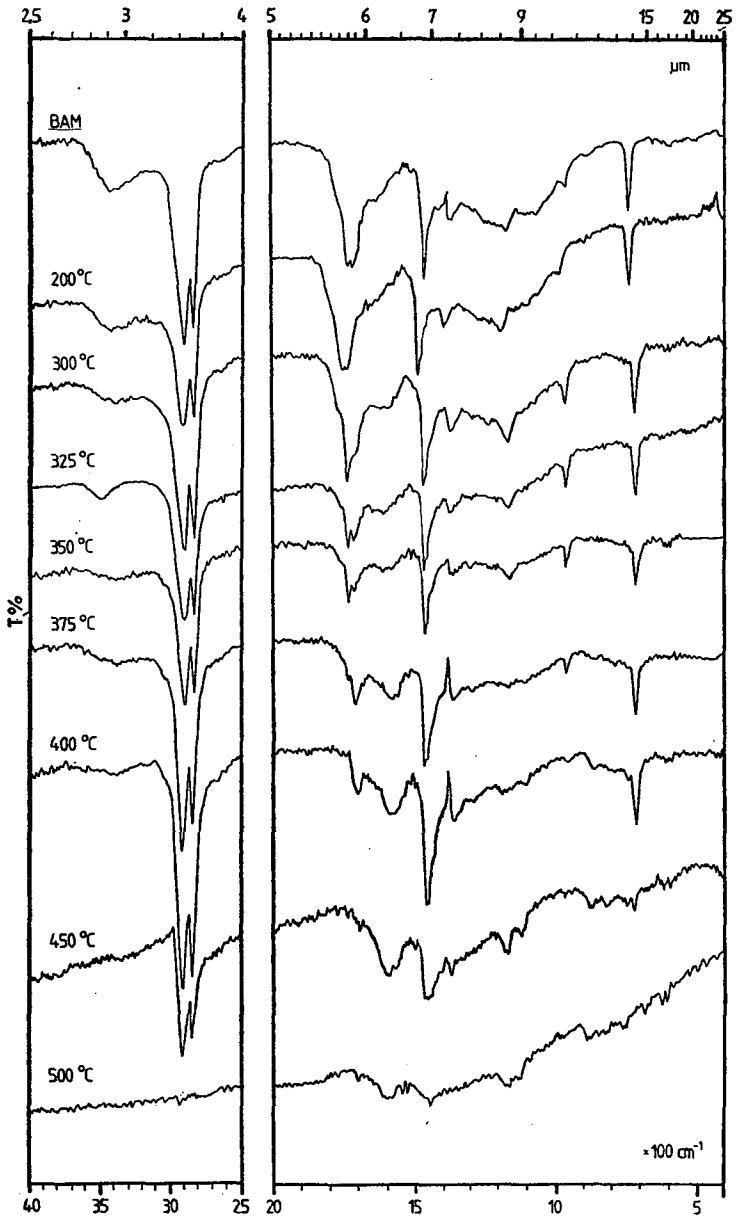

Fig. 2. The IR spectra of starting and thermal residues of BAM-bitumen

TABLE 2

C—H analyses and variation of the ratio of the extinction coefficients of bitumens after thermal treatment

Temperature °C	Bit—A C %	Bit—A H %	Bit—A $\frac{E_{1710}}{E_{1460}}$	Bit—A $\frac{E_{1720-40}}{E_{1460}}$	BAM—bitumen C %	BAM—bitumen H %	BAM—bitumen $\frac{E_{1710}}{E_{1460}}$	BAM—bitumen $\frac{E_{1720-40}}{E_{1460}}$
200	78.2	12.6	0.76	0.76	73.2	12.2	1.09	1.09
300	81.0	13.8	0.52	0.71	80.4	12.8	0.81	1.02
325	81.6	13.9	0.46	0.59	81.4	14.0	0.62	0.71
350	83.4	14.0	0.48	0.50	82.9	14.1	0.55	0.62
375	84.7	13.7	0.46	0.14	85.2	13.2	0.48	0.28
400	86.1	12.9	0.25	0.00	84.9	12.2	0.29	0.00
450	96.0*		0.00	0.00	87.6	10.3	0.00	0.00
500	100.0*		0.00	0.00	91.1*		0.00	0.00

* The carbon contents were determined by Carmhograph 8 apparatus.

200 °C caused considerable oxygen loss, which continued somewhat moderately up to 350 °C. From 375 °C the records refer to the break off of smaller carbon chains in addition to the process above.

On the contrary, in case of the thermal residues of the BAM-bitumen the thermal treatment of 200 °C did not produce remarkable change in the state of bitumen as compared to the initial one. (At this temperature no condensate could be collected.) Nevertheless, the oxygen loss at 300 °C proved to be considerable, then parallel with increasing temperature this trend is continued somewhat more moderately up to 350 °C. At 375 °C and above the decrease of hydrogen quantity refers to the break off of units fo smaller carbon chains. Data obtained at 450 °C support the information indicated by the IR spectra, *i.e.* a part of the paraffinic and alicyclic skeletons survived the thermal effect.

Under increasing thermal conditions the qualitative changes of the thermal residues are fairly well indicated by the extinction ratios of carbonyl and methylene groups of the given compounds measured at given wavenumber. The overall tendency it that the band of 1710 cm^{-1} decreases to greater extent in case of Bit-A up to 300 °C and in case of BAM-bitumen up to 325 °C, than the band of 1720—40 cm^{-1}. Up to 375 °C the measure of decrease is reversed, while the intensity of the band of 1710 cm^{-1} is nearly constant or decreases only to small extent. This fact was concluded from the fact that up to 300 and 325 °C, respectively, mostly carboxylic acids, subordinately esters are released from the bitumens. After the loss of carboxylic acids the decomposition of the esters is accelerated from esters and residues consisting of ketons, up to 375 °C, while the quantity of the keton-type matter remaines nearly constant or shows some decrease. Taking into account the C—H data it can be stated that about one-fifth of the original oxygen-bearing compounds of the bitumens are preserved after the thermal treatment at 400 °C.

Based on the IR spectra, the condensate produced by Bit-A at 200 °C consists mainly of the mixture of carboxylic acids, esters and hydrocarbons (*Fig. 3*). Between 300 and 350 °C in the spectra the band of carboxylic acids in dimeric cyclic association (3500—2400 cm^{-1}) gradually disappears, the base-line of the fingerprint range is increasing, *i.e.* the quantity of the oxygen-bearing compounds of the condensate is decreasing. At 375 °C and above the long unbranched hydrocarbons and cycloparaffins are predominating, in addition to the small quantities of ketons and ester

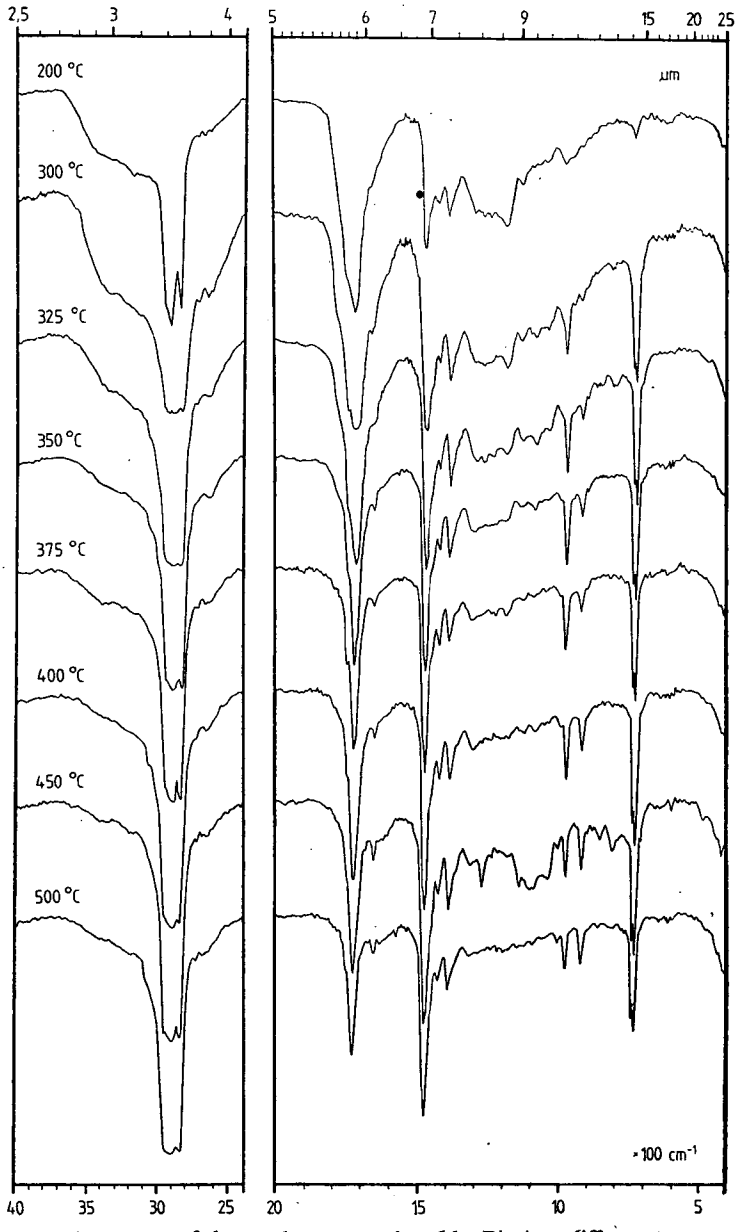

Fig. 3. The IR spectra of the condensate produced by Bit-A at different temperatures

type compounds. In the spectra of the Pula Bit-A condensates the bands characteristic of the aromatic structure are lacking. In all spectra bands referring to isolated double bonds are found, at 200 °C as a shoulder at 1640 cm^{-1} and as small band at 910 cm^{-1}, while at 500 °C in form of bands at 1640, 990 and 910 cm^{-1}. The band pair of 990—910 cm^{-1} is characteristic of the matter of $RHC=CH_2$ type.

In the degradation processes related to kerogen the occurrence of terminal vinyl groups is also well-known. This is the result of the homolytic scission of C—C bonds (HENDERSON *et al.*, 1968; BROOKS and SMITH, 1969; DOUGLAS *et al.*, 1970; CONNAN, 1973; ESNAULT, 1973; KIRAN and GILLHAM, 1976; LARTER, 1978; see in: ALLAN *et al.*, 1980), and the lack of these terminal olefins is just surprising. Taking into account the qualitative composition of the Pula bitumens it seems to be very probable that the occurrence of terminal vinyl groups is caused by the degradation of fatty acids and carbonic acid esters, respectively, disregarding the reaction mechanism of degradation (DOUGLAS *et al.*, 1970; JURG and EISMA, 1970; BASET *et al.*, 1980).

The peculiarities determined for the Bit-A condensates are characteristic also of the condensates of BAM-bitumen (*Fig. 4*), only the temperature values are different. At 200 °C no condensate could be collected. Between 300 and 375 °C in the condensates much carboxylic acid and esters are found, in addition to hydrocarbons. Above 400 °C the hydrocarbon character predominates, the quantities of ketons and esters are subordinate. Between 300 and 500 °C the amount of terminal vinyl groups is increasing parallel with the temperature. No aromatic compounds are indicated by the spectra.

The C—H analyses as well as the ratios of carbonyl and methylene groups of the corresponding compounds measured at given wavenumber (Table 3) indicate

TABLE 3

C—H analyses and variation of the extinction coefficients of organic condensations generated from bitumens after thermal treatment

Temperature °C	Bit—A C %	Bit—A H %	Bit—A $\frac{E_{1710}}{E_{1460}}$	Bit—A $\frac{E_{1720-40}}{E_{1460}}$	BAM—bitumen C %	BAM—bitumen H %	BAM—bitumen $\frac{E_{1710}}{E_{1460}}$	BAM—bitumen $\frac{E_{1720-40}}{E_{1460}}$
200	72.7	11.6	2.80	1.78	—	—	—	—
300	79.6	13.4	1.21	0.98	72.9	11.5	2.93	1.45
325	80.0	14.1	0.90	0.40	76.6	11.4	1.95	0.84
350	79.7	13.8	0.97	0.33	78.6	13.2	1.26	0.76
375	80.9	14.0	0.77	0.27	81.2	13.1	1.01	0.39
400	80.1	13.9	0.66	0.18	79.9	12.8	0.96	0.40
450	80.5	14.0	0.66	0.22	80.1	13.0	0.63	0.21
500	79.8	14.0	0.58	0.18	79.3	12.6	0.48	0.16

that the condensate produced by Bit-A at 200 °C contains considerable amounts of oxygen-bearing compounds. As compared to 200 °C, the oxygen quantity is considerably decreased at 300 °C, then between 325 and 500 °C a decrease of smaller extent can be observed, while the C and H values are constant within the measurement error values. In the condensate of the BAM-bitumen the amount of oxygen-bearing compounds is high at 300, 325 and 350 °C, further it decreases with increasing temperature. Above 375 °C the oxygen loss is of smaller extent than at lower temperatures and the C and H values vary only within narrow extreme limits. In the condensates no aromatic compunds are indicated by the IR spectra, *i.e.* it can be assumed that without catalysis no aromatic compounds are generated from the alkyl and cycloalkyl compounds of bitumens within the temperature range applied.

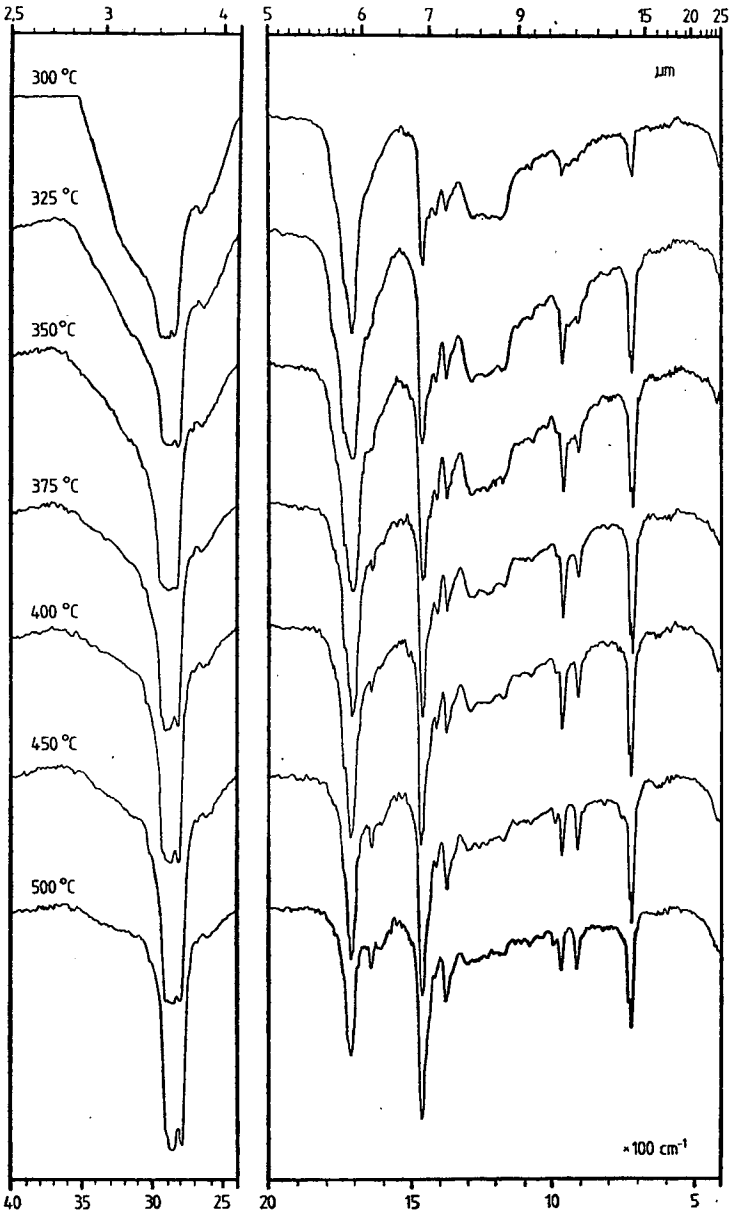

Fig. 4. The IR spectra of the condensate produced by BAM-bitumen at different temperatures

SUMMARY

Based on the simulated maturation processes of the Pula bitumens it can be stated that both the Bit-A and the BAM-bitumen loss their relatively high oxygen content only gradually. At lower temperatures the oxygen is released mainly in

form of carboxylic acid, esters and ketons. Above 400 °C all the oxygen-bearing compounds are lacking in the thermal residue. Considerable parts of the long unbranched paraffin chain and of the alicyclic skeleton are preserved up to 400 °C, though when condensates are generated the scission of C—C bonds can also be presumed at 200 °C in case of Bit-A and at 300 °C in case of BAM-bitumen, being indicated by the occurrence of terminal vinyl groups. At 450 °C small amounts of paraffinic parts can be observed in case of Bit-A, while at the same temperature much more paraffins survive the thermal effect. The difference between their thermal resistivity can be observed also at 500 °C, because the thermal residue of Bit-A is strongly coalified (coke-like), the residue of the BAM-bitumen is similar to that of 450 °C.

The condensates produced by bitumens and isolated from water are characterized by remarkable amounts of oxygen-bearing compounds (carboxylic acids and esters). This value decreases with increasing temperature and mainly above 400 °C it comes close to the oil state of paraffin base, though the products generated at 500 °C contain also some oxygen-bearing compounds. The quantity of terminal olefins increases with increasing temperature. No aromatic compounds could be identified in the condensates.

As a function of increasing temperature, the oxygen loss of bitumens, the break off of aliphatic units, the simultaneous increasing coalification of the thermal residue and the trend towards the graphite-state, as well as the occurrence of terminal olefines in the condensates are experimental results showing similarities to the data described from the thermal investigation of kerogens (HARWOOD, 1974; TISSOT *et al.*, 1974; 1978; DURAND and ESPITALIÉ, 1976; ROBIN and ROUXHET, 1978; TISSOT and WELTE, 1978; ALLAN *et al.*, 1980; MONIN *et al.*, 1980; ROUXHET *et al.*, 1980).

Nevertheless, the aromatization in case of bitumens is less unambiguous. In the condensates no aromatic compounds could be determined, in the thermal residues aromatic compounds were indicated by the IR spectra at 375 °C and above. The appearance of these compounds in the spectra, however, is not due to aromatization, but rather to the relative concentration increase of the aromatic compounds of the starting bitumens, generated by the thermal effect.

ACKNOWLEDGEMENTS

I am thankful to dr. M. HETÉNYI, for the thermal investigations and to dr. L. KÖRMÖCZI (Department of Botany) for making the nitrogen determination.

REFERENCES

ALLAN, J., M. BJOROY and A. G. DOUGLAS (1980): A geochemical study of the exinite group maceral alginite, selected from three Permo-Carboniferous torbanites. In: Advences in Organic Geochemistry 1979 (eds. A. G. DOUGLAS and J. R. MAXWELL), Pergamon Press. p. 599—618.

BASET Z. H., R. J. PANCIROV and T. R. ASHE (1980): Organic compounds in coal: Structure and origins. In: Advences in Organic Geochemistry 1979 (eds. A. G. DOUGLAS and J. R. MAXWELL), Pergamon Press. p. 619—630.

BROOKS J. D. and SMITH J. W. (1969): Diagenesis of plant lipids during the formation of coal, oil and gas—II. Coalification and formation of oil and gas in the Gippsland Basin. — Geochim. Cosmochim. Acta **33**, p. 1183—1194.

BRUKNER-WEIN, A. and I. VETŐ (1981): Origin and migration of hydrocarbons in the southeastern Danube-Tisza Interfluve (in Hungarian with English resume). — Bull. of the Hungarian Geol. Soc., **111**, p. 98—118.

BRUKNER-WEIN A. and I. SZŰCS (1982): Bitumen contents of the fish-scale clay-marl in the Mecsek mountains, S Hungary (in Hungarian with English resume). — Annual Report of the Hungarian Geological Institute of **1980,** p. 487—500.

CANE, R. F. (1969): Coorongite and the genesis of oil shale. — Geochim. Cosmochim. Acta **33,** p. 237—265.

CANE, R. F. ALBION, P. R. (1973): Organic geochemistry of torbanite precursors. — Geochim. Cosmochim. Acta **37,** p. 1543—1550.

CONNAN, J. (1973): Diagenese naturelle et diagenese artificielle de la matiere organique a elements vegetaux predominants. In: Advences in Organic Geochemistry, 1973 (eds, B. TISSOT and F. BIENNER) Editions Technip, Paris. p. 73—96.

COSTA NETO, C., A. M. P. MACAIRA, R. C. P. PINTO, H. T. NAKAYAMA and J. N. CARDOSO (1980): New analytical approaches to organic geochemistry: solid phase functional group extraction for bitumens and functional group markers for kerogens. In: Advences in Organic Geochemistry (eds. A. G. DOULAS and J. R. MAXWELL), Pergamon Press. p. 249—263.

DOUGLAS, A. G., EGLINTON, G. and W. HENDERSON (1970): Thermal alteration of the organic matter in sediments. In: Advences in Organic Geochemistry, 1966 (eds., G. D. HOBSON and G. C. SPEERS), Pergamon Press. p. 369—388.

DURAND, B. and ESPITALIÉ, J. (1976): Geochemical studios the organic matter from the Duala Basin (Cameroon)—II. Evalution of kerogen. — Geochim. Cosmochim. Acta **40,** p. 801—808.

ESNAULT, C. (1973): Evolution thermique des acides gras combinées genése des paraffines normales dans las sédiments. Ph. D. Thesis L 'Université de Pau et des Pays de l'Adour.

GLEBOVSKAYA, E. A. (1971): Primenenie infrakrasnoy spektrofotometrii v neftyanoy geohimii. Nedra, Leningrad.

GRASSELLY, GY., M. BERTALAN and Cs. SAJGÓ (1977): Contributions to the knowledge of the Hungarian oil shale kerogen II. Results of preliminary DTA and IR-investigations on the kerogen of the oil shale occurrence at Pula. — Acta Miner. Petr., **XXIII/1,** p. 177—196.

HARWOOD, R. J. (1977): Oil and gas generation by laboratory pyrolysis of kerogen. — AAPG Bull., **61,** p. 2082—2102.

HENDERSON, W., EGLINTON, G., SIMMONDS, C. and LOVELOCK, J. E. (1968): Thermal alteration as a contributory process to the genesis of petroleum. — Nature, **219,** p. 1012—1016.

HETÉNYI, M., K. MAITZ and É. TÓTH (1977): Contributions to the knowledge of the Hungarian oil shales kerogen I. Preliminary report on the results of the pyrolysis and selective oxidation. — Acta Miner. Petr., **XXIII/1,** p. 165—175.

HETÉNYI, M. and K. SIROKMÁN (1978): Structural information on kerogen from the Hungarian oil shale. — Acta Miner. Petr., **XXIII/2,** p. 211—222.

HETÉNYI, M. (1979): Thermal degradation of the oil shale kerogen of Pula (Hungary) at 473 and 573 K. — Acta Miner. Petr., **XXIV/1,** p. 99—111.

HETÉNYI, M. (1980): Thermal degradation of the organic matter of oil shale of Pula (Hungary) at 573—773 K. — Acta Miner. Petr., **XXIV/2,** p. 301—314.

HETÉNYI, M., J. TÓTH and GY. MILLEY (1982): On the role of temperature and pressure in the artificial evolution of organic matter of the Pula oil shale (Hungary). — Acta Miner. Petr., **XXV/2,** p. 131—146.

HOLLY, S. and P. SOHÁR (1975): Absorption spectra in the infrared region. Akadémiai Kiadó, Budapest.

JÁMBOR, Á., G. SOLTI (1975): Geological condition of the Upper Pannonian oil shale deposite recovered in the Balaton Highland and Kemeneshát (Transdanubia, Hungary). — Acta Miner. Petr., **XXII/1,** p. 9—28.

JÁMBOR, Á. (1980): The results of oil shale exploration in Hungary (1980) (in Hungarian). — Földt. Kutatás **XXIII/4,** p. 5—8.

JURG, J. W. and E. EISMA (1970): The mechanism of the generation of petroleum hydrocarbons from a fatty acid. In: Advences in Organic Geochemistry, 1966 (eds. G. D. HOBSON and G. C. SPEERS), Pergamon Press. p. 367—368.

KIRAN, E. and GILLHAM, J. K. (1976): Pyrolysis-molecular weight chromatography: a new on-line system for analysis of polymers. II. Thermal decomposition of polyolefins: polyethylene, polypropylene, polyisobutylene. J. appl. polymer Sci., **20,** p. 2045—2068.

LARTER, S. R. and DOUGLAS, A. G. (1978): Low molecular weight aromatic hydrocarbons in coal maceral pyrolysates as indicators of diagenesis and organic type. In: Environmental Biogeochemistry and Geomicrobiology. Vol. 1. The Aauatic Environment (ed. W. E. KRUMBEIN) p. 373—386. Ann Arbor, Sci. Pub. Inc., Michigan.

MONIN, J. C., B. DURAND, M. VANDENBROUCKE and A. Y. HUC (1980): Experimental simulation of the natural transformation of kerogen In: Advances in Organic Geochemistry 1979 (eds, A. G. DOUGLAS and J. R. MAXWELL), Pergamon Press. p. 517—530.

NAGY, E. (1976): Palynological investigation of Transdanubian oil-shale exploratory boreholes (in Hungarian with English resume). — Annual Report of the Hungarian Geological Institute of **1974,** p. 247—262.
PÁPAY, L. (1979): Several features of the oil shale and oil-shale-kerogen bitumen of Pula (Hungary). — Acta Miner. Petr., **XXIV/1,** p. 113—124.
PÁPAY, L. (1982): IR and NMR characterization of oil generated from some Hungarian oil shale at 773 K. — Acta Miner. Petr., **XXV/2,** p. 147—156.
ROBIN, P. L., and ROUXHET, P. G. (1978): Characterization of kerogens and study of their evolution by infrared spectroscopy: carbonyl and carboxyl groups. — Geochim. Cosmochim. Acta **42,** p. 1341—1349.
ROUXHET, P. G., P. L. ROBIN and G. NICAISE (1980): Characterization of kerogens and their evolution by infrared spectroscopy. In: Kerogen insoluble organic matter from sodimentary rocks (ed. B. DURAND) Éditions Technip, Paris. p. 163—190.
TISSOT, B., B. DURAND, J. ESPITALIÉ and A. COMBAZ (1974): Influence of nature and diagenesis of organic matter in formation of petroleum. — AAPG Bull., **58,** p. 499—506.
TISSOT, B., G. DEROO, A. HOOD (1978): Geochemical study of the Uinta Basin: formation of petroleum from the Green River formation. — Geochim. Cosmochim. Acta **42,** p. 1469—1485.
TISSOT, B. P. and D. H. WELTE (1978): From kerogen to petroleum. In: Petroleum formations and occurence (eds. B. P. TISSOT and D. H. WELTE), Springer-Verlag. p. 148—184.
YEN, T. F. (1976): Structural aspects of organic components in oil shales. In: Oil shale (eds. T. F YEN and G. V. CHILINGARIAN), Elsevier Scientific Publishing Company. p. 129—148.

Manuscript received, July 31, 1984

Acta Mineralogica-Petrographica, Szeged, XXVII, 165—170, 1985

HUMIC ACIDS IN SUBSURFACE WATERS FROM THE SOUTHERN GREAT PLAIN, HUNGARY

I. VARSÁNYI*

ABSTRACT

Subsurface water samples from different depths were analysed in the Southern part of the Great Hungarian Plain. Permanganate oxidizability and concentration of humic acid were measured. These data showed that there are humic and non-humic organic material in subsurface waters of different ages. The proportion of this organic materials is characteristic on the age of the waters. On the basis of this proportion can be concluded the reaction of organic matarials taking place in waters after burial.

INTRODUCTION

The aim of our investigation is to draw conclusions on the diagenetic changes affecting the organic material in shallow subsurface and deeper Pleistocene and thermal waters. For this purpose the $KMnO_4$ consumption i.e. the permanganate oxidizability of waters and the quantity of total humic acid were determined in waters of different types.

MATERIALS AND METHODS

66 shallow (5—30 m), 82 deeper (75—604 m) subsurface waters and 19 thermal water samples (504—1945 m) were analysed. These waters come from the wells of the Southern part of the Great Hungarian Plain.

Estimating permanganate oxidizability analysis were made in the presence of sulfuric acid. The determination of total humic acid was carried out by CHALUPA's (1963) method; after adding into the water sample sulfuric acid and n-amylalcohol, the mixture was shaken and separated, and than the amylalcohol phase reextracted by dilute NaOH solution. The alkaline extract was measured colorimetrically at 420 nm wavelength. Calibration curve was used to calculate the results.

The data were evaluated by mathematical methods of statistics. Regression analysis was made. The regression constant and coefficient and the correlation coefficient were calculated between O_2 consumption and humic acid content in different types of waters.

RESULTS

The waters are characterised by the permanganate oxidizability (O_2 consumption) and the concentration of total humic acid (THA) of waters and by the O_2 consumption of 1 mg of the THA $\left(\frac{O_2 \text{ cons}}{\text{THA}}\right)$.

* H-6726 Szeged, Csíz u, 7/6, Hungary

The average of these results for different types of waters are summarized in Table 1. Because of the great number of the data only the average values are listed in the Table 1 but each result is used for making *Fig. 1.* The thermal water was divided into two groups: the first group is the thermal water with lower (35—45 °C) temperature and the second one is with higher (>70 °C) temperature. These two types seem to differ from each other on the basis of their chemical character. The thermal water with lower temperature comes from Upper Pliocene and Upper Pannonian strata, the water samples of the other group come from Pannonian strata.

Relation between O_2 consumption and the concentration of humic substances can be seen on *Fig. 1.* The regression constants and coefficients and the correlation coefficients were computed for all the curves (Table 2). On the basis of *Fig. 1.* and Table 2 it can be concluded that the closest connection between O_2 consumption and the concentration of THA is in deeper Pleistocene and in 35—45 °C thermal waters (r: 0.93, 0.95). In shallow subsurface waters and in >70 °C thermal waters

TABLE 1

O_2 consumption, humic acid concentration and O_2 consumption of 1 mg of the humic acid in different types of waters

Type	Number of the samples	O_2 cons. mg/l	THA mg/l	Number of the samples*	O_2 cons* mg/l
Groundwater	66	10.2	5.2	25	2.54
Deeper Pleistocene water	79	4.2	4.6	33	0.77
35—45 °C thermal water	6	8.3	9.7	5	0.95
>70 °C thermal water	13	17.2	6.5	11	3.30

* Number of the samples contains the samples with >2 mg/l humic acid concentration

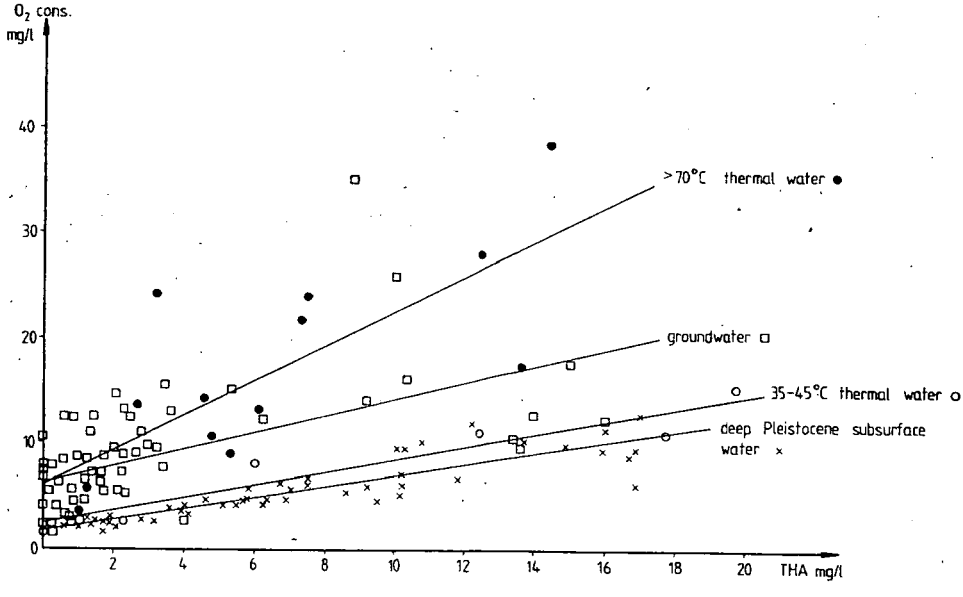

Fig. 1. Relation between O_2 consumption and concentration of humic acid

TABLE 2

The regression constants (b) and coefficients (m) and the correlation coefficients (r) between O_2 consumption and THA in different types of waters

Type	Number of the samples	*b*	*m*	*r*
Groundwater	66	6.57	0.77	0.87
Deeper Pleistocene water	79	1.78	0.52	0.93
35—45 °C thermal water	6	2.23	0.62	0.95
>70 °C thermal water	13	6.67	1.60	0.75

the correlation is not so close but it is strong enough to suppose the connection (r: 0.87, 0.75).

The O_2 consumptions extrapolated to 0 mg/l THA content *(b)* are higher values for shallow subsurface and >70 °C thermal waters (6.57, 6.67 mg/l) than for the deeper Pleistocene and 35—45 °C thermal waters (1.78, 2.23 mg/l).

The three curves are parallel and two of them — the curves of the deeper Pleistocene and 35—45 °C thermal waters — run very close to each other. The slope of >70 °C thermal waters is greater than that of the other ones. These results are reflected by the regression coefficients too.

DISCUSSION

According to our results we supposed that a larger quantity of oxidizable organic material other than humic acid may be present in shallow subsurface — and thermal waters. This assumption is on the basis of *b*: 6.57, 6.67 values which means the O_2 consumption when the concentration of humic acid is 0 mg/l.

Because of their different slope (*m;* 0.77, 1.60) we concluded that the quantity of non-humic organic materials is proportional to the quantity of humic substances in the >70 °C thermal waters having a higher (*m;* 1.60) regression coefficient, but in shallow subsurface waters it is independent of the quantity of humic acid and approximately constant.

The O_2 consumption/THA ratios were regarded as a function of the concentration of humic acid on the *Fig. 2, Fig. 3* and *Fig. 4.* The O_2 consumption/THA curve of shallow and deeper groundwater *(Fig. 2, Fig. 3)* is exponential, i.e. the ratio is decreasing with increasing THA concentration. The curve of thermal waters *(Fig. 4)* is not exponential. The O_2 consumption — neglecting the O_2 consumption of inorganic ions — consists of two parts: one belongs to the humic acid (O_2 $cons_1$), the other to the non-humic acid (O_2 $cons_2$). So:

$$\frac{O_2\ cons}{THA} = \frac{O_2\ cons_1}{THA} + \frac{O_2\ cons_2}{THA}$$

It can be supposed that in the waters of the same age, the precursors of organic material, the circumstances of sedimentation and the diagenetic alteration before and after burial are similar, so the oxidizability of humic acid is similar in the waters derived from the strata of the same age. In this case the O_2 $cons_1$/THA ratio is independent of the concentration of humic acid. It is constant (k_1) and corresponds to the O_2 consumption of 1 mg of humic acid.

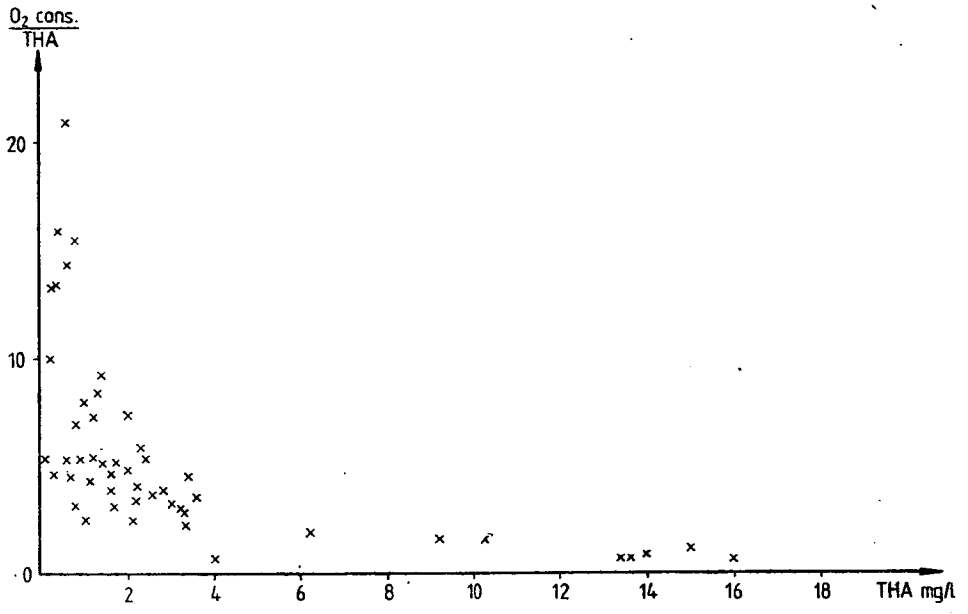

Fig. 2. Relation between O_2 cons./THA ratios and the concentration of humic acid in shallow subsurface waters

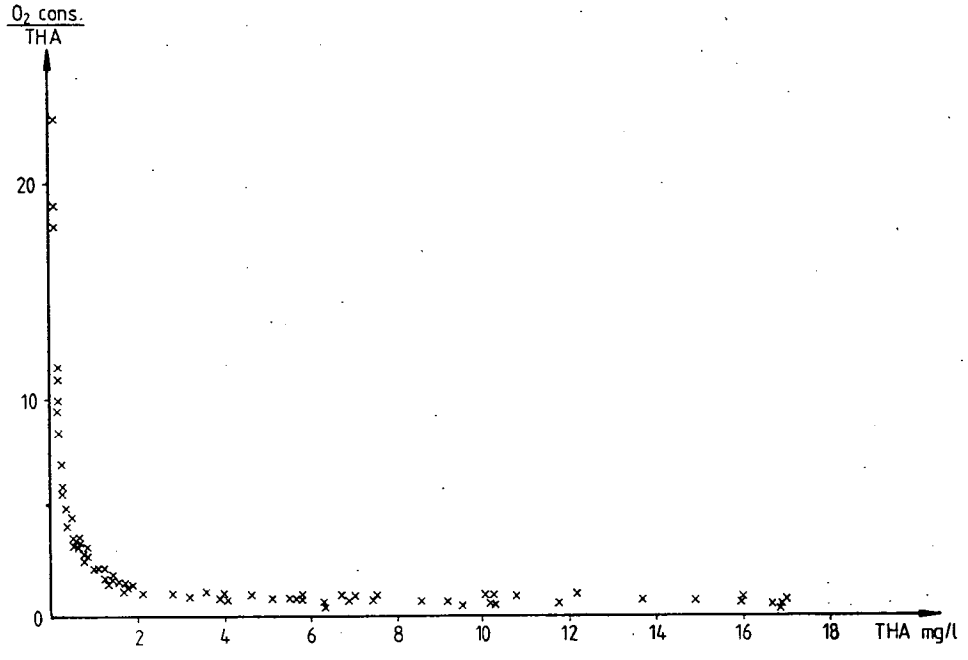

Fig. 3. Relation between O_2 cons./THA ratios and the concentrations of humic acid in deeper Pleistocene subsurface waters

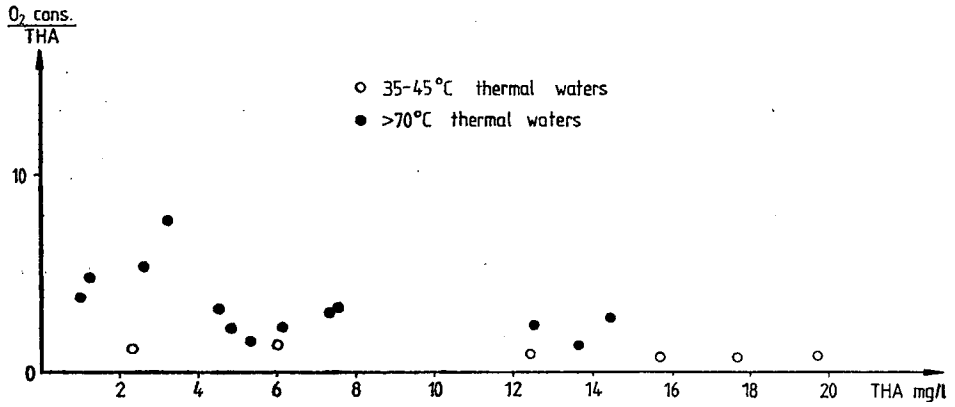

Fig. 4. Relation betwen O_2 cons./THA ratios and the concentration of humic acid in thermal waters

$$\frac{O_2\,\text{cons}}{\text{THA}} = k_1 + \frac{O_2\,\text{cons}_2}{\text{THA}}$$

Interpreting this equation two cases have to be taken into consideration. One is when the quantity of non-humic oxidizable organic materials are constant, the other is when the quantity of them depends on the concentration of humic acid. In this latter case the precursor of the non-humic oxidizable organic materials may be humic acid or its condensation derivatives.

When the quantity of non humic oxidizable organic materials is constant, the O_2 $cons_2$ is constant too independently of the humic acid concentration, so the O_2 $cons_2$/THA ratio decreases with increasing THA concentration. The O_2 cons/THA ratio converges to k_1 constant when THA concentration is high enough to neglect O_2 $cons_2$/THA ratio. The connection is exponential between the O_2 cons/THA and humic acid concentration. This is in shallow and deep subsurface Pleistocene waters *(Fig. 2, Fig. 3)* in which the quantity of non-humic oxidizable organic materials is constant independently of the humic acid concentration. In these cases the regression constant *(b)* between O_2 consumption and humic acid concentration gives the O_2 consumption of the non-humic organic materials. These are 6.57 mg/l and 1.78 mg/l for shallow groundwaters and deep Pleistocene subsurface waters, respectively. On the basis of these data there is a larger quantity of the non-humic oxidizable organic materials related to the total oxidizable organic materials in shallow groundwater than in the deeper Pleistocene waters.

When the quantity of the non-humic organic materials depends on the humic acid concentration:

$$O_2\,\text{cons}_2 = k_2 \cdot \text{humic acid concentration}$$

with the k_2 proportion factor. Its values depend on the proportion of the humic and non-humic organic materials. In this case

$$\frac{O_2\,\text{cons}}{\text{THA}} = k_1 + k_2$$

According to this equation the O_2 cons/THA ratio independent of the humic acid concentration and it is a constant value. The regression coefficient of the connection between O_2 cons and humic acid concentration gives the k_1 and the regression constant gives the k_2 values. On the *Fig. 4* it can be seen that there is not exponential connection between O_2 cons/THA ratio and humic acid concentration, though the scattering of the O_2 cons/THA ratio is higher at lower humic acid concentrations.

On the basis of the data it has been assumed that because of the elevated pressure and first of all elevated temperature the degradation of humic acid and of its condensation derivatives starts in the Pannonian thermal waters. During this degradation water-soluble oxidizable non-humic organic materials are formed. Their quantity is proportional to the concentration of humic acid from which they formed.

CONCLUSIONS

Evaluating the $KMnO_4$ *i.e.* O_2 consumption of waters and their humic acid content it can be concluded as follows:

— In waters of different age and depth there are humic and non-humic organic materials.
— The proportion of humic and non-humic organic materials differs in the waters of different types.
— On the basis of the connection between O_2 consumption and humic acid concentration the shallow and deep Pleistocene subsurface waters and the thermal waters can be distinguished. In the ground waters large quantity of non-humic oxidizable organic material is related to the total organic material. In the deep Pleistocene subsurface waters humic acid predominates, and in the thermal waters the proportion of non-humic organic materials is increased again. The thermal waters with lower temperature (35—45 °C) are between Pleistocene and Pannonian thermal waters.
— In the thermal waters the degradation of humic acid takes place and non-humic organic materials are formed.

REFERENCE

CHALUPA, J. (1963): Humic acids in water I. Methods of preparation and determination. Scientific Papers from Institute of Chemical Technology, Prague 1963. 18—47.

Manuscript received, March 27, 1984

Acta Mineralogica-Petrographica, Szeged, XXVII, 171—174, 1985

HUMIC ACID AS AN INDICATOR OF SUBSURFACE WATER MOVEMENTS

I. VARSÁNYI[1] and M. BERTALAN BALOGI[2]

ABSTRACT

Concentration of humic acids and their E_4/E_6 ratio in shallow groundwater, deeper subsurface water and thermal water samples were determined. Humic acids were isolated from several samples and their C and H contents were also measured.

The E_4/E_6 and H/C ratios of humic acids differ to each other in shallow ground- and in thermal waters. The E_4/E_6 ratio of humic acids in deeper Pleistocene waters of less Cl^- content is similar to that of the shallow groundwaters and those of higher Cl^- content is similar to that of the thermal waters. The E_4/E_6 ratio shows an upward migration of deep waters along fault line, where this migration was supposed on the basis of the higher Cl^- concentration of waters.

INTRODUCTION

In the Hungarian Great Plain, based on observations regarding the anomalies of well yields, geothermal gradient and Cl^- ion concentration, respectively, several authors presumed the presence of structural lines penetrating from the depth to the surface (ERDÉLYI, 1964; URBANCSEK, 1965; SCHERF, 1967). The authors mentioned assume the migration of water along these structural lines from the deeper aquifers.

According to the investigations of CASAGRANDE *et al.*, (1980) each depth interval represents a given horizon of diagenetic transformation. So, it can be assumed that the investigation of the organic material dissolved in the waters offers rather valuable informations than that of the concentration of inorganic salts. Thus, analyzing the organic matter dissolved the question can presumably be answered either the water in the given sedimentary layer can be considered as syngenetic to the sedimentation or it migrated later into the layer from greater or shallower depth.

This paper attempts to conclude to probable movements of subsurface waters by determining the degree of diegenesis of humic acid.

MATERIALS AND METHODS

The amount of dissolved humic acid was determined in 66 samples taken from shallow groundwaters, in 82 samples from Pleistocene layers (depth interval from 75 to 604 m) and in 19 thermal water samples taken from the depth interval from 504 to 1945 meter according to CHALUPA's method (1963).

The absorbance of humic acid in 0.5% NaOH solution was also measured at the wavelength of 465 and 665 nm and their ratio (E_4/E_6) was calculated. The E_4/E_6 ratio

[1] H-6726 Szeged, Csiz u. 7/6, Hungary

[2] Department of Mineralogy, Geochemistry and Petrography, Attila József University, H-6701 Szeged, Pf. 651, Hungary

is suitable — on the basis of KONONOVA's results (CHEN *et al.*, 1977) — to conclude the aromatic or aliphatic character of the humic acids. This ratio is independent of the humic acid concentration in water.

The humic acid content of two samples of groundwaters, six samples of deeper Pleistocene waters and four samples of thermal waters was isolated in acid medium by n-amylalcohol and after drying by rotation vacuum evaporator the C and H content were determined. Determinations were made by CHN—1 analysator at 800—820 °C, with silverpermanganate catalysator under oxygen atmosphere. The CO_2 and H_2O were carried into a Porapack-Q-filled column by He carrier gas. Their quantities were determined by thermal conductivity measurements after their absorption and desorption.

The comparison of data was carried out by the STUDENT's *t*-test (SVÁB, 1981), if this proved to be necessary.

RESULTS

The average values of the E_4/E_6 quotient are listed in Table 1. Calculating the average values only the water samples containing more than 2.0 mg/l humic acid were involved. When the concentration of humic acid is smaller than 2.0 mg/l the very low absorbance measured at 665 nm makes the calculations uncertain. Having compared the average values of the E_4/E_6 quotient of different waters by the *t*-test it was stated that there is no significant difference between the shallow groundwater and the deeper Pleistocene water, at a confidence level of 5%. The humic acid content in thermal waters were examined separately in waters of lower temperature (35—45 °C) and of higher temperature (more than 70 °C) since their chemical characters are different. The waters of lower temperature derive from Upper Pliocene and Upper Pannonian, those of higher temperature from Pannonian strata. Based on their E_4/E_6 quotients the thermal waters of higher temperature differ both from the shallow groundwaters and from the deeper Pleistocene waters. The E_4/E_6 qoutient of the thermal waters of lower temperature does not differ significantly from the other water types, these waters are transitional ones between the Pleistocene and Pannonian waters.

According to CHEN *et al.* (1977) the ratio E_4/E_6 depends on the molecular weight, thus it is related to the pH-value affecting the molecular weight, to the carbon and oxygen contents depending on the molecular weight and to the carboxyl groups, as well. Smaller E_4/E_6 values refer to greater molecular weight and to higher carbon and lower carboxyl group contents. KONONOVA (CHEN *et al.*, 1977) suggested that the smaller E_4/E_6 ratios refer rather to the aromatic, the greater ones rather to the aliphatic structures. Taking into consideration this suggestion it can be stated that humic acid in the Pannonian thermal waters is rather aromatic, it has a greater molecular weight, and it contains less carboxyl groups ($E_4/E_6=2.77$) related to the shallow groundwaters and deeper Pleistocene waters ($E_4/E_6=4.44$; 4.30).

In one part of the studied region, i. e. in the Danube — Tisza interfluve, in the territory east of the river Tisza, but close to it, the humic acid concentration is low in the deeper Pleistocene waters, and due to the small absorbance values the E_4/E_6 ratio cannot be determined. In the other areas, however, this value can be fairly well measured. The extremely high Cl^- ion concentration as compared to the environment has been attributed to the waters migrating upward along fault lines. The Cl^- ion concentration is lower than 10 mg/l in water samples almost from the whole area, but it is about 30 mg/l in some samples *(Fig. 1)*. The E_4/E_6 ratios of these two types of water were compared. In the areas where the Cl^- ion concentration is extremely

TABLE 1

The E_4/E_6 quotient in waters of different types

Type of water	Number of samples	E_4/E_6 average	Variance
Shallow groundwater	25	4.44	7.21
Deeper Pleistocene water	37	4.50	1.00
Thermal water of lower temperature	54	4.06	1.30
Thermal water of higher temperature	11	2.77	2.16

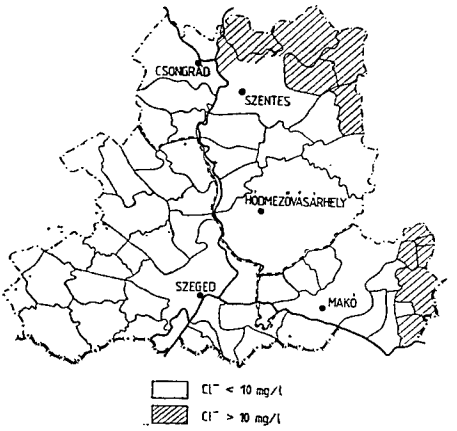

Fig. 1. Regional distribution of Cl^- concentration in drinking waters in the area studied

high as compared to the environment, the average of the E_4/E_6 ratio is 3.9 while in the areas characterized by lower Cl^- ion concentration this value is 4.7. Taking into account the different element number of the groups and the different deviation, based on the *t*-test the E_4/E_6 ratios show significant differences on a confidence level of 5%.

In Table 2 the waters of more or less Cl^- ion content are compared with the thermal waters based on the E_4/E_6 ratio. The *t*-test proves that at $P=5\%$ confidence level the average value of the E_4/E_6 ratio of the Pleistocene waters of low Cl^- ion concentration considerably differs both from the waters of greater Cl^- ion concentration and of thermal waters, too. Nevertheless, waters of greater Cl^- ion concentration do not show any considerable differences as compared to the thermal waters.

All these suggest that in the waters of high Cl^- ion concentration the humic acid structure becomes similar to that of the thermal waters and this is a new evidence to the upward migration of abyssal waters along fault lines.

TABLE 2

The E_4/E_6 quotient in the deeper Pleistocene waters of more or less Cl^- ions and in thermal waters

Type of water	Number of samples	Cl^- (mg/l) average	E_4/E_6 average	Variance
Deeper Pleistocene water of less Cl^-	20	6	4.90	1.23
Deeper Pleistocene water of more Cl^-	17	26	3.90	0.22
Thermal water	16	41	3.20	2.03

The H/C atomic ratio was determined from isolated humic acids, the data are listed in Table 3.

TABLE 3

The H/C atomic ratios in humic acids isolated from waters of different types

Locality	Type of water	Depth of well (m)	H/C atomic ratio
Apátfalva	shallow groundwater	20	1.90
Nagyér		20	1.85
Nagymágocs	deeper Pleistocene water, <10 mg/l Cl^-	207	1.91
		358	1.79
Apátfalva		386	1.63
Ambrózfalva	deeper Pleistocene water, >10 mg/l Cl^-	189	1.59
Eperjes		386	1.75
Nagyér		498	1.70
Ásotthalom	thermal water, 35—45 °C	415	1.69
Eperjes		580	1.60
Apátfalva	thermal water, >70 °C	1700	1.55
Hódmezővásárhely		1735	1.58

The H/C atomic ratio shows smaller values in the organic matter with more aromatic compounds. TISSOT and WELTE (1978) showed that the H/C ratio is 1.3—1.5 in the organic matter of terrestrial origin and 1.7—1.9 in that of marine origin. According to the present investigations the C/H ratios in the humic acid changes between 1.55 and 1.91. The value is highest in the humic acids isolated from groundwaters (Table 3). This fact corresponds fairly well to that obtained on the basis of E_4/E_6 ratios, i. e. in the thermal waters more aromatic humic acids are found than in shallow groundwaters. The upward migration of the waters supposed by hydrogeological methods can be proved by the E_4/E_6 ratio and the H/C atomic ratio of the humic acid dissolved in deeper Pleistocene water which is similar to that of the thermal waters.

REFERENCES

CASAGRANDE, D. J., K. GRONLI and N. SUTTON (1980): The distribution of sulfur and organic matter in various fractions of peat: origins of sulfur in coal. Geochim. Gosmochim. Acta, **44**, 25—32.

CHALUPA, J. (1963): Humic acids in water. Sci. Papers from Inst. of Chem. Technol., Prague, 18—47.

CHEN, Y., N. SENESI and M. SCHNITZER (1977): Information provided on humic substances by E_4/E_6 ratios. Soil Sci. Soc. Am. J., **41**, 352—358.

ERDÉLYI, M. (1964): Tracing of the subsurface structure and fault lines on sedimentary lowlands by using indirect geological method. Acta Geol. Ac. Sci. Hung., **8**, 364—376.

SCHERF, E. (1967): Microtectonical and hydromorphological interrelations on the southern region. of the Plainland and the practical importance thereof. Hidr. Közl. **6**, 322—331. (in Hungarian)

SVÁB, J. (1981): Biometrical methods in research. Mezőgazd. Kiadó, Budapest. (in Hungarian).

TISSOT, B. P., D. H. WELTE (1978): Petroleum formation and occurence. Springer-Verlag.

URBANCSEK, J. (1965): Quaternary profund structures in the Hungarian Plains. Hidr. Közl., **3**, 111—125. (in Hungarian).

Manuscript received, July 10, 1984

Acta Mineralogica-Petrographica, Szeged, XXVII, 175—183, 1985

STUDY OF ORGANIC MATTER ON SOME CENOZOIC SAMPLES FROM THE DSDP WALWIS RIDGE LEG 75 HOLES, WITH EMPHASIS ON ITS ORIGIN AND ITS PETROLEUM POTENTIAL

A. WEIN-BRUKNER, F. GÓCZÁN, K. IKRÉNYI, I. SZŰCS and J. VETŐ

ABSTRACT

The authors have studied the organic matter content of 11 Cenozoic core samples from four Walwis Ridge Leg 75 Holes by means of organogeochemical and palynological techniques. The kerogen concentrates of the Paleogene to Early Miocene samples contain planktonic and land-derived particles. These samples are scarce in organic matter (C_{org}<0.4%) due to the low sedimentation rate and/or the low surface biological productivity. The Upper Miocene to Pleistocene samples, rich in organic matter (C_{org} mostly>1%) also contain planktonic and land-derived organic particles. The proportion of the planktonic organic matter and C_{org} content increase from the Upper Miocene up to the Pleistocene. These observations can be explained by an upward increase in surface productivity and/or sedimentation rate. The upper, organic-rich part of the Cenozoic sequence accumulated in oxygen-depleted environment caused by the high plankton production due to the Benguela upwelling evolved in Late Miocene time. This part of the sequence may be regarded as a good potential oil source rock but the generation of a substantial amount of hydrocarbons in it has not started yet.

INTRODUCTION

The objectives of this study are to characterize the amount and composition of organic matter preserved in Walwis Ridge Cenozoic sediments and to evaluate of some conditions of their deposition and their petroleum potential.

We have received 11 frozen core samples from four holes — 530 A, 530 B, 532 A, 532 B — of the Leg 75 (Fig. 1). Their geological ages range from Pleistocene to Paleocene. The samples are diatomaceous and/or nanno-ooze and marl. They were studied for C_{org}, extractible organic matter and kerogen. For the chemical characterization of the kerogen a special pyrolysis device was used.

METHODS

The analyses of the samples started after their thewing. They were checked in UV-light and the stainings visible with eyes or by fluorescence were eliminated. Each samples were cut in two and one part was grinded in a Fritsch ball mill.

The extraction of rock powder was carried out with $CHCl_3$ (200 ml). The IR spectra of the extracts were recorded on Zeiss-Jena Spekord IR 75 spectrophotometer using KBr disc technique, and evaluated by baseline method.

Asphaltenes were precipitated from the chloroform extracts with a large excess of petroleum ether (40—70 °C). Asphaltene-free extracts were separated on silica gel

Hungarian Geological Survey, H-1442 Budapest, Népstadion út 14, P. O. Box 106, Hungary

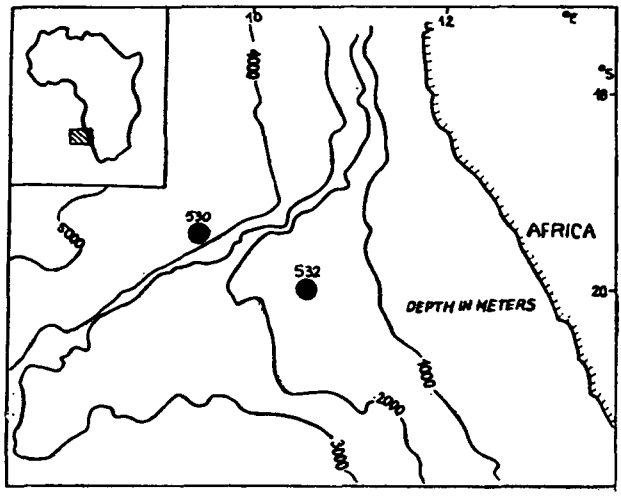

Fig. 1. Location of the Holes

column by elution technique. Eluents were: petroleum ether (40—70 °C) for the saturated HC fraction; benzene for the aromatic HC fraction; benzene-methanol (1 :1) mixture for the resin fraction.

The saturated HC fraction was analysed on a CHROM ROM 41 type gas chromatograph using a 20 m×0.25 mm capillary column coated with OV—1 stationary phase. The chromatograph was programmed from 100 to 250 °C at 6 °C per min. H_2 was the carrier gas. The n-alkane peaks were identified by addition of n-alkane standards, and response factors were applied.

The exracted rock powder was treated by hydrochloric acid to eliminate the carbonates. The C_{org} content of the carbonate-free samples was measured in a special equipment using CO_2-free dry air as a carrier gas and a catalytic postburner. The samples were heated up 700—800 °C at 6 °C per min. heating rate. The volatile C_{org} was measured in the same way but using purified N_2 gas as a carrier gas.

The second part of the sample was crushed, then it was treated with hydrochloric and hydrofluoric acid and centrifugated in $ZnCl_2$-solution. The concentrate was mounted on a glass slide and examined microscopically.

The path of the sample preparation and the analysis are shown on a flow chart *(Fig. 2)*.

RESULTS

The organogeochemical and palynological data are shown in the Tables 1—3 and Figs 3—6.

A separation of the samples in two groups is clearly visible from these data.

The Paleogene to Early Miocene samples are characterized by a low C_{org} content (0.04—0.36%) and a relatively high extract to C_{org} ratio (78—1100 mg/g) (Table 1, *Fig. 3*).

The absence of the 960 cm^{-1} absorption band, the predominance of the esthers as carbonyl bearing molecules and the presence of absorption bands in the 600—

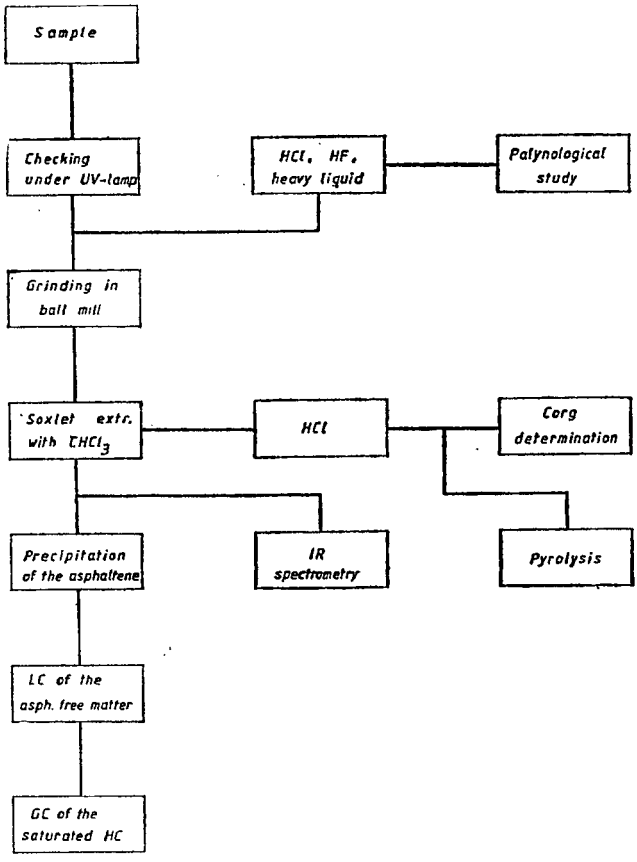

Fig. 2. Flow chart of the analytical procedures

400 cm^{-1} range (organic sulphur compounds) in IR spectra are characteristic for the extracts (Table 2, *Fig. 4 b*).

The palynological concentrate does not contain woody particles, the sporomorphs are very scarce. *(Fig. 5)*. The palynomorphs proved to be well preserved and light.

The Upper Miocene to Pleistocene samples are characterized by a high C_{org} content (0.39—3.66%) and a relatively low extract to C_{org} ratio (23—39 mg/g) (Table 1, *Fig. 3*), the 29.2 sample from the Hole 532 A has a petroliferous odor. The presence of a 960 cm^{-1} absorption band (saturated cyclic hydrocarbons) and the predominance of the acids and ketones as carbonyl-bearing molecules in IR spectra are characteristic for the extracts (Table 2, *Fig, 4. a*).

The quantity of extract obtained from these samples was sufficient for the determination of the bulk composition and for GC-study of the alkanes (Table 3, *Fig. 6*). The extracts are characterized by a high resin content (55—75%). In the n-alkane spectra the $C_{23}+$ molecules are dominating and a strong odd predominance was found. The pristane to phytane, pristane to n-C_{17} and phytane to n-C_{18} ratios are varying between 0.75—1, 0.5—0.8 and 0.8—1.2, respectively.

TABLE 1

C_{org}, extract and HCl-insoluble residue data of the Leg 75 samples

Site	Core	Section	Sub-bottom depth m	C_{org} %	mg extract / g rock	mg extract / g C_{org}	HCl-insoluble residue %
530 A	5	5	162	1.65			90
	13	5	249	0.39	0.15	39	62
	24	6	343	0.21			71
	37	3*	467	0.04—0.05	0.13—0.55	380—1100	50—47
	43	1	523	0.08	0.15	190	48
530 B	1	1	0	0.36	0.28	78	22
	33	1	126	0.95	0.35	36	49
532 A	7	3	25	3.39	0.93	27	37
	29	2	121	3.66	0.98	27	52
	49	2	199	1.96	0.43	22	44
532 B	63	1	256	0.63	0.19	29	29

* The sample was separated to two parts before grinding

TABLE 2

Significant bands and the position of maximum of broad overlapped bands in IR spectra of extracts of the Leg 75 samples

Site	Core	Section	Sub-bottom depth m	Position of absorption bands. Wawe number (cm^{-1})												
				3500—3200	2960—2850	1740–1670 maximum 1740	1740–1670 maximum 1710	1650—1600	1460	1370	960	900—690 maximum 870	900—690 maximum 790	720	600—400	
530/A	13	5	249	+	+	+	+	+	+	+	+	+		+	+	
	37	3/A	467	+	+	+		+	+	+		+	+	+	+	
	37	3/B	467	+	+	+		+	+	+		+	+	+	+	
	43	1	523	+	+	+		+	+	+		+		+	+	
530/B	1	1	0	+	+	+		+	+	+		+	+	+	+	
	33	1	126	+	+		+	+	+	+	+		+	+		
532/A	7	3	25	+	+		+	+	+	+	+			+		
	29	2	121	+	+		+	+	+	+	+			+		
	49	2	199	+	+		+	+	+	+	+	+	+	+		
532/B	63	1	256	+	+		+	+	+	+	+			+		

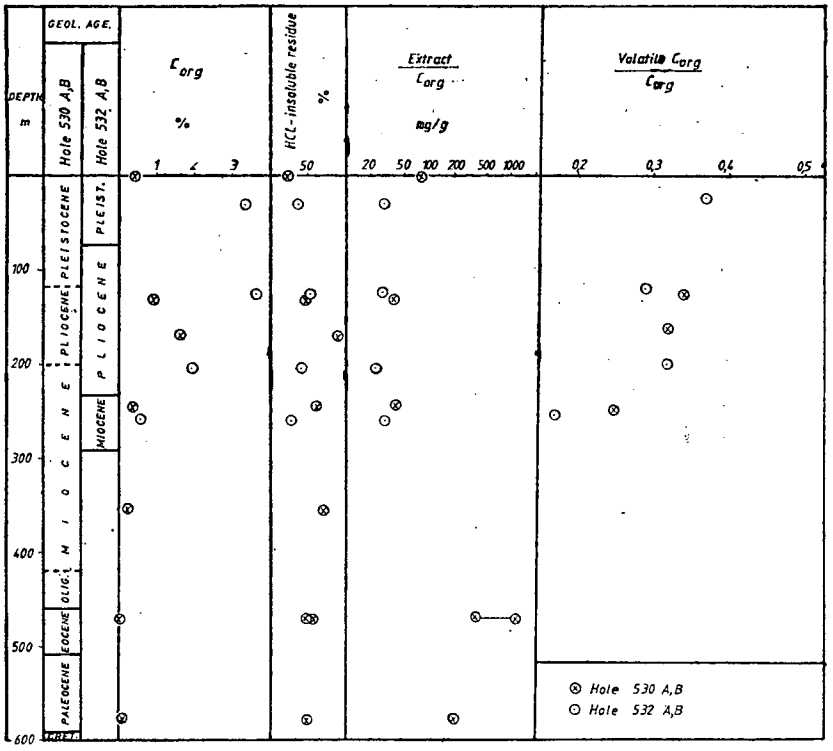

Fig. 3. Basic organogeochemical parameters *vs* depth in the Leg 75 samples

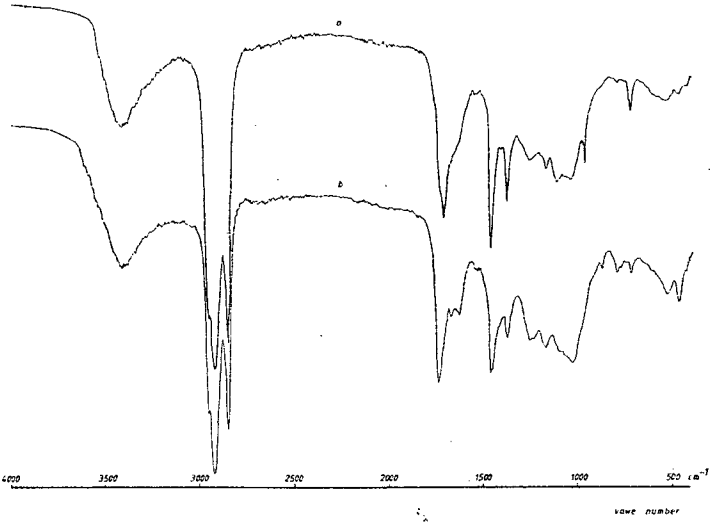

Fig. 4. Typical IR spectra of the Leg 75 samples
a) Hole 532 A, 29-2 sample
b) Hole 530 A, 37-3

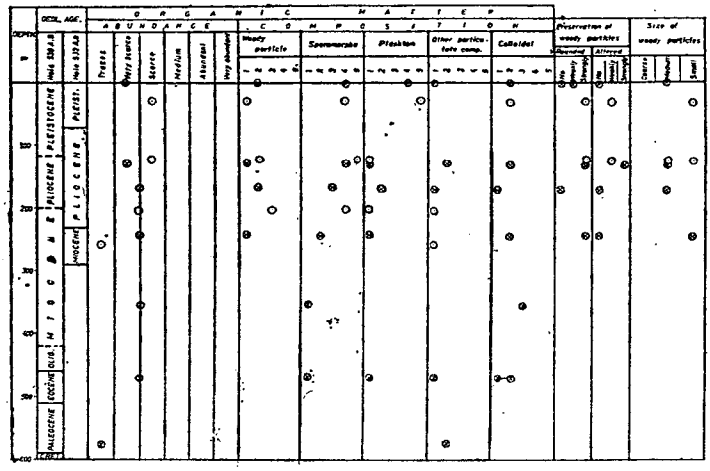

Fig. 5. Characters of the particulate organic matter *vs* depth in the Leg 75 samples. 1) very scarce, 2) scarce, 3) medium, 4) abundant, 5) very abundant
(For other explanations, see *Fig. 2*)

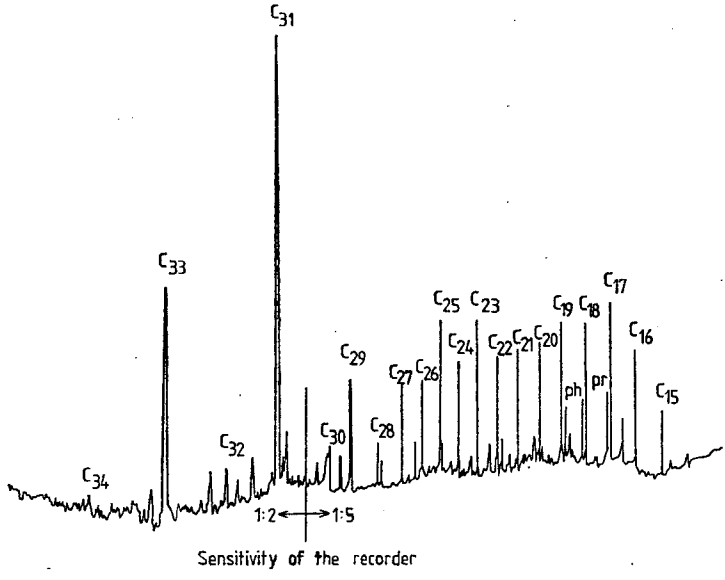

Fig. 6. GC spectra of the saturate fraction of the extract from the Hole 532A, 49-2 sample

In the palynological concentrate mainly woody particles, sporomorphes and plankton remains can be observed *(Fig. 5.)* The 7—3 and 29—2 samples of the Hole 532 A contain a lot of microscopic resinite grains. The palynomorphs proved to be well preserved and light.

The volatile C_{org} to C_{org} ratio decreases with increasing depth (Table 3).

The 1—1 sample of the Hole 530 B and the 13—5 sample of the Hole 530 A show intermediate character between the two sample groups.

TABLE 3

Extract bulk composition, alkane distribution parameters and kerogen pyrolysis data of the Leg 75 samples

Site	Core	Section	Sub bottom depth m	Saturated HC	Aromatic HC	Resins	Asphalt	$\frac{n\text{-}C_{22}^-}{n\text{-}C_{23}^+}$	CPI ($n\text{-}C_{24}$—$n\text{-}C_{34}$)	$\frac{pr}{ph}$	$\frac{pr}{n\text{-}C_{17}}$	$\frac{ph}{n\text{-}C_{18}}$	Volatile C_{org} / C_{org}
				% in extract									
530 A	5	5	162										0.32
	13	5	249										0.25
530 B	33	1	126	16.7	8.1	57.4	11.7	0.77	2.08	0.83	0.81	1.05	0.34
532 A	7	3	25	8.7	4.9	64.0	21.4	0.39	3.05	0.85	0.75	1.17	0.37
	29	2	121	7.7	5.3	68.6	16.9	0.43	3.51	0.79	0.76	1.17	0.29
	49	2	199	6.1	6.1	73.2	12.6	0.26	3.53	0.91	0.58	0.82	0.32
532 B	63	1	256	17.7	6.2	76.0		0.42	2.21	0.91	0.68	0.94	0.17

DISCUSSIONS AND CONCLUSIONS

Because of the low organic matter content of the Paleogene to Early Miocene samples these could not be analyzed for pyrolysis or gas chromatography, respectively. For this reason, only tentative conclusions can be drawn as to the sequence in question.

The palynological concentrate is composed of planktonic and land-derived particles *(Fig. 5)*. but their ratios do not enable us to draw any quantitive conclusion concerning the composition of the kerogen (POWELL *et al.*, 1981). The predominance of bands corresponding to esther-type carbonyl groups in the IR spectra of the extracts (Table 2) suggests the organic matter of marine origin to play an important role (MAKSIMOV *et al.*, 1975).

The low C_{org} content may be due to both the low quantity of organic matter reaching the sea bottom or an intense bacterial oxidation owing to the low sedimentation rate (4.5 m/m. y.). The organic sulphur compounds found in the extracts also suggest an intense bacterial oxidation (NERUCHEV *et al.*, 1975).

The palynological concentrate of Upper Miocene to Pleistocene samples is richer in both sporomorphs and planktonic organisms than it is the case with the Paleogene to Earlier Miocene samples, the abundance of woody particles and resinite being conspicuous *(Fig. 5)*. The predominance of the $C_{23}+$ molecules in the n-alkan spectra (Table 3) proves the importance of the land-derived components, too. All these circumstances, however, do not allow us to conclude quantitatively as to the kerogen composition.

The definite increase of the volatile C_{org}/C_{org} ratio up in the vertical section *(Fig. 3)* cannot be ascribed to a depth-controlled maturation, as the extract/C_{org} ratio in the interval in question is low (a maximum of 40 mg/g), the CPI values being higher than 2 and one of the maturation parameters does not show any correlation with depth (Table 3). Therefore it is considered doubtless that the upward growth of the volatile content of the kerogen is caused by a change in the character of the original organic matter, i. e. that the proportion of planktonic organic matter increases from the Upper Miocene up to the Pleistocene. Since the quantity of C_{org} increases in the same direction, an increase in biological production and/or the sedimentation rate must be suggested. Let us remark that in the uppermost 400 m (Upper Miocene-Pleistocene) of Hole 362 located at less than 2 nautic miles away from Hole 532 the kerogen was observed to become more and more enriched in C^{13} isotope (ERDMAN and SCHORNO, 1970). (Table 3) proceeding up the section which suggests an upward growth of the proportion of organic matter of marine origin.

According to our earlier experiences (BRUKNER and SZŰCS, 1982; BRUKNER, unpublished data) the absorption observed at 960 cm^{-1} in the IR spectra of the extracts suggests an very oxygen-depleted environments of sedimentation and a still immature organic matter.

The high C_{org} content, the marine character of the organic matter and the oxygen-depleted environment can be attributed to a very high plankton production due to upwelling. These results and conclusions are in good accordance with the opinion suggesting that the Benguela upwelling in the vicinity of Walwis Ridge evolved in Late Miocene time (HAY, SIBUET *et al.*, 1982).

HYDROCARBON POTENTIAL

The C_{org} content of the Paleogene to Early Miocene sequence is too low to consider it as a potential source rock. According to the colour of the palynomorphs and their preservation state, the kerogen is immature. The comparatively high extract (C_{org} ratio) does not contradict this, since this is generally the case at a low C_{org} content (the so-called VASSOEVICH—USPENSKI rule known from the Russian-language literature). The significant extract content observed in the sample 37/3 of Hole 530 A may be considered a migration trace, the IR spectrum providing no ground for suspecting a contamination.

The average C_{org} content of the Upper Miocene to Pleistocene sequence is over 1%, i. e. the sediments may be regarded as good source rocks. Its kerogen seems to oil-prone. Judging by the colour and preservation state of the palynomorphs and the immature character of the extracts, the oil generation has not started yet in the sequence.

ACKNOWLEDGEMENTS

We wish to thank BERND R. T. SIMONEIT for giving us the possibility to work on the Leg 75 samples. The analytical assistance of I. FABÓK and K. PIRINGER is highly appreciated.

REFERENCES

BRUKNER, A., SZŰCS, I. (1982): Bitumen contents of the fish-scale clay-marl in the Mecsek Mountains, S Hungary (in Hungarian). Annual Report of the Hungarian Geological Institute of 1980, 487—500

ERDMAN, J. G., SCHORNO, K. S. (1978): Geochemistry of carbon: Deep Sea Drilling Project Leg 40 DSDP. In: Rep. Supplement to **XXXVIII—XLI**, 651—658.

HAY, W. W., SIBUET, J. C., E. J. BARRON, R. E. BOYCE, S. BRASSELL, W. E. DEAN, A. Y. HUC, B. H. KEATING, C. L. MCNULTY, P. A. MEYERS, M. NOHARA, R. E. SCHALLREUTER, J. C. STEINMETZ, D. STOW and H. STRADNER (1982): Sedimentation and accumulation of organic carbon in the Angola Basin and Walwis Ridge: Preliminary results of Deep Sea Drilling Project Leg. 75. Geol. Soc. Amer. Bull., **93**, 10, 1038—1050.

MAXIMOV S. P., T. A. BOTNEVA, M. K. KALINKO, YE. S. LARSKAYA, K. F. RODIONOVA and O. P. CHETVERIKOVA (1975): Facial-genetic types of dispersed organic matter, their chemical and physical characteristic. Adv. in Org. Geoch. (Eds R. CAMPOS, and J. GONI). Enadisma, Madrid, 487—491.

NERUCHEV S. G., G. M. PARPAROVA, E. A. ROGOZINA, S. S. FILATOV, S. N. BELECKAJA, A. V. ZSUKOVA, E. M. FAJZULINA, I. A. SAKSZ, I. A. ZELICSENKO, L. S. BELJAJEVA, A. I. SAPIRO, G. M. SIROVA and U. M. SUMENKOVA (1974): A new classification of the diagenetic and catagenetic alteration of planktonogenic (sapropelic) dispersed organic matter (in Russian). In: Study of Organic Matter. (Ed. by VASSOEVICH, N. B.), Nauka, Moscow, 81—106.

POWELL, T. G., L. R. SNOWDON, S. CREANEY (1981): Intercorrelation of organic geochemical and organic petrographic data. Lecture to be presented at Symposium on Organic Geochemical Correlation. GSA Meeting, 4th November, San Diego.

Manuscript received, March 22, 1984

Acta Mineralogica-Petrographica, Szeged, XXVII, 185—192, 1985

GEOLOGICAL IMPORTANCE OF SOME CHEMICAL FEATURES OF COALS IN HUNGARY

Á. JÁMBOR[1] and GY. WOLF[2]

ABSTRACT

Geochemical characteristics of sedimentary rocks, including coals and especially those of their ashes and detrital rocks, respectively, are primarily determined by geological setting of the denudation area. Significant influencing factors are supposedly the weathering factors, especially the climate. It seems to be possible to approach the question of climate by analysing the modulus of coal ashes.

INTRODUCTION

During the investigation of distribution of major elements of variegated clays from the Transdanubian Central Mountains (JÁMBOR *et al.*, 1968) it was evidenced that the modulus of the clayey rocks shows comparatively significant variation in different eras of the Earth's history. As far as both pelitic and variegated clayey rocks were concerned the significant role of climatic differences was thought of as possible cause of differences.

The collection and publication of data concerning coal beds being mined regularly in Hungary (KOVATSITS and WOLF, 1980) provided the possibility for further consideration. Data in this publication cited contain three-month averages of the daily collected quality control data for the different mining products. From this publication mainly data, concerning ash content were used furthermore the geological relations of total water and organic carbon content of coals were also studied. As a first step of data processing the analytical data from the 25 plants operating in the country, arranged into 7 groups according to geological age (Table 1) were averaged (Table 2). For better understanding both Table 1 and Table 2 include these data.

DISCUSSION

Modulus

The modulus (Al_2O_3/SiO_2) is a value used mainly in the evaluation of bauxites and it is dependent on the quantitative and qualitative relation of allitic and siallitic components in bauxites. In clayey rocks containing allitic components this value is

[1] Hungarian Geological Survey
H-1442 Budapest, Népstadion út 14, P. O. Box 106, Hungary
[2] Central Institute of Mining Development
H-1027 Budapest, Varsányi I. u. 40/44, Hungary

TABLE 1

Geological age and some characteristics of mined coal deposits in Hungary

Occurrence and age	Classification	Country rocks
1. Mecsek (Liassic)	medium to high volatile bituminous	argillite, aleurolite and sandstone
2. Ajka (Upper Cretaceous)	high volatile bituminous C	clayey marl, marl
3. North Transdanubian (Eocene)	subbituminous A	clay, aleuritic limestone
4. Tokod (Oligocene)	subbituminous C	clay, aleurite
5. Nógrád and Borsod (Lower Miocene)	lignite A	clay, aleurite
6. Várpalota (Middle Miocene)	lignite B	clay, oil shale
7. Mátraalja (Pliocene)	lignite B	clay, aleurite, sand

over 1.0, in average clayey rocks from 0.2 to 0.5 but can reach the value of 1.0, which is over the value for pure kaolinite (0.85). It means that the modulus is connected with the chemical composition of claystones as well and, being related to the progress of diagenesis, it is significantly influenced by the intensity of burial, namely diagenesis tends to continually reduce the modulus in an extent unknown at present, since in great depth of 2000 to 3000 meters rocks contain only illites and chlorites of hardly known chemical composition, the modulus of which is lower than that of kaolinite. Naturally, in determining of modulus of a claystone besides clay minerals other mineral components, first of all the quantity of quartz and feldspar grains in the silty fraction are also important. Their ratio, however, is influenced by the climate just like that of clay minerals. Warmer and more humid climate results in the increase of the modulus.

It is evident that the modulus of claystones can not be considered as a measure for the definition of warm and humid climates but it may give a good point of orientation besides palaeontological data.

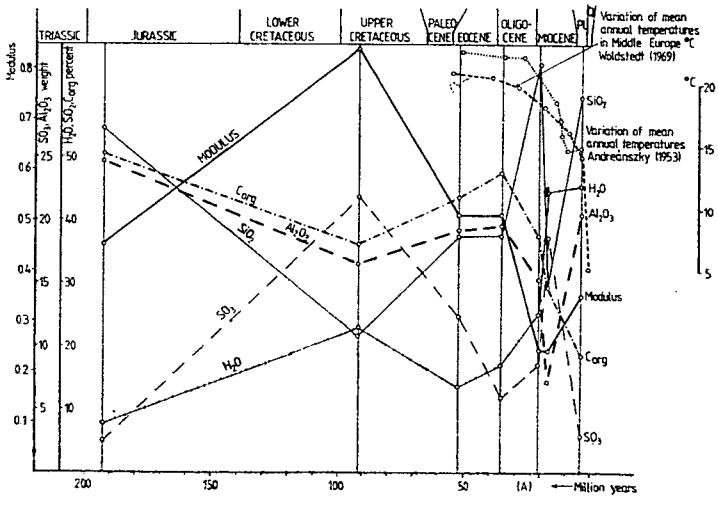

Fig. 1. Variation of averages of some chemical components in coals mined in Hungary

TABLE 2

Some components (in average) of Hungarian coals and their ashes

	SiO_2	Al_2O_3	Fe_2O_3	CaO	MgO	K_2O	Na_2O	SO_3	Total H_2O	Modulus	K_2O/Na_2O	CaO/MgO	C_{org}
1. Liassic	54.5	24.7	10.6	1.7	1.1	3.1	0.4	2.5	7.8	0.45	7.8	1.5	50.1
2. Upper Cretaceous	19.7	16.5	8.9	28.5	3.4	0.3	0.3	21.7	22.8	0.84	1.0	8.4	36.0
3. Eocene	37.8	19.1	9.2	11.8	3.5	1.1	1.6	12.3	13.9	0.51	0.7	3.4	43.8
4. Oligocene	37.9	19.6	20.6	7.0	4.3	1.4	3.0	6.0	15.1	0.51	0.46	1.6	47.6
5. Lower Miocene	64.3	15.2	10.5	8.8	2.3	1.4	1.2	8.7	25.0	0.24	1.2	3.8	37.5
6. Middle Miocene	29.5	7.1	7.7	28.9	4.4	1.6	0.8	18.7	44.1	0.24	2.0	6.6	29.0
7. Pliocene	59.3	20.5	6.4	4.8	2.0	0.9	0.2	2.9	45.3	0.35	4.5	2.2	18.4

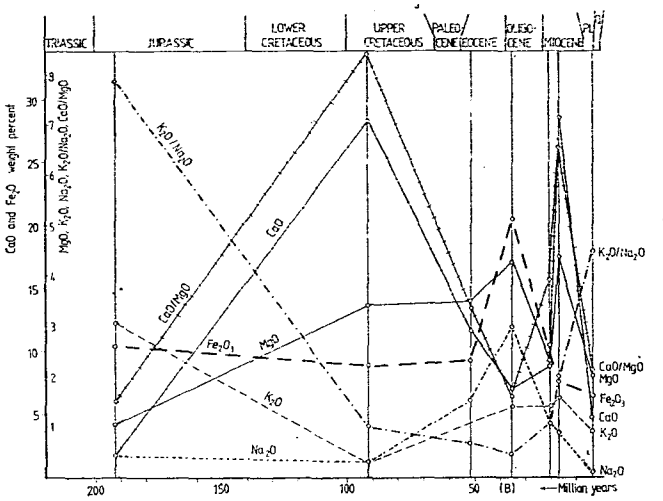

Fig. 2. Variation of averages of some chemical components in coals mined in Hungary

The modulus of Hungarian Upper Cretaceous coals is extremely high (0.84). It is in close concordance with the data from palynological analyses (GÓCZÁN, 1972). These show that climate in the Upper Cretaceous was tropical warm and humid but still insufficient for the formation of bauxites. The modulus is sharply decreasing from the Upper Cretaceous to the Badenian. The value for Liassic coal ashes is slightly lower than that for Eocene and Oligocene coals, whereas the modulus of Pliocene (Upper Pannonian) lignite is again higher. Decrease from the Upper Cretaceous to the Middle Miocene is interpreted as evidence of decrease in temperature. The modulus of Eocene and Oligocene coals is similar although in the Oligocene

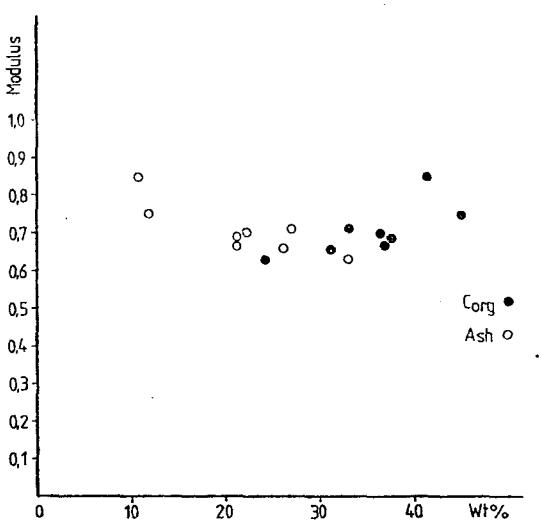

Fig. 3. Relation of modulus — ash and modulus — C_{org} in Upper Cretaceous coals

a cooler climate was unambigously evidenced. This similarity can be explained by the more humid climate in the Oligocene.

The decrease of modulus in the Liassic can be interpreted by a more disadvantageous climate on one hand and an advanced stage of the diagenesis on the other (Table 1). Increase of the modulus in the Pliocene can be regarded as sign of a lower degree of diagenesis as compared to that in the Miocene.

Chemical composition of ashes of the mining products depends on two components. These are on one hand inorganic components taken up from the soil by the plants and incorporated in their body and preserved during the process of coalification and embedding rocks inevitably entering the product during mining and processing as well as the nature of embedded rock fragments on the other.

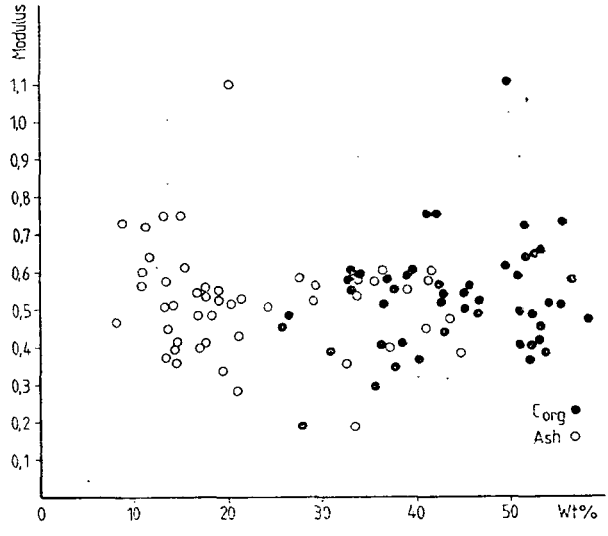

Fig. 4. Relation of modulus — ash and modulus — C_{org} in Eocene coals

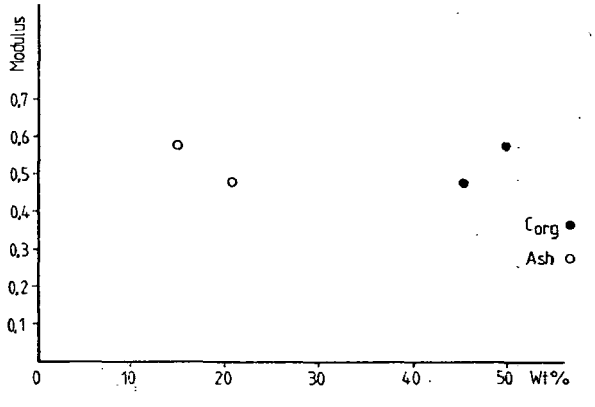

Fig. 5. Relation of modulus — ash and modulus — C_{org} in Oligocene coals

Using the possibility of analyses it was investigated whether the coal-rich products or products containing less coal have higher modulus and whether there is a difference between the modulus of coal ashes and that of barren rocks. *Figs 3* to *6* unambiguously show that finer coal products are cleaner. At the same time their modulus in Upper Cretaceous, Lower Eocene, Oligocene and Lower Miocene coals is in most cases higher. Thus the material taken up and incorporated by the plants evidences higher temperature, a more humid climate than do the bedrocks.

Naturally, SiO_2 and Al_2O_3 content of coal ashes unequivocally evidences the changes in the denudation area. From the Liassic to the Oligocene both factors are of similar quantity. In the Lower Miocene a large gap was formed between the two factors in favour of SiO_2. The situation remained the same in the course of the history of Earth in accordance with palaeogeographic facts.

Sulphur content

Sulphur content of the coal-ashes, as it is known since long time, depends on the abundance of carbonate rocks on the denudation area. This is unequivocally proved by the variation of sulphur content in Hungarian coals of different geological age. Liassic coals from the Mecsek Mountains contain the least sulphur. It proves that although a theoretical possibility of an outcrop of Middle Triassic carbonate com-

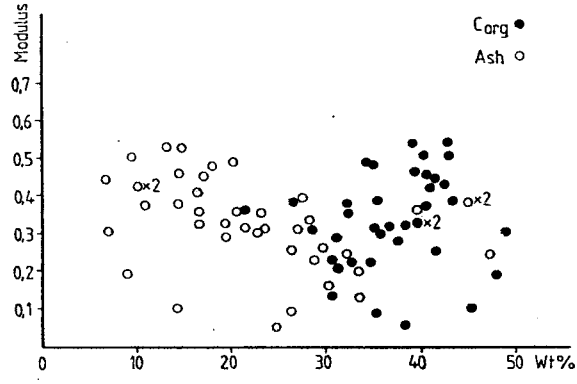

Fig. 6. Relation of modulus — ash and modulus — C_{org} in Lower Miocene coals

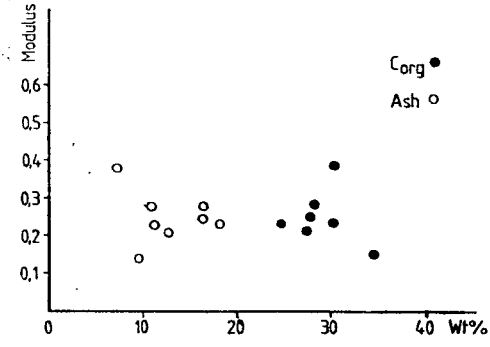

Fig. 7. Relation of modulus — ash and modulus — C_{org} in Middle Miocene coals

plexes existed in the SW foreland of the Mecsek Mountains (NAGY, 1962), the chemistry of coals indicates that the denudation area was absolutely free from carbonate rocks.

The high sulphur content of the Upper Cretaceous coal beds of Bakony, Ajka is in close relation with the well known palaeogeographical picture (HAAS, 1979), namely that carbonate rocks played an important or determinative role in the denudation area. Transgression over the Mesozoic limestone-dolomite mass of the Transdanubian Central Mountains is well perceivable even in the course of the transgression in the Lower Eocene. At the beginning of the Oligocene there are hardly any carbonate masses on the surface, most part of the Transdanubian Central Mountains became sedimentary area again. Here, sulphur content is again in concordance with the knowledge obtained in the course of the thorough complex analysis (KORPÁS, 1981). These facts are important, since part of the specialists repeatedly arrived at different conclusions from the present picture of a block mountain.

The medium sulphur content of the Upper Miocene coals of North Hungary and the high sulphur content of the Middle Miocene coal seams of Várpalota is also in close concordance with the palaeogeographical facts (HÁMOR, 1981). In the surroundings of the Lower Miocene beds there were only few carbonate rocks on the denudation area. On the contrary the Middle Miocene coal swamp of Várpalota was surrounded by hills consisting of carbonate rocks.

Sulphur content of the Pliocene coal beds verifies that the denudation area was almost totally free of carbonate rocks, a fact evident from the known palaeogeographical summaries (BALÁZS *et al.*, 1981).

With a little boldness, on the basis of the close agreement of data it can be declared that from the sulphur content of the coals numerical data can be obtained concerning the role of the carbonate rocks in the denudation area.

CaO content of coal ashes, naturally, varies in close connection with the carbonate surroundings, consequently, also with the sulphur content, although no mineralogical connection exists between them. Calcium appears mainly in form of carbonates and sulphur is mainly found as pyrite.

MgO content is higher in carstic coals than in coals of non-carstic origin but whilst CaO dominates in carstic ones it never does in the case of non-carstic coals (Liassic, Oligocene, Lower Miocene, Pliocene). CaO/MgO ratio is in accordance with this, although there is some discrepancy in the Lower Miocene deposits.

Other inert components

The amount of total iron as Fe_2O_3, K_2O and Na_2O can be interpreted only with greater difficulty. Iron content is relatively stable ranging between 6 and 10 per cent. Disregarding the iron content (21 per cent) in the Oligocene beds, it shows a slightly decreasing tendency in the course of the Earth's history and a relatively close correlation with the Na_2O content can be established.

The geohistorical background of both the correlation of the two components and the anomalous values in the Oligocene beds is not known at present.

Variation of K_2O content can also be contradictory interpreted. Although the highest value in Liassic formations is in close connection with the potassium abundance in the granitic denudation areas. Minimum in the Upper Cretaceous and increasing K_2O values in the Eocene and Oligocene show that this value is low in coals of carstic type but the relatively high values in the Middle Miocene and low values in Pliocene are contradictory.

High K_2O/Na_2O ratio in the majority of cases indicates beds of carstic type well, but this ratio is contradictory in the Oligocene and Middle Miocene beds.

Water and organic carbon

Comparison of water and organic carbon (C_{org}) content in coals untangles a close reverse correlation. Both factors depend on the extent of epigenesis, *i. e.* on the progress of the coalification. The high water and low C_{org} content of the Upper Cretaceous coals is noteworthy. It proves the low epigenetic stage of the Upper Cretaceous beds which is the result of the thin cover, formed over them in the Tertiary. Unlike the above cases this provides data for palaeogeographic investigation since it evidences that the Upper Cretaceous deposits of Ajka and Padragkút were only covered by thin sedimentary layers in the course of the Paleogene as well as the Neogene time. Higher grade of coalification of the coals from Eocene beds can be explained by the fact that coals of Dorog, Tatabánya and Felsőgalla are mined in greater depth. Lower coalification of coals from the mines in Oroszlány and Dudar-Balinka definitely indicates a thinner Oligocene/Neogene cover.

Higher coalification of Oligocene coals revealed in their C_{org} content as compared to Eocene ones is only apparent. Low C_{org} content of the Eocene coal products is the result of pollution occurring in the mining technology, a less frequent problem in Oligocene deposits, containing less barren embeddings.

Water content of coals continuously increased from 12 per cent in the Eocene to 46 per cent in the Pliocene. It seems that the total water content of the coals in this early stage of the epigenesis, namely in the upper gas zone, just like the free water content of clay minerals (HALMAI *et al.*, 1982) is a more sensible indicator of coalification than the vitrinite reflexion which changes here only between 0.2 and 0.5.

REFERENCES

ANDREÁNSZKY, G. (1953): Paleobotany. Akadémia Kiadó, Budapest, pp 320.

BALÁZS, E. *et al.* (1981): Molasse formations in Hungary. Special publication of the Hungarian Geological Survey, pp 179.

GÓCZÁN, F. (1972): Comparative palynology and the paleoclimate of bauxite formation — Hungary. In: Unesco Ref. Coll. 1971 in the fields of Stratigraphy and Micropaleontology, Final Report. — Jahrb. Geol. B. A. (1972) Sonderband **19**, pp 36—37.

GÓCZÁN, F. (1973): Oberkretazische Kohlenbildung in Ungarn im Lichte de Palynologie. In: Proc. III. Internat. Palynological Conf., Moscow, pp 28—35.

HAAS, J. (1979): Upper Cretaceous Ugod Limestone Formation in the Bakony Mountains. In: Annales of the Hungarian Geological Institute No. **61**, pp 148.

JÁMBOR, Á. and KORPÁS, L. (1968): Stratigraphic analysis of Upper Oligocene-Neogene varicoloured clay formations in the Bakony Mountains. Data base ot the Hungarian Geological Institute. (Manuscript)

KORPÁS, L. (1981): Oligocene — Lower Miocene formations in the Transdanubian Central Range. Annales of the Hungarian Geological Institute No. **64**, pp 140.

KOVATSITS, M. and GY. WOLF, (1980): Quality register of the Hungarian commercial coal products. KBFI — MSZT. Budapest—Tatabánya, pp 449.

NAGY, E. (1962): Geological re-analysis of the Pécs Lower Liassic Coal Complex. Data base of the Hungarian Geological Institute.

ÓDOR, L. (1969): Report on the geochemical analyses of the Eocene brown coal complex in Balinka II territory. In: Annual Report of the Hungarian Geological Institute (1967), pp 315—343.

SZÁDECZKY-KARDOSS, E. (1952): Lithology of Coals. Akadémiai Kiadó, Budapest.

HALMAI, J. *et al.*, (1982): Geological results from the borehole Tengelic 2. Annales of the Hungarian Geological Institute No. **65**, pp 325.

Manuscript received, June 14, 1984

Acta Mineralogica-Petrographica, Szeged, XXVII, 193—212, 1985

THE SILURIAN AND DEVONIAN IN THE SURROUNDINGS OF NEKÉZSENY (SOUTHERNMOST UPPONY MTS, NORTHERN HUNGARY)

K. BALOGH* and H. KOZUR

ABSTRACT

The athrogenic and volcanic sequence (Strázsahegy Formation) of the Strázsa-hegy section; at first regarded as Middle Triassic and later assumed to be Lower Devonian (Lochkovian), could be placed into the Middle Devonian. From olistolites within the tuffitic parts of this formation a complete highly fossiliferous Silurian sequence (similar to the Silurian of the Cellon section in the Carnic Alps, and consisting mainly of pelagic micritic limestones, among these also nautiloid limestones) could be reconstructed. The geological evolution of the Uppony Mts from the Upper Ordovician up to the Bashkirian (Middle Carboniferous) is briefly discussed (*Fig. 1 and 2*).

INTRODUCTION

In northern Hungary ORAVECZ, J. (1965) reported a black chert pebble with a *Radiolarian* cross-section in the Gosau conglomerate of Nekézseny as belonging to Silurian. But this spumellarian *Radiolaria* is specifically undeterminable. The first *Silurian conodonts* of northern Hungary were found by KOZUR, H. (in press *a, c*) in lydite pebbles of the Upper Carboniferous Taróf conglomerate of the borehole Nagybátony—324 (NW of Mátra Mts) and of Felsőszőlőköve in the Bükk Mts. But the richest conodont faunas could be found *in the Strázsa-hegy section at Nekézseny* (southernmost Uppony Mts). They are very well preserved (even conodont apparatuses are present) and they belong to the richest Silurian conodont faunas in Middle Europe. *Almost all Silurian conodont zones are present, indicated mostly by their index species.*

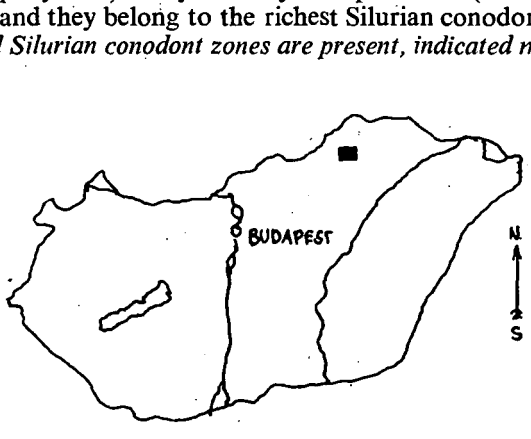

Fig. 1. Location sketch of the Uppony Mts.

* *Hungarian Geological Survey,*
1H-442 Budapest, Népstadion út 14, P. O. Box 106, Hungary

The Strázsa-hegy section yielded also Lochkovian (deeper part of Lower Devonian) conodonts, for the first time reported by KOVÁCS, S. (1981) on the basis of one conodont-bearing sample of the investigated 6 ones. Now rich Lochkovian and more rarely also Pragian, Emsian and Eifelian conodont and ostracod faunas could be found. *The Jőcsös-völgy section* (about 1 km W of the the Strázsa-hegy) yielded Pragian to Lower Eifelian conodonts. One sample (not in situ) yielded also Lochkovian conodonts.

GEOLOGICAL SETTING

The Uppony Mts with its SSE-dipping Paleozoic beds play an important role in the tectonics of northern Hungary. It is regarded as the tectonically separated, slightly metamorphic, stratigraphically downward continuation of the southeastward following Fennsík-nappe of the Bükk Mts with its southalpine—dinaric Middle Carboniferous to Upper Triassic (? and Jurassic) sequence.

Because of scarcity or lack of macrofossils and bad exposures, formerly only hypothesis existed about the precise age of the Uppony Paleozoic. According to SCHRÉTER, Z. (1945, 1960), PANTÓ, G. (1954) and BALOGH, K. (1964) the small Uppony block, surrounded mostly by Neogene deposits, has been assumed to have a more or less continous sequence, beginning in the NW with Devonian (or Tournaisian) deposits and ending in the SE with Viséan ones.

Among the in this time discriminated main units, the light, massive *"Uppony Limestone,,* was placed at first into the Devonian, later into the Lower Tournaisian.

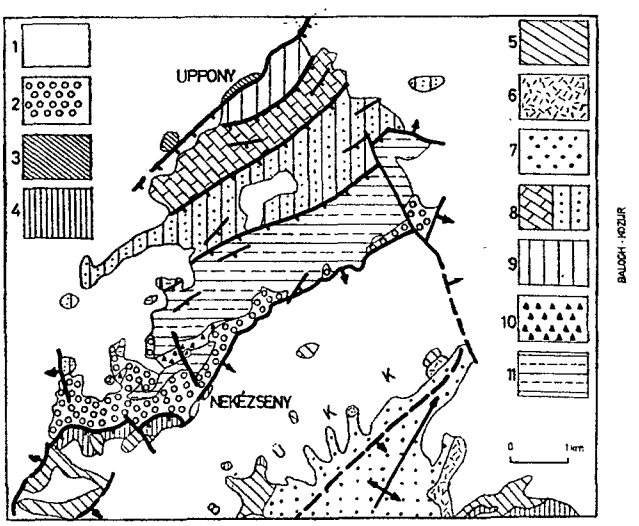

Fig. 2. Geologic sketch of the Uppony Mts.
1: Miocene. *2:* Gosau conglomerate (Senonian). — *Rudabánya Mts: 3:* Lower and Middle Trias. — *Bükk Mts.: 4:* Lower Trias. *5.* Upper Permian. *6:* Middle Permian. *7:* Middle and Upper Carboniferous. — *Uppony Mts.: 8:* "Lázbérc Formation": *a)* Upper Devonian to Tournaisian *(left). b)* Viséan to Lower Bashkirian *(right). 9:* "Uppony Limestone Formation" (partly Middle? Devonian). *10:* Strázsahegy and "Jőcsösvölgy" Formations (mainly Middle Devonian. *11:* "Tapolcsány Formation" (age undetermined).

① Strázsa-hegy section. ② Jőcsös-völgy section

The overlying>1200 m thick "*Limestone—Shale* sequence" was regarded as Upper Tournaisian. The third unit (= "*Tapolcsány Formation*") built up of grey sandstones and shales with some black cherts, manganese lenses and subordinately diabases and their tuffes, was assumed to be Viséan.

KOZUR, H.—R. MOCK (1977) found Upper Devonian conodonts in the tuffitic part of the "Limestone—Shale sequence". But another parts of this complex (now named as "Lázbérc Formation" yield Lower Carboniferous to Lower Bashkirian conodonts; thus it can be divided into two tectonic units. After KOVÁCS's personal communication also the "Uppony Limestone" (considered earlier as a coherent, unfossiliferous sequence) can be divided into several tectonic slices, one of which contains Viséan conodonts, and only the remaining light limestones may belong to the (Middle ?) Devonian.

The nearly unmetamorphic "Nekézseny Limestone" and the accompanied basic volcanics (=today *Strázsahegy Formation*) was regarded by SCHRÉTER and BALOGH as northwestward overthrusted wedges of Bükk Triassic. KOVÁCS, S. (1981) and KOVÁCS, S.—E. VETŐ-ÁKOS (1983) placed it into Lochkovian (lower part of Lower Devonian). The Strázsahegy Formation can only be found in the southernmost Uppony Mts in small wedges tectonically separated from the "*Tapolcsány Formation*". Both formations are transgressively overlain by the Senonian Gosau Conglomerate.

All the former authors regarded the various rocks of the *Strázsahegy section* as contemporaneous deposits. But new artificial outcrops show that the Strázsahegy Formation consists here of altered diabases, limy diabase tuffs (schalstein) with some small limestone and altered diabase inclusions further diabase tuffites with large amounts of limestone blocks that are — according to the here presented conodont data — all olistolites mostly considerably older than the tuffitic matrix. These olistolites are highly fossiliferous and only partly altered by hematite metasomatosis.

In the Jőcsös-völgy section a limestone wedge occurs that is to a large part metasomatically altered. This is the Jőcsösvölgy Formation by KOZUR, H. The Strázsahegy Formation of Jőcsösvölgy consists of tuffites with small limestone olistolites from the underlying Jőcsösvölgy Formation.

STRATIGRAPHICAL RESULTS

In general samples of about 1 kg were taken. Only from small olistolites samples of about 0.2—0.7 kg were solved and the weight of the ostracoda-bearing sample *Sh 19* was about 5 kg. In the Silurian often more than 500 conodonts/kg were found. In the Lower Devonian the conodont frequencies decreases to fewer than 100 specimens/kg. Only in the basal Pragian sample *Ne 4* more than 1000 specimens/kg were present, but only two species. The conodont content of the samples is listed in Table 3.

Among other (rare) microfossils mostly *ostracods* and *fish remains* were found. *Scolecodonts* (only in Přidolian). *Muellerisphaerida* (microfossils of incertae sedis, only in the Lochkovian) and *graptolite* remains (only in the Lochkovian) are extremely rare.

Both the Silurian and Lower Devonian limestones are partly rich in macrofaunas. In the Silurian above all *orthocone nautiloids, brachiopods,* more rarely *pelecypods, crinoids* and very rarely *corals* could be found. In the Lower Devonian large *crinodi stem fragments,* higher up also *corals* are frequent. *Brachiopods* and *pelecypods* are rare.

Strázsa-hegy section:

If not other data are given, the samples are olistolites from the tuffitic part of the Strázsahegy Formation.

Sample Sh 1: Brownish-red nodular nautiloid limestone (0.2 kg). *Age:* The occurrence of *Kockelella variabilis* (WALLISER) without *Polygnathoides siluricus* BRANSON et MEHL indicates the *Kockelella variabilis* zone (Lower Ludlowian).

Sample Sh 2: Pink micritic nautiloid limestone. *Age:* Upper Ludlowian *Ozarkodina crispa* zone indicated by the index species.

Samples Sh 2a, Sh 3, Sh 16, Sh 16a, Sh 18: Pink micritic limestone, in sample *Sh 16* with few nautiloids. The sample *Sh 16a* is more light-grey to almost white and it derives from the upper part of the same olistolite as for sample *Sh 16* (lower part of this olistolite). The sample *Sh 18* is more red-coloured. *Age:* Upper Ludlowian (*Ozarkodina bohemica* to *O. crispa* zones). There is no index species, but huge amounts of *Ozarkodina excavata* (BRANSON et MEHL) are present, partly together with several *Panderodus* species. This very rich occurrence and absolute dominance of *O. excavata excavata* (BRANSON et MEHL) is characteristic for the Upper Ludlowian.

Samples Sh 4: Dark grey micritic to sparitic limestone with some brachiopods and large crinoid stem fragments. *Age: Panderodus praesemicostatus* KOZUR occurs in the Upper Lochkovian and Lower Pragian. *Pandorinella frankenwaldensis* (BISCHOFF et SANNEMANN) is characteristic for the *Ancyrodelloides deltus* zone of Middle to Upper Lochkovian. Therefore an Upper Lochkovian age (deeper part of Lower Devonian) is indicated.

Sample Sh 5 (=sample 3 by KOVÁCS, S. 1981): Dark-grey micritic limestone with some crinoid stem fragments, brachiopods and pelecypods. *Ostracoda,* very rarely *graptolite fragments* and *Muellerispaerida (Armstrongisphaera upponyensis* KOZUR*)* are also present. — *Age:* Upper *Ancyrodelloides deltus* zone indicated by the joint occurrence of *A. deltus* KLAPPER et MURPHY and *A. asymmetricus* (BISCHOFF et SANNEMANN). Upper Lochkovian.

Sample Sh 6: Dark-grey to black marly crinoid-bearing limestone with greenish tuffites. *Age:* Lower *Ozarkodina sagitta* zone (*rhenana* subzone) indicated by the joint occurrence of *P. sagitta* (WALLISER) and *Dapsilodus sparsus* BARRICK that does not occur above the lower *O. sagitta* zone. Middle Wenlockian.

Sample Sh 8: Reddish, a little nodular limestone (0.5 kg). *Age:* The conodont fauna consists almost exclusively of single cone conodonts (mostly *Decoriconus* COOPER). Such faunas are typical to the Middle Wenlockian.

Sample Sh 9 (immediately above a mark *A 3*): Black to grey micritic limestone with some crinoid stem fragments. *Age: Ancyrodelloides omus* MURPHY et MATTI characterizes the lower part of the *Ancyrodelloides deltus* zone (Middle Lochkovian.)

Sample Sh 10 (3 m SE of the mark *A 3*): Light-grey limestone with single large crinoid stem fragments. *Age: Pelekysgnathus serratus serratus* JENTZSCH occurs mostly in the Pragian, but it was rarely reported also from the higher Lochkovian.

Sample Sh 11: Light grey limestone with pebbles that consist of ferruginous limestone, greenish-grey calcareous sandstone, greenish siltstone and acidic tuff. *Age: Pterospathodus pennatus pennatus* (WALLISER) from the matrix characterizes the middle to higher *Pterospathodus celloni* zone of higher Llandoverian.

Sample Sh 12: Grey limestone with reddish fissure fillings. *Age:* Lower *Ozarkodina sagitta* zone (*rhenana* subzone) indicated by the index species both of the zone and the subzone. Middle Wenlockian.

Sample Sh 13: Dark-grey limestone; *sample Sh 30:* coarsely sparitic limestone with large crinoid stem fragments. *Age: Icriodus solatericrescens—Ozarcodina*

zone *(= Ancyrodelloides deltus* zone*)* indicated by the occurrence of *Ozarcodina repetitor* (CARLS et GANDL). Middle to Upper Lochkovian.

Sample Sh 14: Inclusion in the schalstein. Coral-bearing limestone with *Multisolenia* cf. *tortuosa* FRITSCH (determined and placed into the Llandoverian by KOVALEVSKIJ and TESAKOVA). Because the Wenlockian is only represented by pelagical limestone in the Strázsa-hegy section, a Llandoverian age is tentatively assumed.

Sample Sh 15: Small inclusion of crinoidal limestone in the schalstein (0.25 kg). *Age:* Only very few badly preserved conodonts *(Ancyrodelloides* sp., *Ozarkodina cf. remscheidensis)* indicate an early Lower Devonian (Lochkovian) age.

Sample Sh 19: Yellow-brownish-grey crinoid and coral bearing sparitic limestone (5 kg). *Age:* Only ostracods. Similar strongly carinate *Kozlowskiella* species occur only in the Upper Emsian (topmost Lower Devonian) and Middle Devonian.

Sample Sh 20: Grey micritic limestone (0.4 kg). *Age: Ozarkodina remscheidensis* (ZIEGLER) indicates Lower to Middle Lochkovian.

Sample Sh 22: Dark-grey limestone, partly marly, with some juvenile pelecapods *(? Cardiola)* and brachiopods (2 kg). *Age: Polygnathus siluricus* zone (Middle Lochkovian) indicated by the index species.

Sample Sh 23: Greenish-grey micritic limestone with pink spots, slightly tuffitic (0.7 kg); *sample Sh 28:* dark, partly black, micritic, somewhat marly brachiopod-bearing limestone with some greenish tuffites. *Age: Ozarkodina excavata inflata* (WALLISER) and *O. excavata posthamata* (WALLISER) are both restricted to the upper part of the *Ancyrodella plockensis* zone. Topmost Lower Ludlowian.

Sample Sh 23a: Crinoidal limestone. *Age:* The exclusive occurrence of typical *Ozarkodina remscheidensis* (ZIEGLER) indicates Lower Lochkovian.

Sample Sh 24: Grey micritic limestone (0.6 kg). *Age:* Upper *Ozarkodina sagitta* zone (*bohemica* subzone) indicated by the occurrence of *Ozarkodina sagitta bohemica* (WALLISER). Upper Wenlockian to basal Ludlowian.

Sample Sh 25: Light-grey sparitic limestone (0.4 kg). *Age:* Only *Belodella devonica* (STAUFFER) is present, but very frequent. Tis species is long-ranging, but large amounts of the species without any other conodonts seems to indicate Lower Devonian.

Sample Sh 26: Coral-bearing limestone (0.2 kg). *Age: Ozarkodina buchanensis* (PHILIP) indicates basal Pragian.

Sample Sh 29: Light-grey micritic limestone. *Age: Ancyrodelloides asymmetricus* (BISCHOFF et SANNEMANN) indicates the upper part of *Ancyrodelloides deltus* zone. Upper Lochkovian.

Sample Sh 31: Yellow-grey micritic limestone (0,5 kg). *Age: Ozarkodina stygia* (FLAYS), morphotype δ, *O. pandora* MURPHY; MATTI et WALLISER and *Panderodus praesemicostatus* KOZUR occur in the higher *Ancyrodelloides* deltus zone and in the lower *Pedavis pesavis — Pandorinella optima* zone. Upper Lochkovian.

Sample Sh 32: Iron-bearing limestone. *Age: Belodella devonica* (STAUFFER) is moderately frequent. No other conodonts. A Lower Devonian age is probably.

Sample Sh 34: Small grey limestone inclusion in the schalstein, marginally contact metamorphically altered (0.12 kg). *Age:* The conodont association with *Polygnathus angustipennatus* BISCHOFF et ZIEGLER and *P. linguiformis* HINDE indicates the *Tortodus kockelianus* to basal *Polygnathus xylus ensensis* zone of Middle to Upper Eifelian (Middle Devonian).

Sample Sh 35: Light-grey sparitic limestone with some crinoid stem fragments (0.2 kg). *Age: Ozarkodina eosteinhornensis* zone indicated by its index species.

Sample Sh 36: Brownish-red nodular limestone (0.3 kg). *Age: Hadrognathus patulus* zone indicated by the index species. Lower Wenlockian.

Sample Sh 37: Grey limestone with large crinoidal stem fragments and some corals. *Age:* Basal Pragian indicated by *Ozarkodina buchanensis* (PHILIP) and *Belodella striata* KOZUR.

Sample Sh 28: Coral-bearing limestone. *Age:* No microfossils. The corals indicate most probably higher part of Lower to Middle Devonian.

Jőcsös-völgy section:

Sample Ne 4: Grey micritic limestone. Lower part of the non-metasomatical limestone. *Age:* Basal Pragian indicated by *Ozarkodian buchanensis* (PHILIP) and *Belodella striata* KOZUR.

Sample Ne 5: Grey sparitic crinoidal limestone, higher part of the limestone sequence. *Age: Panderodus semicostatus* TIEGLER et LINDSTRÖM indicates Upper Emsian (topmost Lower Devonian) to Lower Eifelian (basal Middle Devonian).

Sample Ne 8: Grey crinoidal limestone with large crinoid stem fragments, collected from debris. *Age:* Some *Ancyrodelloides fragments* indicate the *A. deltus* zone of Middle to Upper Lochkovian.

Sample Ne 9: Bulk sample of several very small limestone olistolites within the tuffite of the sample Ne 9a. Grey micritic limestone (0.08 kg). *Age:* Because of the small amounts of available rock only some conodonts could be founad, but the fauna with *Belodella striata* KOZUR seems to indicate basal Pragian.

Sample Ne 9a: Crinoid and coral-bearing tuffite with small olistolites. *Age:* Among corals *Heliolites* is present. This genus ends in the top of the Middle Devonian. Therefore these tuffites cannot be younger than Middle Devonian.

Sample Ne 12: Dark-grey sparitic limestone. *Age:* Basal Pragian indicated by *Ozarkodina buchanensis* (PHILIP).

Samples Ne 15—20: Reddish to brownish coral limestones and coral-algal limestones. *Age:* There are no microfossils for an exact age determination. The corals with *Heliolites* indicate higher Lower Devonian to Middle Devonian, but they had to be still investigated by coral specialists for more precise age determinations.

4. GEOLOGICAL EVOLUTION IN THE PALEOZOIC OF THE UPPONY MTS

According to the Tables 1 and 2 the oldest fossil-dated rocks belong to the *Upper Llandoverian.* This fauna derives from the matrix of a limestone olistolite with unfossiliferous pebbles (above all greenish-grey calcareous sandstone) that may represent Upper Ordovician. Also a coral limestone is tentatively assigned to the Llandoverian. The missing evidence of Lower Llandoverian olistolites may either result from the scarcity of Llandoverian olistolites or may be caused by a gap that could be indicated by the pebbles of older rocks within the Upper Llandoverian olistolite.

On the contrary to the Llandoverian *the Wenlockian* and *Ludlowian* is well documented by olistolites. These consist of red to pink, grey, greenish-grey and black, mostly micritic limestones and nautiloid limestones (the latter ones are sometimes nodular) and dark-grey to black marly limestones (Table 1). The presence of black shales, not preserved as olistolites, may be assumed from olistolites of black marly limestones to marls that could be found within the lower *O. sagitta* zone (Middle Wenlockian) and in the *O. siluricus zone* (Middle Ludlowian). The *ostracode* faunas

TABLE 1

Silurian sequence from the Strázsa-hegy at Nekézseny reconstructed from olistolites within higher Emsian to Middle Devonian tuffites. Comparison with the Silurian of the Cellon section (Carnic Alps)

Carnian Alps	Strázsa-hegy	Conodont zone	Age
Megaerella Beds (light, partly fossiliferous limestones)	Light, partly fossiliferous limestones	*Ozarkodina eosteinhornensis*	Přidolian
Alticola Limestone (grey and pink nautiloid limestones)	Grey and pink limestones and nautiloid limestones	*O. crispa*	Ludlowian
		O. snajderi	
Cardiola Beds (black limestones and shales)	Dark grey limestones ank marls	*P. siluricus*	
Kok Limestone (brownish ferruginous nodular limestone)	Greenish-grey limestones with ferruginous spots, brownish to reddisch-brownish ferruginous nodular limestone and nautiloid limestone	*K. variabilis* I / II	
		O. sagitta III / IV	Wenlockian
Trilobite and Aulacopleura Beds (alternating shales and ferruginous limestone beds)	Grey limestones with intercalations of reddish-brownish ferruginous limestones, black marly limestones	*Hadrognathus patulus*	
	* Light gray limestone with pebbles	*P. amorphognathoides*	
		P. celloni	Llandoverian
Lower Beds and Uggwa Limestone Formation	Not fossil-proven	Bereich I	Ordovician

I = *Ancoradella ploeckensis* zone; II = *Ozarkodina crassa* zone; III = *Ozarkodina sagitta bohemica* subzone; IV = *Ozarkodina sagitta rhenana* subzone

* The pebbles consist of ferruginous limestone, greenish-gray calcareous sandstone, greenish siltstone and subordinately acidic tuff.

from the Wenlockian and Ludlowian limestones indicate water depth of about 50—150 m.

A certain tectonic unrest is indicated by fissure fillings of reddish limestones in grey ones. These are typical for tensional tectonic activity or indicate block faulting. Weak synsedimentary basic volcanism can be traced in Wenlockian and Lower Ludlowian limestones by some minor greenish tuffite intercalations within the limestone olistolites.

TABLE 2

Lower and Middle Devonian sequence of the Uppon Mts

Upper Devonian		Grey, rarely reddish bedded limestones, nodular limestones, tuffs, subordinately shales
Givetian	Strázsa-hegy Formation	Diabases and schalstein with limestone inclusions; Tuff, tuffite with limestone olistolites; Uppony Limestone Formation: massive, light reef limestone; Light to dark grey limestone
Eifelian		
Emsian		
Siegenian	Pragian	Jőcsös-völgy Formation: Grey to yellowish coral-bearing and crinoidal limestones
Gedinnian	Lochkovian	Light to dark gray, mostly sparitic, partly also micritic limestone and crinoidal limestone
Silurian		

In the highest Silurian *(Přidolian)* the water depth decreases and the pelagic micritic limestones are partly displaced by shallow water crinoid-brachiopod limestones. In the *Lochkovian* the geological situation is similar compared with the Přidolian, but shallow water crinoid-brachiopod limestones prevail over dark micritic limestones. No traces of volcanism could be found in the Lochkovian olistolites within the Strázsahegy Formation.

In the *Pragian* the shallowing of the depositional area continued: crinoidal and coral limestones were deposited. Only in some of these beds conodonts are still present. The *ostracods* indicate maximum water depth of about 20 m, but mostly fewer. No traces of volcanic activities.

The environmental conditions were unchanged during the *Emsian,* but for the Upper Emsian the beginning of the volcanism can not be excluded. Namely the fauna of the olistolites within the tuffitic part of the Strázsahegy Formation indicates an Upper Emsian to Middle Devonian age. Likewise in the higher Jőcsös-völgy Formation below the tuffites an *Upper Emsian* to *Lower Eifelian* conodont fauna could be found. Therefore *the tuffites cannot be older than uppermost Emsian, but most probably they belong to the Middle Devonian.*

For the schalstein and altered diabases above the tuffites and tuffs the oldest age can be more exactly determined. An inclusion within the schalstein yielded Middle to Upper Eifelian conodonts. *The schalstein and diabases have therefore most probably a*

TABLE 3

Distribution of the conodonts in the samples of Strázsa-hegy and Jőcsös-völgy near Nekézseny

Conodont species	Sh 1	Sh 2	Sh 2a	Sh 3	Sh 4	Sh 5	Sh 6	Sh 8	Sh 9	Sh 10	Sh 11	Sh 12	Sh 13	Sh 16	Sh 16a	Sh 18	Sh 19	Sh 20	Sh 22	Sh 23	Sh 23a	Sh 24	Sh 25	Sh 26	Sh 28	Sh 29	Sh 30	Sh 31	Sh 32	Sh 34	Sh 35	Sh 36	Sh 37	Ne 4	Ne 5	Ne 9	Ne 12
Ancyrodelloides asymmetricus (BISCHOFF et SANNEMANN)						+																				○										
Ancyrodelloides deltus (KLAPPER et MURPHY)						○																														
Ancyrodelloides cf. *omus* (MURPHY et MATTI)									○																											
Ancyrodelloides transitans (BISCHOFF et SANNEMANN)									○																○											
Ancyrodelloides sp. indet.						○																														
Belodella devonica (STAUFFER)		○	+	+	○			+		+		+	+		○		○	+		○			×					○	+			○	○	×		+	+
Belodella erecta (RHODES et DINELEY)					×					×																×		+								
Belodella silurica BARRICK												○								○																
Belodella striata KOZUR																																	○	+		○	
Dapsilodus obliquicostatus (BRANSON et MEHL)							+					○										○														
Dapsilodus praecipuus BARRICK											○																									
Dapsilodus sparsus BARRICK							+					○																								
Dapsilodus sp.												○																				○				
Dapsilodus sp. sensu BARRICK, 1977							○	○																												
Decoriconus fragilis (BRANSON et MEHL)							×	×				×										○										+				
Decoriconus magnistriatus KOZUR																									○											
Decoriconus sp.								×																												
Hadrognathus patulus (WALLISER)																																○				
Kockelella variabilis WALLISER	○																		+																	
Neopanderodus hungaricus KOZUR									○																											
Neopanderodus sp.																																		○		○	
Ozarkodina buchanensis (PHILIP)																							+											+			○
Ozarkodina confluens (BRANSON et MEHL)																																○					
Ozarkodina cf. *crassa* (WALLISER)																									○											
Ozarkodina crispa (WALLISER)		○																																		
Ozarkodina eosteinhornensis (WALLISER)																																○				
Ozarkodina excavata excavata (BRANSON et MEHL)	+	+	×	×				○						×	×	×			×	×					×											
Ozarkodina excavata inflata (WALLISER)																				○					○											
Ozarkodina excavata posthamata (WALLISER)																				○					○											
Ozarkodina orta WALLISER							+																													
Ozarkodina pandora MURPHY; MATTI et WALLISER						×																						+								
Ozarkodina remscheidensis (ZIEGLER)																		+			+															
Ozarkodina repetitor (CARLS et GANDL)						○			○				○													×	○	⊙								
Ozarkodina cf. *sagitta* (WALLISER)							○																													
Ozarkodina sagitta bohemica (WALLISER)																						○														
Ozarkodina sagitta rhenana (WALLISER)												○																								
Ozarkodina sagitta sagitta (WALLISER)												×																								
Ozarkodina stygia (FLAYS)																										×		○								
Ozcrkodina wurmi (BISCHOFF et SANNEMANN)																										×										
Ozarkodina cf. *wurmi* (BISCHOFF et SANNEMANN)					○																							○				○	+			
Ozarkodina sp.										+																	○									
Ozarkodina sp. indet.																									○											
Panderodus barricki KOZUR	○	×	○																○	×					○											
Panderodus gracilis (BRANSON et MEHL)		×	○	○							○	+								+												○				
Panderodus praesemicostatus KOZUR					○	○																				+		+								
Panderodus recurvatus densistriatus KOZUR											×	+													○								○				'
Panderodus recurvatus recurvatus (RHODES)	○	+															+		○	×																
Panderodus semicostatus ZIEGLER et LINDSTRÖM																																			○		
Panderodus simplex (BRANSON et MEHL)			○	○					○		+	○								+																
Panderodus spasovi DRYGANT								○				○																					○				
Panderodus unicostatus (BRANSON et MEHL)		×	+	+				○				+								+													+				
Panderodus n. sp. *A*																	○																				
Panderodus n. sp. *B*																		○																			
Panderodus n. sp. *C*																		○																			
Panderodus sp. indet.					○				○											○							○							○			
Pandorinella frankenwaldensis (BISCHOFF et SANNEMANN)						○																				○										
Pandorinella sp.										○																											
Pelekysgnathus serratus JENTZSCH										○																											
Polygnathoides emarginatus (BRANSON et MEHL)																									○											
Polygnathoides siluricus BRANSON et MEHL																			+																	
Polygnathus angustipennatus BISCHOFF et ZIEGLER																														○						
Polygnathus linguiformis linguiformis HINDE																														+						
Pseudooneotus beckmanni (BISCHOFF et SANNEMANN)						×		○	○			○						○							○			○								
Pseudooneotus tricornis DRYGANT											○																									
Pterospathodus pennatus pennatus (WALLISER)											○																									

× = very frequent; + = moderately frequent ○ = rare

Givetian (or topmost Eifelian). The upper age range could be only determined for the tuffites that contain *Heliolites* unknown above the Middle Devonian.

Thus we can say that after a quiet time in the Lower Devonian, the Middle Devonian was a time of tectonic and volcanic activity. The depositional area of the Uppony Mts was now subdivided in ridges and basins and the whole area subsided slowly. On the subsiding ridges thick pure (probably reef-) limestones of the "Uppony Limestone Formation" were deposited. In the basinal parts light to dark-grey conodont-bearing limestones, but on the slopes limestones with reef detritus settled down. The third heteropic facies in the Middle Devonian was represented by the volcanic and athrogenic Strázsahegy Formation. In connection with the Middle Devonian volcanic activity huge slide masses of Silurian and Lower Devonian limestones sliped into the basins where tuffs and tuffites were deposited nearly contemporaneously with the diabases and schalstein. — The Upper Devonian consisted of limestones, shales, tuffs and tuffites.

During the Lower Carboniferous to basal Bashkirian basinal limestones and shales settled down. The overlying Tapolcsány Formation consisting of a flyschoid sequence of shales, aleurolites, strongly pressed sandstones, siliceous shales and black cherts with ferromanganese nodules includes olistolites of Middle and Upper Devonian and Lower Carboniferous limestones in some places (e. g. at the cliff Éleskő; *Plate 7: 4)*. Also some Lower Bashkirian conodonts were found in the beds adjacent to the fossiliferous Lower Carboniferous. But for lack of sufficient determinable microfossils the exact age of the bulk of the Tapolcsány Formation is still unknown. Thus it is also possible that it shall be devided in the future into divers stratigraphic and tectonic units.

As pointed out by KOZUR, H.—R. MOCK (1977) and KOVÁCS, S.—H. KOZUR—R. MOCK (1983) no stratigraphic gaps are known in the Uppony Mts from the Middle Devonian up to the Bashkirian. So the effects of the older phases of Hercynian orogenesis could net be strong. The slightly epimetamorphic character of the Middle Devonian—Bashkirian sequence in the northern part of the mountains (ÁRKAI, P., 1983) can be explained by the existence of tectonic slices that underwent an alpine metamorphosis of different degree. *It is possible,* however, *that the tectonic slices of the almost unmetamorphic Silurian to Bashkirian at Nekézseny* (at the south margin of the Uppony Mts) *belong geologically to the Bükk Mts.* These tectonic slices were thrusted on the Uppony Mts before the deposition of the Gosau beds. The Carboniferous, Permian and Triassic sequences of the immediately southward following parts of the northern Bükk Mts are likewise only weakly affected by alpine metamorphosis.

ACKNOWLEDGEMENT

The authors thank PROF. DR. W. ZIEGLER, Frankfurt a. M. for sending literature and important data for conodont determination and biostratigraphic evaluation.

REFERENCES

ÁRKAI, P. (1983): Very low- and low-grade Alpine regional metamorphism of the Paleozoic and Mesozoic formations of the Bükkium, NE-Hungary. — Acta Geol. Hung., **26**, 83—101, Budapest

BALOGH, K. (1964): Die geologischen Bildungen des Bükk-Gebirges. — Jahrb. Ungar. Geol. Anstalt, **48**, 2. 245—719, Budapest.

BALOGH, K. and G. PANTÓ (1954): Recherches géologiques dans les environs de Nekézseny. — MÁFI évi jel. **1953,** 1, 17—27, Budapest.
ERBEN, H. K. (1962): Unterlagen zur Diskussion der Unter) Mitteldevon-Grenze. — *In:* Sympos. 2. Internat. Arbeitstag. über die Silur/Devon-Grenze und die Stratigr. von Silur und Devon, Bonn—Bruxelles, 1960, 62—70, Stuttgart.
ERBEN, H. K. and K. ZAGORA (1968): Devonian of Germany. — *In:* OSWALD, D. H. (ed.): Internat. Sympos. Devonian System, Calgary, 1967, **1,** 53—68, Calgary.
FÜLÖP, J. *et al.* (1983): Magyarország litosztratigráfiai formációi. — Budapest.
KLAPPER, G. and W. ZIEGLER (1979): Devonian conodont biostratigraphy. — *In:* The Devonian System. — Spec. Paper in Paleont., **23,** 199—224. London.
KOVÁCS, S. (1981): Lower Devonian conodonts from the Strázsa-hegy, near Nekézseny; Uppony Mts., North Hungary. — MÁFI évi jel. **1979,** 65—79, Budapest.
KOVÁCS, S., H. KOZUR and R. MOCK (1983): Relations between the Szendrő—Uppony and Bükk Paleozoic in the light of the latest micropalaeontological investigations. — MÁFI évi jel. **1981,** 155—175, Budapest.
KOVÁCS, S. and É. VETŐ-ÁKOS (1983): On the age and petrology of the basic volcanics in the Uppony Mts, NE Hungary. — MÁFI évi jel. **1981,** 177—199, Budapest.
KOZUR, H. (in press *a*): On the age and tectonical significance of the prae-Oligocene sequence of the water exploration bore hole Nagybátony 324. — Földt. Közlöny, Budapest.
KOZUR, H. (in press *b*): Fossilien aus dem Silur von Ungarn (vorläufige Mitteilung). — Proc. Geoinst., Beograd.
KOZUR, H. (in press *c*): Biostratigraphic evaluation of Upper Paleozoic conodonts, ostracods and holothurian sclerites of the Bükk Mts. Part I. Conodonts and holothurian sclerites of the Upper Moskowian and Upper Carboniferous. — Acta Geol. Hung., Budapest.
KOZUR, H. (in press *d*): *Muellerisphaerida* n. ord., eine neue Ordnung von Mikrofossilien unbekannter systematischer Stellung aus dem Silur und Devon von Ungarn. — Geol. Paläont. Mitt., Innsbruck.
KOZUR, H. and R. MOCK (1977): On the age of the Paleozoic of the Uppony Mountains (North Hungary). — Acta Miner. Petr., Szeged, **23,** 1, 91—107.
PANTÓ, G. (1954): Le levé des gîtes métalliques dans la montagne de Uppony. — MÁFI évi jel. **1952,** 91—111, Budapest.
SCHÖNLAUB, H. P. (1979): Das Paläozoikum in Österreich. — Abhandl. Geol. B.—A., **33,** 124 p. Wien.
SCHRÉTER, Z. (1945): Geologische Aufnahmen im Gebiete von Uppony, Dédes und Nekézseny, ferner im Gebiete von Putnok. — MÁFI évi jel. **1941—42,** 1, 161—237, Budapest.
SCHRÉTER, Z. (1960): Die geologischen Verhältnisse des Bükkgebirges. — Karszt- és Barlangkutatás, **1,** 7—36, Budapest.
WALLISER, O. H. (1964): Conodonten des Silurs. — Abh. hessisch. L. Anst. Bodenforsch., **41,** 106 p., Wiesbaden.
WEDDIGE, K. (1977): Die Conodonten der Eifelstufe im Typusgebiet und in benachbarten Faziesgebieten. — Senckenberg. Letaea. **58,** 4/5, 271—419, Frankfurt a. M.
ZIEGLER, W. (1979): Historical subdivision of the Devonian. — *In:* The Devonian System. — Spec. papers in Palaeontol., **23,** 23—47, London.

Manuscript received, July 31, 1984

EXPLANATION OF PLATES

Plate I

All figured conodonts are from Silurian limestone olistolites within the tuffitic part of the Middle Devonian Strázsahegy Formation. Strázsa-hegy section at Nekézseny.

1: *Panderodus simplex* (BRANSON et MEHL), conodont apparatus, lateral view, sample Sh 12, grey limestone with brownish-red fissure fillings, lower *Ozarkodina sagitta* zone *(rhenana subzone),* Middle Wenlockian, ×160, rep.-no. S 9

2: *Decoriconus fragilis* (BRANSON et MEHL), sample and age as for fig. 1, ×200, rep.-no. S 103
3: *Panderodus recurvatus densistriatus* KOZUR, obverse side, sample and age as for fig. 1, ×150, rep.-no. S 90
4; 6: *Ozarkodina sagitta sagitta* (WALLISER), sample and age as for fig. 1, ×120, *fig. 4:* rep.-no. S 14, *a)* upper view, *b)* lateral view; *fig. 6:* upper view, rep.-no. S 13
5: *Ozarkodina sagitta rhenana* (WALLISER), lateral view, sample and age as for fig. 1, ×150, rep.-no. S 108
7: *Dapsilodus obliquicostatus* (BRANSON et MEHL), sample Sh 6, dark bluish-grey to black, crinoid-bearing, micritic and marly limestone with greenish tuffitic intercalations, *Ozarkodina sagitta* zone (Wenlockian), ×160, rep.-no. S 109

Plate II

All figured conodonts are from Silurian and Lower Devonian limestone olistolites within the tuffitic part of the Middle Devonian Strázsa-hegy Formation. Strázsa-hegy section at Nekézseny.

1, 2: *Decoriconus fragilis* (BRANSON et MEHL), 2 different elements, sample Sh 6, dark bluish-grey to black crinoid-bearing micritic and marly limestone with greenish tuffitic intercalations, *Ozarkodina sagitta* zone (Wenlockian), ×200, rep.-no. S 110 (fig. 1) and S 117 (fig. 2)
3: *Polygnathoides siluricus* BRANSON et MEHL, upper view, sample Sh 22, dark grey to black, partly marly limestone, *Polygnathoides siluricus* zone (Middle Ludlowian), ×32, rep.-no. S 10
4: *Panderodus recurvatus recurvatus* (RHODES), reverse side, sample Sh 2, pink micritic nautiloid limestone, *Ozarkodina crispa* zone (Upper Ludlowian), ×100, rep.-no. S 122
: *Ozarkodina sagitta bohemica* (WALLISER), sample Sh 24, grey limestone, upper part of *Ozarkodina sagitta* zone (*bohemica* subzone), Upper Wenlockian to basal Ludlowian ×150, rep.-no. S 8
6: *Neopanderodus hungaricus* KOZUR, reverse side, sample Sh 9, grey crinoidal limestone, deeper part of *Ancyrodelloides deltus* zone (Middle Lochkovian, deeper part of Lower Devonian), ×130, rep.-no. D 509
7: *Kockelella variabilis* WALLISER, upper view, sample Sh 1, brownish-red nodular nautiloid limestone, *Kockelella variabilis* zone (Lower Ludlowian), a 150, rep.-no. S 12

Plate III

All figured conodonts are from the Strázsa-hegy section at Nekézseny.

1: *Ozarkodina confluens* (BRANSON et MEHL), sample Sh 35, olistolite of light grey, sparitic crinoid-bearing limestone, *Ozarkodina eosteinhornensis* zone (Přidolian), ×72, rep.-no. S 99
3: Carinate *Kozlowskiella* sp., Strázsa-hegy at Nekézseny, sample Sh 19, olistolite of yellow-brownish-grey crinoidal-coral limestone within the tuffitic part of the Strázsahegy Formation, ×44, rep.-no. D 539

4: *Palmatolepis* cf. *P. tenuipunctata* SANNEMANN, eastern bank of the Uppony reservoir, olistolite within the Tapolcsány Formation, Lower Famennian, ×78, rep.-no. D 544

2: *Polygnathus angustipennatus* BISCHOFF et ZIEGLER, sample Sh 34, limestone inclusion in the Middle Devonian schalstein, *Tortodus kockelianus* to basal *Polygnathus xylus ensensis* zone (Middle to Upper Eifelian), ×60, rep.-no. D 501, *a)* upper view, *b)* lateral view

3: *Ozarkodina crispa* (WALLISER), juvenile specimen, anterior part of blade broken away, sample Sh 2, olistolite of pink, micritic nautiloid limestone within the tuffitic part of the Middle Devonian Strázsahegy Formation, *Ozarkodina crispa* zone (Upper Ludlowian), ×320, rep.-no. S 119

4: *Ozarkodina excavata inflata* (WALLISER), sample Sh 23, olistolite of greenish-grey micritic limestone with pink spots, slightly tuffitic, within the tuffitic part of the Strázsahegy Formation, upper part of *Ancoradella ploeckensis* zone (topmost Lower Ludlowian), ×130, rep.-no. S 112, *a)* upper view, *b)* lateral view

5: *Dapsilodus obliquicostatus* (BRANSON et MEHL), sample Sh 24, olistolite of grey limestone within the tuffitic part of the Strázsahegy Formation, upper part of *Ozarkodina sagitta* zone (*bohemica* subzone), Upper Wenlockian to basal Ludlowian, ×100, rep.-no. S 118

Plate IV

All figured conodonts are from limestone olistolites within the tuffitic part of the Strázsahegy Formation; Strázsa-hegy section at Nekézseny.

1, 2: *Ozarkodina excavata excavata* (BRANSON et MEHL); *fig. 1:* lateral view, sample Sh 3, pink micritic limestone, Upper Ludlowian, ×100, rep.-no. S 120; *fig. 2:* lateral view a little obliquely from above, sample Sh 16, pink micritic limestone with some nautiloids, Upper Ludlowian, ×72, rep.-no. S 102

3: *Panderodus barricki* KOZUR, obverse side, sample Sh 23, greenish-grey micritic limestone with pink spots, slightly tuffitic, upper part of *Ancoradella ploeckensis* zone (topmost Lower Ludlowian), ×130, rep.-no. S 21

4, 6: *Ozarkodina remscheidensis* (ZIEGLER), sample Sh 23a, grey sparitic crinoidal limestone, Lower Lochkovian; *fig. 4:* lateral view, ×86, rep.-no. D 523; *fig. 6:* upper view, ×60, rep.-no D 524

5: *Ancyrodelloides asymmetricus* (BISCHOFF et SANNEMANN), sample Sh 29, light grey micritic limestone, upper part of *Ancyrodelloides deltus* zone (Upper Lochkovian), ×180, rep.-no. D 527, *a)* a little oblique upper view, *b)* lateral view

Plate V

All figured conodonts are from the Strázsa-hegy section at Nekézseny.

1: *Ancyrodelloides asymmetricus* (BISCHOFF et SANNEMANN), sample Sh 5, olistolite of dark grey crinoid and brachiopod-bearing limestone within the tuffitic part of the Strázsahegy Formation. Upper part of *Ancyrodelloides deltus* zone (Upper Lochkovian, rep.-no. D 526, *a)* upper view, ×48, *b)* lateral view, ×44

2: *Ozarkodina pandora* MURPHY; MATTI et WALLISER, lateral view, sample and age as for fig. 1, ×100, rep.-no. D 525

3: *Ozarkodina repetitor* (CARLS et GANDL), sample Sh 31, olistolite of yellow-grey micritic limestone within the tuffitic part of the Strázsahegy Formation, upper part of Ancyrodelloides deltus zone to lower part of *Pedavis pesavis — Pandorinella optima* zone (upper Lochkovian, ×150, rep.-no. D 533

4: *Polygnathus linguiformis linguiformis* HINDE, upper view, sample Sh 34, limestone inclusion in the schalstein, *Tortodus kockelianus* to basal *Polygnathus xylus ensensis* zone (Middle to Upper Eifelian), ×72, rep.-no. D 502

5: *Pelekysgnathus serratus serratus* JENTZSCH, lateral view, sample Sh 10, light grey limestone with few crinoid remains, olistolite within the tuffitic part of the Strázsahegy Formation. Higher Lochkovian to Pragian (deeper to middle part of Lower Devonian), ×150, rep.-no. D 541

6: *Ozarkodina stygia* (FLAYS), sample Sh 29, light grey micritic limestone, olistolite within the tuffitic part of the Strázsahegy Formation. Upper part of *Ancyrodelloides deltus* zone (Upper Lochkovian), ×200, rep.-no. D 542, *a)* lateral view, *b)* upper view

Plate VI

1, 2: *Belodella striata* KOZUR, Jőcsös-völgy near Nekézseny, sample Ne 4, grey micritic limestone, basal Pragian, *fig. 1:* denticulated element, rep.-no. D535, *á)* detail of upper part, ×480, *b)* detail of middle part, striation well visible, ×360, *c)* complete specimen, ×78; *fig. 2:* undenticulated element, striation well visible, ×150, rep.-no. D 504

Plate VII

1: *Panderodus* sp., obverse side, probably transitional form between *P. praesemicostatus* KOZUR and *P. semicostatus* ZIEGLER et LINDSTRÖM, Strázsahegy at Nekézseny, sample Sh 4, olistolite of dark grey micritic to sparitic limestone with few large crinoid stem fragments and brachiopods, probably Pragian (middle part of Lower Devonian), ×84, rep.-no. D 543

2: *Panderodus semicostatus* ZIEGLER et LINDSTRÖM, obverse side, Jőcsös-völgy near Nekézseny, sample Ne 5, grey sparitic crinoidal limestone, Upper Emsian to Lower Eifelian, rep.-no. D 522, *a)* detail from the middle part of the specimen, ×300, *b)* complete specimen, ×94

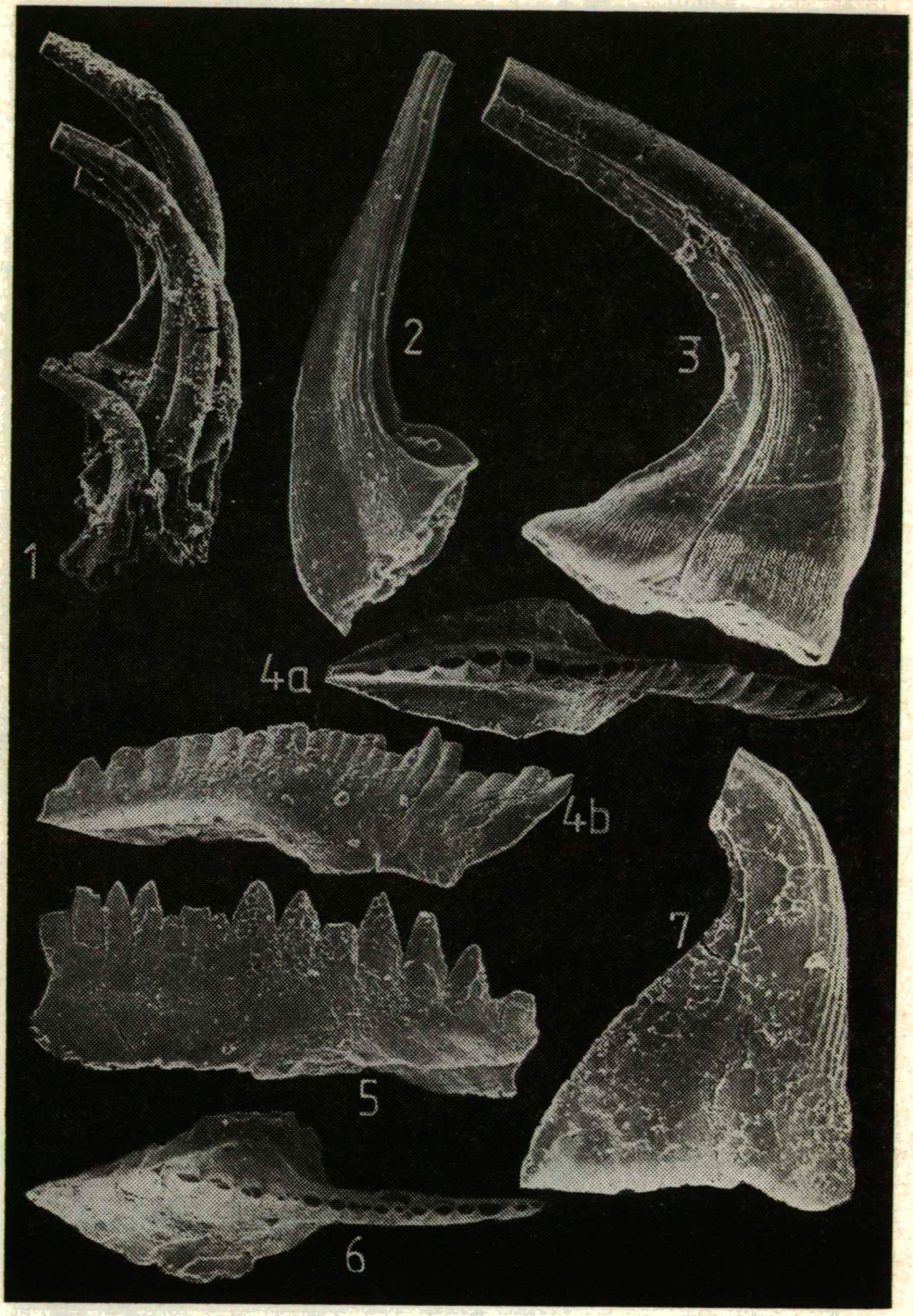
1
2
3
4a
4b
5
6
7

Plate II

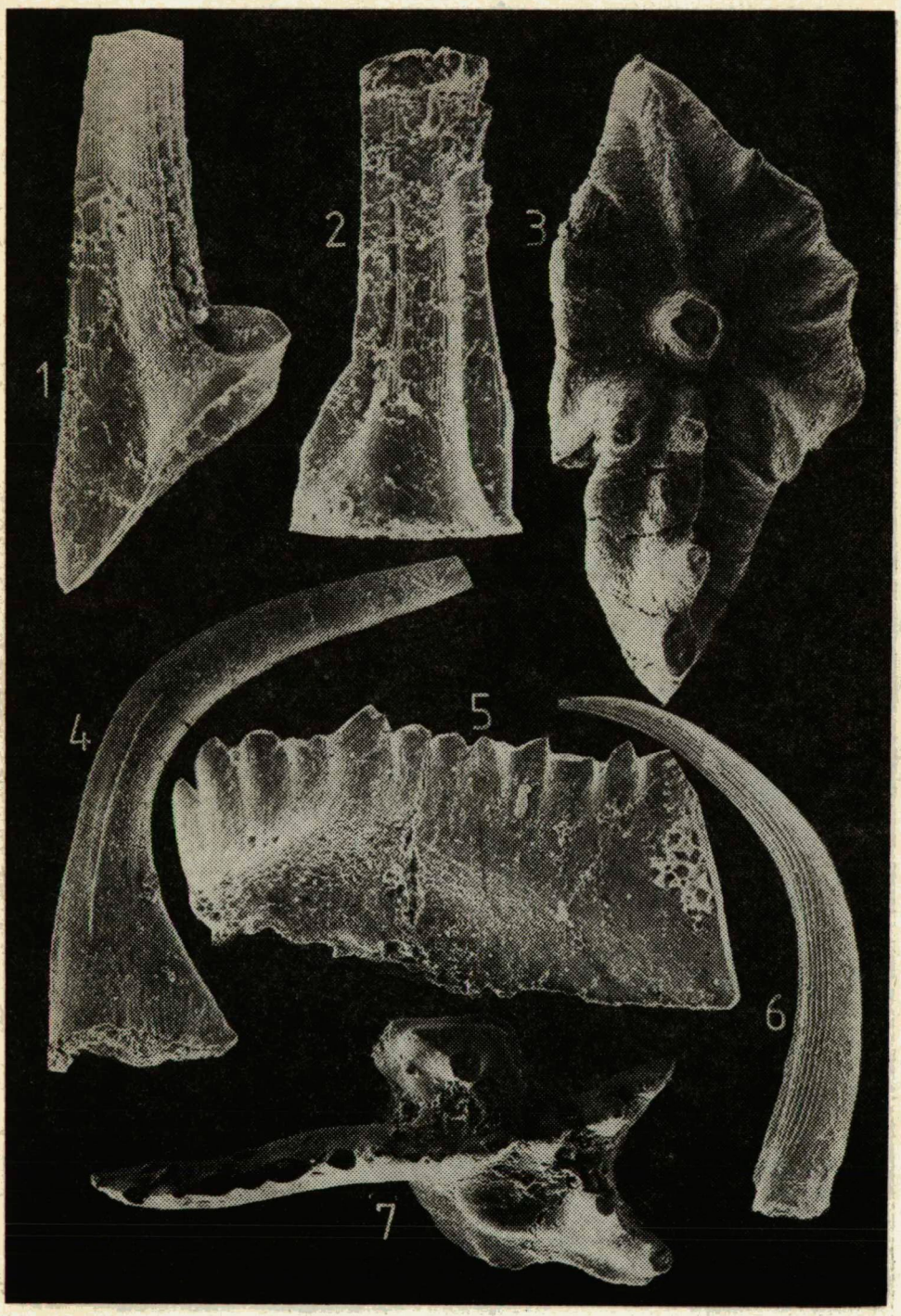

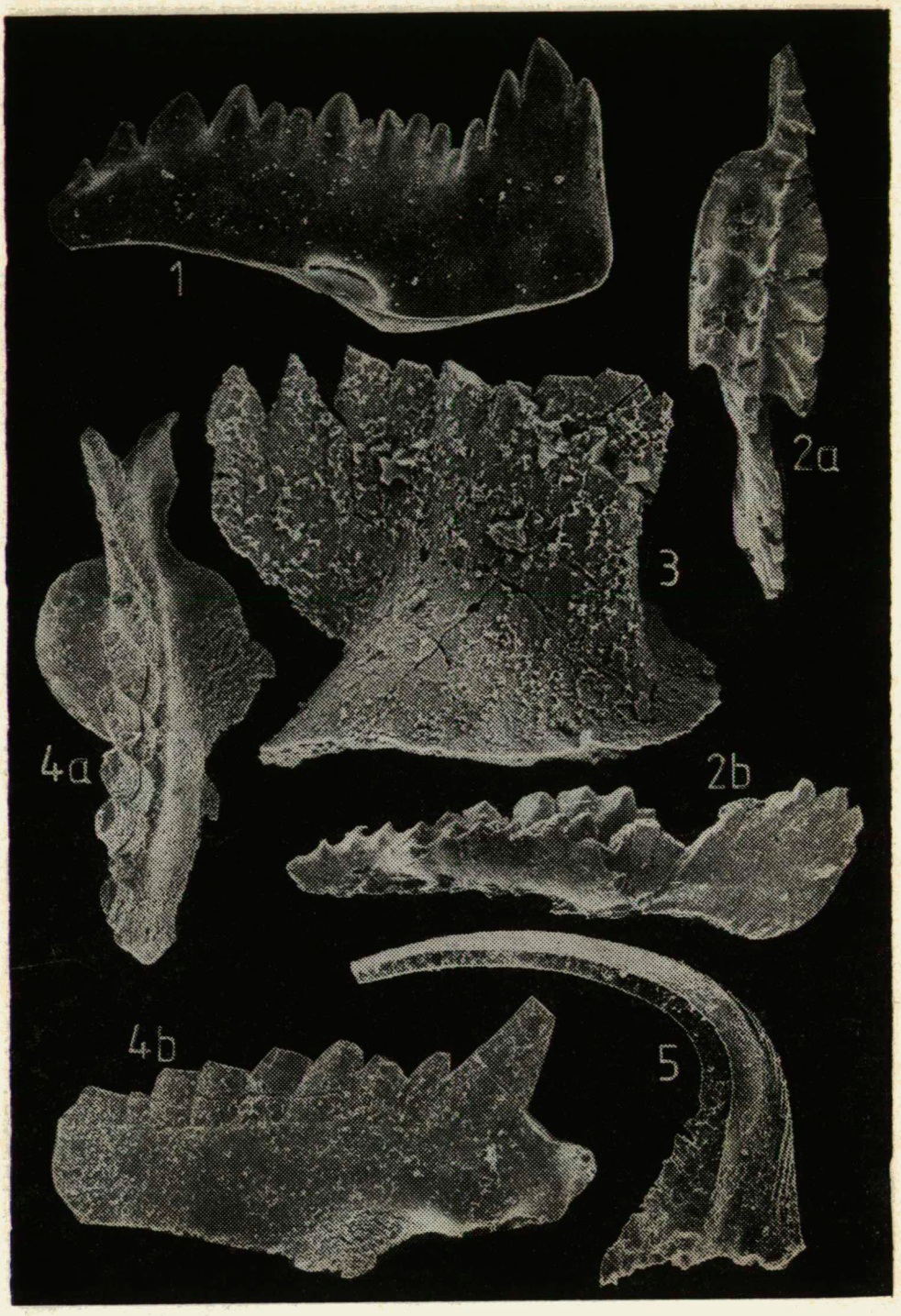
1
2a
3
4a
2b
4b
5

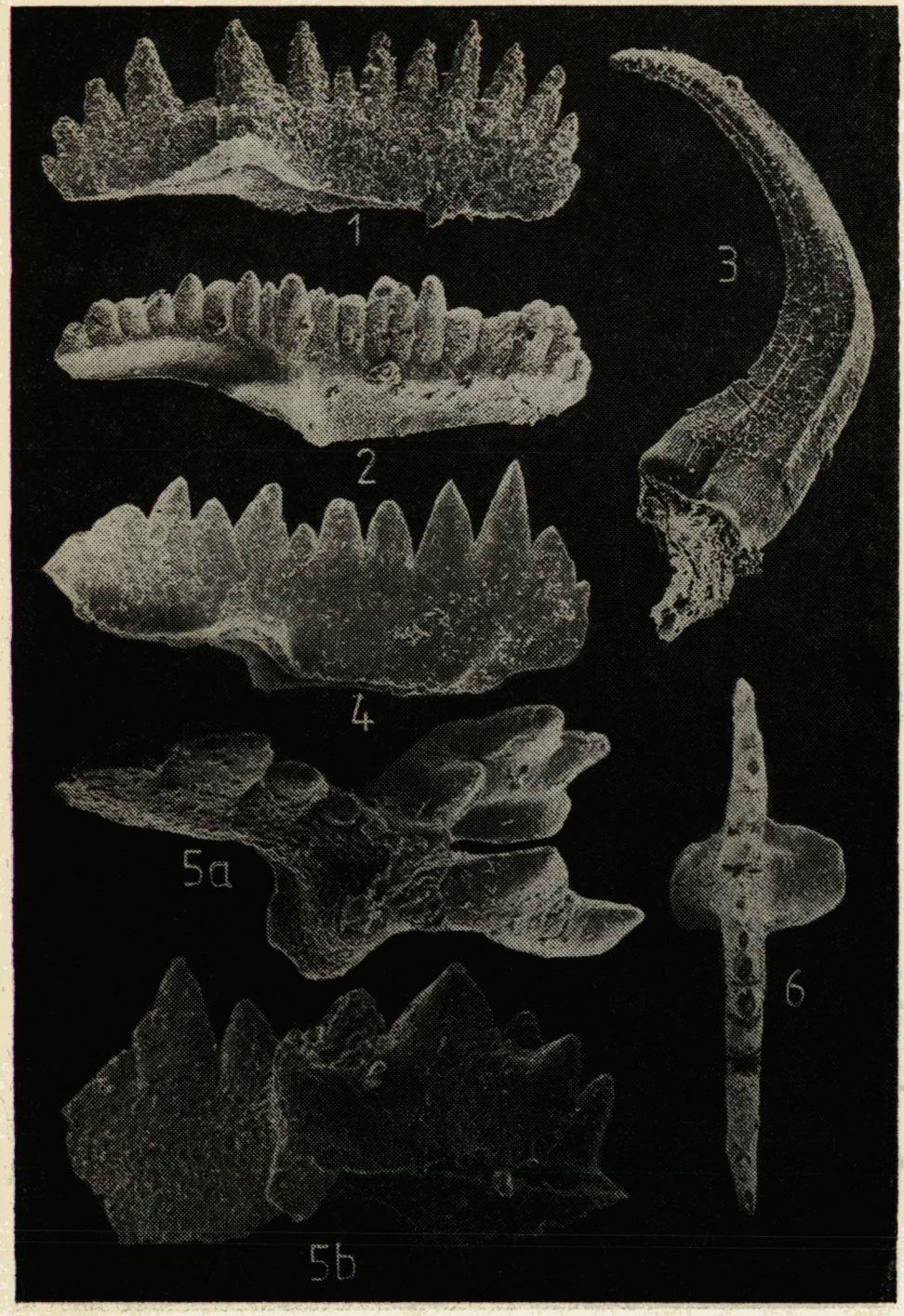
1
2
3
4
5a
5b
6

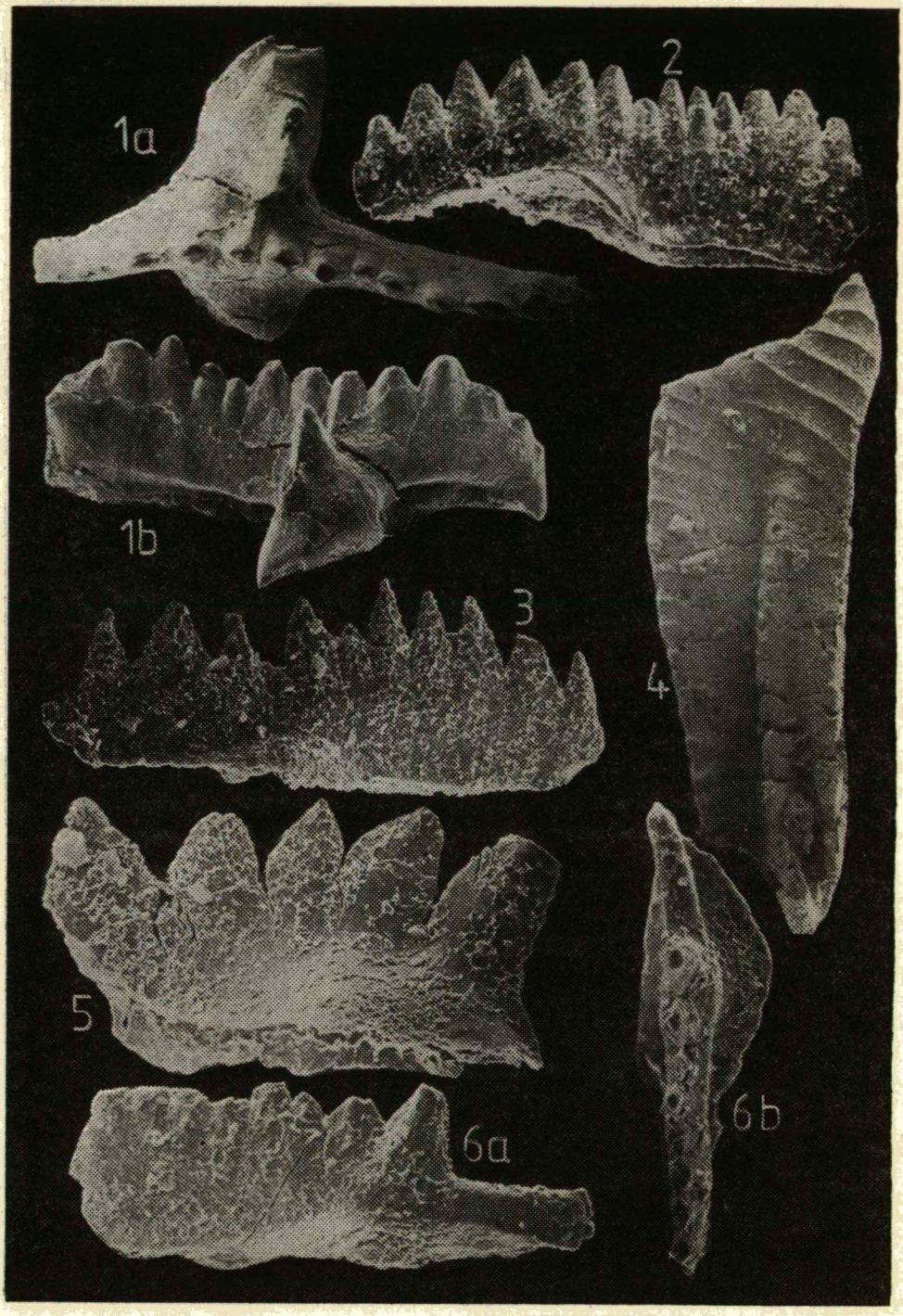
1a
2
1b
3
4
5
6a
6b

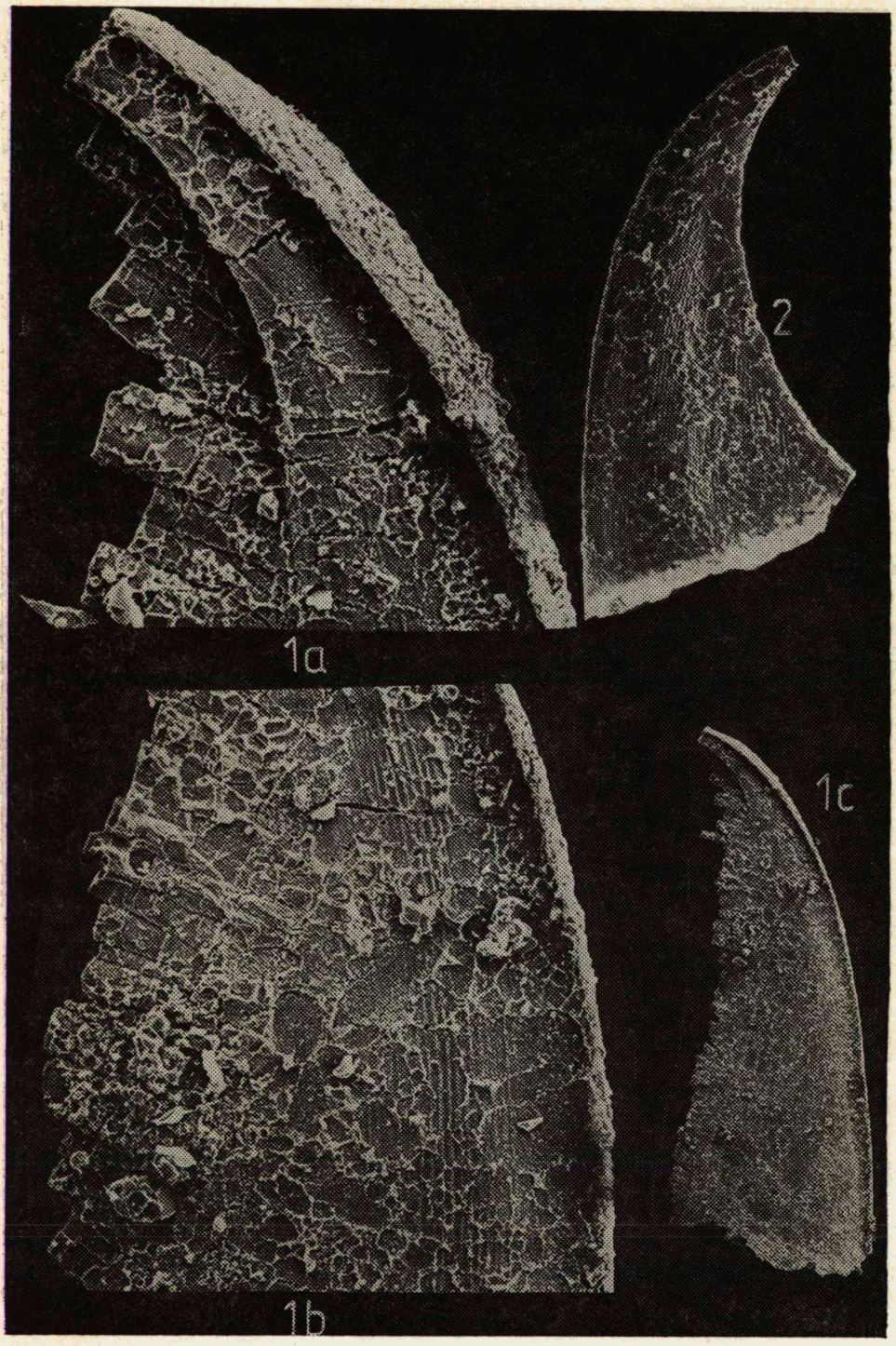
2
1a
1c
1b

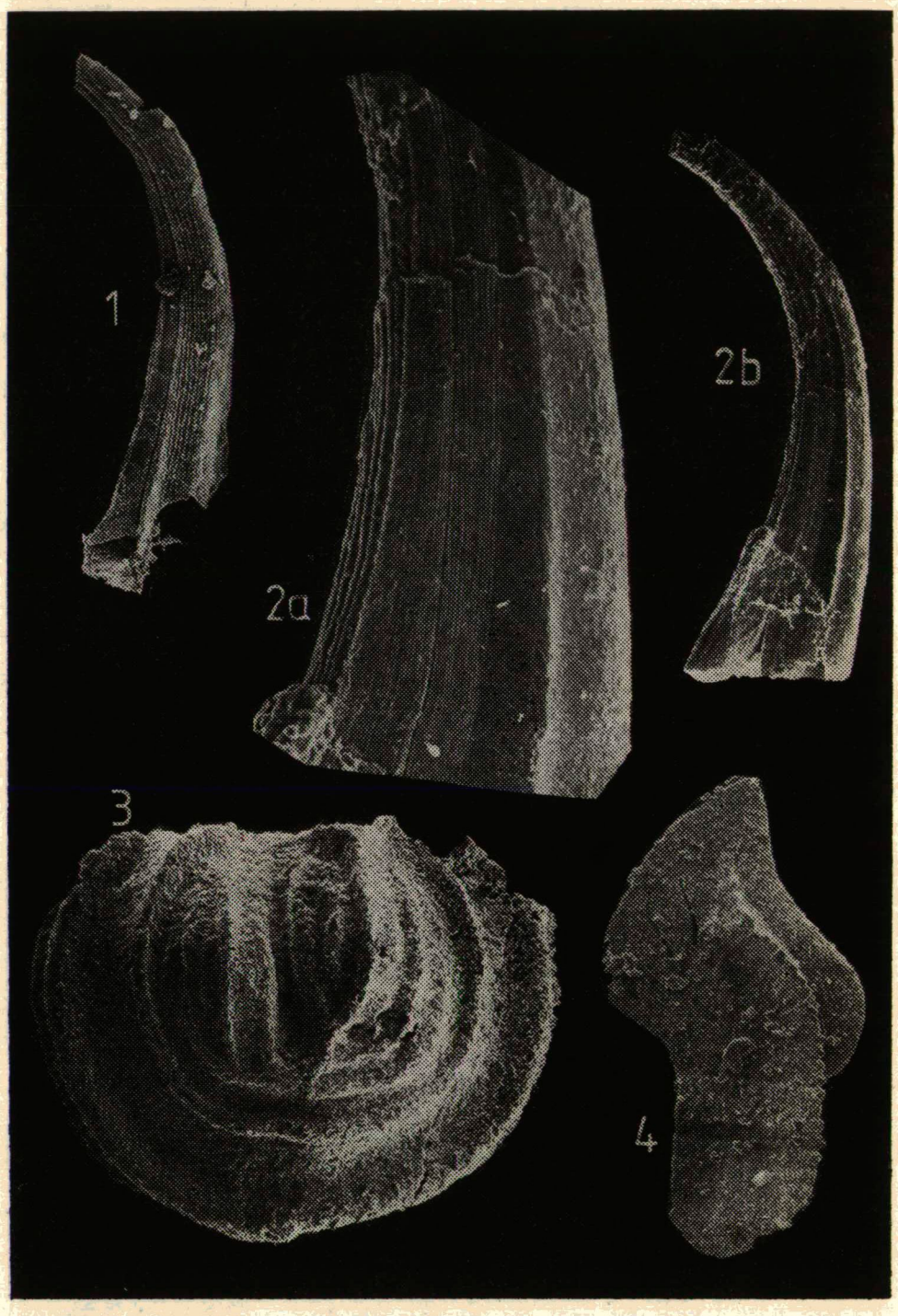
1
2a
2b
3
4

Acta Mineralogica-Petrographica, Szeged, XXVII, 213—218, 1985

REPORT ON THE SYMPOSIUM ON THE GEOLOGY AND GEOCHEMISTRY OF MANGANESE AND ASSOCIATED METALS; 27TH INTERNATIONAL GEOLOGICAL CONGRESS, MOSCOW

A. B. VEIMARN[1] and I. M. VARENTSOV[2]

The Symposium S. 12. 2. 2 Geology and Geochemistry of Manganese and Associated Metals was held August 5—9, 1984, in the framework of the 27th International Geological Congress. 39 reports covering the following 3 main problems were discussed: 1. mineralogy and geochemistry of manganese—4 reports; 2. genesis of manganese deposits on the continents — 15; 3. manganese and associated metals on the floors of recent basins — 20. The problem was discussed at the joint sessions with the theme C. 06. 1. 3. entitled. "Regularities of the Origin and Distribution of Metalliferrous Sediments and Ferromanganese Nodules."

The Symposium was organized by the Commission on Manganese of the International Association on the Genesis of Ore Deposits (IAGOD) and by the Project 111. "Genesis of Manganese Ore Deposits" of the International Geological Correlation Programme.

1. On the problem of *Mineralogy and Geochemistry of Manganese* the review by R. GIOVANOLI (University of Berne, Switzerland) "Layer Structures and Tunnel Structures in Manganates" was of great scientific interest. Ternary Mn oxide phases often having a layer structure were classified as phyllomanganates. Synthetical experiments have shown that they have a relatively rigid lattice and can accomodate a considerable amount of Co and Ni ions without any alteration of the unit cell. These associations are known as asbolites. Among the 10 Å- phyllomanganates there is a group of Mn oxides the structure of which is stable only in the presence of Co, Ni, Zn, Cu or other transition metal ions which are accumulated and built into the lattice of these compunds. The dehydration products of this group of 10 Å-manganates form the group of 7 Å-phyllomanganates including two minerals — birnessite and ranciéite.

In the presence of ions the radius of which is about 1.5 Å, like K^+, NH_4^+, Ba^{2+} manganates (IV) preferably form a lattice with tunnels accomodating these ions. These tectonomanganates (IV) include such minerals as hollandite and psilomelane (lately known as romanéchite). Upon heating psilomelane transforms *via* structural intergrowth into hollandite. It's notable that tunnel manganates (IV) cannot exchange ions. Studies of monomineral samples have shown that todorokite is a mineral though its structure is still debatable.

[1] Moscow State University
[2] Geological Institute of USSR Academy of Sciences, Moscow

These are valuable data for the interpretation of Mn, Ni, Cu and other transition metals ore formation in the ocean as the highest concentrations of these metals in nodular ores are associated, as a rule, with 10 Å- manganate phases.

In the report "Mineralogy and Mineral Chemistry of Metamorphosed Manganese-Oxide Ores and Manganese Silicate-Oxide Rocks — the example from the Precambrian Sausar Group, India" by BHATTACHARYYA, P. K. DASGUPTA, S., ROY, S. (Jadavpur University, Calcutta, India), FUKUOKA, M., HIROWATARI, F. (Kyushu University, Fukuoka, Japan) it was shown that in the process of progressive metamorphism fO_2 was different in ores and enclosing pelitic rocks. The authors came to the conclusion that the composition of the fluid phase in the contrasted environment was internally buffered by the reacting minerals.

The report by CHERNYSHEV, L. V., GELETII, V. F. (Institute of Geochemistry of the Siberian Branch of the USSR Academy of Sciences, Irkutsk) "On Geochemistry of Manganese in Endogenic Processes" contains experimental data contributing to the understanding of formation processes of hydrothermal manganese ores and metal-bearing sediments. It is shown that manganese is accumulated in endogenic fluids in wide temperature ranges and remains in them (stable forms in solutions and absence of efficient precipitants) even after removal of other ore minerals from the aqueous solutions. The accumulation of manganese due to its removal from the fluid system is predominantly going on in the superficial environment while oxygen is the main precipitant of the element.

The report by KALININ, V. V. (Institute of Geology of Ore Deposits, Petrography, Mineralogy and Geochemistry of the USSR Academy of Sciences, Moscow, USSR. "Alkaline and Alkaline-Earth Mineralization at Manganese Ore Deposits of the USSR Far East" presents the characteristics of new manganese minerals, formed when the processes associated with the Mesozoic magmatism were superimposed on the Paleozoic and, probably, originally volcanogenic sedimentary manganese ores.

2. The problem of *Genesis of Manganese Deposits on the Continents* was dealt with in the report "Genetic Aspects of Manganese Deposits Formation in the Geological History of the Earth Crust" by VARENTSOV, I. M. (Geological Institute of the USSR Academy of Sciences), RAKHMANOV, V. P., GURVICH, E. M. (Institute of Lithosphere of the USSR Academy of Sciences) and GRASSELLY, GY. (Szeged University, Hungary). The authors made an attempt to synthesize data on the evolution of the manganese ore process. The study revealed that from the Archean till the Paleozoic there was no evidence of manganese ore sedimentation in deep-water basins, the sedimentation was registered in the shallow-water environment practically in all the regions. In the Jurassic the formation of nodules and accumulation of metalliferous sediments was established in pelagic conditions (Alpine region, Timor and Roti Islands). At the Paleogene-Neogene boundary the intensive formation of ferromanganese nodules in the World Ocean took place which followed the invasion of Antarctic waters northwards.

Another interesting report on this theme was made by BEUKES, N. J. (Rand Afrikaans University, Johannesburg, South Africa) "Sedimentology of the Proterophytic Kalahari Manganese Deposit, Transvaal Supergroup, South Africa". The author presented the data on geology and conditions of formation of the gigantic hydrothermal sedimentary manganese deposit of Kalahari situated in the Hotazel formation of the Early Proterozoic Transvaal Supergroup. The estimated ore resources amount to 7500 million tons with the content of Mn 30—48% and Fe 4—15%. It is a bedded deposit, manganese ores are interbedded with iron-ore jaspilitic formations. The deposit consists of tree beds of relatively non-metamorphosed peloidal

kutnahoritic braunite lutite. According to BEUKES, N. J., the ores are of volcanogenic sedimentary origin and belong to the greenstone jasperoid association bound to manganese deposits. The ores are overlaid and interfingered by andesitic pillow lavas and hyaloclastites. Jaspilites were deposited more proximally to the volcanic source while manganolutites rather more distal. The ore-bearing sequence grades upwards into clastic deep water carbonates deposited in the front of a prograding shallow water carbonate platform.

The report by VEIMARN, A. B. (Moscow State University), BUZMAKOV, E. I., ROZHNOV, A. A. and SCHIBRIK, V. I. (the Ministry of Geology of the Kazakh SSR, USSR) "Famennian Manganese Ore Epoch in Kazakhstan" was devoted to genetically close hydrothermal sedimentary ferromanganese ore formations. However, the resources of Kazakhstan ore deposit are considerably less in comparison with Kalahari deposit, and the volcanic activity is also less manifested. The main deposits are associated with siliceous-carbonate flyshoid formation.

The report by the Australian geologists BOLTON, B. R. (La Trobe University) and FRAKES, L. A. (Monash University) "On the Origin of Manganese Giants: A Preliminary Comparative Investigation of the Chiatura (USSR) and Groote Eylandt (Australia) Deposits" and the report by the same authors together with MCHUGH, L. "The Geology and Geochemistry of Secondary Manganese Deposits on Groote Eylandt" were of considerable interest. The papers give general characteristics of the genesis of the deposits laying the emphasis on the hypergene processes in the formation of the most rich cryptomelan-pyrolusite ores of the Groote Eylandt.

VUJANOVIĆ, V. (Geological Institute, Beograd) in his report "Genetic Characteristics of Manganese Deposits in Yugoslavia" comes to the conclusion that they are mainly of moderate size, predominantly of volcanic-sedimentary origin and are situated in the "Diabase-chert formation" (from the Devonian to the Cretaceous including).

MORITANI, T. (Geological Survey of Japan) in his paper "Geology of Neogene Bedded Manganese Ore Deposits of Japan" characterized these deposits as hydrothermal sedimentary and divided them into two subtypes. Those occurring on the Japan Sea Coast show more sedimentary features, while the others occurring in the Kuroko Belt, show more influence of the hydrothermal activity.

KOSKI, R. A. and HEIN, J. R. (Geological Survey of the USA) in the report "Volcanogenic-Hydrothermal Manganese Deposits in the Western Cordillera" distinguish three groups of deposits: 1) deposits in chert-basalt and chert-graywacke sequences of the Paleozoic (Nevada) and of the Mesozoic (the Franciscan assemblage in California); 2) deposits in sequences of pelagic limestone and basalts (the Eocene of the Olympic Peninsula); 3) deposits in continental sedimentary and volcanic rocks. The first two groups are represented by numerous small deposits. The third group is represented by large Miocene and Pliocene deposits of low grade oxide manganese ores, interbedded in sandstone, conglomerate, tuff and gypsum overlying latitic andesites. The sequence was formed during incipient rifting related to the opening of the proto-Gulf of California.

A number of reports made by the Soviet geologists contained new data on manganese deposits of the USSR: GRIBOV, E. M., CHUKHNINA, L. S. (Institute of Lithosphere of the USSR Academy of Sciences) "Manganese Accumulation in the Area of the Enisei Chain of Hills"; YASHVILI, L. P. (Institute of Geological Sciences of the Academy of Sciences of the Armenian SSR) "Mineral Peculiarities of Different Genetic Types of Manganese Ores in the Armenian Republic"; DANILOV, I. S.

(Dnepropetrovsk State University) "Some Aspects of Genesis of Nikopol Manganese Ores"; MACHABELI (Caucasian Institute of Mineral Resources) "Genetic Model of Manganese Ore Formation in the Oligocene Deposits in the Caucasus"; LIPAEVA, A. V., PAVLOV, D. I. (Institute of Ore Deposits Geology, Petrography, Mineralogy and Geochemistry of the USSR Academy of Sciences) "Iron, Manganese and Metals Closely Linked with Them Occurring in the Paleochannel ways of Discharged Subterranean Waters in the Northern Near-Aral Sea Area".

The reports delivered by MACHAMER, J. F. (US Steel Corporation, USA) "Classification of Manganese Deposits. The Point of View of a Field Geologist" and by MSTISLAVSKIY, M. M. (Ministry of Geology of the USSR) "The Mechanism of Manganese Deposits Formation on the Continents" presented the analysis of data on a great number of deposits in the World.

3. The most informative reports on the problem of *Manganese and Associated Metals on the Floors of Recent Basins* contained data on formation conditions, on the regularities of distribution and on evaluation of Co-rich ferromanganese crusts on the Ocean floor: HALBACH, P. and PUTEANUS, D. (Institute für Mineralogie und Mineralische Rohstoffe, Technische Universität, Clausthal, FRG) "Cobalt-Rich Ferromanganese Crusts from Central Pacific Seamount Regions — Composition and Formation"; HEIN, J. R. (USA) "Cobalt-Rich Ferromanganese Crusts from the Central Pacific"; MANHEIM, F. T. and LANE, K. M. (US Geological Survey) "A World Wide Data Base for Ferromanganese Crusts in the Oceans". These crusts are considered as potential ores due to a high cobalt content (up to 2%). According to the data of the expedition convened on the MRV "Sonne" (FRG) in 1981, which were lately confirmed by the study of the US Geological Survey, the Mid-Pacific Seamounts region is the most promising for the industrial development. In the region of the Mid-Pacific Mountains of the Line Islands the crust thickness riches 2 cm containing 1—2% Co at the depth of 2500 m. At present the US Geological Survey carries out a wide programme of studies of these Co-rich ores a computer data base is set up, oceanographic and geochemical surveys using the most advanced technology are planned. It is emphasized that the oxidizing diagenesis plays a certain role in the development of the nodules in the abyssal regions, the bottom waters reflecting geochemical processes in the ocean is the source responsible for the formation of crusts and nodules on the seamounts.

The paper by MORITANI, T., USUI, A., NAKAO, S. and NOKARA, M. (Geological Survey of Japan) "Manganese Nodule Deposits in the Northern Central Pacific Basin" presents the results of a five year programme. There are detailed data on the distribution of different morphologic types of nodules reflecting the source of ore components supply. *a)* Interstitial waters as the metal source for the nodules of rough surface, characterized by 10 Å manganate and high grade of Mn, Ni, Cu; *b)* bottom waters were the metal source for the nodules with a smooth surface, characterized by δ-MnO_2, rich in Fe, Co. The emphasis is laid on the correlation between types of nodules and geological setting, water currents and peculiarities of sedimentation.

The report by SKORNYAKOVA, N. S., BATURIN, G. N. and MURDMAA, I. O. (Shirshov Institute of Oceanology of the USSR Academy of Sciences) "Ferromanganese Nodules of Subequatorial Ooze of Radiolarian Belt of the Pacific Ocean" is devoted to the variations in mineral and chemical composition of nodules occurring in the zone of high biological productivity related to the latitudinal zonation. It is shown that the highest Ni, Cu, Mn concentrations occur in the nodules on the both sides from the equator along the periphery of the biologically productive zones. Three

types of nodules are distinguished: sedimentary (hydrogenic), sedimentary-diagenetic and diagenetic.

SHNJUKOV, E. F. and ORLOVSKY, G. N. (Institute of Geological Sciences of the Academy of Sciences of the Ukranian SSR, USSR) in their report "Iron-Manganese Nodules of Northern and Equatorial Part of Indian Ocean" show wide distribution of multilayered bodies of nodules, underlying the role of endogenic processes as a source of ore-bearing components.

As a rule, the reports on this theme contain a lot of factual data usually presented in the graphic form. Most reports are detailed regional studies: HAYNES, B. W, LAW, S. L. and BARRON, D. C. (Bureau of Mines, Avondale, Maryland, USA) "The Mineralogy and Geochemistry of Pacific Manganese Nodules"; APLIN, A., CRONAN, D. S. (Imperial College, London, UK) "Ferromanganese in the Western Central Pacific"; PLÜGER, W. L., KUNZENDORF, H. and FRIEDRICH, G. (Technical University, Aachen, FRG) "Rare Earth Elements in Manganese Nodules from the South West Pacific Basin"; BOLTON, B. R., BURNS, R. B. and FRAKES, L. A. (Australia) "On the Geochemistry and Origin of Polymetallic Crusts from the d'Encastieaux Zone, South-West Pacific Ocean"; PIPER, D. Z., SWINT, T. P. (US Geological Survey) "Distribution of Ferromanganese Nodules in the Pacific Ocean"; BAZILEVSKAYA, E. S. (Commission on the Problems of the World Ocean of the USSR Academy of Sciences) "About the Mechanism of Manganese Nodules Formation"; EMELYANOV, E. M. (Shirshov Institute of Oceanology of the USSR Academy of Sciences, Atlantic Department, Kaliningrad, USSR) "Geochemistry of Manganese and Iron in the Atlantic Ocean Basin"; MAKEDONOV, A. V., GOLOVIENOK, O. M. and KRIVULINA, Y. A. (All-Union Geological Research Institute, USSR) "Classification of Recent Manganese Nodules"; WAKEFIELD, S. J. (University of Swansey, UK) "Deep Sea Metalliferrous Deposits: How Significant Are They?"; GRAM-OSIPOV, L. M., BYCHCOV, A. S., VOLCOVA, V. S., TISHENKO, P. YA. and CHICHKIN, R. V. (Pacific Oceanological Institute of the Far East Scientific Centre of the USSR Ac. of Sci., Vladivostok, USSR) "Physical and Chemical Problems of Formation of Ferromanganese Nodules". The report "World Distribution of Metal-Rich Subsea Manganese Nodules: a Summary" by MCKELVEY, V. E., WRIGHT, N. A. and BOWEN, R. W. (US Geological Survey) was of considerable interest. General characteristics of distribution of ferromanganese nodules in the World Ocean were inferred on the basis of computer processing of geochemical data.

The following reports were devoted to the study of fossil nodules: MINDSZENTY, A., GALÁCZ, A., DODONY, I. (Eötvös L. Univ., Budapest, Hungary), CRONAN, D. S. (UK) "Paleoenvironmental Significance of Ferromanganese Oxide Concretions from the Hungarian Jurassic", VARNAVAS, S. (Univ. of Patras, Greece) "Comparative Study of Fossil Manganese Nodules from Two Areas in Greece".

The theses of almost all the above mentioned reports were published by the "Science" Publishing House.

The sessions of the Symposium were held at M. V. Lomonosov Moscow State University. The participants visited the exhibition "Manganese Ores of the USSR and Other Countries" which was specially organized for the 27th International Geological Congress, at the Museum of the Earth Science of Moscow State University, We should mention the report made by SOREM, R. K. on the establishment of the Museum of manganese ores at Pullman University (Washington, USA). The author urged the participants of the Symposium to contribute to the museum collection, for all the materials would be available for specialists from all states.

During the Symposium a joint organizing meeting of the Commission on Manganes of the IAGOD and of the Project 111 "The Genesis of Manganese Ore Deposits" of the IGCP was held. There were made the reports on the work of the Commission and of the Project. It was decided to prepare a summarizing report on the results of the Project 111 and to start carrying out the new project of the IGCP "Global Correlation of Manganese Metallogeny to Paleoenvironments". Provisions were made to convene a session on geology and geochemistry of manganese in the framework of the VII IAGOD Symposium, Sweden, 1986.

The Symposium was a great international event which contributed to the intensive exchange of scientific information and to the consolidation of efforts of geologists and geochemists of the world in the field of geology and geochemistry of manganese and associated metals.

Manuscript received, June, 1985

Felelős kiadó: Grasselly Gyula
85-2946 — Szegedi Nyomda — Felelős vezető: Dobó József igazgató
Készült: Monószedéssel, íves magasnyomással, 19,25 A/5 ív terjedelemben,
az MSZ 5601—59 és 5602—55 szabvány szerint
Példányszám: 625

Illustrations

Figures should be used only where they are essential to elucidate the text.

The illustrations should be numbered according to their sequence in the text, and in the text references should be made to each figure.

All illustrations should be given separately, not stuck on sheets and not folded. The number of the figure and the authors name should be noted on the reverse side of the photographs and on the lower frontside of drawings, indicating at the same time the top of the figure where it is necessary.

Captions for all figures should be given typewritten on a separate list at the end of the manuscript. Drawn text in the figures should be kept to a minimum.

Drawings should be made on tracing paper by Indian ink. The thickness of the lines and the size of the lettering should be big enough to allow a necessary reduction.

Photographs of good contrast and intensity on glossy paper are only acceptable. Colour photographs or drawings cannot be accepted.

Use bar scale on all illustrations instead of numerical scales that must be changed if reduction is necessary.

References

All references to publications made in the text should be made by quoting the author's name (without initials) and year of publication in parenthesis.

The list of references at the end of the manuscript should be arranged alphabetically by author's names and chronologically per author.

If the referred publications are written by more than two authors, in the text only the name of the first author should be indicated, the other co-authors are denoted by "et al.", however, in the list of references the names of authors and all co-authors should be mentioned.

In the list of references all references should be written, e. g. Balogh, K., A. Barabás (1972): The Carboniferous and Permian of Hungary. Acta Miner. Petr., Szeged, XX/2, 191—207.

At references to books beside the author's name, year of publication, title and the publishing house should also be mentioned.

In the case of references for symposium volumes, special issues or multi-authors books, the following system should be used: Roser, B. P., C. W. Childs, and G. P. Glasby (1980): Manganese in New Zealand. In: I. M. Varentsov and Gy. Grasselly (Editors): Geology and Geochemistry of Manganese, Vol. II. Akadémiai Kiadó, Budapest, 199—211.

Manuscripts that are not adequately prepared will be returned to the author(s).